Continuous Twin Screw Wet Granulation: A Step towards Mechanistic Understanding

Sushma Vijay Lute

Department of Chemical and Biological Engineering
The University of Sheffield

A thesis submitted in fulfilment of the requirements for the degree of Doctor in Philosophy

September 2018

Abstract

Twin screw granulation is the most recent technique used for continuous wet granulation across the pharmaceutical industry. The research works published so far are pioneering but more work needs to be done to bring twin screw granulation from a developing state to a fully industrialised and commercialised state in the pharmaceutical industry.

Currently, one of the main challenges and deterring issues in twin screw granulation is the limited control on granule attributes (size, amount of small and large granules etc.) owing to the limited mechanistic understanding of granulation process. For an instance, TSG generally produces granules with bimodal, wide size distribution, which is often not desirable during tabletting as it can lead to variability in the tablet attributes. This requires milling of oversize granules resulting in increase in process time, cost and potentially production of more fines. Such bimodal size distribution from TSG has to be turned into monomodal and narrow granules size distribution. Hence, there is a need to address such challenges to increase the acceptability of the twin screw granulation as an efficient continuous wet granulation technique.

Therefore, in this research work an attempt was made to develop a thorough mechanistic understanding of twin screw wet granulation process with respect to effects of various formulation (L/S, type of powders) and process (type of screw element, screw configuration, screw speed, powder feed rate, fill level, barrel temperature) variables on the granule properties such as size, shape and structure and tablet tensile strength. Increasing number of kneading elements the granule become bigger in size, elongated, smoother and denser due to coalescence and consolidation (as result of higher shear and compaction stresses acting on granules). However, addition of conveying elements after kneading elements in the screw configuration resulted in decrease in granule size and elongation, due to cutting and chopping action of the conveying elements. As L/S increased above critical level (which is L/S-0.1 in case of lactose) the granule size increased.

It was also found that, material property plays more important role while studying fill level. Lactose powder maintained granule size at changing barrel fill levels (SFL and PFN).

In addition to the experimental studies, an attempt was made to develop the mechanistic understanding of twin screw granulation process by using population balance method (PBM) based models incorporated in an advanced process modelling platform i.e. gSolids followed by the experimental validation of the models. From both experimental and modelling works, it was demonstrated that the granules (and thereby tablets) with preferential properties can be produced through a systematic approach based on mechanistic understanding of the twin screw wet granulation.

Acknowledgements

I would like to thank my research supervisor Professor Agba D. Salman, for his excellent supervision. I sincerely appreciate his enthusiastic support in project, directive comments and discussions provided throughout the whole research programme.

My special thanks to Dr. Ranjit Dhenge for his support. Really thanks for all the encouragement and support you provided during this study.

I would also like to thank Prof. Jim Litster for his kind guidance and discussions on the work of population balance modelling and providing access to gSolids. I would like to thank Dr Dana Barasso from Process Systems Enterprise for helping me to understand gSolids.

I would also like to thank all of my PPG colleagues Dr. Chalak Omar, Dr. Mohammad Saleh, Dr. Riyadh Bakir, Dr. Syed Islam, Ali Hassan, Osama Mahmah, Bilal Khorsheed for their company and help during PhD. I could not imagine Sheffield without you.

Thanks goes to my Indian Society friends Arthi Rajkumar and Dr. Menan Balshanmugam. Life could have been more difficult during PhD without you two. Thanks for those many relaxed Indian meetings and I am still looking forward many more to happen in future. Special thanks to Arthi's delicious food and her constant support and care like a sister.

Last but not least, I am really grateful to my Parents, Mr. Vijay Lute and Mrs. Sandhya Lute for giving me special support and care during all years of my life and studies. Thanks also goes to my brother Amit and other family members for their well wishes and constant support.

List of Journal Publications and Conference Papers

- ✓ Sushma V. Lute, Ranjit M. Dhenge, Agba D. Salman, Twin Screw Granulation: An Investigation of the Effect of Barrel Fill Level, Pharmaceutics 2018, 10(2), 67

- ✓ Sushma V. Lute, Ranjit M. Dhenge, Agba D. Salman, Twin Screw Granulation: Effects of Properties of Primary Powders, Pharmaceutics 2018, 10(2), 67

- ✓ Sushma V. Lute, Ranjit M. Dhenge, Michael J. Hounslow, Agba D. Salman, Twin screw granulation: Understanding the mechanism of granule formation along the barrel length, Chemical engineering research and design, Volume 110, June 2016, Pages 43-53

- ✓ Sushma V. Lute, Ranjit M. Dhenge, Michael J. Hounslow & Agba D. Salman, Twin screw granulation: Effect of fill level. 7th International Granulation Workshop, UK, 2015.

- ✓ Sushma V. Lute, Ranjit M. Dhenge, Michael J. Hounslow, Agba D. Salman, Twin screw granulation: A steps towards granule designing, 7th International Granulation Workshop, UK, 2015

- ✓ Sushma V. Lute, Ranjit M. Dhenge, Michael J. Hounslow & Agba D. Salman, Twin screw granulation: Effects of properties of primary powders. 8th International Granulation Workshop, UK, 2017.

- ✓ Sushma V. Lute, Ranjit M. Dhenge, Dana Barasso, Jim D. Litster, Michael J. Hounslow & Agba D. Salman, Twin screw granulation: A step towards developing predictive mechanistic models based on population balance method. 8th International Granulation Workshop, UK, 2017.

Table of Contents

List of Figures

List of Tables

Notations

ø	Helix (flight) angle (°)
d_{50}	Median granule size (µm)
s	Second
h	Hour
L/D	Barrel length/ Barrel diameter
L/S	Liquid to solid ratio
K	Compressibility factor
σ	Strength of tablet (N/m^2)
F_{max}	Maximum force (N)
D	Tablet diameter (mm)
T	Thickness of tablet (mm)
β	Aggregation kernel
R_{agg}^{form}	Formation of granules due to aggregation
R_{agg}^{dep}	Depletion of granules due to aggregation
i,j	Size classes (µm)
$\beta_{i,j}$	Aggregation kernel
β_0	Aggregation efficiency
$\beta_{i,j}$	Collision frequency
K_{break}	Breakage rate kernel
v, *w*	Particles of respective volumes (m^3)
β, ϒ, φ	Constant parameters (Fragment distribution Function)
Gm	maximum growth rate
Mpowder	mass of fine powder the lower bound of the particle classes (g)
Mi	mass of particles in the ith size class (g)
x_c	moisture content
x_{wc}	critical moisture
k, α	fitting parameter

Abbreviations

API	Active pharmaceutical ingredient
CE	Conveying element
DME	Distributive mixing element
HSG	High-shear granulator
ID	Inside diameter (of the screw)
KE	Kneading element
L/D	Barrel length/Barrel diameter
LPCE	Long pitch conveying elements
MCC	Microcrystalline cellulose
SPCE	Short pitch conveying elements
TSG	Twin screw granulator

1 INTRODUCTION

1.1 GRANULATION

Granulation is a process of bringing two or more powder particles together to form larger aggregates or granules. It is commonly used in food, pharmaceutical, ceramic, fertilizer, detergent industries to improve physical and mechanical properties and aesthetics of powders such as density, flowability, homogeneity etc.

In pharmaceutical industry, the direct compression (no granulation) of bulk powders (excipients) and active pharmaceutical ingredient (API) into the tablets is desired. However, this is not possible in the most cases as the compressibility of most of the APIs or excipients is poor. Furthermore, in some cases the API and excipient are so sensitive to the excess stresses that they melt during compaction. Hence, in such cases the granulation of API with excipient becomes very important.

Granulation is of two types; dry granulation and wet granulation. Dry granulation is carried out by compression of dry powder under high pressure. This can be carried out using roller compactor in which two counter rotating rollers compact the powder particles to form sheets or ribbons and then desired size is achieved through milling. This type of granulation is useful for materials having sensitivity to the moisture. In wet granulation, the liquid binder is added onto a dynamic powder bed under the influence of impeller (in high shear granulator), screws (in twin screw granulator) or air (in fluidised bed granulation) (Dhenge et al. 2010). The agitation imparted into the system along with the wetting of the powder particles results in the formation of wet granules (Iveson et al. 2001). A basic schematic of wet granulation is shown in Figure 1-1.

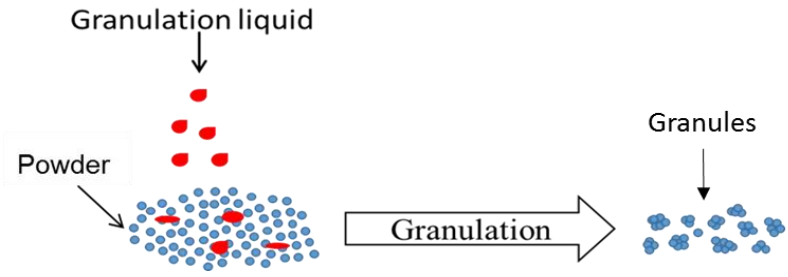

Figure 1-1 Schematic of the wet granulation process

1.1.1 Basic theory of wet granulation

Granule formation by wet granulation has generally been considered more complex than dry granulation as it involves various rate processes viz., wetting & nucleation, consolidation & coalescence and attrition & breakage as shown in Figure 1-2 (Iveson et al. 2001). The knowledge and understanding of these rate processes has ever been evolving in the area of batch wet granulation. In the context of the present study i.e. continuous twin screw wet granulation it is important to summarise the basic understanding of the wet granulation in order to build the mechanistic knowledge.

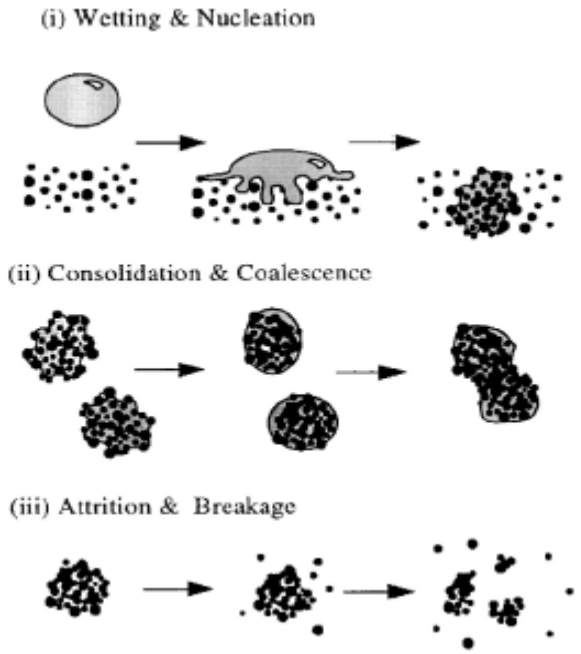

Figure 1-2 Different rate processes within wet granulation (Iveson et al. 2001)

1.1.1.1 Wetting & Nucleation

The first stage in the wet granulation is nucleation, where liquid comes in contact with powder to form nuclei. The process of nuclei formation and dispersion of liquid has been described by Iveson et al. (2001), Dhenge et al. (2012a) and Vercruysse, Bellandi, et al. (2014). The nuclei are formed immediately after addition of liquid onto the powder. These nuclei are very weak, loose and easy to break. After wetting and nucleation the nuclei go through some mechanical agitation or mixing which causes proper distribution of liquid.

It is very important to distribute the liquid uniformly throughout the powder otherwise; it can result in bimodal size distribution indicating a sample with varying amounts of lumps of nuclei and ungranulated dry powder. The nucleation can exhibit two types of mechanisms; i) Immersion, ii) Distribution as described by Schæfer et al. (2004).

1.1.1.2 Consolidation & Coalescence

After liquid addition, nuclei undergo further process called consolidation and coalescence. Consolidation is a process in which densification of nuclei occurs (Liu et al. 2009, Dhenge et al. 2012a, Kumar, Vercruysse, Bellandi, et al. 2014, Lute et al. 2016). During granulation, the granules collide with the vessel wall of the granulator or with other granules. Due to this process the granules become denser and the interstitial liquid in their structure comes on the surface to promote granule growth (Liu et al. 2009).

When consolidation of granules occurs, the granules undergo process of coalescence and layering. These processes are mainly responsible for granule growth. Coalescence occurs due to the deformation of granules in which liquid comes on surface of granules. When liquid covered particles collide with each other, the kinetic energy of particles is dissipated with the deformation of particles. The layering occurs when the granules squeeze out liquid on the surface due to deformation and the dry powder sticks over that surface (Iveson et al. 2001, Kumar, Vercruysse, Bellandi, et al. 2014).

1.1.1.3 Attrition & Breakage

Attrition is a process in which the surface of the granules chips away with respect to time in an opposite process of coalescence (Liu et al. 2009, Kumar, Vercruysse, Bellandi, et al. 2014, Sayin, El Hagrasy, et al. 2015, Lute et al. 2016). Breakage occurs due to collision or impact of granules on the barrel wall of the granulator. Both attrition and breakage affects granule size distribution and other properties of granules. However, amount of breakage depends on the strength of the granules. So, the strength and breakage can be controlled by different formulation variables such as amount and viscosity of granulation liquid and process variables such as speed of the impeller/screw/fluidising air during granulation.

1.1.2 Types of wet granulation

There are various techniques used for wet granulation of powders. Vervaet and Remon (2005) reviewed various batch and continuous granulation techniques which are used for the production of granules in the pharmaceutical industry. Example of batch techniques is high shear granulation while that of continuous technique is twin screw granulation.

1.1.2.1 Batch wet granulation

It is a traditional method of granulation. This method is suitable for industries which generally deal with small to median volumes of materials.

1.1.2.1.1 High shear granulation

It is type of batch wet granulation where powder is mixed with liquid binder with the help of impeller and chopper at high rotational speed. Granules produced using high shear granulation have high density as well as regular and spherical shape.

High shear granulation technique is very well established and well known for the product quality and is suitable for flexible operation. However, it has some limitations. This technique is batch and/or semi continuous in operation, and suffer from problems during process and product optimisation and scale up resulting in high production cost.

1.1.2.2 Continuous wet granulation

Not many instances yet of use of TSG in pharma production but it is under development widely in industry. Continuous granulation is used in the pharmaceutical sector as it offers several advantages over batch granulation such as reduced production time, labour, waste, high energy efficiency and thereby reduced cost and increased profitability (Isaac et al. 2003). The twin screw granulator (TSG) is used for continuous wet granulation in the pharmaceutical industry.

1.1.3 Twin screw wet granulation

In twin screw granulation, the binder is added on the screw conveyed powder resulting in granules (Isaac et al. 2003). The schematic of the twin screw wet granulation is shown in Figure 1-3.

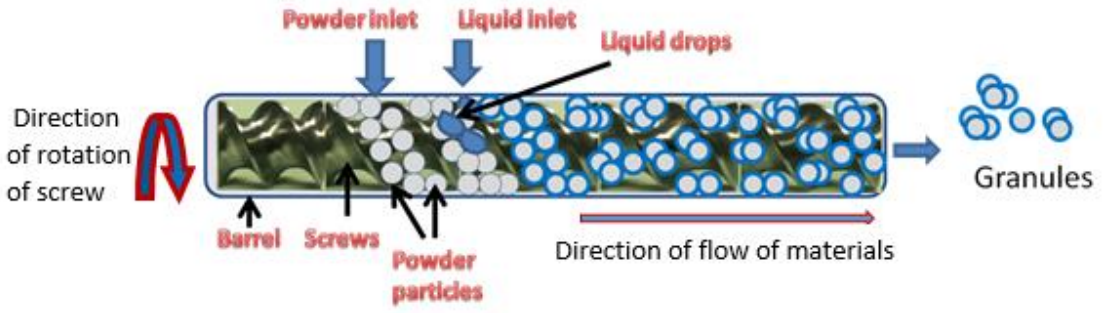

Figure 1-3 Schematic of twin screw wet granulation process

The twin screw granulator is derived from the twin screw extruder which is commonly used for the food and the polymer processing purposes. The die in the extruder is removed to produce the granules. The heart of TSG are the two co-rotating, closely intermeshing screws which are used to transport powder in the forward direction. The various key terms used in describing the screw elements and the TSG are mentioned in the following section (Chokshi 2004) and in Figure 1-4 and Figure 1-5.

L/D of the barrel- This is the ratio of length (L) to diameter (D) of the barrel bore of the granulator. L/D is commonly used to describe the granulator dimension. Increasing diameter (D) of the granulator increases its capacity (throughput and volume).
Screw diameter- The width of the screw measured from one flight tip to other. The screw diameter is slightly narrower than the barrel diameter.
Root diameter- The width of the part of the screw that the flight is wound around. The root diameter can vary.
Flight- The conveying surface or thread of the screw element.
Pitch- The distance between two matching points on the same screw. The pitch can vary.
Channel- This is the space between the flights in which the material moves down the barrel.

Helix angle- The angle made by flight with horizontal screw base. The standard helix angle of screws calculated as follows:

Helix Angle = arctan $\left(\frac{Pitch}{\pi D}\right)$ Eq. 1

1.1.3.1 Conveying elements

Conveying elements are the key parts of the screw configuration in the TSG. Conveying elements are available in various forms and sizes depending on the manufacturer and their role in the screw configuration. Different types of conveying elements have different pitch length and flights (single or double). These different terms are illustrated in Figure 1-4

Both screws of twin screw granulator commonly consist of conveying elements, kneading elements and screw shaft. Conveying elements are used for feeding or discharge purpose (Dhenge et al. 2012a).

Depending on the pitch length, conveying elements are of two types i) Short pitch conveying element (SPCE) ii) Long pitch conveying element (LPCE). The length of LPCE is twice that of SPCE in case of the equipment used in study. As the pitch length increases channel width of conveying element also increases, resulting in increase in conveying capacity. The screw elements can be arranged in a different manner in order to make screw configuration suitable for intended application.

1.1.3.1.1 Long pitch conveying elements (LPCE)

LPCE has larger channel width (12 mm in the present study), volume and conveying capacity. It helps to avoiding over feeding of powder in feeding zone. Hence, it carries more volume of material. Conveying elements rotate and apply compression and shear force inside the barrel. The helix angle in LPCE is bigger as compared to SPCE. Long pitch conveying elements are shown in Figure 1-4(a).

1.1.3.1.2 Short pitch conveying elements (SPCE)

SPCE has shorter channel width (8 mm in the present study), volume and conveying capacity. It helps carrying powder in the forward direction. It carries small volume of

material compared LPCE due to small channel width. The helix angle in SPCE is steeper compared to LPCE. Short pitch conveying elements are shown in Figure 1-4 (b).

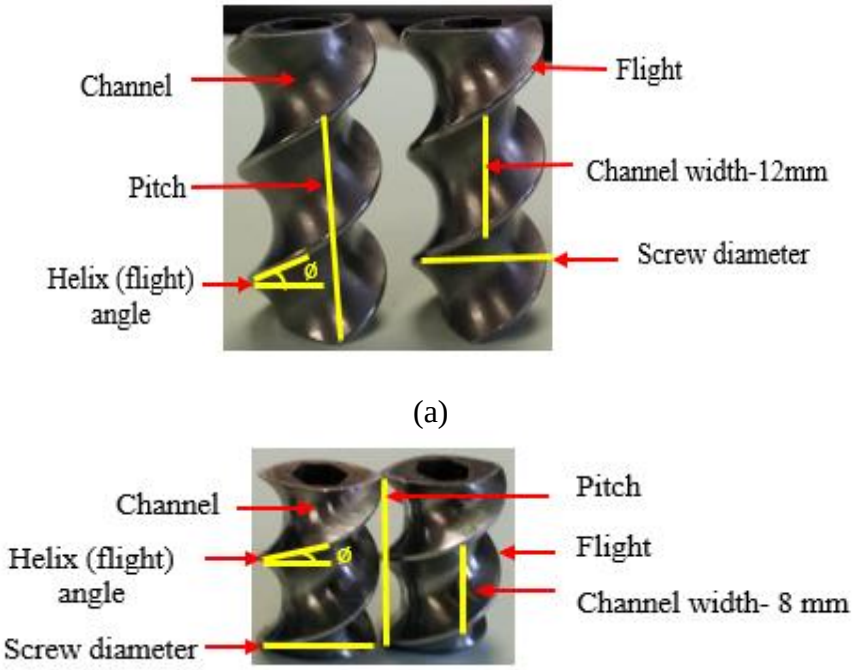

Figure 1-4 Types of conveying elements (a) LPCE (b) SPCE (used in this study)

1.1.3.2 Kneading elements

One or more kneading elements (KEs) or discs are used along with the conveying elements in the screw configuration during twin screw granulation process. These elements are used for mixing and proper distribution of granulation liquid within powder. Kneading elements are also used in many different ways like conveying elements. The angle between two KEs is called staggering angle. The KEs having staggering angle of 30°, 60° and 90° can be used depending upon product requirement. These elements can be arranged in forward or reverse direction. The KEs used in this study are arranged in forward direction having staggering angle of 60°. With the increase in the staggering angle, the mixing of material increases while the resultant conveyance of material decreases (Thiele 2003). The thickness of kneading element is $1/4^{th}$ (4 mm in the present study) of SPCE (16 mm). Increasing number of KEs results in proper mixing and

redistribution of granulation liquid with material. Varying number of KEs and staggering angle causes change in properties of granules. KEs (used in this study) are shown in Figure 1-5.

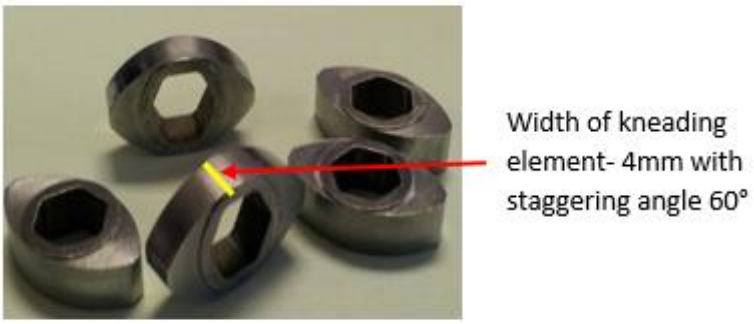

Figure 1-5 Kneading discs with staggering angle of 60° (used in this study)

2 LITERATURE REVIEW, SCOPE FOR RESEARCH & OBJECTIVES

Since last decade, twin screw wet granulation has gained the popularity as a continuous wet granulation technique in the pharmaceutical industry as it offers edge over the conventional batch granulation techniques such as high shear and fluidised bed granulation (Isaac et al. 2003). Most importantly twin screw granulation delivers continuous, high throughput, high quality product with efficiency and at reduced cost. It provides an easy compliance with ongoing Food & Drug Administration (FDA) initiative of implementation of continuous manufacturing and Process Analytical Technique (PAT) to monitor and control the process and reduce the process inconsistency.

In general, a large portion of the studies published so far in twin screw granulation area have focused on the parametric evaluations of effect of process (powder feed rate, screw configurations and screw speed) and formulation variables (liquid to solid ratio (L/S), viscosity of the liquid binder and primary particle size) on the dependant variables (torque and residence time) and granule properties (median size, size distribution, shape and strength) (see Table 2-1). Papers have also been published on understanding the granulation behaviour inside the twin screw granulator (Dhenge et al. 2012a, Dhenge et al. 2012b, Mu and Thompson 2012, Dhenge et al. 2013, Tu et al. 2013). Dhenge et al. (2012a) first attempted to give a simplistic view of how granule formation occurs along the length of barrel of TSG. They classified the length of TSG into 4 different regions namely nucleation, coalescence, consolidation and breakage. Dhenge et al in their series of publications (Dhenge et al. 2012a, Dhenge et al. 2013) also proposed regime maps for the twin screw granulation process to predict the regime and/or properties of granules (produced using mixture of lactose and microcrystalline cellulose powders). The maps were not tested and validated for different materials and processing conditions. The formation and flow of granules across the screw channel of the twin screw granulator were demonstrated using Particle Image Velocimetry (PIV) by Dhenge et al. (2013).

Twin screw granulation is influenced by the several variables. Effects of some of the key process and formulation variables on the granulation behaviour and granule

properties and on secondary or dependant variables from literature are summarised in the following sections.

2.1 EFFECT OF POWDER FEED RATE

The powder feed rate is only surrogate for the degree for fill level at fixed speed which in turn can affect the compressive and shear stresses, dependant variables such as residence time and torque and ultimately granule properties.

In twin screw granulation, barrel fill level refers to the ratio of the volume occupied by powder to the total available volume of screw channel. Previously, the barrel fill level was estimated by Lee et al. (2012) and Dhenge et al. (2013) in their studies to understand the material occupancy inside the granulator. Few studies considered barrel fill as a primary or input variable and investigated its impact on granule attributes (Thompson and Sun 2010, Gorringe et al. 2017, Meier et al. 2017). The background about barrel fill level is discussed in more details in chapter 6.

The residence time is the time for which the materials are mixed, granulated within the granulator (Dhenge et al. 2010). When feed rate is low the residence time of materials inside the granulator is longer. So, the distribution curve is wide and its peak location is on the right (Ainsworth et al. 1997). Dhenge et al. (2010) and Dhenge et al. (2011) showed that increasing the powder feed rate decreases the residence time of wetted powder mass. When feed rate is low, the relatively low degree of channel fill would generate a lower throughput force, which will slow down the material conveying speed and take a longer time. Study carried out by Vercruysse et al. (2012) showed agreement with finding from Dhenge et al. (2010) and Dhenge et al. (2011).

Torque is a measure of twisting force acting on screws to rotate them (Dhenge et al. 2010). The torque values are considered an indication of extent of compaction of powder inside the barrel. The torque required to rotate the screws depends on the amount of powder available in the barrel (Dhenge et al. 2011). Dhenge et al. (2010) studied the effect of powder feed rate on the torque. As expected, the torque increased with increasing powder feed rate due to increase in the barrel filling. The results were further reconfirmed by Dhenge et al. (2013). Liu et al. (2017) observed that effect of powder feed rate on

torque depends on liquid to solid ratio (L/S). At low to moderate L/S, increasing powder feed rate does not significantly influence torque while opposite is the case at high L/S (i.e. torque increases with increasing powder feed rate).

The powder feed rate also influences the granule properties as investigated by Keleb et al. (2004). They granulated lactose powder and found that increasing the total input rate had no influence on all the granule properties except the granulation yield (granule fraction between 250-1000 μm), which increased as the total input rate increased. Djuric et al. (2009) also granulated lactose powder and studied the interaction between the total input rate and the twin screw granulator type [Leistritz and APV]. They found that the Leistritz granulator produced much larger granules, but a limited effect was observed in the case of the APV granulator when increasing the total input rate. They also observed that increasing the total input rate decreased the friability of the granules which also means higher granule hardness and strength. Dhenge et al. (2010) and Dhenge et al. (2011) showed that increasing the powder feed rate decreased the size but increased sphericity and strength of granules. Lee et al. (2012) also observed similar results. This was attributed to the increase in the barrel fill at higher powder feed rates which increased the particle packing contributing to increase overall granule strength. But increased powder feed rate also led to more particle-particle and particle-wall friction meaning more attrition and breakage of the formed granules making them smaller in size and spherical or rounder in shape.

Vercruysse et al. (2013) also studied the influence of powder feed rate at varying screw configurations and barrel temperature on the granule size in terms of amount of fines (<150 μm), yield (150 μm to 1400 μm) and agglomerates (>1400 μm). They found that with the increasing powder feed rate the amount of fine, yield and agglomerates do not change significantly. However, the authors observed that the amount of fines and amount of oversized agglomerates varies significantly with change in the number of kneading element and the barrel temperature. Increasing the number of kneading elements in the screw configuration produced less amount of fines and more amount of oversized agglomerates. These results agree with the findings from previous researchers (Djuric et al. 2009, Thompson and Sun 2010). A similar effect was observed when barrel

temperature was increased owing to increased solubility of powder in the granulation liquid.

All the studies mentioned above were carried out using kneading elements in the screw configuration. Dhenge et al. (2013) were first to investigate the granulation behaviour using only conveying elements in the screw configuration. They observed that granulation of powder at higher feed rate the powder is conveyed in plugs with poor axial mixing and granulation inside the granulator. This results in production of large fraction of fines with few bigger granules meaning overall reduction in the granule size. It was also found that the amount of the fines decreases while that of bigger granules increased with increasing powder feed rate. Authors explained that the bigger agglomerates formed in the beginning of the granulation retain the granulation liquid with them due to limited shearing from the conveying elements leaving rest of the powder mass poorly wetted or partially granulated.

2.2 EFFECT OF SCREW SPEED

Similar to powder feed rate, screw speed is also a surrogate to barrel fill level and can affect dependant variables such a residence time and torque and ultimately granule properties (Thompson and Sun 2010). Dhenge et al. (2010) studied the effect of varying screw speed on the mean residence time. The dye was injected in the powder inlet of the granulator and time at which first coloured granule appeared on the exit was called as residence time. It was observed that increasing screw speed decrease the residence time. Vercruysse et al. (2014) supported this observation in their study; however, they calculated the mean residence time by noting the total time for the tracer drug (theophylline) to come out of the granulator completely. In both studies, the shortening of the residence time was attributed to high conveying capacity of fast rotating screws at high screw speed. The torque also decreases as the conveying load on the screw decreases at higher screw speed (Dhenge et al. 2010).

The effect of screw speed on the granule properties has also been studied previously. Keleb et al. (2004) varied the screw speed during the granulation of lactose powder using two types of granulation liquids to understand the effect on the size of granules. In first granulation liquid polyvinylpyrolidone (PVP) was dissolved in water while the second

granulation liquid was pure water (no PVP). They found that granules size increase with increasing the screw speed only when PVP was dissolved in water. According to them, this effect was due to incomplete filling of the granulator barrel at higher screw speed which resulted in less friction and collision between the granules and thus allowing granules to grow. Djuric et al. (2009) and Dhenge et al. (2010) also studied the effect of varying screw speed on the granule size using water as granulation liquid. Both these studies found that granule size does not change significantly with screw speeds. Dhenge et al. (2010) argued that increasing screw speed limits the granule growth by breaking the bigger agglomerate at high shear forces and agglomerating granules after breakage due to availability of liquid, hence, change in granules was not noticeable. Vercruysse et al. (2013) also studied the influence of screw speed on the granule size in terms of amount of fines (<150 µm), yield (150 µm to 1400 µm) and agglomerates (1400 µm). They found that with increasing screw speed, the amount of fines, yield and agglomerates do not change significantly. Authors did not describe the reasons why such effect in size was observed.

According to Dhenge et al. (2010), with increasing screw speed, the fraction of elongated and irregular granules increased due to increase in shearing forces. Authors further describe that the screw speed also results in the low residence time at higher screw speed which prevents the powder to compact and interlock on the granule surface consequently making granules less spherical.

Keleb et al. (2004), Djuric et al. (2009) and Dhenge et al. (2010) studied the effect of varying screw speed on the strength of granules. They all did not notice any significant influence on the granule strength.

2.3 EFFECT OF SCREW CONFIGURATION

In twin screw wet granulation, the type of screw configuration is a key input variable since it directly impacts and determines the granule attributes. Twin screw granulator (TSG) provides a great flexibility in terms of different types of possible screw elements [conveying (forward/reverse), kneading (different angles, width), distributive feed (combing), distributive mixing etc.] that can give a number of possible configurations that

can be used during granule engineering or designing. Furthermore, these screw elements also directly influence granulation rate processes like nucleation, growth and breakage that occur in a regime separated manner along the length of the twin screw granulator (Dhenge et al. 2011, Dhenge et al. 2012a). Therefore, it is important to understand the role of various type and location of screw elements in the screw configuration. The pioneering study by Keleb et al. (2004) investigated the impact of modifying the screw configuration by replacing conveying elements at the barrel end with conveying elements on the granule yield. They observed that use of conveying screw element in place of discharge elements significantly reduce the built up of pressure at barrel end, hence reducing the lump formation by compaction of the wet granules. Djuric and Kleinebudde (2008) in their study used different types of screw elements (kneading, combing and conveying) to understand their effect on granule and tablet attributes. It was found kneading element produce larger, denser and stronger granules which resulted in weaker tablets. Conveying elements resulted in exactly opposite scenario compared to kneading elements. Combing or distributive feed screw elements produced granules and tablets with intermediate characteristics between the kneading and conveying elements. Thompson and Sun (2010) also carried out systematic evaluation of implications of using different screw elements in the screw configuration on granulation behaviour and the granule properties. Similar to the findings by Djuric and Kleinebudde (2008), use of kneading and combing elements produced coarser granules than that while using conveying elements. However, Thompson and Sun (2010) fed pre-wetted lactose powder into the TSG which is not a very common approach. So, the granulation mechanisms for pre-wetted powder in TSG are more likely to be different than the dry powder as a starting material. Researchers have also tested impact of distributive mixing elements (DMEs) on the residence time, liquid distribution and granule attributes, especially size (Sayin, El Hagrasy, et al. 2015, Pradhan et al. 2017). Pradhan et al. (2017), examined the impact of orientation (reverse vs. forward) and placement (adjacent vs. spaced) of the distributive mixing elements on the residence time, liquid distribution and granule size. It was found that DMEs placed in reverse orientation in both adjacent as well spaced placement or configurations resulted in granules with mono-modal size distribution and relatively better liquid distribution. However, no clear impact on granule shape and porosity and mean residence time was observed. Pradhan et al. (2017) noticed that distributive mixing

elements, when placed at the end section of TSG, exhibits granule breakage in the form of chipping and crushing mechanisms. Furthermore, space between teeth of the distributive mixing element and barrel determine the size of the resultant granule fragments.

Dhenge et al. (2010), Dhenge et al. (2011) and Dhenge et al. (2012a) showed that the location of kneading and conveying element blocks in the screw configuration dictates the granulation mechanisms, thus granule properties. As granules progress along the length of granulator, they become smaller, denser and stronger. The use of conveying elements at the end of granulator acts as a wet milling section which helps reducing oversized granules in the final product. Increasing number of kneading elements in the screw configuration also influence the residence time, torque, degree of mixing, barrel fill level and properties granules (yield and density) and thereby tablet properties (Vercruysse et al. 2012). The presence of more number of kneading elements increase the shear and compressive forces acting on the granules and improve the liquid distribution (owing to more distributive mixing) (Vercruysse et al. 2012, Kumar, Vercruysse, Toiviainen, et al. 2014). Thus, the granules become denser and consist less fines which upon compression into tablet reduce the disintegration time. The staggering angle of kneading element or disc (30°, 45°, 60° or 90° degrees) also has direct impact on the conveyance, residence time, torque, barrel fill level and overall granule properties in TSG (Lee et al. 2012). For instance, compared to 30° and 60°, kneading element with 90° staggering angle has poor conveyance, longer residence time, higher torque, high fill level and produce denser granules. Despite poor conveyance, long residence time and high barrel fill level, there is some degree of axial mixing that takes place when 90° kneading elements are used in the screw configuration. However, there is a critical limit for having such elements in the screw configuration since, excess barrel fill can result in poor dispersion and ultimately jamming the screws.

2.4 EFFECT OF LIQUID/SOLID RATIO (L/S)

The amount of liquid added to the granulator is a critical variable in wet granulation whether it be a batch or a continuous approach. In continuous twin screw wet granulation, the liquid is injected into the port just after the powder feeding port on the granulator. The

liquid to solid ratio (L/S) in twin screw wet granulation is actually the ratio of powder and liquid feed rates (kg/h). There are many studies in literature which focussed on effect of L/S on granulation dependant variables and granule properties. Dhenge et al. (2010) showed that the increasing L/S increase the residence time of the granules in the granulator. The increase in residence time was attributed to the increase in the consistency/viscosity of granulating mass. With higher L/S, powder become more wetted and behave like paste and take longer time to come out of barrel of granulator. Similar results were presented by Vercruysse et al. (2013) but they calculated the mean residence time from residence time distribution of the tracer drug, theophylline in twin screw granulator. Change in the granulating mass consistency (pasty and sticky) with increase in L/S also results in increase in the force required to rotate the screws meaning the resultant torque is higher (Dhenge et al. 2010, Vercruysse et al. 2013). Dhenge et al. (2010) found that the torque increases with L/S initially and then declines as the granulating mass becomes less sticky.

In general, the increasing liquid amounts (L/S) results in increase in the granule size (Keleb et al. 2004, Djuric and Kleinebudde 2008, Djuric et al. 2009, Dhenge et al. 2010, Dhenge et al. 2011). Tu et al. (2013) observed that higher L/S results in production of a number of bigger granules and reduction in the amount of fines. According to Dhenge et al. (2012b), when the L/S increases, the granules become more wetted and form inter-granular bridges leading to the increase in the strength of the granules. This in turn causes the granules to resist the shearing forces and friction in the barrel and thus increases the large granules fraction. At low L/S, the fraction of fines becomes higher and the mean granule size decreases. This is also confirmed by Dhenge et al. (2010), Lee et al. (2012) and El Hagrasy et al. (2013a). Furthermore, with increasing L/S, the granule size distribution shifts from bimodal to monomodal (Vercruysse et al. 2013).

Increasing L/S also changes shape and structure of the granules (Dhenge et al. 2010). At low liquid to solid ratio, the granules become more elongated and rough because of low pore space saturation (El Hagrasy et al. 2013a). With the increase in liquid levels the granules become more spherical and smoother because of the high pore space saturation. The granule sphericity also improves with increase in L/S. This is because the wet sticky

powder mass is easy to roll and spheronise on the rotating screw surface (Dhenge et al. 2010).

2.5 EFFECT OF GRANULATION LIQUID VISCOSITY

Similar to L/S, the granulation liquid viscosity is also an important variable in wet granulation. During wet granulation, liquid bridges formed between powder particles give the mechanical strength to the granules. During drying, these liquid bridges solidify to form final granules. The viscous granulation liquid (dry binder powder dissolved in liquid) results into stronger wet and dry granules compared to plain distilled water as granulation liquid. In twin screw granulation, very few studies have investigated the influence of granulation liquid viscosity on the torque, residence time, granule attributes and granulation behaviour. Dhenge et al. (2012b) granulated lactose based formulation using granulation liquid with varying viscosity. The granulation liquid viscosity was varied by dissolving different amounts of (hydroxypropyl cellulose) HPC in the water. It was observed that increasing granulation liquid viscosity torque, residence time, granule size increased (size distribution become mono-modal) and granule porosity decreased. It was concluded that the presence of HPC dissolved in the granulation liquid reduces the L/S required during granulation compared to that granulation liquid with no binder. These results were in agreement with findings by Dhenge et al. (2012b) who used polyvinylpyrrolidone (PVP) solutions (in water) as granulation liquids. Keleb et al. (2004) observed similar behavior for hydroxypropylmethyl cellulose (HPMC) solution as granulation liquid. Saleh et al. (2015) also investigated the effect of varying amount of HPMC powder in the granulation liquid on the granule size distribution while granulating lactose and MCC powders separately using two types of screw configurations i.e. with conveying elements only and with both conveying and kneading elements. They observed that while using screw configuration with conveying elements only, both lactose and MCC powders resulted in a broader granule size distribution when the HPMC amount was increased in the granulation liquid. Granulation of lactose and MCC powders at varying amounts of HPMC in the granulation liquid while using kneading elements in the screw configuration resulted in limited change in case of lactose while MCC produced

granules with narrow size distribution compared to that with screw configuration with conveying elements only.

2.6 EFFECT OF PRIMARY POWDER PARTICLE SIZE

The effect of particle size of primary powders is hence of high importance in the granulation. In twin screw wet granulation, the effect of primary powder particle size has received limited attention compared to the high shear wet granulation. El Hagrasy et al. (2013b) investigated the impact of using three different grades of lactose powder (with different particle size) as a major excipient in the formulation at different L/S on granule size and porosity. A limited impact on granule size and porosity was observed. Fonteyne et al. (2014) granulated different grades of anhydrous theophylline (with different particle size) in the formulation and studied the impact on granule attributes. It was observed that the granule size was directly proportional to the primary powder particle size.

A brief summary of previous works in twin screw wet granulation area is presented in Table 2-1.

Table 2-1 Summary of previous studies

Reference	TSG type and size & screw configurations used	Formulation	Parameter space covered	Key results
Keleb et al. (2004)	MP 19 TC 25 (APV Baker, Newcastle-under-Lyme, UK) (L/D: 25/1) Conveying element, Kneading element, discharge screw element	Powder: α-lactose monohydrate 200M, PVP Liquid: Water	Screw speed: 200–450 rpm Powder feed rate: (5.5–9.5 kg/h) L/S :8.5 and 7.5% (w/w) for formulations without and with 2.5% (w/w) PVP	Increasing the total input rate had no influence on the granule properties except on the granulation yield (granule fraction between 250-1000μm), which increased as the total input rate increased. In general the increasing liquid amounts (L/S) resulted in increase in the granule size.
Djuric et al. (2009)	Leistritz Micro 27GL/28D co-rotating twin-screw extruder (Leistritz Extrusionstechnik GmbH, Nuremberg, Germany) with screw diameter 27mm and MP19 TC25, APV Baker, Newcastle-under-Lyme, United	Powder : Dicalcium phosphate, Povidone Granulation Liquid: Water	Screw speed: 150, 225 and 300 rpm Powder feed rate: 2, 4 and 6 kg/h L/S: 11% and 7.5% (w/w)	The interaction between the total input rate and the extruder type [Leistritz and APV]. They found that the Leistritz extruder produced much larger granules, but a limited effect was observed in the case of the APV extruder when increasing the total input rate.

	Kingdom) with screw diameter 19mm. Conveying element, Kneading elements (30°, 60° and 90° advance angles)			Also observed that increasing the total input rate would decrease the friability of the granules which in reverse means more granule hardness and strength
Dhenge et al. (2011)	Euro lab 16 TSG, Thermo Fisher Scientific, UK (L/D : 25/1) Conveying elements, Kneading elements (60°)	Powders: MCC, Lactose, Cross carmellose cellulose, HPC, Sodium Chloride Granulation Liquid: Water	Screw speed: 400 rpm Powder feed rate: 2, 3.5, 5 and 6.5 kg/h L/S: 0.3	Increasing the powder feed rate would increase the barrel fill level and inter-particle bonds. The higher barrel fill would increase the compaction forces on the powder mass resulting in decrease in the granule porosity, hence, increase in the strength.
Vercruysse et al. (2012)	Granulation unit of ConsiGmaTM-25 system (L/D: 25/1) Conveying Kneading: (2, 4, 6, and 12 discs; advance angles of 30°, 60°, 90°)	Powder: α-lactose monohydrate (filler) Theophylline anhydrate (model drug, 30%)	Screw speed: 600 rpm – 950 rpm Powder feed rate: 10 – 25 kg/h Liquid feed rate: adjusted to achieve 9%	Increasing powder feed rate and screw speed resulted in increase in higher torque value and increase in barrel temperature due to increased friction with barrel wall of elements. Higher number of kneading elements resulted in reduced amount of fines

		PVP (binder, 2.5 wt%) Liquid: Distilled water (when PVP was added to dry powder)	wt concentration on wet mass	and increase in oversized and less friable granules. The number of KEs also affects tensile strength, disintegration time and dissolution profile. More number of KEs produces denser granules with less deformability during compression. Desired granules can be obtained by adjusting process variables such as number of kneading elements, barrel temperature and binder addition method helps to get granules and tablet of desired attributes.
Lee et al. (2012)	GEA Pharma Systems, UK (Screw diameter: 19 mm) Conveying elements, Kneading elements (30°, 60°,90°)	Powders used: MCC Granulation Liquid: Water	Screw speed: 150, 300 rpm Powder feed rate: 10 g/min, 20 g/min	The mean residence time is inversely proportional to screw screw speed and material throughput. However, the shape of the distribution curve remains similar for various screw geometry and process conditions because the axial mixing is similar for different screw configurations.

				Moreover, the fill level in the granulator is increases with increase in powder feedrate and decreases with increasing screw speed.
Dhenge et al. (2013)	Euro lab 16 TSG, Thermo Fisher Scientific, UK (L/D : 25/1) Conveying elements	Powders: MCC, Lactose, Cross carmellose cellulose, HPC, Sodium Chloride Granulation Liquid: Water	Screw speed: 400 rpm Powder feed rate: 2, 3.5 and 5 kg/h L/S : 0.3	Median granule size decreased with increase in the powder feed rate. The powder at higher feed rate is conveyed in plugs with poor mixing and granulation inside the granulator. This results in generating high fraction of fines and few very large agglomerates. It was also found that the strength of the fines decrease while that of bigger granules increase with increasing powder feed rate.
Vercruysse et al. (2014)	Granulation unit of ConsiGma^{TM}-25 system (L/D: 20/1) Conveying	Powder: α-lactose monohydrate (model excipient) theophylline anhydrate (tracer)	Screw speed: 600 - 950 rpm Powder feed rate: 15-25 kg/h	Increased screw speed and lower moisture content resulted in lower mean residence time with narrower distributions. More number of KEs and increasing moisture

	Kneading (one or two kneading blocks; 6 discs in each block; advance angle of 60°)	Liquid: Distilled water	Liquid feed rate: 2.3–6.7% (wt/wt, based on wet mass)	content resulted in lower mean residence time narrower residence time distribution. Different experiments were performed to understand the effect of moisture content, screw speed and powder feed rate on the mixing efficiency of the powder and liquid phase. It was found that only increasing the moisture content can improved the granule liquid distribution significantly.
Kumar, Vercruysse, Toiviainen, et al. (2014)	25 mm granulator in the ConsiGma-25 unit (L/D: 20/1) Conveying Kneading (2-12 discs; each disc is of thickness ¼ D; advance angle of 30°, 60°, 90°)	Powder: α-lactose monohydrate (model excipient) theophylline anhydrate (tracer) Liquid: Distilled water	Screw speed: 500, 700, 900 rpm Powder feed rate: 10, 17.5, 25 kg/h Liquid feed rate: to achieve liquid content of 11.5% (wt/wt)	The results showed that screw speed is one of the most important parameter to understand residence time distribution. Increasing screw speed lower mean residence time with narrower distributions. Increasing the number of kneading discs resulted in an increase in the TSG driving torque. When 6 and 12 KEs with staggering angle 90° were used , jamming of the barrel

				was observed at all screw speeds. When the number and staggering angle of KEs were increased simultaneously, the driving torque of the TSG increased. It was also found that Increase in advance angle of the KEs increased mean residence time and also reduced the normalized variance of residence time.
Djuric and Kleinebudde (2008)	Leistritz Micro 27GL/28D Granulator Conveying (CE; pitches of 15, 20, 30, and 40 mm) Combing mixer (CME; pitches of 15 and 20 mm) Kneading (KE; advance angles of 30°, 60°, 90°, and 30°R)	Powder: α-lactose monohydrate Liquid: demineralized water	Screw speed: 100 rpm Powder feed rate: 2,4 and 6 kg/h Liquid feed rate: 3 g/min	Conveying elements produces more porous and friable granules compared to KE where agglomeration of lactose produces high density and, least friable granules (density increases with increasing staggering angle). Combing mixer elements (CME) produces granules somewhere between CE and KE. Combining KE and CME resulted in smaller size granules.

Van Melkebeke et al. (2008)	MP 19 TC 25, AVP Baker Granulator (L/D: 25/1) Conveying elements, Kneading elements (8 discs (2.4 mm thickness) with advance angle of 60^0 and 10 discs (4.7 mm thickness) advance angles of 30°, 60°, 90°.	Powder: α-lactose monohydrate (filler), polyvinylpyrrolidone (PVP) (binder) Liquid: Distilled water with PVP, 7.5% (w/w) and 8.5% (w/w)	Total feed rate: 5.6 kg/h Screw speed: 250 rpm	The screw configuration with staggering angle 90° produced lower yield and less friable granules. The conveying element placed at the screw end significantly influence tablet disintegration. Twin screw wet granulation was identified as a robust process.
Thompson and Sun (2010)	27 mm Leistritz Model ZSE-27 HP Granulator (L/D: 24/1) Conveying (30 mm pitch) Kneading (5 discs; advance angles of 30°, 60°, 90°, medium disc thickness), Comb mixing (forwarding, reversing)	Powder: α-lactose monohydrate Liquid: 33% (w/w) PVP in distilled water	Screw speed: 30 and 80 rpm Total feed rate: 2 kg/h Liquid content: 5% - 12% (wt/wt)	Granule size and shape can be tailored successfully using the currently available screw designs in twin screw wet granulation. CEs didn't have a very significant effect on particle size or shape. However, their fill level affected the operation of kneading blocks and comb mixers. Kneading blocks and comb mixers were effective in

				producing coarser particles through different mechanisms.
Lee et al. (2012)	19mm GEA Granulator (L/D: 10/1) Conveying Kneading: (6 or 7 discs; advance angle of 30°, 60°, 90°)	Powder: α-lactose monohydrate (73.5%), MCC (20%), HPMC (5%), croscarmellose sodium (1.5%), all percentages are by weight Liquid: Distilled water	Screw speed:150 rpm and 300 rpm Powder feed rate: 10 g/min and 20 g/min Liquid feed rate: Adjusted to achieve a L/S of 0.35	The 90° kneading block was found to convey the material by a dispersion mechanism which was driven by the fill gradient in the granulator. 30° and 60°kneading blocks were found to have conveying capacity and transported the material even with no fill gradients. The extent of axial mixing was found to be similar for different screw configurations. The granulator fill level was directly proportional to powder feed rate and inversely to screw speed. The mean residence time in the granulator was found to decrease with increasing screw speed and material throughput.

Mu and Thompson (2012)	27 mm Leistritz ZSE-27 HP Granulator (barrel length used: 40L/D) Conveying (pitches of 30 mm and 40 mm) Kneading (5 discs; advance angle of 60°)	Powder: α-lactose monohydrate (filler) Binders: PEG 3350 PEG 8000	Screw speed: 220 rpm Powder feed rate: 5 kg/h Binder concentration: 10% - 20% (wt)	As the number of kneading blocks used in the granulator increases material residence time and axial dispersion in the granulator increases. Three kneading blocks was determined to be the upper useful limit, where further densification took place with little change in granule growth. Viscosity of binder and particle size of binder in powder form were found to be equally influential process variables in granule growth. Immersion mechanism as described by Schæfer and Mathiesen (1996) was concluded to be the nucleation mechanism taking place.
El Hagrasy et al. (2013b)	16mm Thermo Fisher EuroLab Granulator (L/D: 25/1) Conveying (L/D helix; L/D length)	Powder: α-lactose monohydrate (73.5%), MCC (20%),	Screw speed: 400 rpm Powder feed rate: 4 kg/h	The following mechanisms were identified: 1. Breakage followed by layering 2. Shear elongation and breakage, followed by layering

	Kneading (3, 5, and 7 discs; each disc is of ¼ L/D length; advance angles of 30°, 60°, 30°R, 60°R, 90°)	hydroxypropylmethyl-cellulose (HPMC, 5%), croscarmellose sodium (1.5%), all percentages are by weight Liquid: Nigrosin black dye (0.1%, wt/wt) in distilled water	Liquid feed rate: Adjusted to achieve the following L/S (wt/wt): 0.15, 0.20, 0.25, 0.30, 0.35	On one extreme was the 90° configuration with breakage being the dominant mechanism; on the other end was 30°R with shear elongation being dominant; other configurations were in between.
Sayin, Martinez-Marcos, et al. (2015)	Thermo Fisher Process 11 Granulator (11mm) (L/D: 40/1) Distributive feed screw (1 unit) Kneading (7 discs with advance angle of 90°)	Powder: α-lactose monohydrate (73.5%), MCC (20%), HPMC (5%), croscarmellose sodium (1.5%), all	Screw speed: 482 rpm and 724 rpm Powder feed rate: 0.66 kg/h, 1.11 kg/h, and 3.9 kg/h	Distributive feed screw (DFS) improve the size distribution compared to feed screw but kneading elements are more aggressive in terms of liquid distribution compared to DFS.

		percentages are by weight Liquid: Nigrosin black dye (0.1%, wt/wt) in distilled water	L/S ratios (wt/wt): 0.15, 0.20, 0.25, 0.30	DFS provides broader size distribution compared to Kneading element configuration used because it is not as efficient as breaking in bigger granules. However, at high powder feed rate, KEs caused increase in torque and barrel temperature.
Sayin, El Hagrasy, et al. (2015)	Thermo Fisher EuroLab Granulator (16mm) (L/D: 25/1) Conveying element helix, Distributive mixing element (forward and reverse orientations; adjacent and spaced placements)	Powder: α-lactose monohydrate (73.5%), MCC (20%), HPMC (5%), croscarmellose sodium (1.5%) Liquid: Nigrosin black dye (0.1%, wt/wt) in distilled water	Screw speed: 400 rpm Powder feed rate: 4 kg/h L/S ratios used: 0.15, 0.20, 0.25, 0.30, 0.35	Breakage and layering is found to be dominant rate processes taking place in DME section of the granulator. Reverse configuration of DME produces monomodal size distributions due proper redistribution of liquid compared to forward configuration of DME. The granule attributes formed due to DME is helpful to use granules directly in downstream processing.

Vercruysse et al. (2015)	Granulation unit of ConsiGma^{TM} -25 system (L/D: 20/1) Conveying element (0.5D pitch) Kneading element (2, 4, 6 discs; narrow and wide; advance angle of 30°, 60°, 90°) Narrow tooth-mixing (1-3 elements) Wide tooth-mixing (1 element) Screw mixing (2 and 4 units) Cutters (19 screw configurations in total)	Powder: α-lactose monohydrate Liquid: Distilled water	Screw speed: 800 rpm Powder feed rate: 20 kg/h L/S ratio: For CE only configuration: 0.035, 0.040, 0.045, 0.055, 0.070, 0.090 For KE configuration: all the CE only L/S values and 0.095 additionally For screw mixing: 0.070 For tooth mixing: 0.045	Use of only conveying elements in screw configuration results in wide and multimodal distribution. Using KEs narrowed the width of Particle size distribution and homogeneous liquid distribution. Promising results were obtained By combining KEs with screw mixing elements produces size fraction more suitable for tableting.
Lute et al. (2016)	16mm Thermo Fisher Euro lab Granulator (L/D: 25/1)	Powder: α-lactose monohydrate Liquid: Distilled water with 1g of red	Screw speed: 150, 250 and 500 rpm Powder feed rate: 2 kg/h	As the number of KEs increases granule size also increases with more elongated and denser granules due to increase in shear and compaction. Placing conveying element after

	Short pitch Conveying element, Long pitch conveying element, Kneading elements (2, 4, 6, 8, 10, and 12 discs; each disc of thickness L/D: ¼; advance angle of 60°)	dye added in 1 liter of water	Liquid feed rate: L/S ratios: 0.048, 0.07, 0.1, and 0.113	KEs resulted in cutting and chopping of bigger granules. Granule size produced at smaller pitch is smaller compared to larger pitch conveying element. Different granule size and distribution can be obtained with the same powder by understanding the effect of kneading and conveying elements.
Pradhan et al. (2017)	Conveying elements, Distributive mixing elements			The effect of conveying element and distributive mixing elements were studied on granule size in order to understand their geometry. The maximum granule size in conveying element is closely equal to the space available between two flights of conveying element and barrel. The maximum size of granules in DME depends on space available between teeth of the elements and the barrel.

2.7 SCOPE FOR FURTHER RESEARCH & OBJECTIVE

The studies done so far demonstrated the application of the twin screw granulator as a continuous wet granulation equipment. These parametric attempts mostly dealt with a generalised understanding of the effects of process (powder feed rate, screw configuration, barrel temperature and screw speed) and formulation variables (L/S, viscosity of the liquid binder, primary particle size of powder) on the dependant variables (torque and residence time) and granule properties (median size, size distribution, shape and strength). Although, these studies pioneered the twin screw granulation process, there was limited attention on controlling the granule properties especially, median size, size distribution, shape, strength and structure (porosity). These granule properties are very important to pharmaceutical industry as they directly influence the tablet production. Pharmaceutical industry generally prefers smaller granules with narrow and monomodal size distribution, better flowability (regular shape) and porous structure for tableting purpose. Production of desired granules requires thorough understanding of the process.

The main objective of this research is the development of the mechanistic understanding of the twin screw wet granulation process using experimental as well as modelling approaches. In an experimental approach, the objective is to develop an understanding of the roles of the screw elements (kneading and conveying) in the screw configuration, effects of fill level (powder feed rate/screw speed), processing temperatures (barrel temperature) and different types of powders on granulation behaviours and granules properties. In the modelling approach, the objective is to develop the mechanistic understanding of twin screw granulation process by using population balance method (PBM) based models incorporated in an advanced process modelling platform i.e. gSolids followed by the experimental validation of the models. Finally, the ultimate objective to develop a systematic approach to control granule properties (and thereby tablet properties).

3 MATERIALS AND METHODS

The following section describes the materials, experimental methods and conditions used in this study.

3.1 MATERIALS

3.1.1 Powder and granulation liquid

The different grades of lactose and mannitol were used in the present study. Different grades of lactose used are Pharmatose 200M, Spray dried lactose SuperTab11SD, Anhydrous lactose SuperTab21AN, Pharmatose 350M, Pharmatose 450M (supplied by DMV-Fonterra Excipient GmbH and co., Goch, Germany). Different grades of mannitol used are Pearlitol 50C, Pearlitol 200SD and Pearlitol 300DC (supplied by Roquette, France). Microcrystalline cellulose (MCC) (Avicel PH 101, FMC Biopolymer, Cork, Ireland) was also used as a primary powder while investigating the effects of fill level on the granule and tablet properties (results are presented in Appendix 12.3.2). Distilled water was used as a granulating liquid and 1g of red dye (Erythrosine B; Acid red 51, Sigma Aldrich) was added to it in some cases. The different powders with their brand name, particle size and mean sphericity are shown in Table 3-1. The median particle size of the powders was measured using a Camsizer XT (Retsch Technology, Germany).

Table 3-1 Powders used in the study

Powders	Brand name	Particle size (µm)			Mean Sphericity
		d_{10}	d_{50}	d_{90}	
Lactose	Pharmatose 200M	9.3	42.1	110.0	0.78
	SuperTab11SD	45.0	113.4	191.3	0.86
	SuperTab21AN	27.5	172.3	330.0	0.85
	Pharmatose 350M	9.8	35.2	74.2	0.79
	Pharmatose 450M	7.0	22.5	43.8	0.79
Mannitol	Pearlitol 50C	10.1	33.9	114.9	0.76
	Pearlitol 200SD	26.0	145.3	200.9	0.85
	Pearlitol 300DC	58.3	249.9	385.9	0.83
MCC	Avicel PH 101	19.0	57.0	135.0	0.74

Different powders were used in various experiments. The respective experiments are covered as chapters in this thesis. A general information about various powders is provided as follows.

Lactose is one of the most commonly used powders in food and pharmaceutical industry and is available in different grades (sieved, milled, spray dried etc.). There are several studies in literature which used lactose powder as one of the major ingredient in the formulation (Djuric and Kleinebudde 2008, Kumar, Vercruysse, Bellandi, et al. 2014, Yu et al. 2014, Saleh et al. 2015b, Saleh et al. 2015a, Sayin, Martinez-Marcos, et al. 2015, Chan Seem et al. 2016, Gorringe et al. 2017, Verstraeten et al. 2017). It is soluble in cold and hot water. It is white, crystalline, brittle powder which is used as filler in tablet production. It has low compressibility and poor flow ability.

Similar to lactose mannitol is also one of the most commonly used fillers/diluents in tablet making via both wet/dry granulation and direct compaction methods in the pharmaceutical industry (Hansuld et al. 2012, Meier et al. 2016, Vanhoorne, Bekaert, et al. 2016, Gorringe et al. 2017, Morkhade 2017, Pradhan et al. 2017, Willecke et al. 2017). Mannitol, due to its non-hygroscopic nature, sweet taste and negative heat of solution giving cooling sensation, is a preferred excipient for formulating the moisture-sensitive drugs (Westermarck et al. 1998, Kibbe 2000) and producing chewable tablets or lozenges (Wade and Weller 1994, Westermarck et al. 1998). Mannitol is known to exist in different polymorphic forms including α, β, and γ having different compressibility (Debord et al. 1987, Wade and Weller 1994). This is however, not in the scope of this research.

Microcrystalline cellulose (MCC) is also used as a filler in pharmaceutical industry. Strong binding capacity makes it one of the most popular fillers in drug formulations. MCC is widely used in pharmaceutical processes like wet granulation, dry granulation or direct compression. MCC is plastically deforming, crystalline free flowing powder with excellent water absorptive property. It is insoluble in water and organic solvents. Due to capillary effect MCC absorbs water very quickly. This property of MCC makes it requiring 1:1 or more proportion of water for the effective granulation.

3.1.2 Granulation equipment

Co–rotating twin screw granulator (TSG) (Euro lab 16 TSG, Prism, Thermo Fisher Scientific, Karlsruhe, Germany) was used for the granulation trials (Figure 3-1). The TSG has 400 mm long barrel (L) and 16 mm bore diameter (D) (so, L/D- 25/1), screw diameter of 15.6 mm, gap between screw tip and inner barrel wall is about 0.2 mm. Maximum screw speed is 1000 rpm and torque per shaft is 12 Nm while the barrel temperature can be varied between 5°C to 300°C. The TSG consists of a gravimetric, loss in weight twin screw powder feeder (K-PH-CL-24-KT20, K-Tron Soder, Niederlenz, Switzerland) with maximum feeding capacity of 25 kg/h, a pair of co-rotating screws enclosed in metallic barrel to convey, wet and mix the powder and a peristaltic pump (101U, Watson Marlow, Cornwall, UK) to pump the granulation liquid into the granulator.

The TSG also consists of following parts:

- A motor
- Temperature control unit
- Control panel

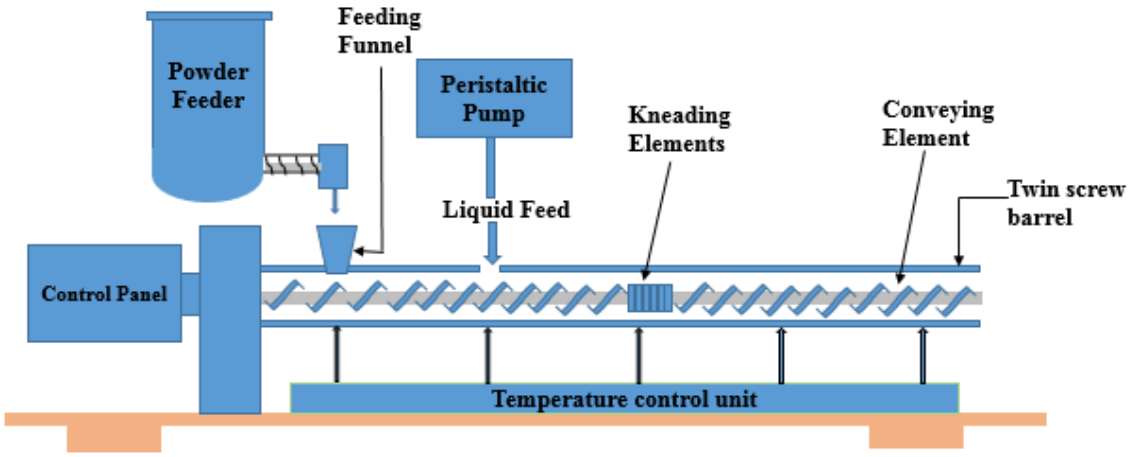

Figure 3-1 Schematic of twin screw granulator used in this study

Various screw configurations were used in this research work. An example screw configuration is shown in Figure 3-2. The screw configuration generally composed of blocks of conveying and kneading elements for transport and mixing purpose respectively. More details about these elements could be found in Section 1.1.1. The screw configuration starts with SPCE, followed by LPCE (channel width- 12 mm) to

rapidly convey powder to SPCE (channel width- 8 mm) and KE for wetting and mixing-kneading respectively. The kneaded powder material is further granulated and transported by SPCE. The flow of material is from left to right in Figure 3-2.

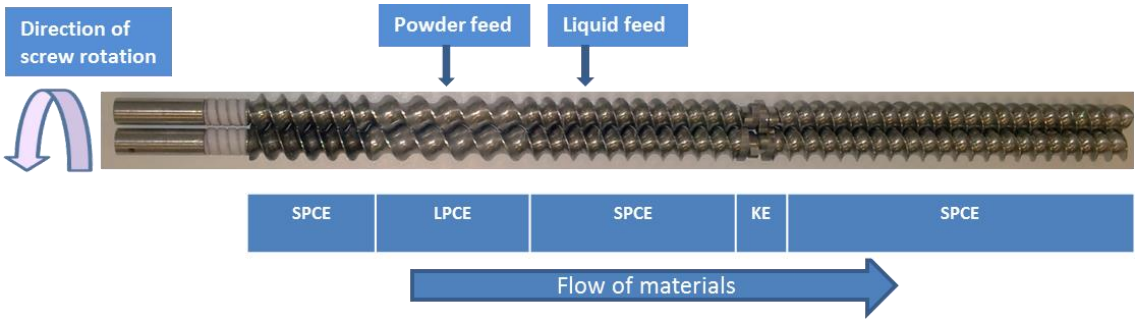

Figure 3-2 Example of screw configuration

3.2 METHODS

3.2.1 Granulation and analysis of granule properties

Powders were fed to the TSG using twin screw feeder and granulated using distilled water, which was pumped into the granulator using a peristaltic pump. The pump was calibrated to obtain desired flow rate at its specific settings (see Appendix 12.1).

3.2.2 Size and shape analysis of powders

Powder particle size and mean sphericity were measured using Camsizer-XT (X-jet module) (Retsch Technology, Germany). The powder shape and surface was studied using scanning electron microscopy (SEM) (Jeol, USA). The lactose and mannitol particles were nonconductive, hence, coated (for 40 s) with thin layer (~25 nm) of gold using coating machine (Leica EM ACE200, Leica Microsystems, UK).

3.2.3 Flowability and compressibility factor of powders

In some cases, the flowability of the powders was measured in terms of effective angle of internal friction and flow factor coefficient (*ffc*) using a ring-shear cell tester RST-XS (Dr. Dietmar Schulze, Germany). The internal angle of friction is an indication of inter-

particle friction while the *ffc* of the powder which is a ratio of the consolidation stress of the corresponding yield locus and the unconfined yield strength, is used as an index to rate the flowability of powders. The internal angle of friction and *ffc*, were measured using a pre-shear load of 5000 Pa and normal load at shear of 1500, 2750, and 4000 Pa. It known that extremely poorly flowing (~non-flowing) powders have *ffc* ⩽ 1, very poorly flowing (very cohesive) have 1–2, poor (cohesive) between 2 and 4, easy or fair between 4 and 10 while the powders with good flowability (free flowing) have *ffc* > 10 (Jenike 1964). Also expectedly, higher the effective angle of internal friction, more difficult it is for the powder to flow.

In addition to the flowability measurement, the compressibility factor (K) for powders was determined from the relationship between the uniaxial stress σ and the resulting powder bed density ρ as shown in Eq. 2. It is known that, the lower the compressibility factor, more compressible is the powder (Johanson 1965). This was measured by compressing about 405 mg of powders in a die (diameter-12 mm) using Instron testing machine (Instron 3367 – USA) under a range of compression forces (1000 to 5000 N) at test speed of 1 mm/min and determining the density of the tablet (from mass and volume). The compressibility factor K was determined from the slope of a logarithmic plot of the density as a function of stress (see linearity plots in Figure 12-28-Figure 12-29).

$$\frac{\sigma_1}{\sigma_2} = \left(\frac{\rho_1}{\rho_2}\right)^K \qquad \text{Eq. 2}$$

where,

σ_1 - major principal stress
σ_2 - minor principal stress
ρ_1 - powder bulk density at σ_1
ρ_2 - powder bulk density at σ_2

3.2.4 Size analysis of granules

After Granulation, the granules were air dried at room temperature for 48 h. The median size (d_{50}) of the granules was measured using the particle size analyser; Camsizer (free-fall module) (Retsch Technology, Germany). Three repetitions were performed for

sieving and therefore for the size analysis. The granules were further sieved into different size classes (212 µm-1400 µm, 212 µm-600 µm, 600 µm-1000 µm and 1000 µm-1400 µm) for tableting.

3.2.5 Shape and morphology of granules

In some cases, the shape characteristic of granules was measured using Camsizer and the morphology was studied using Keyence and Zeiss stereo microscope. The surface characteristics of granule was studied using SEM. The granules were nonconductive, hence, coated with thin layer (25 nm) of gold using coating machine.

3.2.6 Structural analysis of granules

The X-ray tomography (XRT) (µCT 35, SCANCO Medical AG, Switzerland) of granules was carried out to provide information on the change in the internal structure of the granules. Images from the X-ray machine were analysed using ImageJ software to determine the inter-particle porosity within the granules. The black colour in image represents air or void and the grey represents granulated powder mass

3.2.7 Tableting

The granules produced were sieved into different size classes (212 µm-1400 µm, 212 µm-600 µm, 600 µm-1000 µm and 1000 µm-1400 µm) and compressed in a 12 mm die at 10 kN compression force (test speed-1 mm/min) to produce tablets of about 405 mg using Instron testing machine. This was done to study the impact of granule size range on the tabletting (Dhenge et al. 2011). The granules were not pre-lubricated internally or externally, however, punch and die of the compression machine were coated with thin layer of magnesium stearate to minimise sticking and picking.

3.2.7.1 Analysis of tablets

The tablets so produced were analysed for their dimensions (thickness, diameter, structure) and mechanical strength (tensile strength). The thickness and diameter were measured using digital calliper. The tensile strength of tablet was measured by diametric compression method using Zwick/Roell Z 0.5 (Zwick/Roell, Germany) test machine. The

tablets were compressed diametrically (test speed-1 mm/min) until they fracture. The force-displacement data was recorded. 10 tablets were used for each experimental condition to produce reproducible data. The strength of tablets (σ) was determined by inputting maximum force (F_{max}), tablet diameter (D) and thickness (T) in Eq. 2 (Fell and Newton 1970).

$$\sigma = 2\frac{F_{max}}{\pi TD} \quad \text{Eq. 3}$$

4 UNDERSTANDING GRANULATION MECHANISM FOR LACTOSE POWDER ALONG THE BARREL LENGTH

4.1 ABSTRACT

The objective of this chapter was to develop a detailed understanding of the roles and effects of the screw elements in the granule formation along the length of barrel in the TSG by incremental addition of the elements in the screw configuration. The number of kneading and conveying elements in the screw configuration, liquid to solid ratios (L/S) and screw speeds were varied while studying their effects on the mechanism of granule formation and the granule attributes (size, shape and structure). In order to study the granule formation mechanism, the length of TSG barrel was classified into 10 Parts. This was done to mimic and understand the actual granulation process that occurs in the individual Parts (sections) when total barrel length (cumulative length of all 10 Parts) comprising both conveying and kneading zones in the screw configuration is used (for reference see Figure 4-1-Figure 4-10 and Table 4-1). Part-1 consisted of two LPCE followed by 4 SPCE named as nucleation. Part-2 consisted of two KE placed at the end of the granulator after Part-1. Similarly, Part-3 to Part-7 subsequently consisted 4, 6, 8, 10 and 12KE after Part-2. In Part-8, 2SPCE were placed next to 12KE (Part-7) which is named as 12KE + 2SPCE. Same thing was repeated for Part-9 with 4SPCE and Part-10 with 6SPCE after Part-7. In a separate experiment, last 4SPCE in Part-10 were replaced by 2LPCE to study the effect of increase in the screw channel width on the granule size and structure.

It was found that the granules became bigger in size, elongated and denser with increasing number of KE (Part-2 to Part-7) due to increase in shear and compaction forces acting on them. The influence is more evident at higher L/S. However, the presence of SPCE in addition to the KE (Part-8 to Part-10) reduced the size and elongation of granules due to the shearing and cutting action of SPCE. The granule formation and growth in the TSG was found to be the function of the type and number of elements in the screw configuration and the L/S. Presence of 2LPCE at the end of the screw configuration resulted in an increase in the granule size and structural voids due to the coalescence or re-agglomeration of granules.

4.2 INTRODUCTION

Granulation involves different dominant rate processes or mechanisms such as nucleation, coalescence, consolidation (growth) and breakage. Twin screw granulation (TSG) is a continuous and die less process where several mechanisms exist at each regions or compartments along the length of the screw or barrel (Dhenge et al. 2012a).

Dhenge et al. (2012a) studied the granule progression along the barrel length of twin screw granulator, however, their study was more focused on studying the effect of entire blocks of kneading (8 kneading elements) and conveying elements in the screw configuration on the granule size, shape and strength. Although, their study provided pioneering understanding of the granule growth along the barrel length, more specific and detailed effects of kneading and conveying elements on the granule properties need to be studied further.

In this study, an attempt was made to understand the specific roles of kneading and conveying elements in determining the granulation behaviour, granule growth and progression along the length of the screw or barrel. The roles of kneading and conveying elements have also been studied with a unique objective of preferential granulation of powders to produce and control the granule properties (size, shape, surface and structure).

4.3 MATERIAL AND METHODS

4.3.1 Materials

4.3.1.1 Powder, granulating liquid

Lactose powder was granulated using red dyed distilled water (as a granulation liquid) in TSG.

4.3.2 Methods

4.3.2.1 Preparation of granules

The granules (60 g in each experiment) produced using TSG were collected after 1 min when the system reached the equilibrium. The granulation was carried out towards the end section of the granulator using different screw configurations. The different screw elements used to obtain the various screw configurations for the experiments are mentioned with their respective abbreviations in Figure 4-1 to Figure 4-10 and Table 4-1. The length of LPCE (32 mm) is twice that of the SPCE (16 mm). LPCE has a larger channel width (12 mm), larger pitch (25 mm), volume and conveying capacity as compared to SPCE (channel width-8 mm and pitch-16 mm) to avoid over-feeding of powder in feeding zone. Hence, it carries small volume of material. Conveying elements rotate and apply shear and compression forces inside the barrel. Kneading elements (KE) are used along with conveying elements in the screw configuration during the twin screw granulation process.

Ten different screw configurations (each screw configuration is termed as 'Part' henceforth) were used to study the mechanism of granule formation along the barrel length of the TSG more discretely. Table 4-1 shows the various rearrangements of the screw elements, positions of the powder (green coloured boxes) and the liquid binder feeding ports (blue coloured boxes) used to obtain required Parts. The objective was to mimic and understand the actual granulation process that occurs in the individual Parts (sections) when total barrel length (cumulative length of all 10 Parts) comprising both conveying and kneading zones in the screw configuration would be used. Granulation using each Part was carried out separately under the same processing conditions. For each granulation run, elements were rearranged to obtain the desired Part for the granulation. Some configurations required placing the kneading elements at the start of the screw. The powder was fed onto the LPCE which conveyed it to the SPCE where the liquid binder was injected. As in the Part 1, the granulation was supposed to be in its early stage, it was termed as nucleation section where the liquid binder wets powder forming loose, wet, large agglomerates or lumps.

As shown in Table 4-1, Part-2 consisted of two kneading elements placed at the end of the granulator after four short pitch conveying elements (SPCE). Part-3 had four kneading element after 4SPCE. The 2KE were increased subsequently to get Part-4 with 6KE, Part-5 with 8KE, Part-6 with 10KE, and Part-7 with 12KE. In Part-8, 2SPCE are placed next to 12 kneading elements which is named as 12KE + 2SPCE. Same thing was repeated for Part-9 with 4SPCE and Part-10 with 6SPCE. The positions of the powder and liquid binder feeding ports were also changed as per the requirement.

In addition to this, the effect of increase in channel length and volume of screw elements (i.e. increase in the pitch of the screw element) towards the end of screw configuration on the size and structure of the granules was studied. To study this, two screw configurations were used. In one case, screw configuration had 6SPCE at the end (Part-10), whilst in the other case, last 4SPCE at the end of configuration in Part-10 were replaced by 2LPCE keeping the remaining screw configuration same. The experiments were carried out at L/S of 0.1 and at the screw speed of 150, 250 and 500 rpm. The various experimental conditions are shown in Table 4-2. In total, 120 experiments (3 repetitions of each experiment from the same run) were carried out (for Part-1 to Part-10) and cleaning was done in between every condition. The gantt type chart of collection of 3 samples and cleaning is shown in Table 4-3. Each condition was done at four different L/S and three different screw speeds in order to map out the effects of varying process variables on the granule properties (size, shape and structure). The effect of varying screw speed was studied at 150, 250 and 500 rpm with a constant powder feed rate of 2 kg/h and a varying L/S (0.048, 0.07, 0.1 and 0.113).

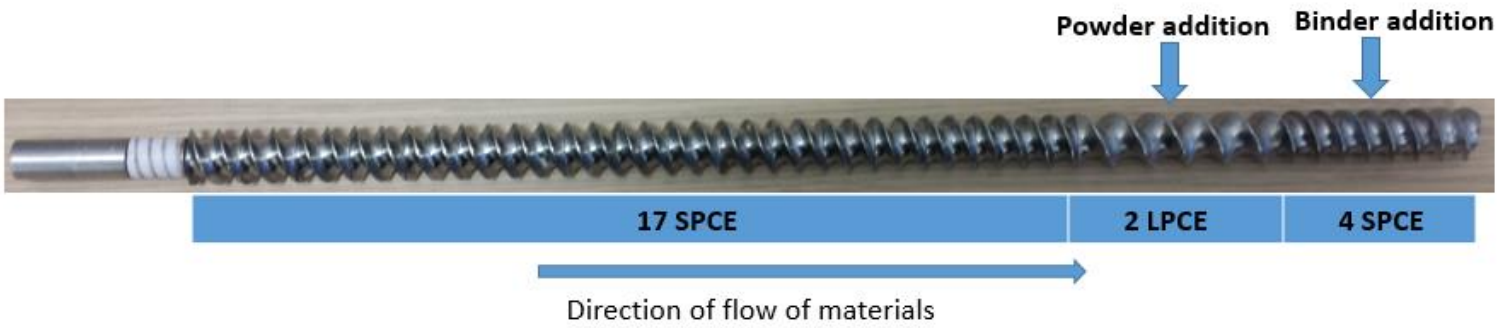

Figure 4-1 Screw configuration for Nucleation (4SPCE) (Part-1)

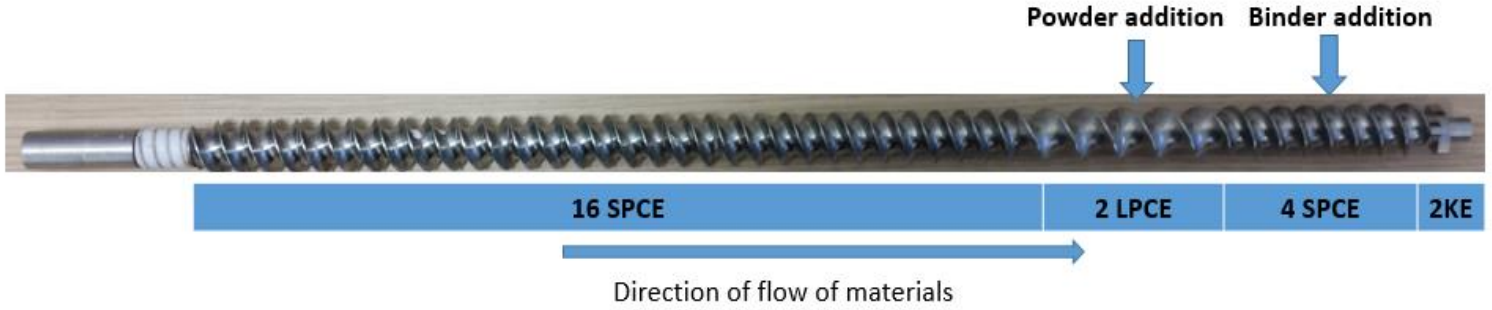

Figure 4-2 Screw configuration for 2 Kneading Elements (2KE) (Part-2)

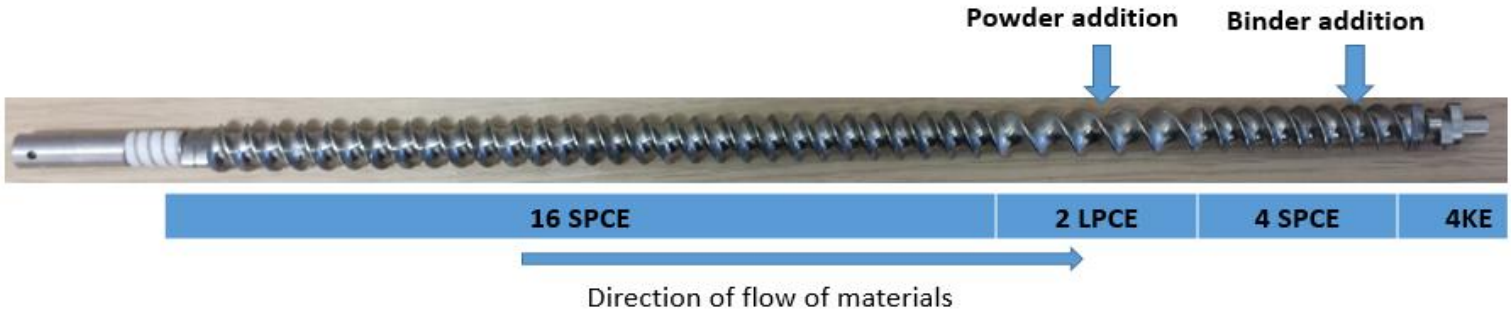

Figure 4-3 Screw configuration for 4 Kneading Elements (4KE) (Part-3)

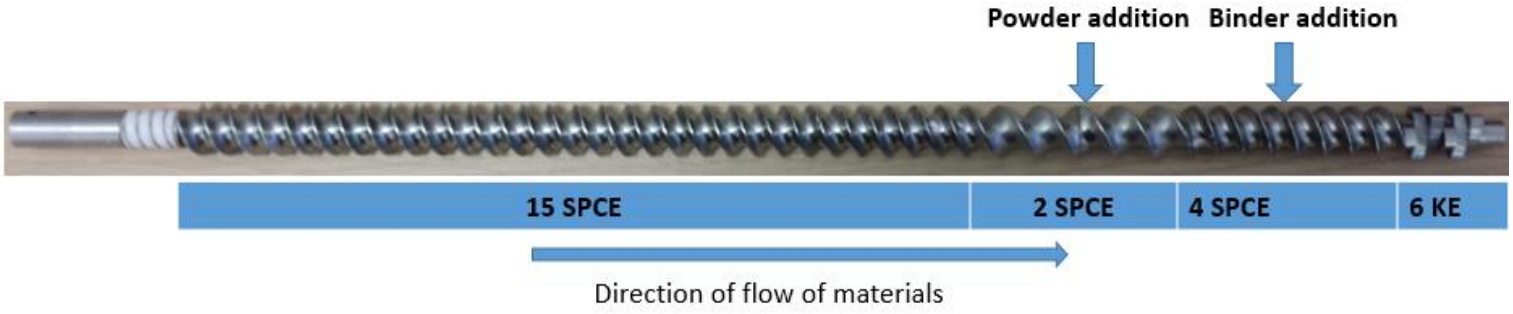

Figure 4-4 Screw configuration for 6 Kneading Elements (6KE) (Part-4)

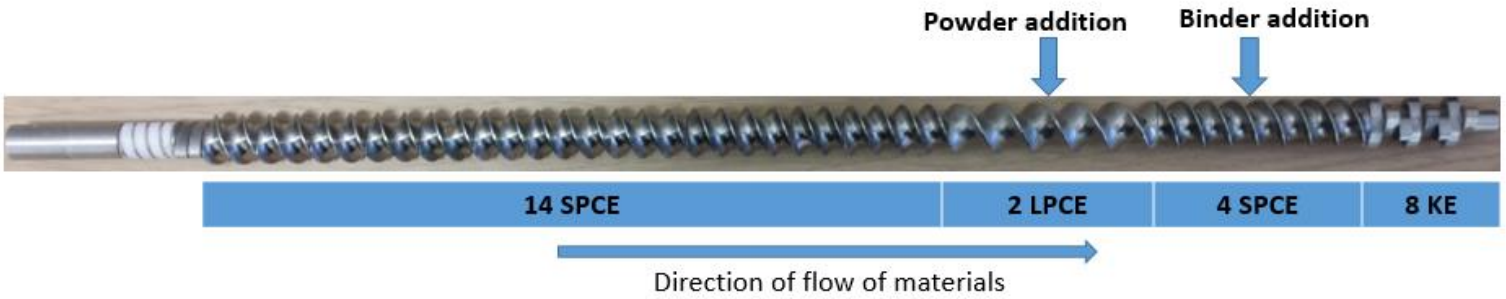

Figure 4-5 Screw configuration for 8 Kneading Elements (8KE) (Part-5)

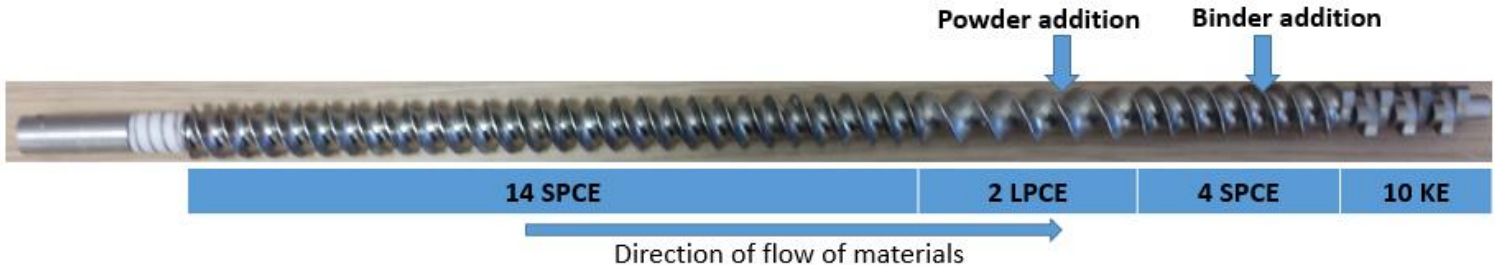

Figure 4-6 Screw configuration for 10 Kneading Elements (10KE) (Part-6)

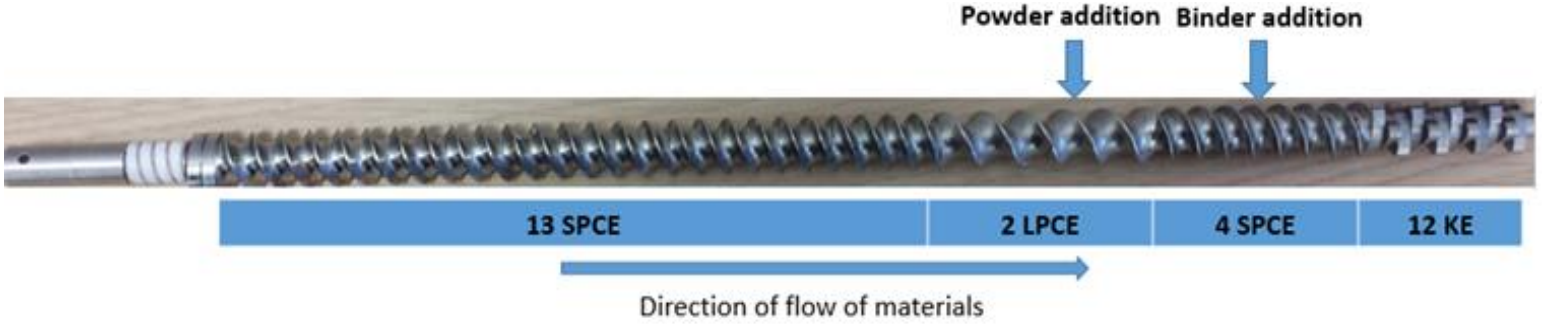

Figure 4-7 Screw configuration for 12 Kneading Elements (12KE) (Part-7)

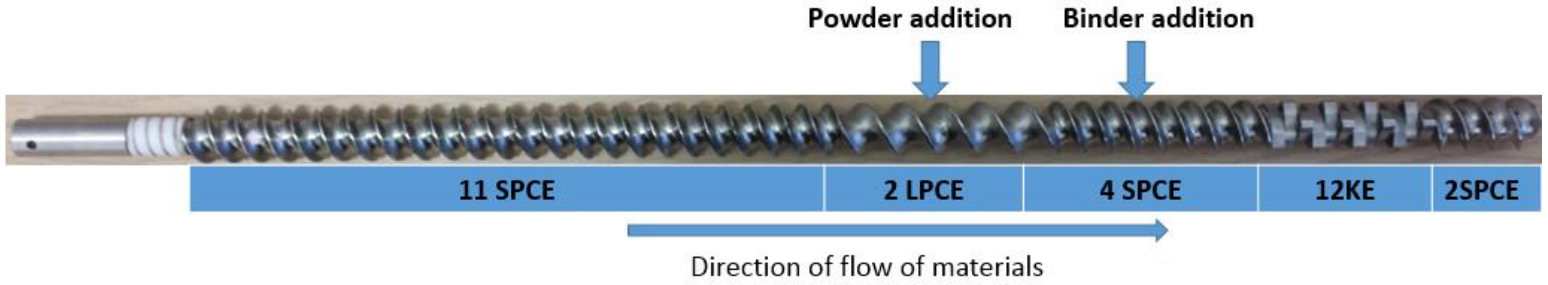

Figure 4-8 Screw configuration for 12 Kneading Elements + 2 Conveying Elements (12KE+2SPCE) (Part-8)

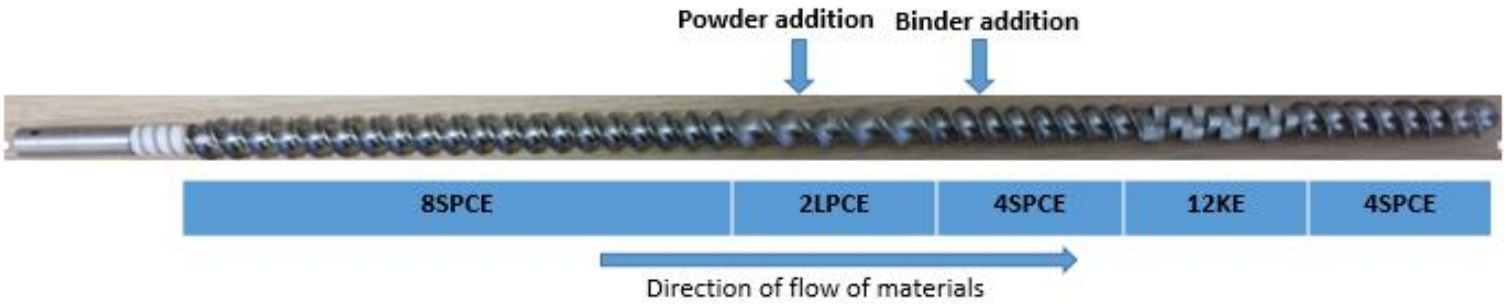

Figure 4-9 Screw configuration for 12 Kneading Elements + 4 Conveying Elements (12KE+4SPCE) (Part-9)

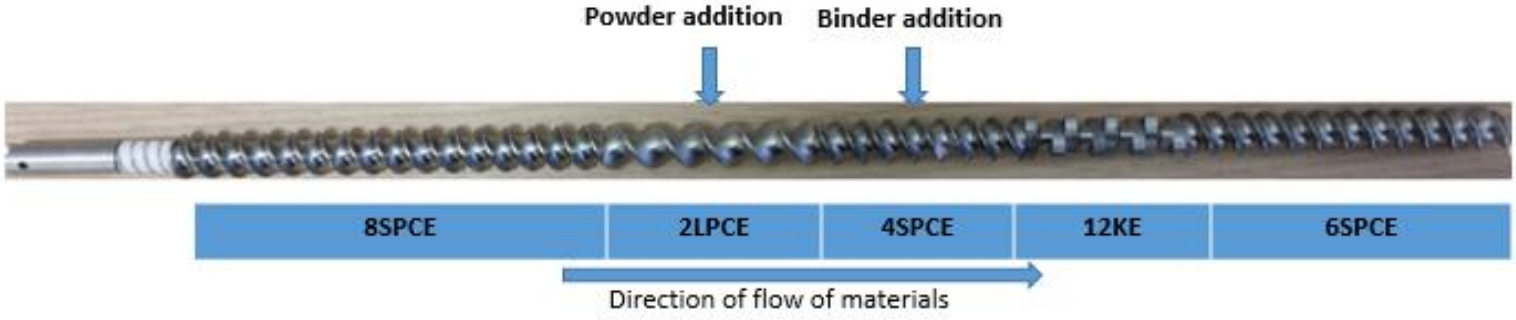

Figure 4-10 Screw configuration for 12 Kneading Elements + 6 Conveying Elements (12KE+6SPCE) (Part-10)

Table 4-1 Screw configurations used in varying Parts along the barrel length

Part No.	Part Code	Screw configuration used to obtain specific part for granulation			
Part-1	Nucleation			2LPCE	4SPCE
Part-2	2KE		2LPCE	4SPCE	2KE
Part-3	4KE		2LPCE	4SPCE	4KE
Part-4	6KE		2LPCE	4SPCE	6KE
Part-5	8KE		2LPCE	4SPCE	8KE
Part-6	10KE		2LPCE	4SPCE	10KE
Part-7	12KE		2LPCE	4SPCE	12KE
Part-8	12KE+2SPCE	2LPCE	4SPCE	12KE	2SPCE
Part-9	12KE+4SPCE	2LPCE	4SPCE	12KE	4SPCE
Part-10	12KE+6SPCE	2LPCE	4SPCE	12KE	6SPCE

Powder addition port Binder addition port

Table 4-2 Experimental conditions and variables used in this study

Experiment	Powder Feed rate (kg/h)	Screw speed (rpm)	L/S	Granulation liquid
Effect of varying screw speed	2	150	0.048, 0.07, 0.1, 0.113	Distilled water
		250	0.048, 0.07, 0.1, 0.113	
		500	0.048, 0.07, 0.1, 0.113	

Table 4-3 Sequence of experiments and cleaning in between

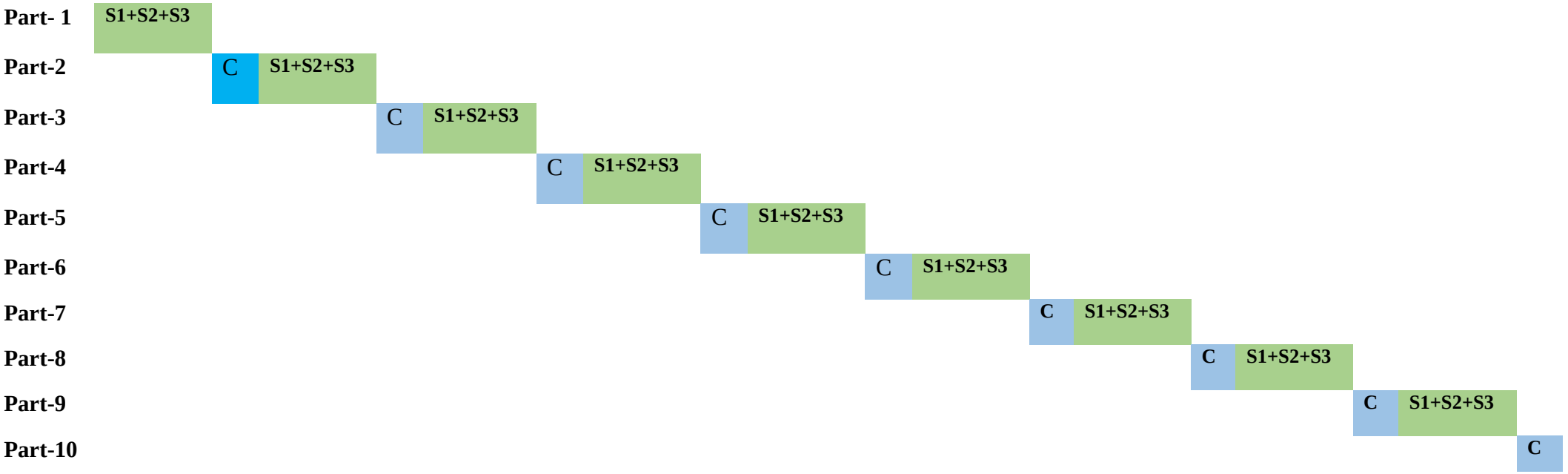

S1+S2+S3	3 Repeated sampling from each run
C	Cleaning after every granulation run

4.3.2.2 Analysis of granules

4.3.2.2.1 Size analysis and sieving of granules

The granules were air dried at room temperature for 48 h and then size of the granules was analysed using Camsizer to obtain median size (d_{50}) and volume density function i.e. q3. The granules were sieved using sieve shaker (Retsch, Germany) with sieve of 212 µm. This was done to separate the granules from poorly granulated powder. The sieving was done at an amplitude of 0.75 mm for 1 min at an interval of 10 s.

4.3.2.2.2 Shape, surface and structural characterization of granules

The granules were analysed for their shape characteristics using Zeiss stereo microscope. In some cases, (while studying the granulation in different Parts), the topology of the granules was studied using SEM to investigate the effect of screw elements on the surface characteristics of the granules. It gives visual evidence of physical surface characteristics such as shape and roughness. The X-ray tomography of granules was carried out to provide information on the change in the internal structure of the granules as they progress along the length of the barrel.

4.4 RESULTS AND DISCUSSION

4.4.1 Size of granules

Figure 4-11-Figure 4-13 show the amount of fines (<212 µm) (%, w/w) produced at screw speed of 150, 250 and 500 rpm respectively (at different L/S of 0.048, 0.07, 0.1, 0.113 and constant powder feed rate of 2 kg/h) in each Part reflecting the extent of mixing of powder and binder. This separation of fines from granules was also meant to allow un-interfered understanding of the roles of conveying and kneading elements in the screw configuration (Part) and their effects on the granule properties [including median size (d_{50}) and density distribution function, i.e. q3].

The amount of fines (%) produced at screw speed of 150, 250 and 500 rpm (at different L/S ratios of 0.048, 0.07, 0.1, 0.113 and a constant powder feed rate of 2 kg/h) in each Part

is shown in Figure 4-11-Figure 4-13, respectively. From the results shown in Figure 4-11, it was observed that Part-1 [also termed as Nucleation] produces more amount of fines (ranging from ~63% at L/S of 0.048 to ~32% at L/S of 0.113) (or the least amount of granules) amongst all the Parts at all L/S. The high percentage of fines or low percentage of granules in Part-1 can be explained as follows. In wet granulation, the nucleation is a process where powder particles are loosely bound together. These loose agglomerates are wet and liquid-rich as they are formed in the beginning of the granulation, with minimum agitation, when liquid droplets come in contact with the powder particles and form nuclei along with fines. The nucleation can occur by two types of mechanism called immersion and distribution (Schæfer and Mathiesen 1996). This mechanism depends on the method of addition of liquid. The method in which the size of the liquid drop is bigger than that of the particle size is called immersion. Distribution type of mechanism is exactly opposite to immersion in which liquid is sprayed onto powder and every small liquid drop is surrounded by some powder particles to form wet mass or nuclei. These big mass or small nuclei undergo a process of consolidation, coalescence and breakage (Iveson et al. 2001, Dhenge et al. 2012a). In TSG, big drop of the binder is injected onto the dry powder in the barrel; this type of nuclei formation is called immersion (Dhenge et al. 2012a). Part-1 is the area in the TSG where the liquid is dripped onto the dry powder in the barrel. This pumping of big drop of liquid results in the formation of big, wet, loose lumps called as nuclei with some poorly granulated and or un-granulated powder (fines). In the present research work, Nucleation (Part-1) was consisted of only four short pitch conveying elements (4SPCE) (after 2LPCE) where the powder was wetted by the liquid to form initial granules called nuclei. As the L/S increased [at Part-1 or Nucleation], the percentage of the fines decreased while that of the granules increased. Granulation at L/S of 0.113 resulted in the lowest proportion of fines and the highest proportion of granules (above 212μm) as the availability of more liquid promoted the more binding between the particles (Dhenge et al. 2012b, Dhenge et al. 2012a, El Hagrasy et al. 2013b). As the wet mass from Part-1 moved to Part-2, the amount of granules increased whilst the fines decreased. This is because the presence of kneading elements promoted the distribution of liquid binder in the powder, forming more granules. From Part-2 to Part-10, the amount of fines (and granules) did not change much at respective L/S.

At the screw speed of 250 and 500rpm, the trend was nearly similar to that of 150rpm. This indicates that an increase in the number of kneading elements from 2 to 12 in the screw configuration alone does not necessarily decrease the amount of fines or increase the amount of granules. However, more number of kneading elements together with L/S could influence the amount of fines or granules.

The median size of granules produced at screw speed of 150, 250 and 500 rpm (at different L/S ratios of 0.048, 0.07, 0.1, 0.113 and constant powder feed rate of 2 kg/h) in each Part is shown in Figure 4-14-Figure 4-16, respectively. At lower screw speed of 150 rpm and lower L/S ratios of 0.048 and 0.07 (Figure 4-14), the median size of granules in Part-1 (Nucleation) was found to be bigger than that in the other Parts. This is because the low shearing short pitch conveying elements (SPCE) in the Part-1 resulted in the formation of big, loose and liquid rich lumps or early stage granules along with the high percentage fines. It is important to mention that this median size was obtained after sieving the whole batch consisting both fines and granules. This was done to understand the amount of granules produce during granulation at different L/S and screw speed.

In Part-2, the two kneading elements (2KE) (which were placed after the Nucleation section) restricted the flow of wetted powder due to poor conveyance (Li et al. 2014), kneaded the wet mass, improved mixing, sheared and broke the bigger agglomerates which causes reduction in median size (d_{50}) (Dhenge et al. 2012a) reducing the median size. The granules from Part-2 (2KE) (in the case of L/S of 0.048 and 0.07) moved further to Part-3 (4KE) where the increased number of kneading elements resisted the flow of granules in the forward direction, sheared, broke and consolidated the granules reducing the median size. After Part-3, the median granule size in the remaining Parts did not show major change.

At higher L/S of 0.1 and 0.113, the granules from Part-1 (Nucleation) were similar in size as in the case of lower L/S (0.048 and 0.07). This may be due to the limited amount of shearing from short pitch conveying elements. In Part-2, the addition of 2KE after the Nucleation section did not influence the granule size at screw speed of 150 and 250 rpm. This is opposite to the results at L/S of 0.048 and 0.07. It may be attributed to the availability of sufficient amount of liquid binder at higher L/S of 0.1 and 0.113 which resisted the breakage due to shearing from 2KE in the screw configuration.

A further increase in the number of kneading elements from two (i.e. in Part-2) to four (i.e. in Part-3) at screw speed 150 rpm increased the shearing and decreased the granule size at L/S of 0.1 indicating the breakage of oversized agglomerates. However, at L/S of 0.113, the effect was still minimum due to more availability of liquid binder resisting the breakage due to shearing. Increasing the number of kneading elements to six (Part-4) and eight (Part-5) resulted in an increase in the granule size at both L/S (0.1 and 0.113). This may be attributed to the synergistic effect of the increased shearing from more number of KE and the availability of more liquid binder at such L/S. The granules were more consolidated promoting growth due to coalescence. In Figure 4-14, the large error bar for 8KE is due to presence of flaky large lumps along with some relatively smaller granules (refer Figure 4-22 for details). This variability decreased with the increasing number kneading elements and screw speed (i.e. shearing and cutting the large lumps) (Figure 4-15 and Figure 4-16).

At L/S of 0.1 (screw speed 150rpm) in Figure 4-14, Part-6 (10KE) appeared to be the critical step in granule progression along the barrel length since after this point the granules size decreased due to breakage, as seen in presence of 12KE in Part-7. This might occur due to the completion of liquid distribution in the powder mass (meaning end of coalescence process) and the excessive stress imparted by increased number of kneading elements in the screw configuration (Dhenge et al. 2012b, Li et al. 2014). So at Part-7 (12KE), breakage due to shearing dominated over the growth due to coalescence.

At L/S 0.113, granule size increased until Part-7 (12KE) due to additional amount of liquid on the surface. It appeared that the critical limit for kneading element to induce breakage was beyond 12KE. There was still sufficient liquid binder to promote granule growth by coalescence increasing the median size (~5000 μm).

At both L/S in Figure 4-14, i.e. 0.1 and 0.113, Part-8 (12KE + 2SPCE), Part-9 (12KE + 4SPCE) and Part-10 (12KE + 6SPCE) exhibited decrease in the granule size. Similar results were reported by Van Melkebeke et al. (2008) and Dhenge et al. (2012a). The reduction in the granule size in presence of SPCE was supposed to be due to the shearing and cutting action exerted by the short pitch conveying elements on the wetted powder as it moves across the intermeshing area between the two screws. To prove this argument, a basic experiment was performed where a handmade wet ball of lactose powder (with diameter that

approximately fits in the screw channel of SPCE) was placed in the screw channel and its progression across the intermeshing area (at very low screw speed of 20rpm) was visualised by recording high speed optical images (using a high speed camera- Photron, Fastcam, 100 K, USA) through a transparent barrel (replacing stainless steel barrel). The snapshots of lactose ball progression across the intermeshing area is presented in Figure 4-17. From figure it can be observed that as the lactose ball is pushed towards the intermeshing area by the flight of the screw, it starts breaking into smaller fragments as it cannot pass through the gap at the intermeshing area i.e. between the pointed edge of the barrel partition and the screws. Although, the solid ball used in this experiment does not fully replicate actual wetted powder mass or granules in granulation experiments, it provides a clear insight into the direction of material flow and shearing and cutting process at SPCE in TSG.

The median granule size at Part-10 was found to be ~1000 μm in all cases except at L/S of 0.113 (screw speed of 150 rpm) which resulted in relatively larger granules (~1900 μm).

At higher screw speeds of 250 rpm (Figure 4-15) and 500 rpm (Figure 4-16), the trend for median granule size at different Parts and L/S was nearly similar to that of 150 rpm but the magnitudes were different. The size of granules at 150 rpm was bigger than that of 250 and 500 rpm. Increasing the screw speed increased the shear and compaction forces and deformation, leading to breakage of granules (Djuric et al. 2009). At screw speed of 250 rpm, the median granule size at Part- 10 (12KE+6SPCE) at L/S 0.113 was found to be (~1500 μm). Interestingly, at screw speed of 500 rpm, the median granule size at Part-10 (12KE+6SPCE) was found to be ~1000 μm at all L/S.

So, it is clear that at lower L/S, the granule size has no potential for growth due to an insufficient availability of liquid. At higher L/S, the granule size increases with increasing number of KE. As granules move from kneading elements to short pitch conveying elements the granule size decreases dramatically due cutting and chopping action of conveying elements.

This clearly demonstrates that the effect of increasing screw speed can dominate over that of L/S (at higher L/S of 0.1 and 0.113). This observation at higher L/S contradicts to some of the findings in the literature, where screw speed showed very limited influence on the granule size (Dhenge et al. 2010, Vercruysse et al. 2012). However, the results at lower L/S

of 0.048 and 0.07 agree with the findings in the literature where granule size does not change at any screw speed due to an insufficient availability of liquid.

The granule size distributions along the length of the barrel at 150 rpm for L/S of 0.048, 0.07, 0.1 and 0.113 (after sieving) are shown in Figure 4-18-Figure 4-21, respectively. The granule size distribution at the low L/S (0.048 and 0.07), screw speed of 150 rpm from Part-1 (Nucleation) to Part-7 (12KE) are bimodal and contains small granules (as granule size distribution curve is shifted more towards the left). Similarly, at high L/S (0.1 and 0.113) and screw speed of 150 rpm, the size distribution curves were bimodal (shifted towards the right) and wide (from Part-1 (Nucleation) to Part-7 (12KE)) due to uneven mixing at the initial stages and compaction and attachment of several granules at later stages (Dhenge et al. 2012a). After kneading elements, the granules pass through short pitch conveying elements. Shearing and cutting action of granules resulted in monomodal and narrow size distribution at 12KE+2SPCE, 12KE+4SPCE and 12KE+6SPCE as shown in Figure 4-18-Figure 4-21, respectively. Compared to high L/S (0.1 and 0.113), at low L/S (0.048 and 0.07), the granule size distribution was narrow and granules had limited potential for growth due to limited availability of liquid. Similar to the median size, it is understood that the monomodality can be influenced by considering fines and granules together and can show different results, mostly in case of Part-1.

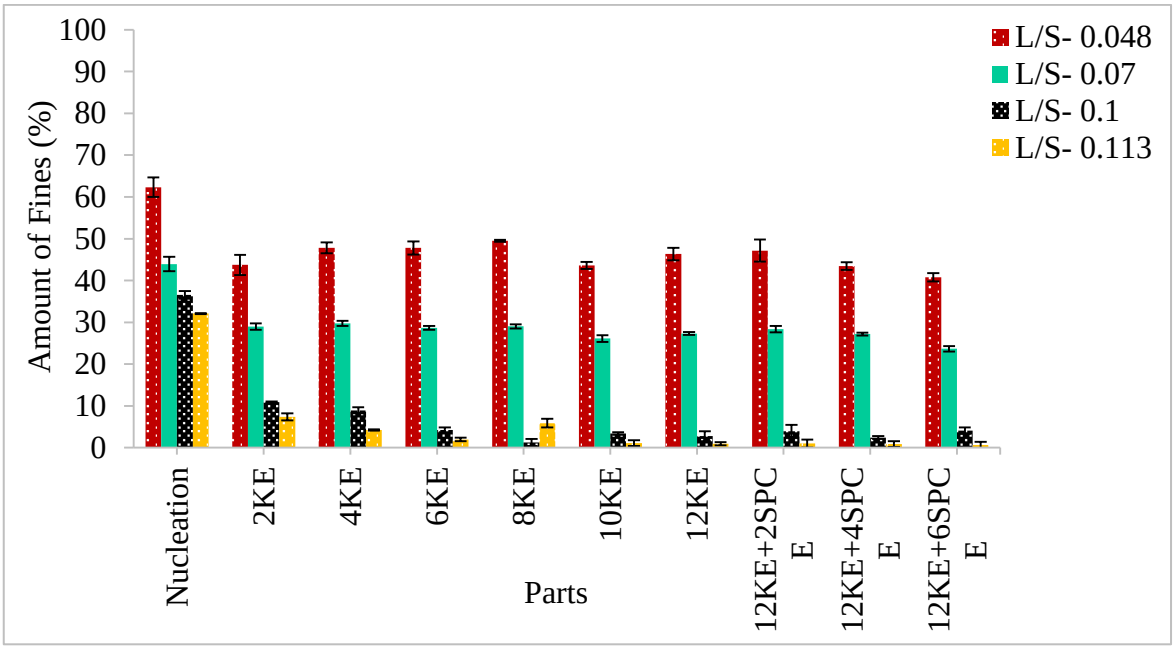

Figure 4-11 Amount of fines (%) produced in different Parts at varying L/S (at 150 rpm)

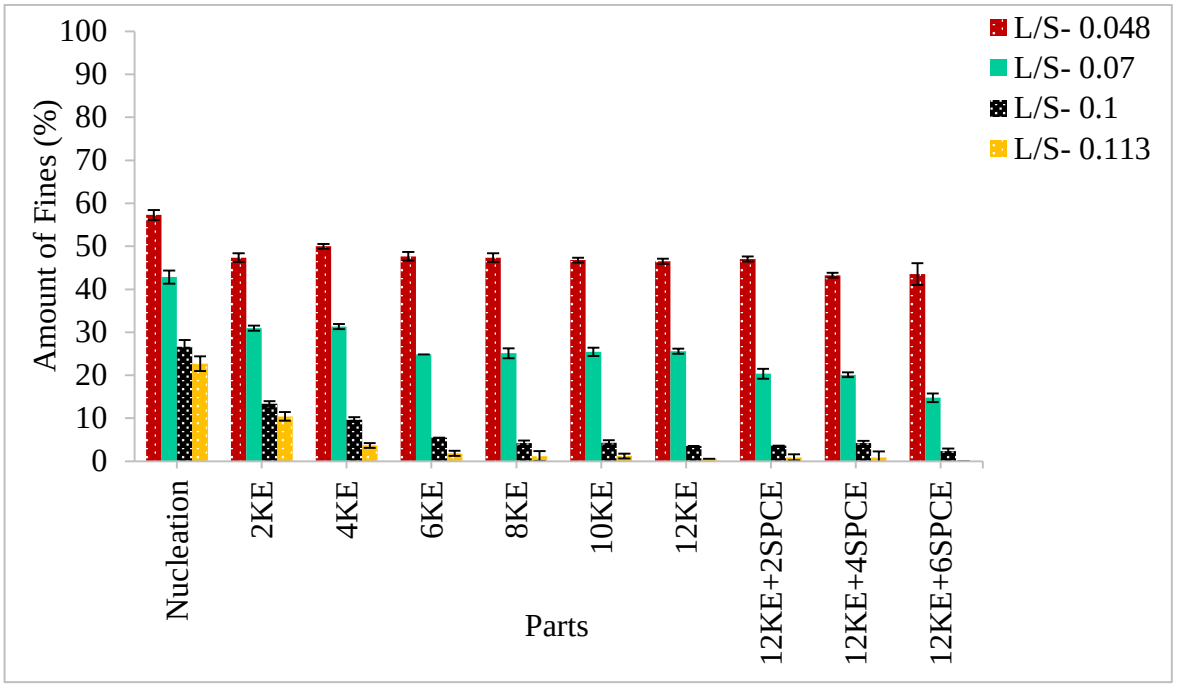

Figure 4-12 Amount of fines (%) produced in different Parts at varying L/S (at 250 rpm)

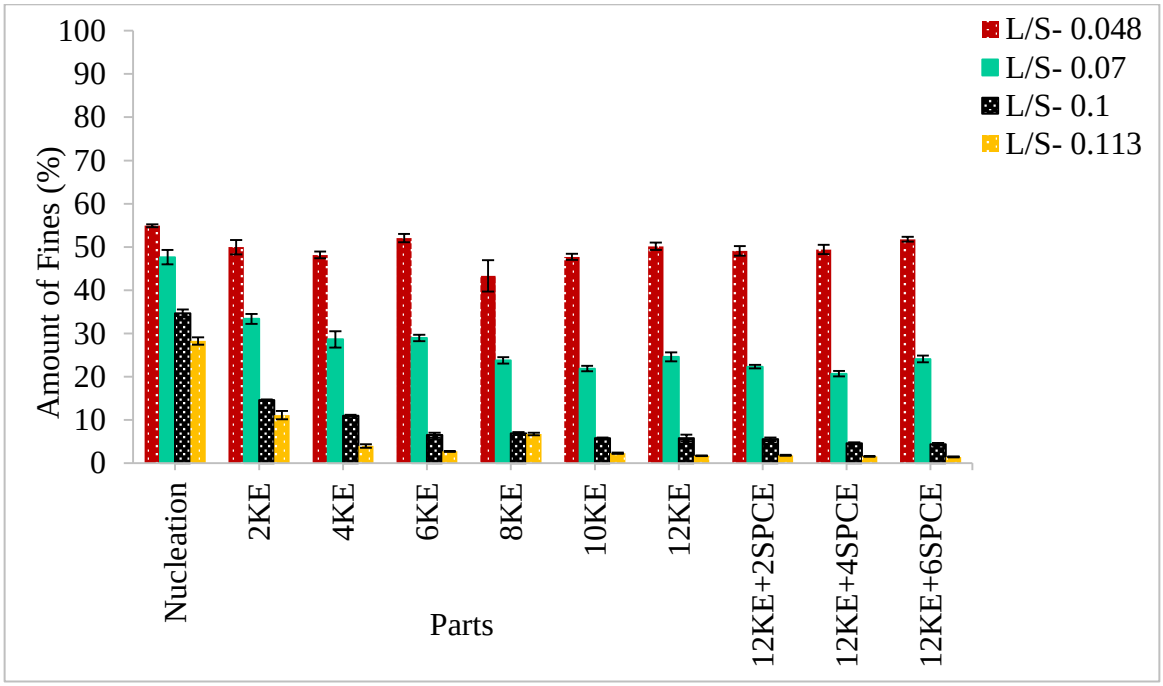

Figure 4-13 Amount of fines (%) produced in different Parts at varying L/S (at 500 rpm)

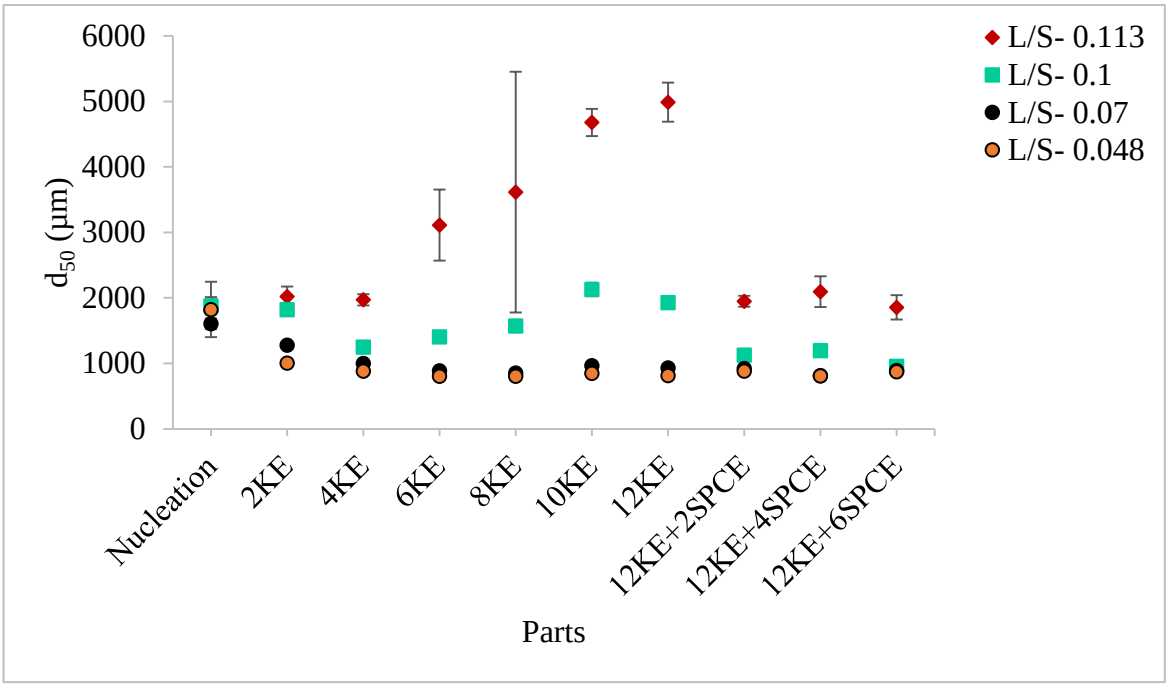

Figure 4-14 Median size of granules (after sieving) in different Parts at varying L/S ratio (at 150 rpm)

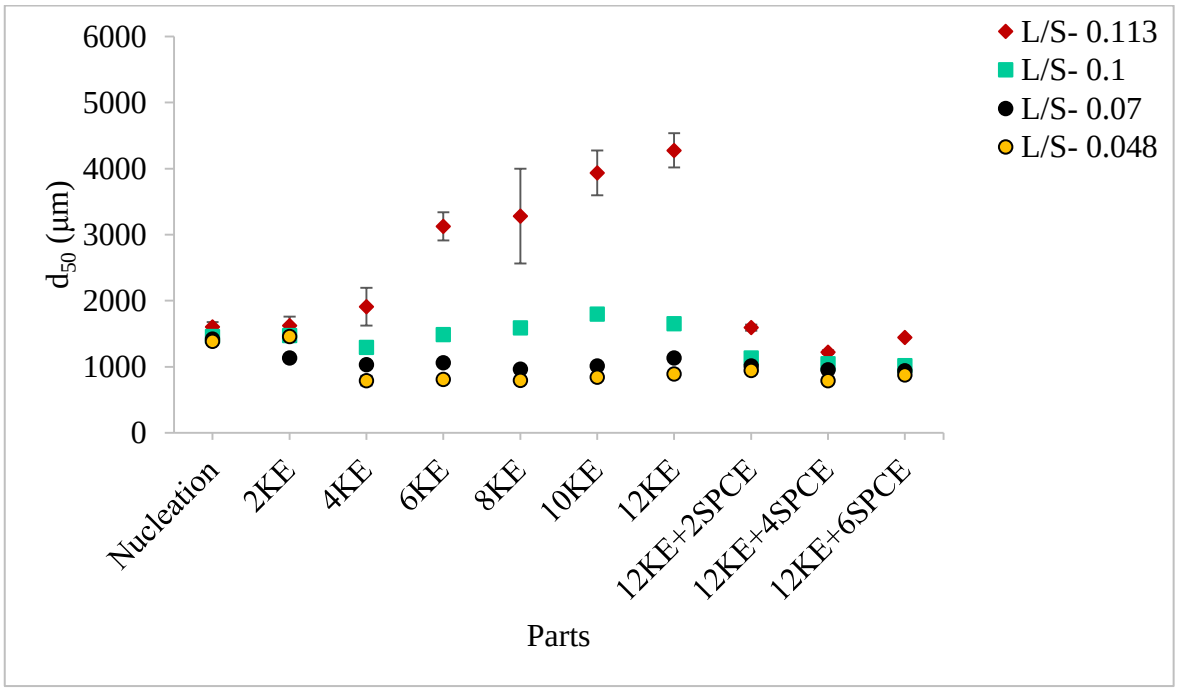

Figure 4-15 Median size of granules (after sieving) in different Parts at varying L/S ratio (at 250 rpm)

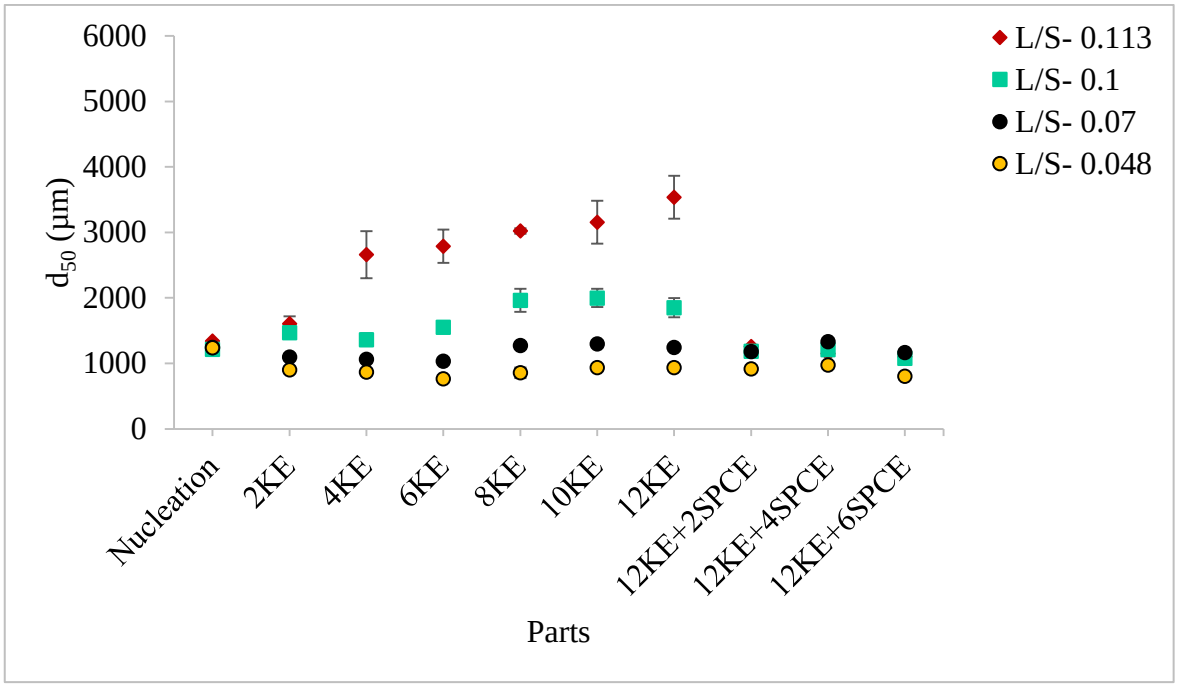

Figure 4-16 Median size of granules (after sieving) in different Parts at varying L/S ratio (at 500 rpm)

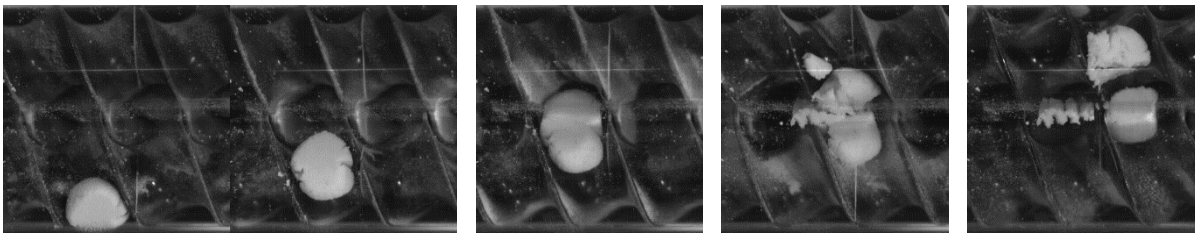

0 t_1 t_2 t_3 t_4

Figure 4-17 Shearing and cutting of wet ball of lactose powder across the intermeshing area of SPCE

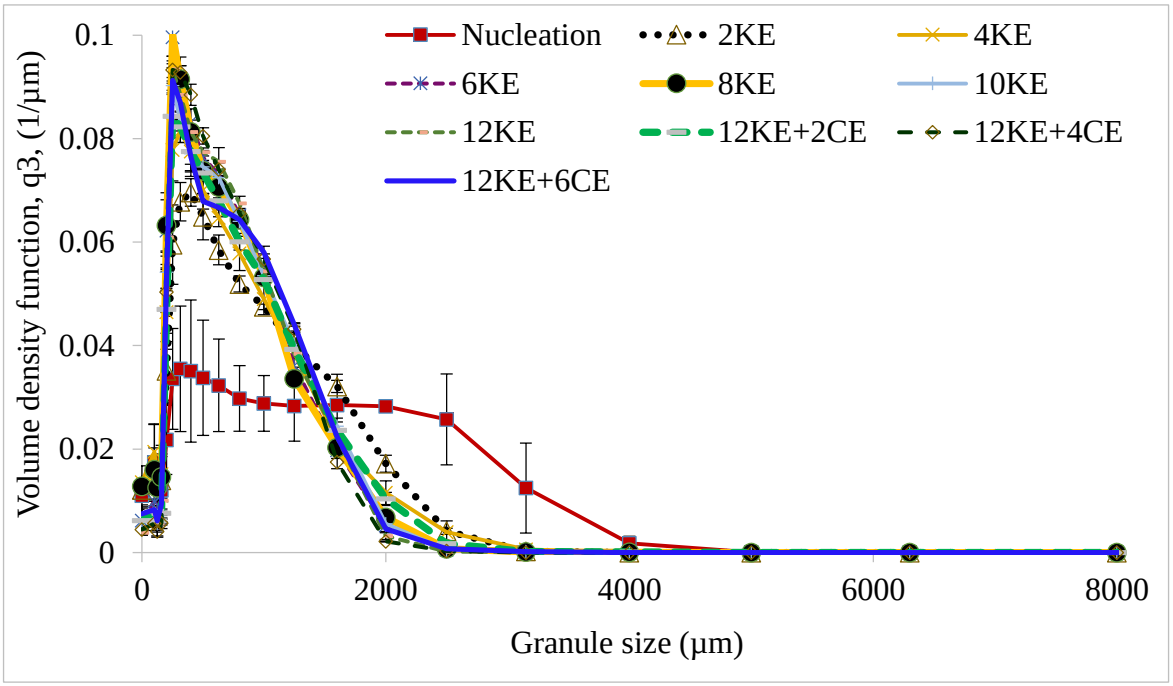

Figure 4-18 Size distribution (after sieving) in different Parts at L/S-0.048 (at 150 rpm)

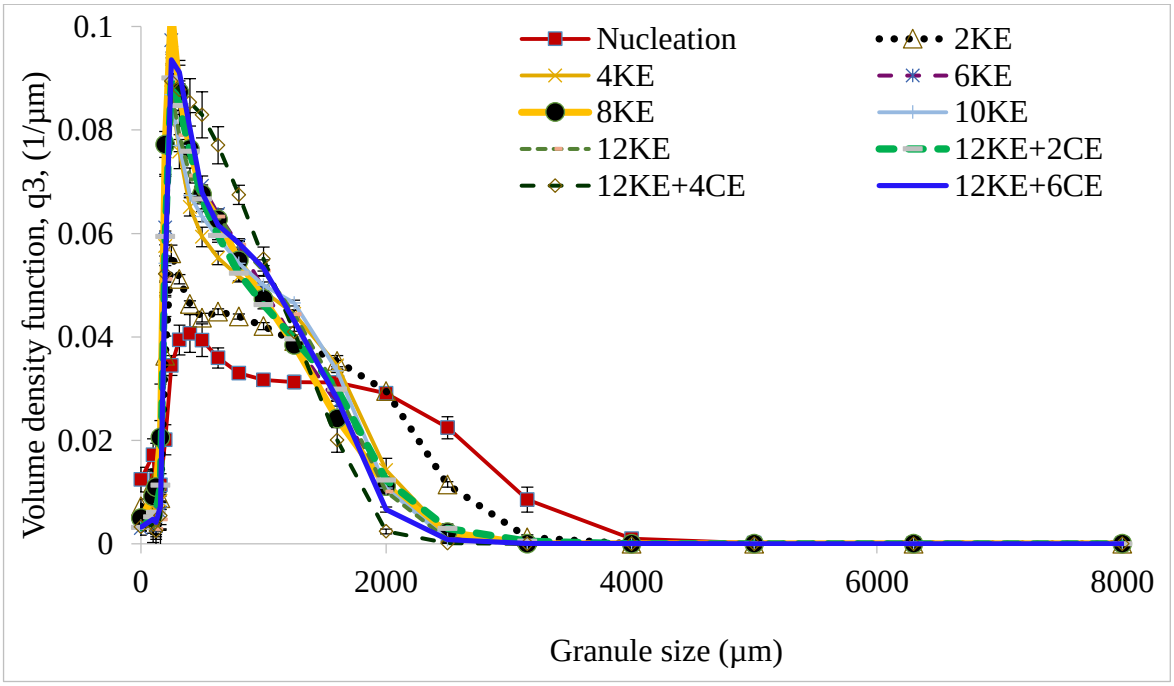

Figure 4-19 Size distribution (after sieving) in different Parts at L/S- 0.07 (at 150 rpm)

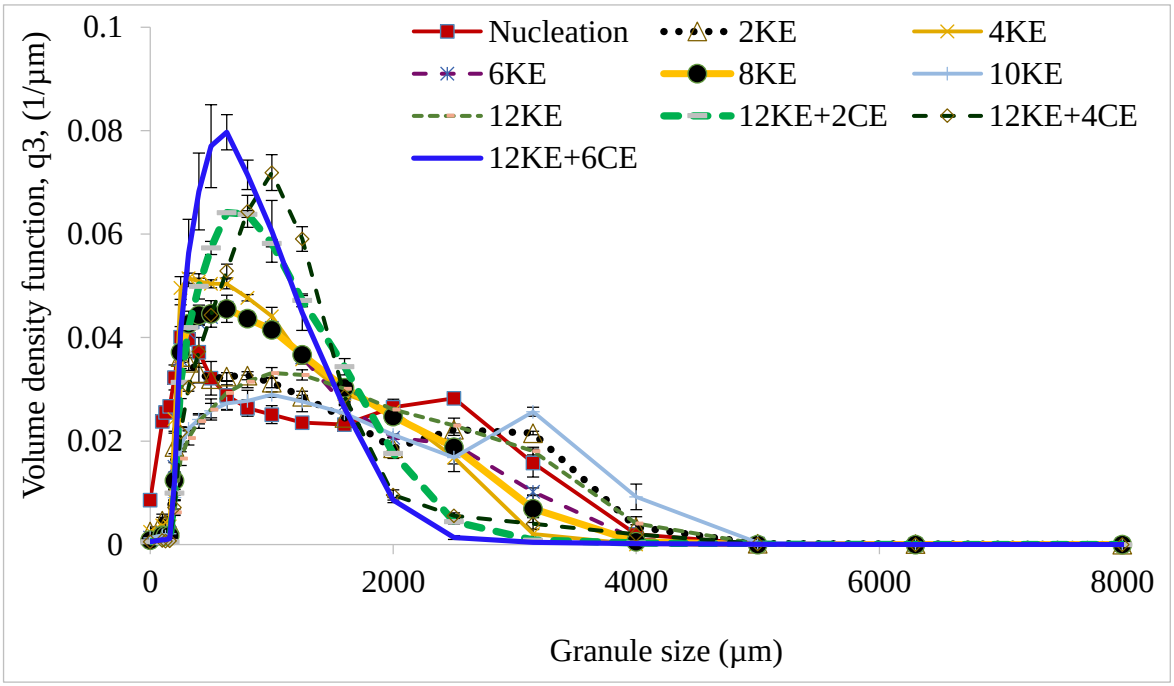

Figure 4-20 Size distribution (after sieving) in different Parts at L/S- 0.1 (at 150 rpm)

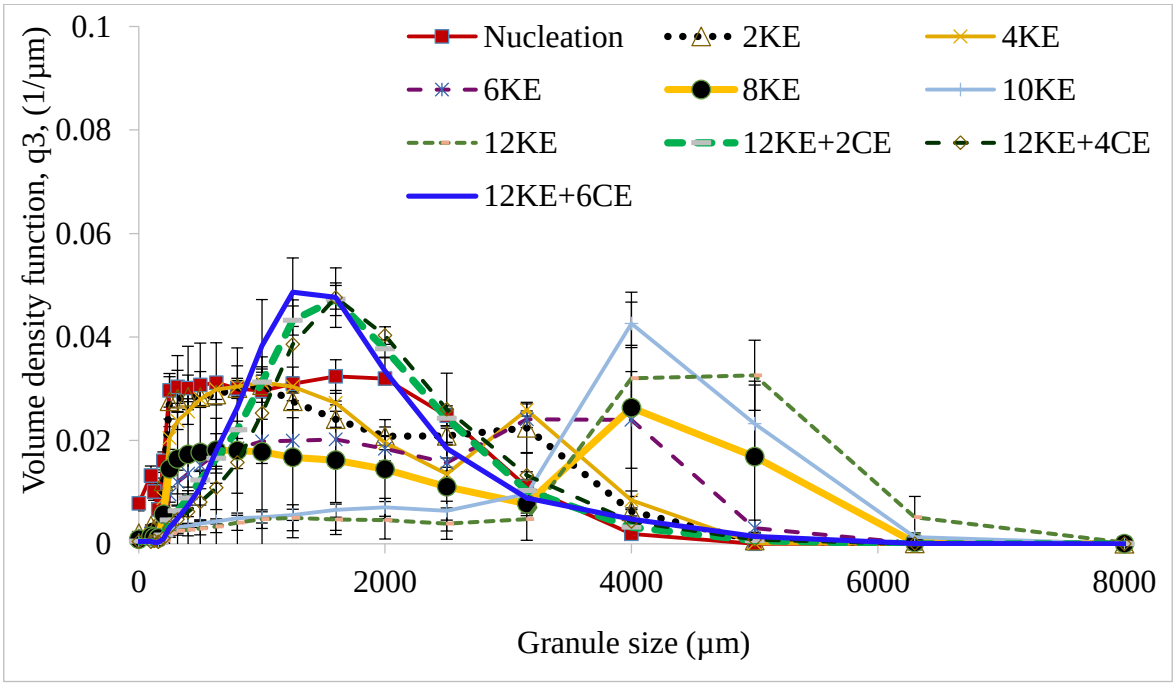

Figure 4-21 Size distribution (after sieving) in different Parts at L/S- 0.113 (at 150 rpm)

4.4.2 Shape of granules

The shape of granules along the length of the granulator (Part-1 to Part-10) was studied at varying screw speeds and L/S using the microscopic images (Figure 4-22-Figure 4-24). The respective process conditions are shown on the left side (L/S_Screw speed) of the Figure 4-22, Figure 4-23 and Figure 4-24. In nucleation (Part-1), all conditions resulted in bigger and relatively spherical granules or nuclei and some amount of poorly granulated and or ungranulated powder. These big and spherical granules/nuclei from Part-1 were then conveyed to the 1st pair of kneading elements i.e. (Part-2). The kneading element shear and compact these bigger agglomerates to reduce their size. The shearing of granules occurs in the gap between the tip of the kneading elements and the barrel wall. The granules from Part-1 were broken and consolidated, and they generally take an elongated shape due to chopping action of kneading element on the wetted powder. As granules move from kneading to conveying elements, granules become relatively spherical due to the cutting and chopping of deformable, elongated granules and their subsequent rolling and rounding on the channels of the conveying elements.

Increasing L/S reduced the amount of elongated granules in general. As the amount of granulation liquid increased the wetted lactose powder became more deformable leading to rounder (less elongated) granules during its breakage and subsequent movement on the screw surface (Dhenge et al. 2010). Increasing screw speed had limited influence on the shape of the granules.

	Nucleation	2 KE	4KE	6KE	8KE	10KE	12KE	12KE+2SPCE	12KE+4SPCE	12KE+6SPCE
0.048_150	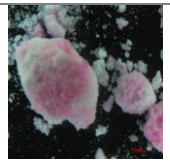	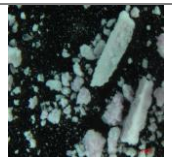	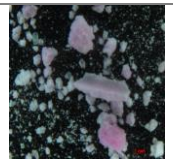		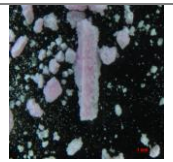	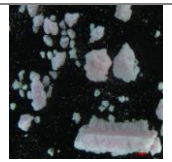	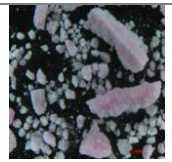	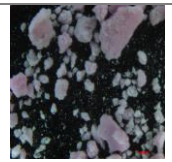	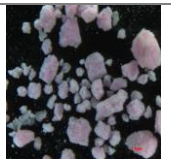	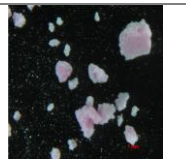
0.07_150	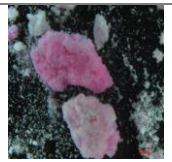	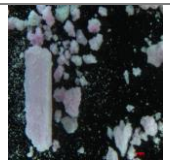	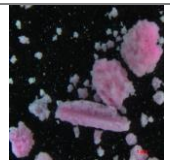	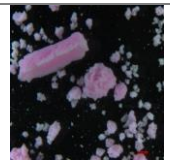	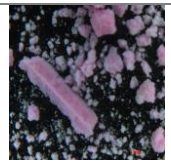	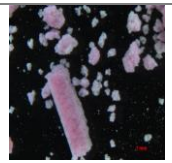	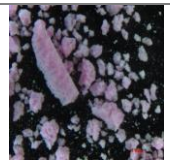	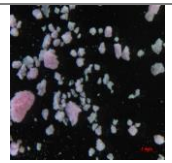	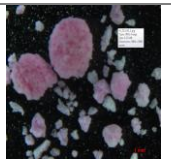	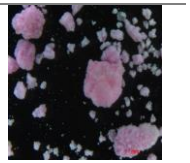
0.1_150	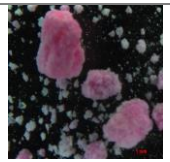	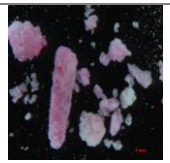	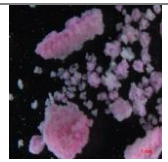	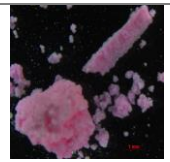	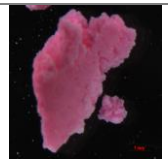	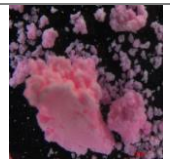	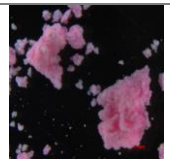	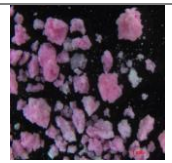	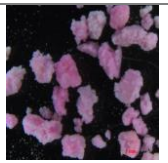	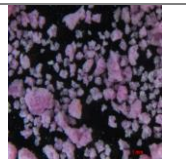
0.113_150	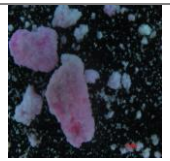	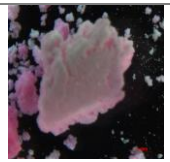	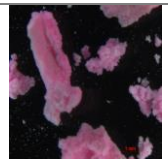	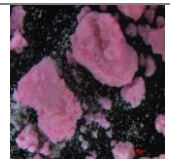	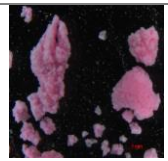	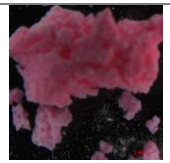	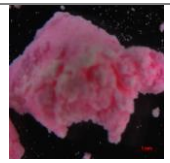	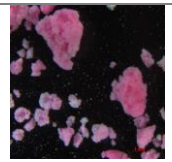	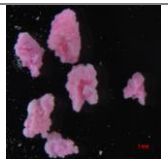	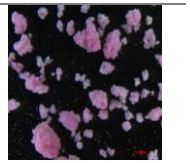

Figure 4-22 Microscopic images of granules produced at different L/S in different Parts at 150 rpm

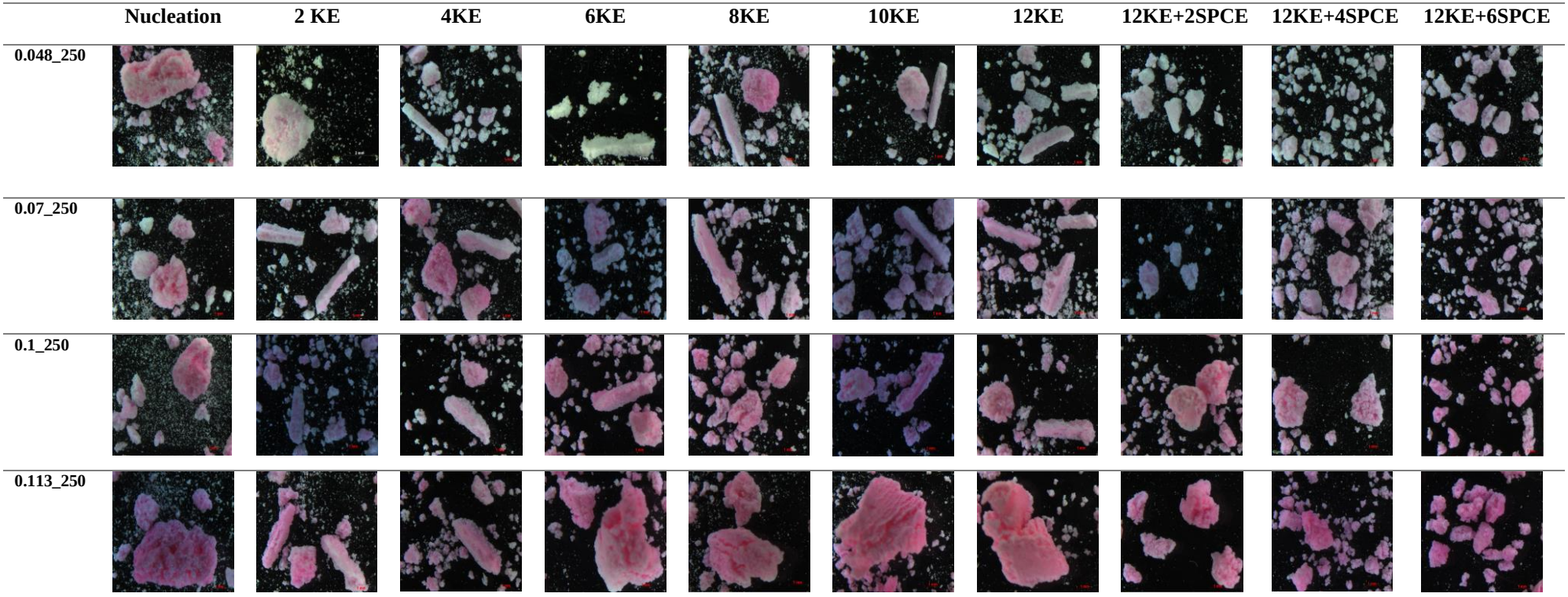

Figure 4-23 Microscopic images of granules produced at different L/S in different Parts at 250 rpm

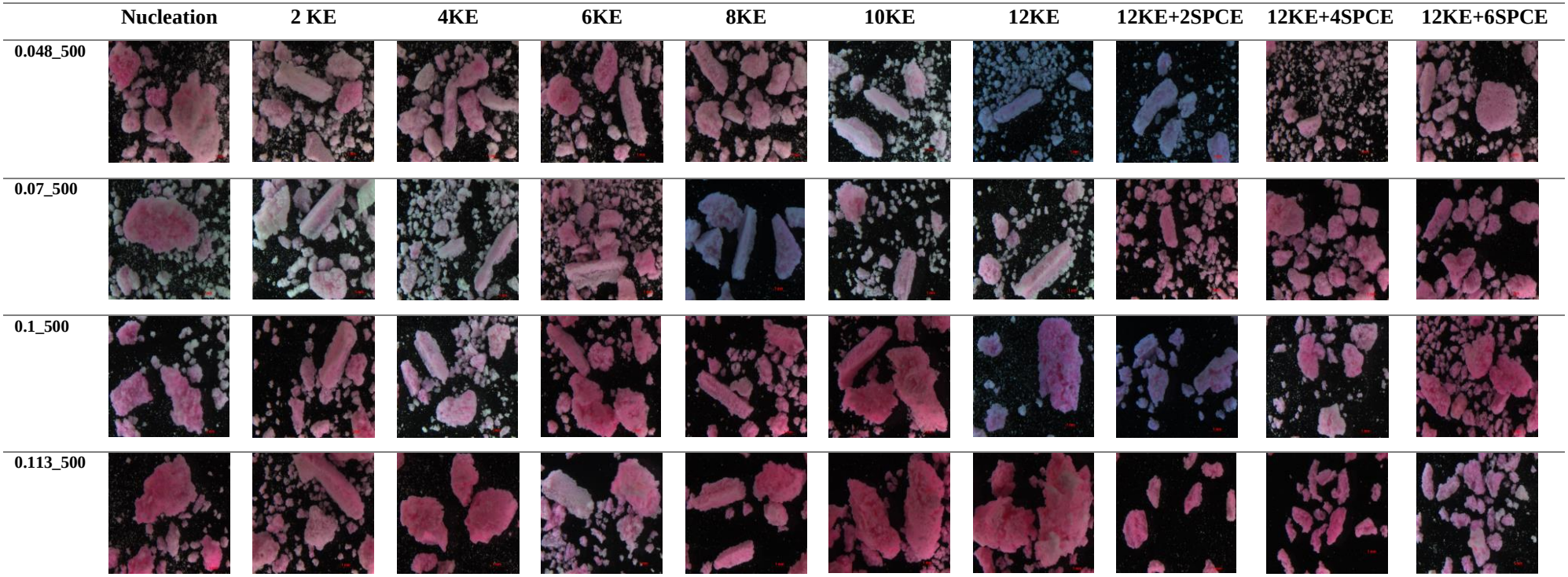

Figure 4-24 Microscopic images of granules produced at different L/S in different Parts at 500 rpm

4.4.3 Surface characteristics of granules

Scanning Electron Microscopy (SEM) was used to study the change in the surface characteristics of the granules produced using various screw configurations. Figure 4-25 shows SEM images of ungranulated lactose powder (Figure 4-25(a)) and the granules produced at L/S 0.1 and screw speed of 500 rpm at varying screw configurations. The reason for selecting only these conditions was to broadly understand the effect of screw configuration on the granule surface. Figure 4-25(b) shows the SEM image of Nucleation condition (Figure 4-1). In Nucleation, the liquid drops interacted with the powder to form wet loose lumps 'nuclei' When liquid evaporates during drying, the liquid bridge between the particles turn into solid bridges forming dry porous granules (called nuclei). In these dry nuclei individual particles can still be distinguished because they were not fully dissolved or compacted to form dense granules as it can be seen in Figure 4-25(b). The particles in the nuclei could still be distinguished and were similar to the ungranulated dry lactose powder particles shown in Figure 4-25(a). This indicated that the Nucleation stage does not impart excessive shear and compressive stresses on the wetted powder to form dense and compacted granules. Figure 4-25(c) shows the SEM image of granule produced using 2KE (Figure 4-2 for screw configuration). In this condition, the 'nuclei' passed through 2KE where they were consolidated and densified as it can be seen in Figure 4-25(c). Then these compacted granules passed through 6 KE (see Figure 4-4 for screw configuration). The granules were deformed and consolidated to make dense granules. The flattening on the surface of granules occurs due to shearing and compaction between kneading elements and barrel wall and intermeshing zone between two screws of the TSG as it can be seen in Figure 4-28(d)-(g). As the number of kneading elements increased further (12 KE) the conveyance of material and residence time of material decreased at constant powder feed rate which results in increase in fill level. Increase in the fill level adds to the compaction, shearing and frictional forces applied on the granules by KE.

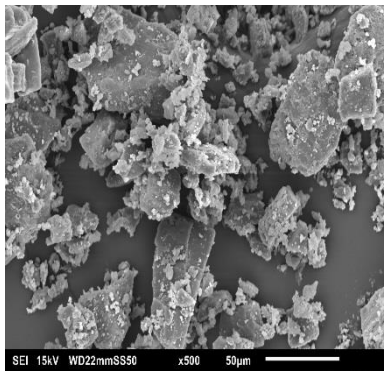

(a) Lactose powder

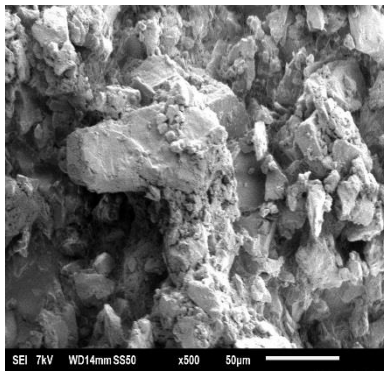

(b) Nucleation

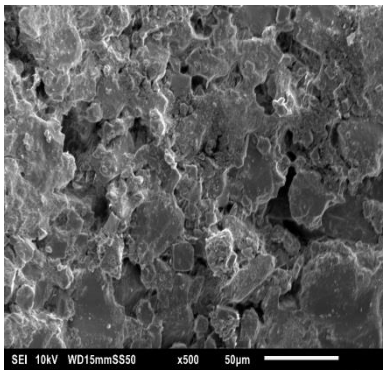

(c) 2KE

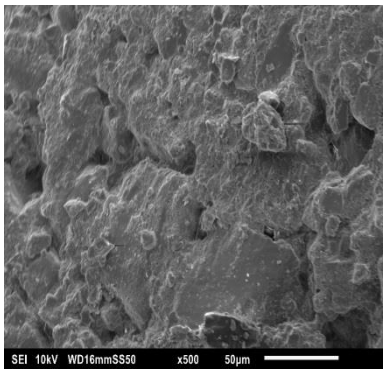

(d) 6KE

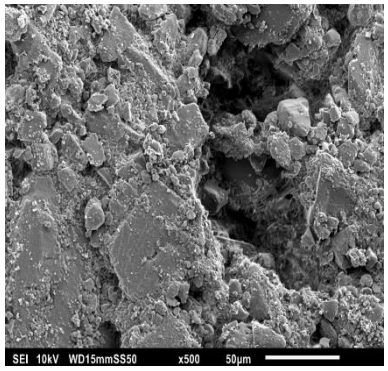

(e) 12KE

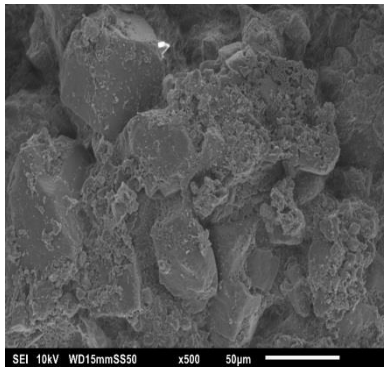

(f) 12KE+4SPCE

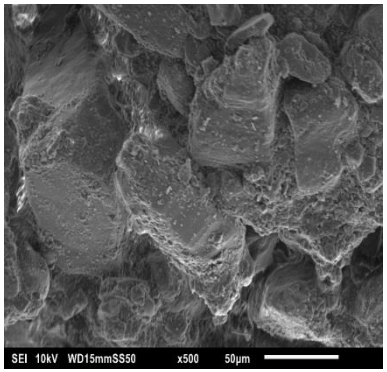

(g) 12KE+6SPCE

Figure 4-25 Scanning Electron Microscopy (SEM) images of granules produced at L/S- 0.1 and speed of 500 rpm in different Parts

4.4.4 Structure of granules

Figure 4-26 shows the X–ray tomographic images of granules (>2000µm) produced in different Parts at L/S 0.1 and screw speed of 500 rpm (similar to SEM study). The X-ray tomography (XRT) (µCT 35, SCANCO Medical AG, Brüttisellen, Switzerland) of granules was carried out to gain more information on the change in the internal structure of the granules. The granules collected from various processing conditions had varying shapes. For this reason, only the middle area of the granules was scanned to determine the porosity. The stack of 240 images (slices) was threshold to differentiate the void and solid particle using ImageJ Software (National Institutes of Health, Bethesda, MD, USA) [26]. The black area in the X-ray images indicates the air (pores), and the white area indicates the granule or powder particle. The porosity of a granule was determined by dividing the area of air by the total area of the image. The XRT images were analysed using ImageJ software to determine the inter-particle porosity within the granules (Figure 4-27). The black colour in image represents air or void and the grey represents granulated powder mass. In Figure 4-26, the first Part is Nucleation, where the granules were less dense because the powder particles were loosely attached to each other and thus the inter-particle porosity was high (Figure 4-27). The nuclei were then granulated further in 'Parts' with increasing number of kneading elements, resulting in denser granules thus lower inter-particle porosity. Some localised densification can be seen the granules produced in Part-2 to Part-10 (see Figure 4-26(b)-(j) and Figure 4-27). This may be attributed to the increase in the shear and compressive forces imparted on granules by the kneading elements.

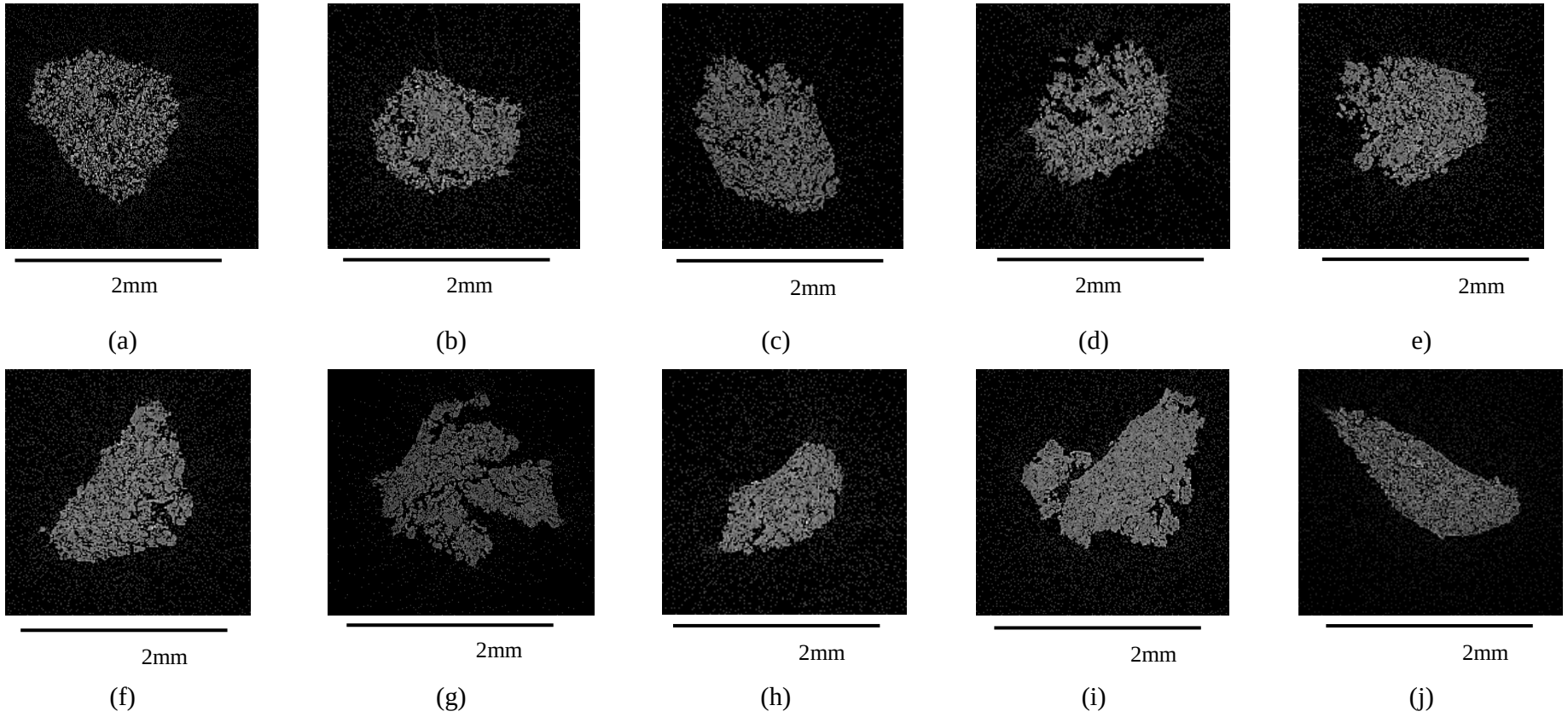

Figure 4-26 X-ray tomographic images of granules produced in different Parts at L/S- 0.1, 500 rpm

(a) Nucleation (b) 2KE (c) 4KE (d) 6KE (e) 8KE (f) 10KE (g) 12KE (h) 12KE +2SPCE (i) 12KE + 4SPCE (j) 12KE +6SPCE

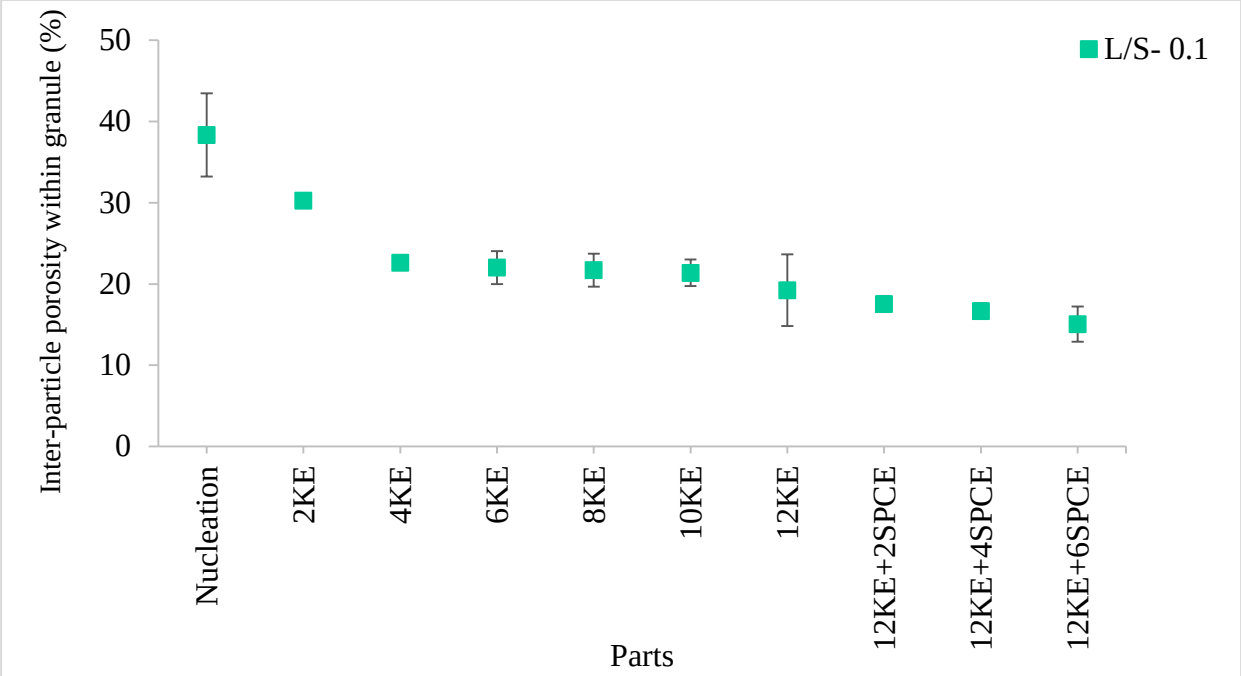

Figure 4-27 Inter-particle porosity within granules produced in different Parts at L/S- 0.1, 500 rpm

4.4.5 Effect of channel width and screw volume on granule size and structure

In addition to the study of granule progression along the barrel length using various 'Parts', the effect of increase in the channel width and volume of screw elements towards the end of screw configuration on granule structure was also studied at L/S 0.1 and 500rpm. In order to study effect of SPCE, screw configuration used in Figure 4-10 where 12KE+6SPCE were used at the end while to study effect of LPCE the four SPCE at the end of screw configuration shown in Figure 4-10 was replaced by two LPCE. Figure 4-28 shows that median granule size produced at SPCE was smaller than that at LPCE, it may be because the SPCE has shorter channel width (8 mm), more number of flights (two flights for 16 mm length of screw compared to one for LPCE over the same length) and steeper helix angle (or flight angle) (17.67◦), which increases the shearing and cutting action reducing the granule size (see section 1.1.3.1). Increasing the screw speed whilst LPCE at the end of the screw configuration increased the median granule size. This may be attributed to the reduction in breakage due to larger channel free space (channel width 12 mm) and helix angle (26.46◦) of LPCE [Shear and impact are proportional to the helix angle which is proportional to the pitch (Liu et al. 2015) (see section 1.1.3.1)]. This consequently increased the coalescence or re-agglomeration of granules resulting in an increase in the granule size. This indicates that it is possible to preferentially design/control the granules size by selecting suitable screw configuration.

Figure 4-29 shows that the granule structure became more porous and fragmented in the case of LPCE than that in SPCE at the end of the screw configuration. The results support the size observations as shown in Figure 4-28 where the granules became bigger due to the increase in coalescence or re-agglomeration of granules. They observed that the apparent porosity of granules decreases with increasing pitch of the screw element. This may be due to the difference in the powder materials used in the experiments of the two studies.

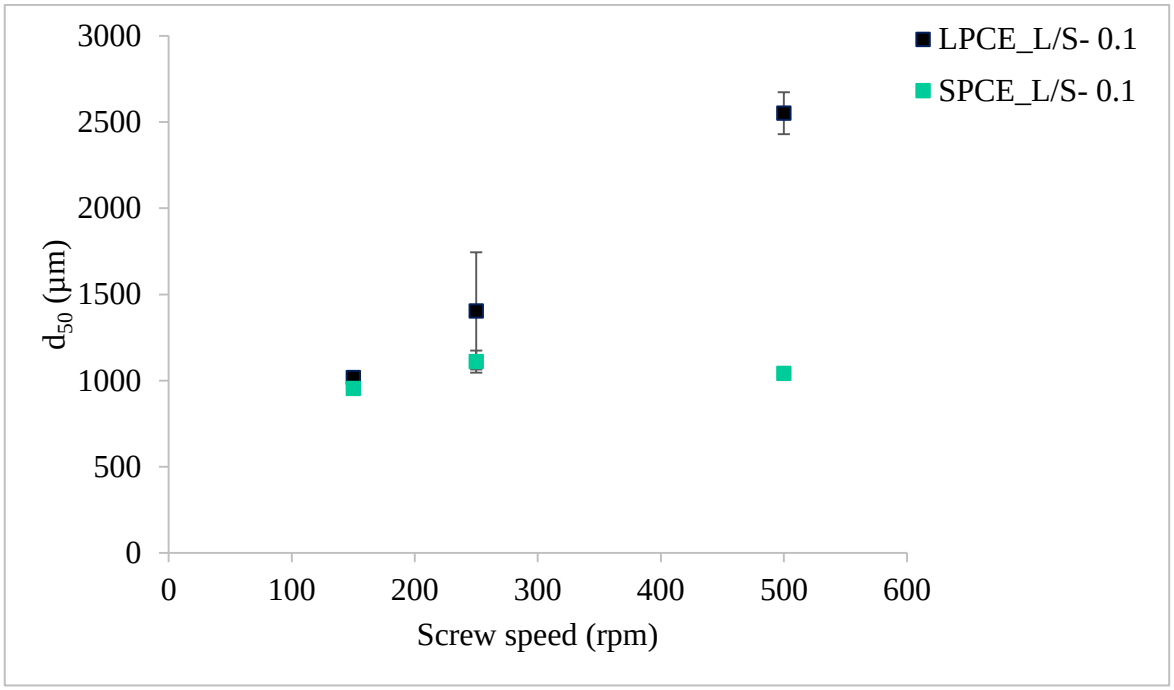

Figure 4-28 Median size of granules produced using different conveying elements at L/S- 0.1 at different screw speeds

(a) (b)

Figure 4-29 X-ray tomographic images of granules using (a) SPCE at L/S- 0.1, screw speed of 250 rpm (b) LPCE at L/S- 0.1, screw speed of 250 rpm

4.5 CONCLUSION

In this study, the specific roles and effects of the screw elements in the formation of lactose granules along the barrel length in the TSG were studied in more detail by incremental addition of the elements in the screw configuration. The stepwise transition of granules in the block of elements was captured successfully. It was observed that the number of kneading and conveying elements in the screw configuration and the L/S can dictate the granule formation and granule attributes. The effect becomes more pronounced as the L/S increases. For instance, increasing the number of kneading elements at higher L/S, the granules became bigger in size, elongated, smoother and denser due to high shear and compaction forces acting on them. However, addition of conveying elements after kneading elements in the screw configuration resulted in decrease in size and elongation of granules due to shearing and cutting action of the conveying elements. Increasing the channel width of conveying elements resulted in an increase in granule size and structural voids indicating the coalescence or re-agglomeration. It was also found that with increase in L/S, the granule size increases. The effect of varying screw speed on granule size was generally dictated by the amount of liquid or L/S and the number of kneading and conveying elements in the screw configuration. It was possible to produce small size granules with monomodal and narrow distribution and less elongation by understanding the effect of kneading and conveying element on the twin screw granulation. In other words, same powder could be granulated to produce granules with different size and distribution. The findings in this study are based on one specific formulation (lactose). The other formulation or materials can also be tested using similar approach to investigate their performance in the TSG.

Furthermore, it was noticed from this chapter that the median granule size started increasing from screw configuration with 8KE (at various L/S and screw speed). Additionally, it was noticed that using 8KE in screw configuration produced granule with median size ranging from ~800 µm to ~1900 µm (at various L/S and screw speed). It was hypothesised that by placing SPCE after 8KE in the screw configuration can be more effective in producing granules with reduced size compared to that with the use of 12KE which produced larger and denser granules due to additional shear and compaction forces imparted on the granules. Furthermore, using 8KE with SPCE can potentially reduce the

median granule size obtained using 8KE without SPCE and provide a median size that is close to a commonly used range (~1000 µm) in the literature for tabletting (Vercruysse et al. 2012, Vercruysse et al. 2015, Vanhoorne, Janssens, et al. 2016, Meier et al. 2017). Hence, it was decided to use the screw configuration with 8KE with SPCE (placed towards downstream of screw configuration) as a standard screw configuration in further chapters in this thesis.

5 EFFECTS OF VARYING BARREL TEMPERATURE

5.1 ABSTRACT

This chapter is focused on developing an understanding about effect of varying temperature of barrel compartments along the length of the granulator on the size, shape and moisture content of granules produced from lactose powder. The experiments were carried out at two different L/S and screw speeds. The study revealed that lower L/S and higher barrel temperature are important process conditions in the twin screw wet granulation as they directly influence the granule attributes.

5.2 INTRODUCTION

In the present study, lactose powder is considered as a powder in twin screw wet granulation. As mentioned in section 3.1, lactose is one of the most popular and commonly used materials for several industrial applications including pharmaceutical granules and tablets production. It is partially soluble in water at room temperature. Figure 5-1 shows the change in solubility of lactose with increase in temperature (DFEpharma 2013).

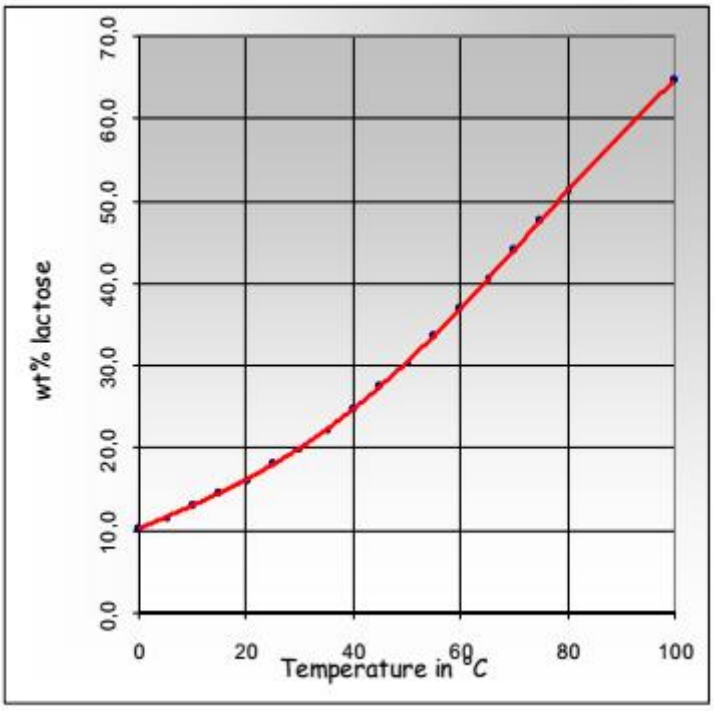

Figure 5-1 Solubility of lactose as a function of temperature (DFEpharma 2013)

Solubility of lactose powder also varies with the particle size. Smaller particles of lactose dissolve rapidly due to availability of higher surface area. The coarse particles dissolve slowly than the smaller particles. The small particles dissolve faster at high temperature which proves useful during granulation as it helps attaching coarse particles together. The soluble lactose has a useful property of recrystallization after drying which is helpful in making the granules stronger post-granulation. The higher barrel temperature is helpful for quicker dissolution and drying. Therefore, the barrel or vessel temperature is very important factor during granulation.

Twin screw granulator at the research facility within The University of Sheffield, is equipped with a temperature controller that regulates the temperature in each compartment of the barrel. The barrel temperature can be varied from 5°C to 300°C. This can offer a great opportunity in changing and controlling the granule properties. However, this important process variable in twin screw wet granulation has received very limited attention (Vercruysse et al. 2012). On the other hand, the barrel temperature is used as process variable in the extrusion cooking of food (Han 1969, Bilgi Boyaci et al. 2012, Dhenge et al. 2012a) and hot melt extrusion of polymers (Hirth et al. 2014).

Therefore, the objective of this work was to understand the effect of changing temperature of the barrel along the length of the granulator (temperature of barrel compartments) on median size, size distribution, shape and moisture content of the granules so produced and thereby improving these granule properties.

5.3 MATERIAL AND METHODS

5.3.1 Materials

5.3.1.1 Powder, granulating liquid and granulation equipment

Lactose powder was granulated using red dyed distilled water (as a granulation liquid) using TSG.

5.3.1.2 Screw configuration

The screw configurations used in this study is shown in Figure 5-2. The granulation was carried out at full length of the screw.

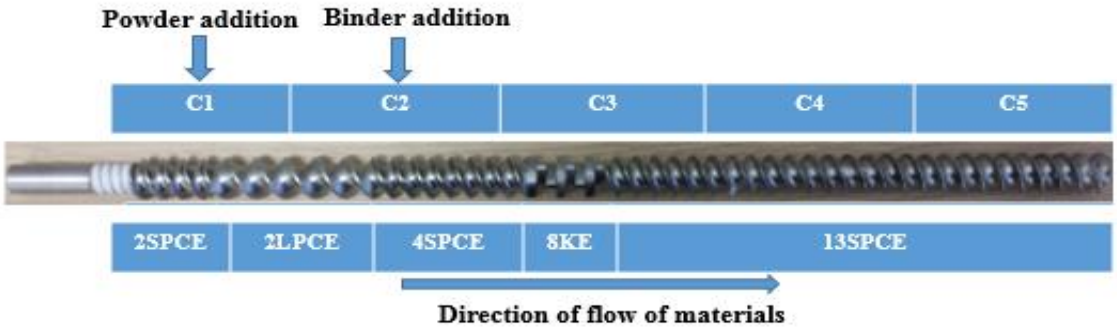

Figure 5-2 Screw configuration with various compartments

5.3.2 Methods

5.3.2.1 Preparation of granules

The experimental plan is shown in Table 5-1. The lactose granules were produced at two screw speeds: 250 rpm and 400 rpm and two L/S: 0.1 and 0.15 at constant powder feed rate of 2 kg/h. At each condition, the temperature of the barrel compartment was varied. The temperature in the initial compartments (C1 and C2) was kept low and fixed because powder and liquid were fed from these two zones. Various temperature settings are denoted with T1, T2, T3 and T4. T1 was considered as a reference condition where temperature of all the compartment was 25°C. The temperature in C3 for T1, T2, T3 and T4 was 25°C, 30°C, 45°C and 100°C respectively. The temperature in the compartment C4 and C5 was 100°C for T2, T3 and T4. In total, 16 experiments (3 repetitions of each experiment) were carried out.

Table 5-1 Experimental plan

Temperature setting	Powder feed rate (kg/h)	Screw speed (rpm)	L/S	Temperature (°C)				
				C1	C2	C3	C4	C5
T1	2	250, 400	0.1, 0.15	25	25	25	25	25
T2		250, 400	0.1, 0.15	25	25	30	100	100
T3		250, 400	0.1, 0.15	25	25	45	100	100
T4		250, 400	0.1, 0.15	25	25	100	100	100

5.3.2.2 Analysis of granules

5.3.2.2.1 Size and shape analysis of granules

The granules were air dried at room temperature for 48 h and then size and shape of the granules was analysed. The size of granules was analysed using the Camsizer. The shape of the granules was studied using Zeiss stereo microscope.

5.3.2.2.2 Moisture content measurement

The freshly produced granules (5 g) from each process condition were collected and their moisture content was measured using Infrared Moisture Analyser, MA35 (Sartorius, UK, Ltd.). This equipment works on loss-on-drying principle.

5.4 RESULTS AND DISCUSSION

Figure 5-3 shows moisture content (%) of granules produced at different temperatures at different L/S (0.048 and 0.1) and screw speed (250 rpm and 400 rpm). The moisture content (%) of granules decreased with increasing temperature from T1 to T4. This indicates that as the granules (~5g) were being collected from the TSG discharge end for the moisture measurement, the granules produced at higher temperature lost some moisture in a short period of time compared to those produced at lower temperature. Figure 5-4 shows the median granule size at different temperature settings (T1, T2, T3 and T4) at two L/S (0.1 and 0.15) at 250 rpm and 450 rpm. It was observed that at L/S of 0.1 (at both screw speed of 250 rpm and 450 rpm), the median granule size did not vary significantly as the temperature increased from T1 to T4. The result of limited change in the granule size with increasing screw speed agrees with the previous studies (Yao et al. 2008). At L/S of 0.15, increasing screw speed from 250 rpm to 450 rpm resulted in limited influence on the granule size which was similar to the observation at relatively lower L/S of 0.1 but the magnitudes of median size were high. Unlike L/S of 0.1, increasing barrel temperature settings from T1 to T4 at higher L/S of 0.15, increased the granule size. This may be explained as follows. As per the experimental setting, the temperature in C3, C4 and C5 compartments in T2, T3, and T4 was higher than that at T1. Based on observations in chapter 4 (see section 1.1.1), when granules progress along the barrel length i.e. from compartment 1 to 5, granules grow or break

depending on amount of liquid added. In the present study, temperature of the compartment along the barrel length was increased at specific L/S. Increasing temperature at L/S of 0.1, resulted in evaporation of water from the granules (also evidenced from reduction in the moisture content, as presented in Figure 5-3) leaving them relatively dry and friable. The dry and friable granules broke due to shearing and attrition from the screws and the size decreased. This effect was overturned at higher L/S of 0.15 and granule size increased as more liquid was available to allow granule growth. This can be explained further using lactose solubility curve shown in Figure 5-1 which shows that the 17% concentration of lactose at 25°C corresponds to 0.2g in $1cm^3$. Similarly, L/S of 0.1 is equivalent to 11.1% and L/S of 0.15 is equivalent to 17.6%. Although, the maximum amount of material that could theoretically dissolve is still small compared to the actual amount present even at high L/S and high temperature, the effect of high L/S could be seen on granule size. The rate of change of dissolution and viscosity changed with increasing barrel temperature from 25°C to 100°C (Figure 5-1). At higher temperature the powder dissolution increases while the viscosity of powder-liquid system decreased. The powder became more wetted with increase in temperature at L/S, hence, it resulted in increase in the granule size.

Figure 5-5 and Figure 5-6 show the granule size distribution at L/S 0.1 and 0.15 respectively. L/S of 0.1, resulted in monomodal and narrow granules size distribution. Due to increase in liquid availability and thus higher solubility at the L/S of 0.15, the lactose powder became over wetted producing bigger granules with wide size distribution.

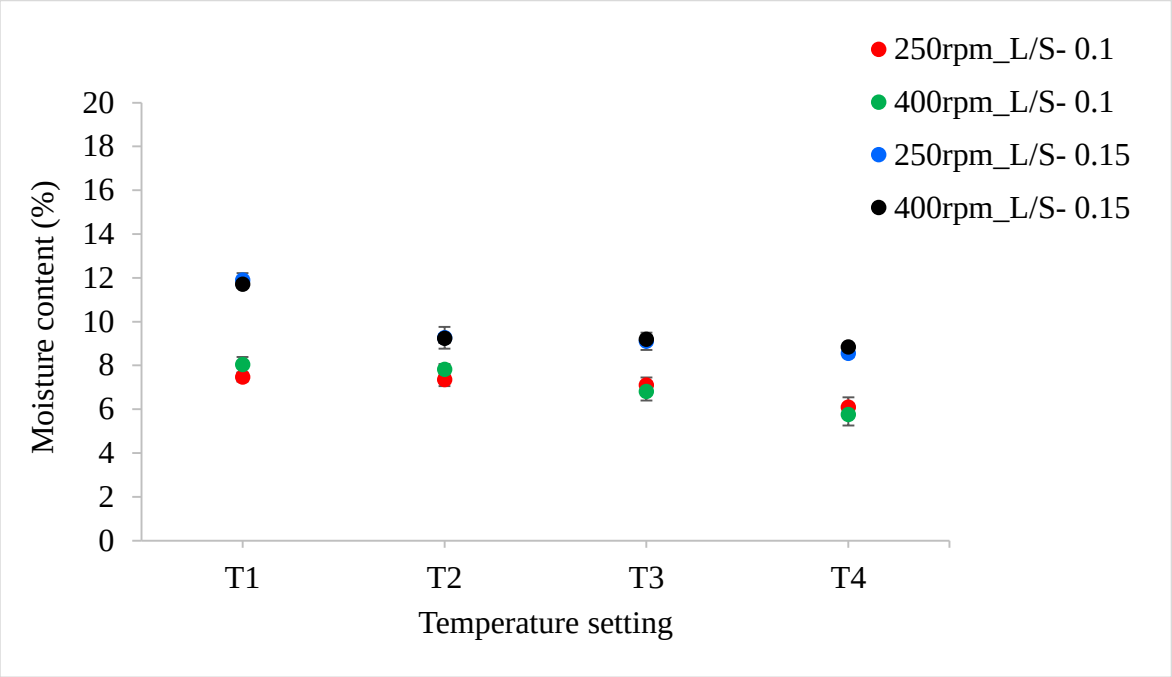

Figure 5-3 Moisture content (%) of granules produced at different temperature settings

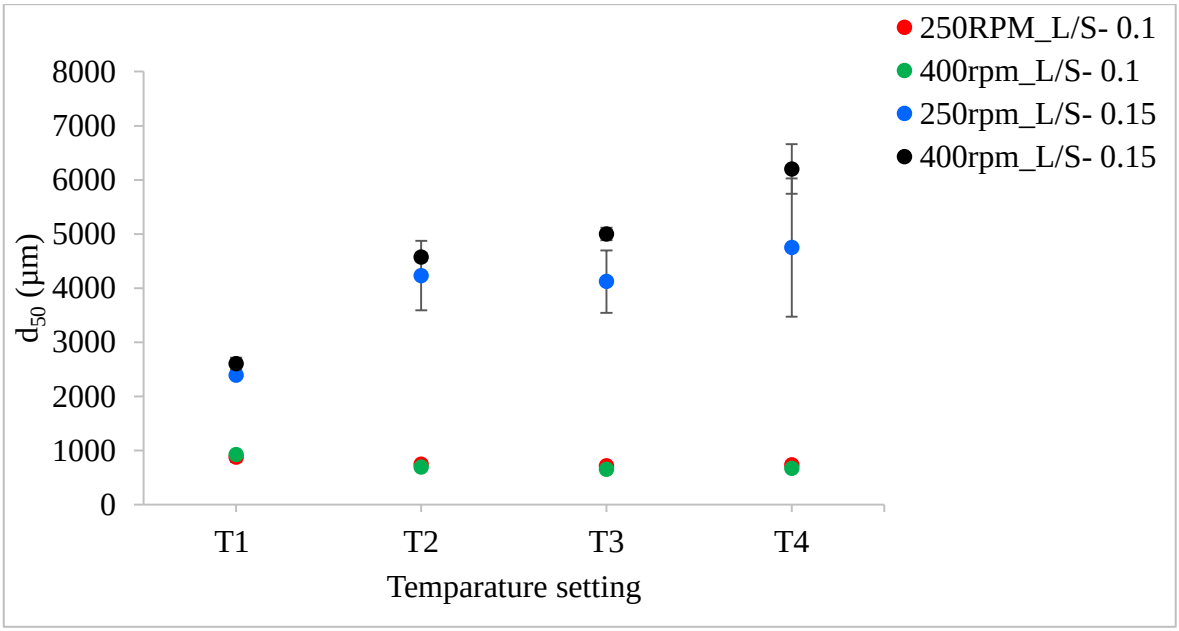

Figure 5-4 Median size of granules at T1, T2, T3 and T4 at different speeds (250 rpm and 400 rpm) at various L/S (0.1 and 0.15)

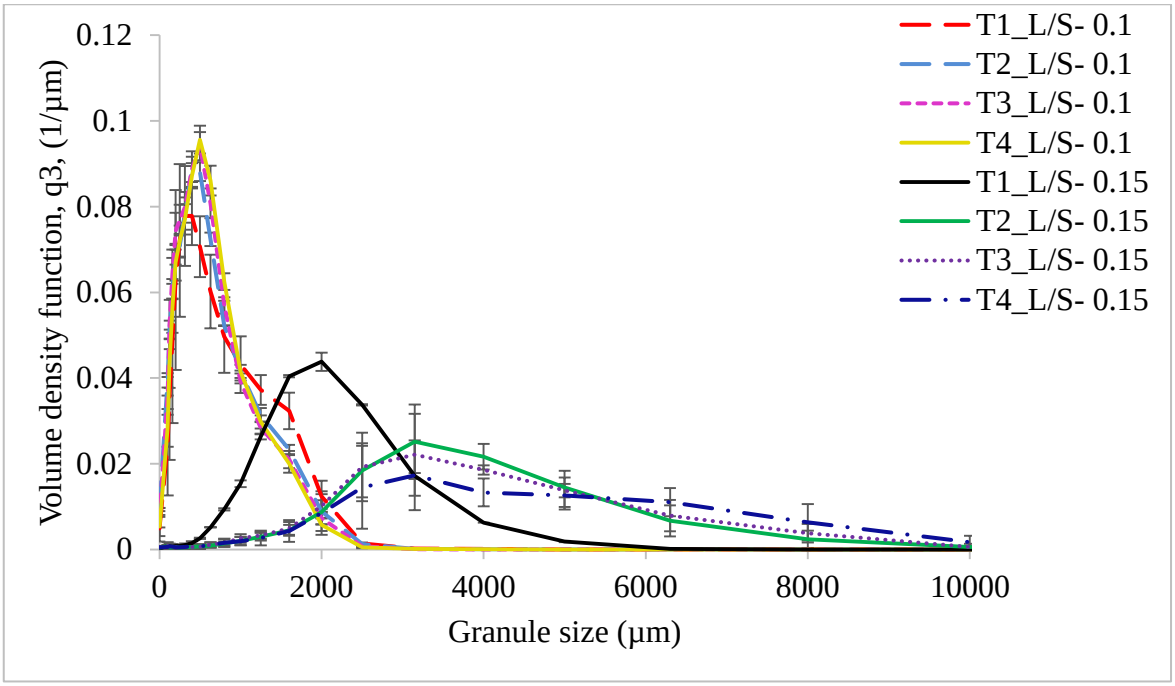

Figure 5-5 Size distribution at T1, T2, T3 and T4 at 250 rpm at L/S of 0.1 and 0.15

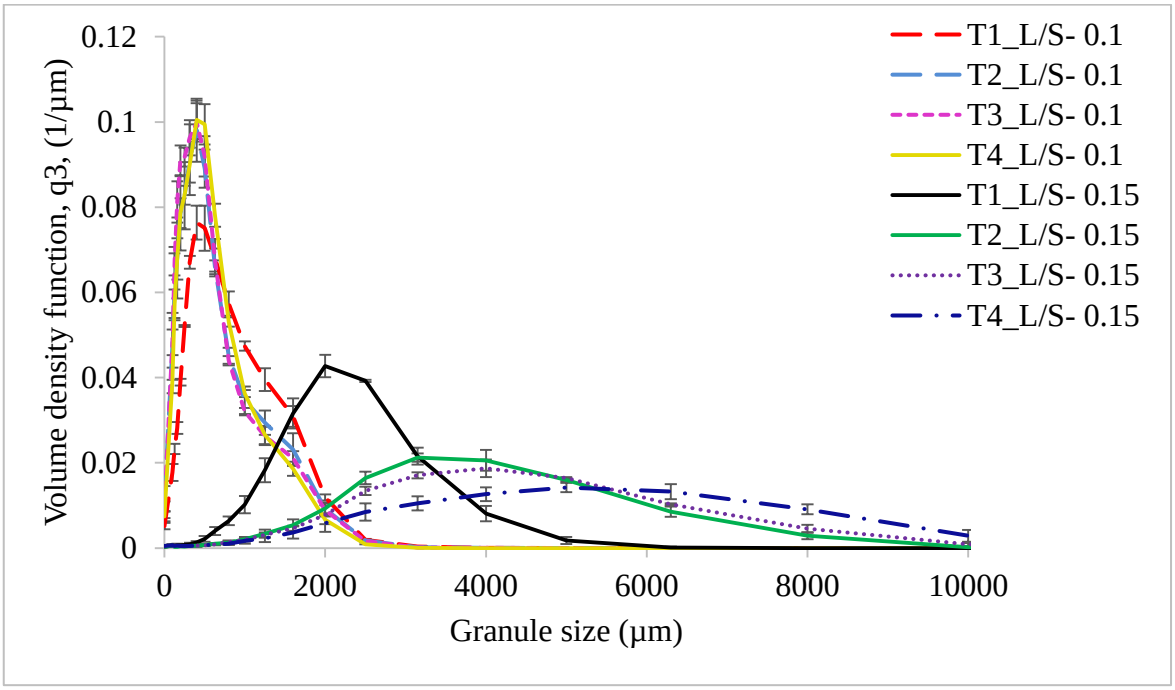

Figure 5-6 Size distribution at T1, T2, T3 and T4 at 400 rpm at L/S of 0.1 and 0.15

Figure 5-7 and Figure 5-8 show the microscopic images of granules produced at different temperature settings (T1, T2, T3 and T4) at 250 rpm and 400 rpm respectively.

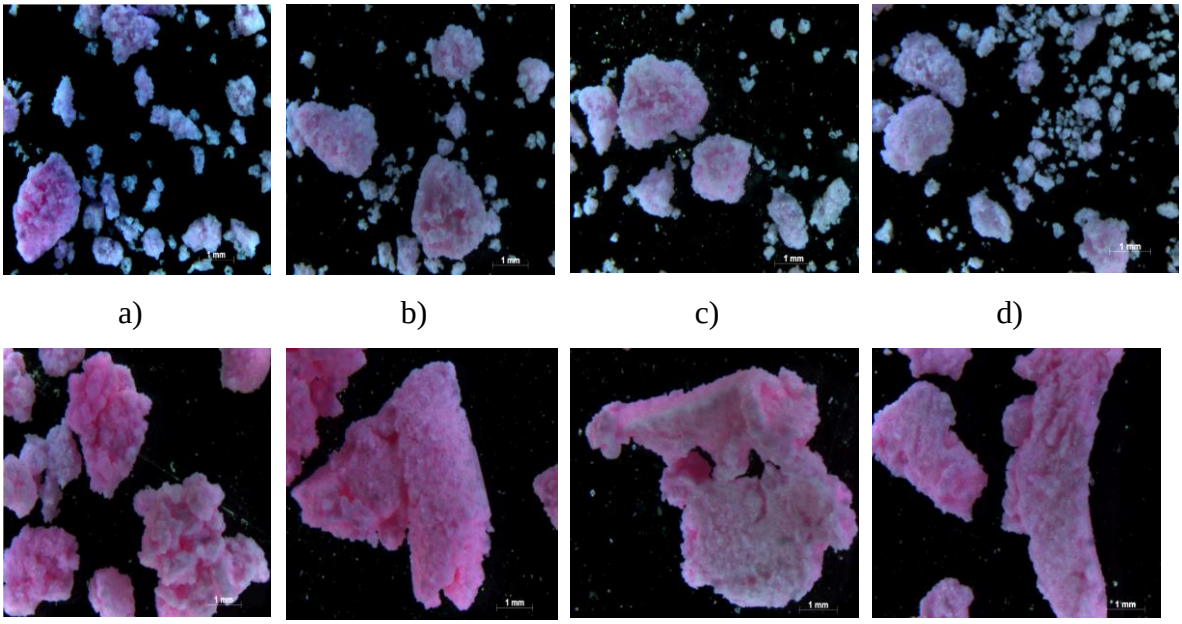

a) b) c) d)

e) f) g) h)

Figure 5-7 Microscopic images of granules produced at 250 rpm at various temperature settings at different L/S
a) T1, L/S- 0.1; b) T2, L/S- 0.1; c) T3, L/S- 0.1; d) T4, L/S- 0.1;
e) T1, L/S- 0.15; f) T2, L/S- 0.15; g) T3, L/S- 0.15; h) T4, L/S- 0.15

As shown in Figure 5-7 and Figure 5-8, at both screw speeds the granule shape supported the median granule size and size distribution observations. The granules produced at L/S of 0.1 (at all temperature settings and at both screw speeds) were more spherical and smaller compared to that at L/S of 0.15. Temperature settings had minimum influence on the granule shape at L/S of 0.1. However, increasing L/S to 0.15 increase granule elongation due to coalescence. The granule elongation increased with increasing temperature.

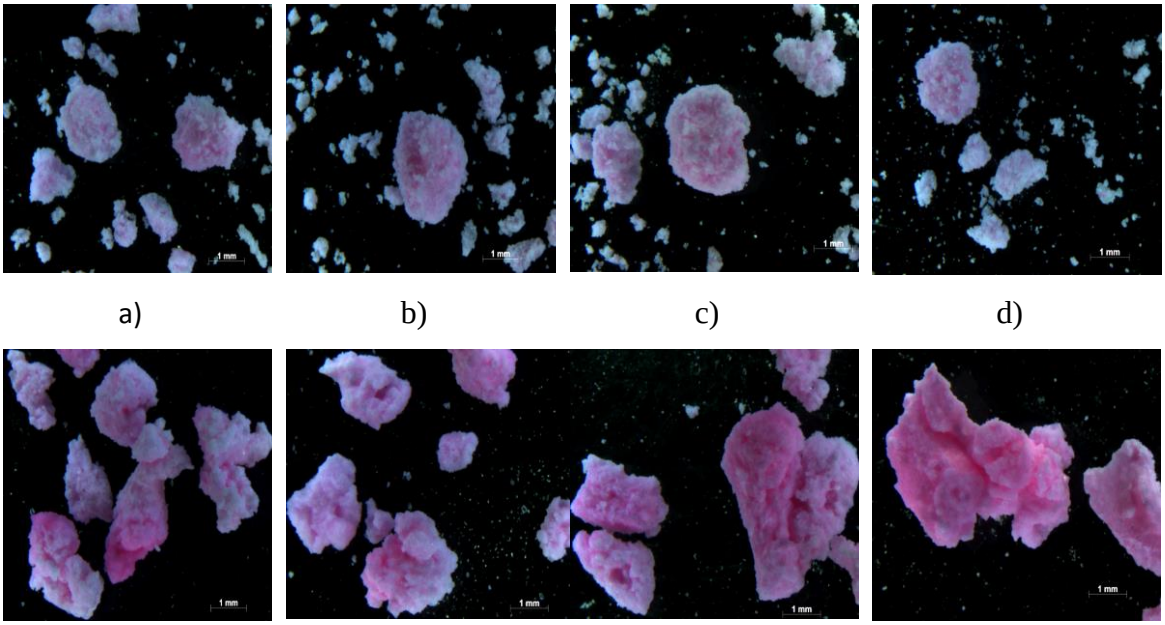

a) b) c) d)

e) f) g) h)

Figure 5-8 Microscopic images of granules produced at 400 rpm at various temperature settings at different L/S
a) T1, L/S- 0.1; b) T2, L/S- 0.1; c) T3, L/S- 0.1; d) T4, L/S- 0.1;
e) T1, L/S- 0.15; f) T2, L/S- 0.15; g) T3, L/S- 0.15; h) T4, L/S- 0.15

5.5 CONCLUSION

This study revealed that L/S and barrel temperature are important input variables in the twin screw wet granulation as they directly impact the granule attributes and moisture content. It was concluded that the L/S is more dominating variable as it promoted production of small size, regularly shaped (less elongated) granules and narrow and monomodal size distribution even at higher barrel temperature settings (at L/S of 0.1). Granulating lactose powder at higher barrel temperature helped granules to dry faster. Hence, produced granules with lower moisture content i.e. faster drying post-granulation. Although, this may be considered as an advantage, the impact of elevated temperature on heat sensitive powders needs to be considered during product development.

6 EFFECTS OF FILL LEVEL

6.1 ABSTRACT

This chapter is focussed on investigating the influence of varying barrel fill levels (for lactose powder) on the mean residence time and granule properties (median size, size distribution and shape) and tensile strength of tablets. Specific feed load (SFL) (powder feed rate divided by screw speed) was considered as a surrogate for the barrel fill level. Lactose was granulated at varying fill levels (SFL) at two different L/S. It was observed that the mean residence time decreased with increasing fill level at both L/S. Finally, it was demonstrated that by controlling barrel fill level the granule size, shape and tablet tensile strength can be maintained at specific L/S.

6.2 INTRODUCTION

As mentioned in section (chapter 2) the most of the studies done so far on twin screw granulation have concentrated on the parametric evaluations which developed a generalised understanding of the effects of process (powder feed rate, liquid to solid ratio (L/S) and screw speed) and formulation variables (viscosity of the liquid binder) on the dependant variables (torque and residence time) and granule properties (median size, size distribution, shape and strength). The most of these studies considered ‘changing one single variable at a time’ (COST) approach (in other words, univariate approach) (as described by Vercruysse et al. (2012)) which means that either powder feed rate or L/S or screw speed was varied at time during particular run or experiment. For instance, some studies concentrated on understanding the effects of varying powder feed rate (Djuric et al. 2009, Dhenge et al. 2010, Djuric and Kleinebudde 2010, Thompson and Sun 2010, Dhenge et al. 2011, Dhenge et al. 2013, Kumar, Dhondt, et al. 2016, Liu et al. 2017) some on L/S (Dhenge et al. 2012b, El Hagrasy et al. 2013b, Kumar, Dhondt, et al. 2016, Liu et al. 2017) while some on binder viscosity (Keleb et al. 2002, Keleb et al. 2004, Dhenge et al. 2012b, Lee et al. 2012, Dhenge et al. 2013, Yu et al. 2014, Saleh et al. 2015a) and screw speed (Keleb et al. 2004, Djuric et al. 2009, Dhenge et al. 2010, Djuric and Kleinebudde 2010, Thompson and Sun 2010, Lee et al. 2012, Kumar, Vercruysse, Toiviainen, et al. 2014) and some on screw configuration (Djuric and Kleinebudde 2010, Thompson and Sun 2010, Dhenge et al. 2012a, El Hagrasy

et al. 2013b, Yu et al. 2014, Lute et al. 2016, Meier et al. 2016, Pradhan et al. 2017). From these COST based studies, it is clear that this approach results in the production of granules with varying attributes (e.g. size, shape, structure). It is known from some studies that variables such as powder feed rate and screw speed impact the dependent or secondary variable i.e. barrel fill/channel fill in the twin screw granulator which influences the granule size, density and structure. For instance, Dhenge et al. (2010) separately investigated the effect of powder feed rate and screw speed on the dependant or secondary variables viz., mean residence time and torque which was considered as an indication of barrel fill level and thereby of shear and compaction forces experienced by powder inside the barrel. The effect of such secondary variables was further correlated with the granule properties. For instance, production of large and porous granules at low powder feed rate was attributed to longer residence time and low barrel fill which led to the restricted particle packing (low shear and compaction forces) as indicated by the low torque. In case of varying screw speed, Dhenge et al. (2010), noticed that median granule size did not change significantly despite noticeable difference in the residence time, barrel fill and torque. However, it was mentioned that the minor differences in the granule size at lower and higher screw speeds were due to the difference in the duration of powder-liquid interactions and the extent of shear and compaction in the granulator.

In twin screw granulation, dimensionless volumetric fill level (i.e. the ratio of the volume occupied by wet mass of powder to the total available volume of screw channel) was estimated by Dhenge et al. (2013) and Lee et al. (2012) in their studies to understand the material occupancy inside the granulator. Although, barrel fill is important in twin screw granulation, only few studies considered barrel fill as a primary or input variable (Thompson and Sun 2010, Lute et al. 2015, Gorringe et al. 2017, Meier et al. 2017, Osorio et al. 2017). The term barrel fill level in twin screw granulation is not surprisingly derived from twin screw extrusion. Kohlgrüber (2008) described the barrel fill level in the form of a dimensionless input variable where with powder mass flow rate was divided by the multiplication of screw speed, screw diameter and the material density in the denominator. Kolter et al. (2012) described specific feed load (non dimensionless) as mass flow divided by the screw speed (i.e. mass transported per screw revolution). Osorio et al. (2017) further explored Kohlgrüber (2008)'s approach of a dimensionless input parameter i.e. powder feed

number (PFN) in their attempt to develop scale up rules for three different size twin screw granulators. They noticed that PFN is not sufficiently applicable in 'scaling up' different size granulators, however, it is useful in 'scaling out' using same granulator. The 'scaling out' in their study meant increasing the production rate or throughput in a granulator. They used one specific powder in their study. Gorringe et al. (2017) investigated influence of volumetric channel fill of conveying elements (i.e. total volumetric fraction of conveying element channels filled with powder) on the granule attributes. They did not consider kneading zone in calculation assuming that it mostly appears filled with powder mass at most of the process parameters. Furthermore, Gorringe et al. (2017) used two powders in their study, however, they did not compare the formulations using same screw configuration. Lute et al. (2015) and Meier et al. (2017) utilised Kolter et al. (2012)'s approach of SFL for one specific drug formulation as surrogate parameter for the volumetric fill level and highlighted that there is need for the further research on this topic. Furthermore, Kumar, Alakarjula, et al. (2016) also emphasized the need for finding and understanding the balance between the powder feed rate and screw speed in order to control the desired product attributes.

This study attempts to further the understanding of the influence of two surrogates for the overall barrel fill level or occupancy i.e. specific feed load (SFL) and powder feed number (PFN) on the mean residence time and thereby the granulation performance of lactose powder using 16 mm TSG. The PFN approach was used in this study along with SFL as it allows comparison between the different powders unlike SFL.

6.3 MATERIALS AND METHODS

6.3.1 Materials

6.3.1.1 Powder, granulating liquid, granulation equipment and screw configuration

Lactose powder (bulk density- 0.5 g/ml) was granulated using distilled water as a granulating liquid in twin screw granulator. The screw configuration used for the experiments was kept constant and is shown in chapter 5.3.1.2 (Figure 5-2). The free volume

(68.67 cm^3) for the screw configuration under consideration was determined using Screw Configuration software from ThermoFisher.

6.3.2 Methods

6.3.2.1 Experimental design

The experimental design for the granulation of lactose powder at varying specific feed load (in g) (SFL) (Eq. 4) and powder feed number (PFN) (-) (Eq. 5) (Osorio et al. 2017) is shown in Table 6-1.

$$SFL(g) = \frac{Powder\ feed\ rate}{Screw\ speed} \quad \text{Eq. 4}$$

$$PFN(-) = \frac{Powder\ feed\ rate}{Powder\ bulk\ density \times Screw\ speed \times Free\ space\ in\ granulator} \quad \text{Eq. 5}$$

Three different SFLs: 0.041, 0.083, 0.166 and were selected to cover lower and upper extremes of the granulation conditions while studying the effect on the residence time and granule attributes. Each time the powder feed rate and screw speed were adjusted accordingly to maintain the SFL. Liquid feed rate was also changed according to powder feed rate in order to maintain respective L/S. PFN was further obtained from SFL using powder bulk density and free space in the twin screw granulator. The liquid was also adjusted to maintain the L/S of 0.048 and 0.1. The barrel temperature was maintained at 25°C (in all barrel compartments). In total, 54 experiments (18 runs × 3 repeats of each experiment) were carried out.

The suitability of SFN or PFN while using different materials (varying bulk densities) was not previously investigated. Hence, this chapter was aimed to test the suitability of these two variables.

Table 6-1 Experimental plan

Expt. no.	Powder feed rate (g/min)	Screw speed (rpm)	SFL (g)	PFN (-) for Lactose	MRT(s) for L/S 0.048	MRT(s) for L/S 0.1
1	6.25	150	0.041	1.71403E-05	14.7436	24.1879
2	10.4167	250			9.2536	12.7324
3	16.6667	400			8.6306	7.2210
4	20.8333	500			7.6831	6.1423
5	31.25	750			4.4866	3.1603
6	41.6667	1000			3.1247	1.5871
7	12.5	150	0.083	3.42806E-05	10.1585	11.8261
8	20.8333	250			5.1881	6.5341
9	33.3333	400			3.5382	4.3143
10	41.6667	500			1.5841	3.3178
11	62.5	750			1.4801	1.8681
12	83.3333	1000			1.2488	0.7139
13	25	150	0.166	6.85612E-05	6.1108	4.2565
14	41.6667	250			3.5668	2.8062
15	66.6667	400			2.5669	1.4937
16	83.3333	500			1.5841	1.0994
17	125	750			1.1844	0.4832
18	166.667	1000			0.6051	0.3608

6.3.2.2 Mean residence time (MRT) measurement

The mean residence time (MRT) was determined using UV spectrophotometer. The blue dye, Patent Blue (Acid Blue 1, Sigma-Aldrich) was used as a tracer. About 30 mg of dye was introduced into the inlet of the granulator after stabilisation of the operating conditions. The samples at the granulator exit were collected at every 5 s until the tracer disappeared in the collected granules. The 2 g of granules were dissolved in 50 ml of distilled water and keep it aside for 2 h. The concentration of tracer in the granules was determined using a UV spectrophotometer at a wavelength λ = 635 nm. The residence time distribution was described by differential outlet age function [$E(t)$] to give the variation of tracer concentration at the exit (Eq. 6).

The *E(t)* curves represent the variation of the tracer concentration with time at the exit. Typical curve for *E(t)* is shown in Appendix 12.3.1 in Figure 12-10.

The area under the curve of the graph of the tracer concentration against the time was normalised by dividing the concentration values by the total area under the curve giving the *E(t)* values:

$$E(t) = \frac{C}{\int_0^\infty C dt} \cong \frac{C}{\sum_0^\infty C_i \Delta t_i} \quad \text{Eq. 6}$$

where, C is tracer concentration appearing at the exit at time t. The MRT (t_m) can be calculated using Eq. 7.

$$t_m = \int_0^\infty tE(t)dt \cong \frac{\sum t_i C_i \Delta t_i}{\sum C_i \Delta t_i} \quad \text{Eq. 7}$$

6.3.2.3 Peak shear rate

The effect of screw speed was also explained in terms of peak shear rate exerted on the powder mass during granulation. The peak shear rate of twin screw granulator was calculated by the following equation.

$$Peak\ shear\ rate = \frac{\pi \times D \times N}{h \times 60} \quad \text{Eq. 8}$$

where, D- Screw diameter (15.6 mm)

N- Screw speed (rpm)

h- Overflight gap (0.2 mm)

6.3.2.4 Size and shape analysis of granules

The granules were air dried at room temperature for 48 h and then size and shape of the granules were analysed. The size of granules was analysed using the Camsizer. The shape of the granules was studied using Keyence microscope.

6.4 RESULTS AND DISCUSSION

6.4.1 Effect of varying SFL-PFN at different screw speed and L/S on mean residence time

The focus of this work (on varying SFL-PFN), was actually on understanding the effect of increasing screw speed at low and high powder feed rates which is further linked to finding the balance between these two process variables to achieve desired product attributes. For this reason, Figure 6-1 is plotted as varying screw speed vs the MRT measured while granulating lactose powder at low L/S of 0.048 at different fill levels [SFL (0.041-0.166) and PFN (1.71403E-05- 6.85612E-05)].

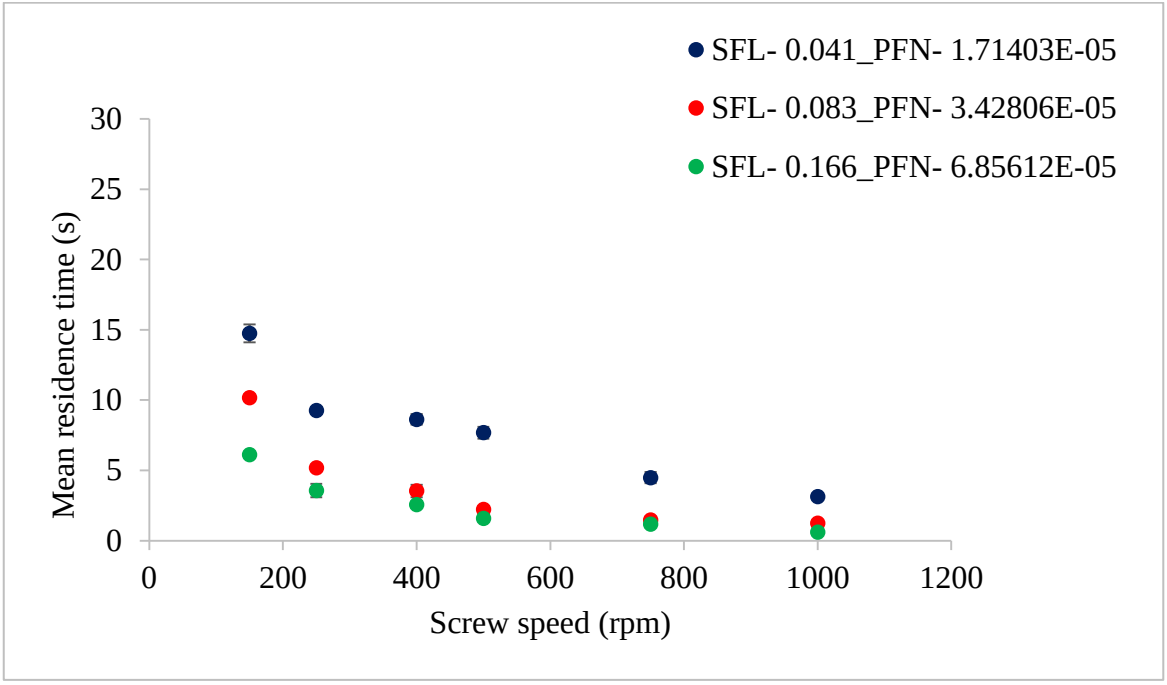

Figure 6-1 Mean residence time at different SFL-PFN at varying screw speed (L/S-0.048)

From Figure 6-1, it can be noticed that the MRT decreases with increase in the screw speed at all fill levels i.e. SFL-PFN. This is because, increasing screw speed increases axial transport rate (drag flow rate) of the powder thereby reducing the time the powder spend in the granulator. Comparing three SFL-PFN at various screw speeds, the highest MRT was at

the lowest SFN-PFN (SFL-0.041 and PFN-1.71403E-05) (i.e. low fill level). This is because the powder throughput or conveyance force (Dhenge et al. 2010) which push the powder in the forward direction in the granulator, was low at low fill level at all screw speeds. In other words, at varying screw speed at a constant powder feed rate, the screws rotate relatively starved of powder and hence, the fill level and throughput force mostly depend on the increase in the powder feed rate. In the present study, the powder feed rate was also varied in proportion to the increase in the screw speed in order to get same specific feed load. Therefore, the relative barrel fill level and thereby the throughput force assumedly remains low for low SFL-PFN at all screw speeds. Thus, the throughput force at low SFN-PFN was relatively low and MRT was high compared to that at higher SFL-PFN conditions where the powder feed rate was higher for corresponding screw speed.

As the fill level increased (i.e. SFL-0.083 and PFN-3.42806E-05), the MRT decreased sharply due to increase in the throughput force. Further increase in the fill level (i.e. SFL-0.166 and PFN-6.85612E-05) did not necessarily result in significant decline in the MRT especially at and after screw speed of 400 rpm compared to that at SFL-0.083 and PFN-3.42806E-05. This indicates that there is a limit for MRT to change with increase in SFL-PFN. As mentioned earlier, in the present study the powder feed rate is varied in proportion to the screw speed in order to maintain same specific feed load or fill level. At SFL-0.166 and PFN-6.85612E-05, the powder feed rate was high but so was the corresponding screw speed. Thus, screw speed could not control the fill level and thereby throughput force and MRT alone as the powder feed rate was also changing at same time.

Similar trend was noticed at L/S of 0.1, however, the magnitude of MRT was higher. This is expected since the powder was more wetted compared to that at L/S of 0.048 which led to powder becoming more sluggish/cohesive or sticky and thus flowing slower in the granulator.

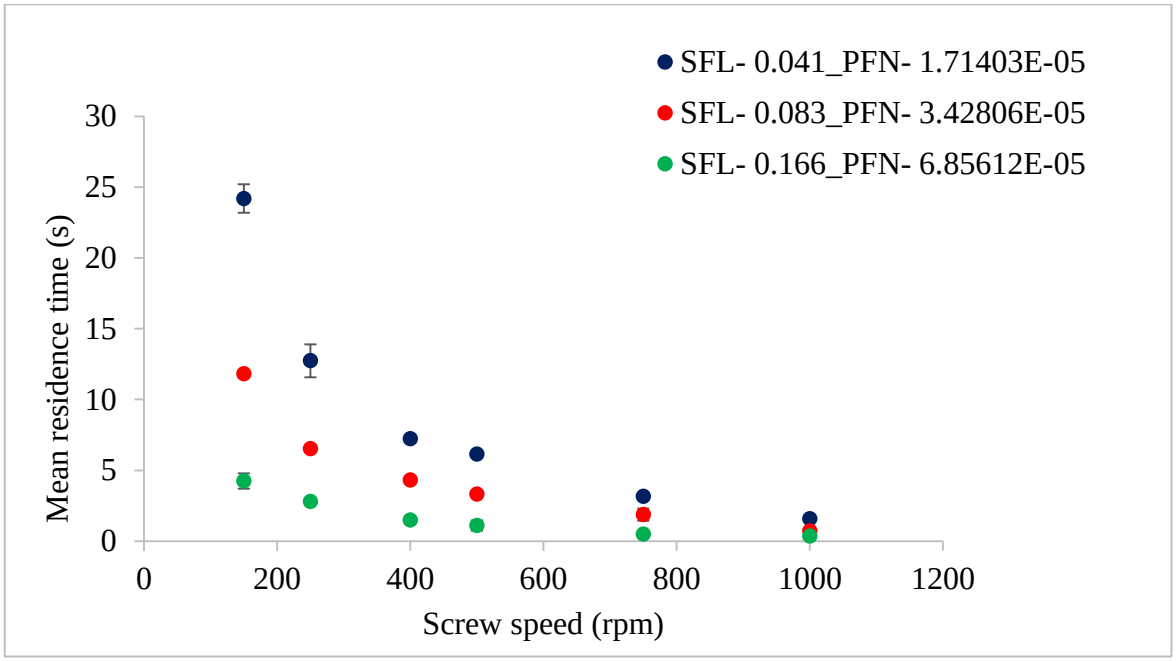

Figure 6-2 Mean residence time at different SFL-PFN at varying screw speed (L/S-0.1)

Also to check how constant fill level is at constant SFN, material hold up (Powder feed rate × MRT) was plotted vs screw speed as shown in Figure 6-3 and Figure 6-4.

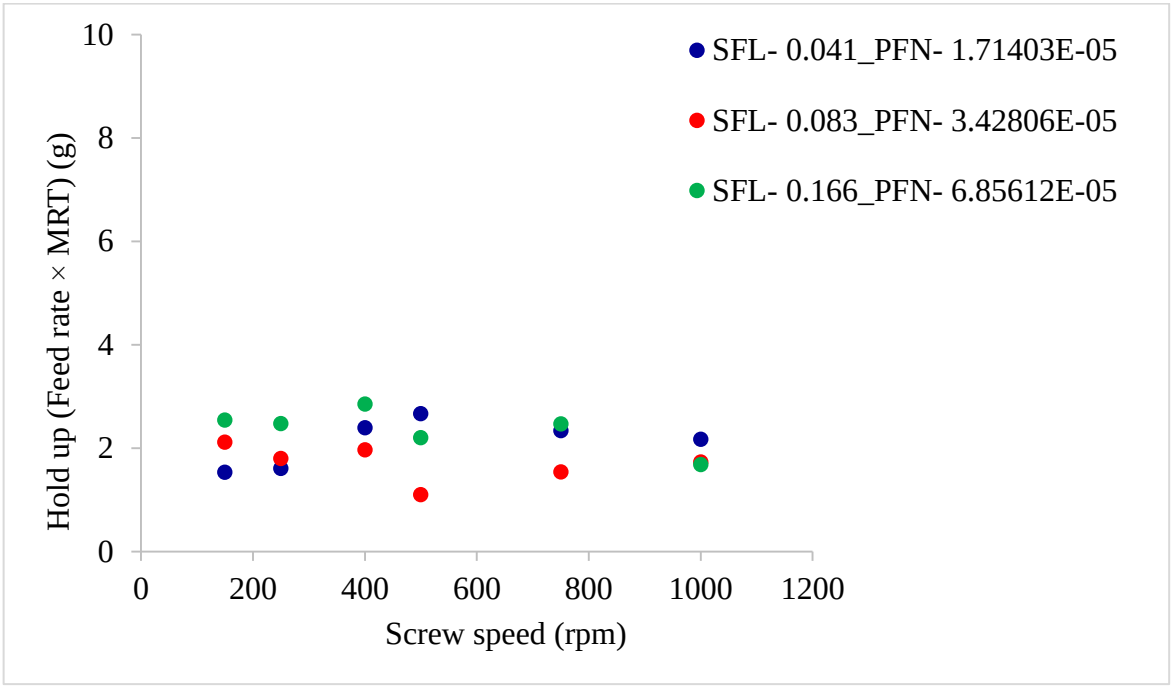

Figure 6-3 Material hold up vs screw speed at L/S- 0.048

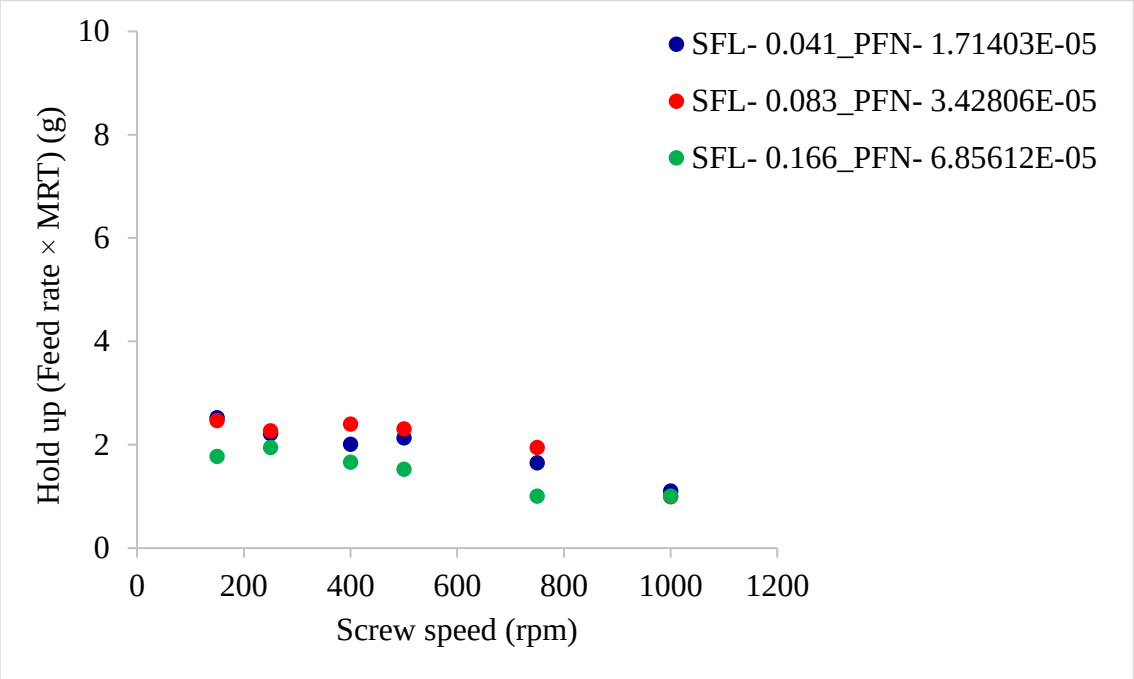

Figure 6-4 Material hold up vs screw speed at L/S- 0.1

6.4.2 Effect of varying SFL-PFN at different screw speed and L/S on granule size

Figure 6-5 shows effect of varying screw speed (i.e. peak shear rates) on median granule size while granulating lactose powder at low L/S of 0.048 at different fill levels [SFL (0.041-0.166) and PFN (1.71403E-05- 6.85612E-05)]. It can be noticed from figure that increasing SFN-PFN i.e. fill level at varying screw speed had no significant impact on the granule size. The median granule size ranged from 585 µm to 758 µm. Considering, the difference in the mean residence time at varying fill levels at L/S 0.048, it was expected that granule size will also change in response to the screw speed and fill level. However, it was not the case, meaning the difference in the mean residence time does not necessarily translate into the change in the granule size when the SFL is kept constant. The granule size can be maintained similar at varying screw speed and fill level for simple powder such as lactose in this case. The results can be explained by understanding the effect of screw speed on the wet granules flow within the twin screw granulator. At low screw speed the peak shear rate, axial mixing and the centrifugal force acting on the wet granules are low (despite keeping same SFL at varying screw speeds). This means the transport of wet granules in granulator was mainly

through convective type of transport and less dispersive one (Kumar, Alakarjula, et al. 2016). This means the more dominant mechanism by which the granules are formed, broken and or reformed is the shearing of wet granules between the screw channel-barrel surface and in the intermeshing area between the screws. The sheared, broken and surface wetted granules undergo sequence of coalescence (granules attach each other as they flow in close proximity at low screw speed) followed by breakage on the surface of the screw as it pushes the granules to opposite screw through intermeshing area in between.

As the screw speed increases the peak shear rate, axial mixing and the centrifugal force acting on the wet granules increase too. High centrifugal force means more dispersion transport and stronger impact of wet granules on the barrel wall, intermeshing section and on the other wet granules. So, the more dominant mechanism at high screw speed is impact of wet granules. Some extent of shearing of wet granules in the intermeshing area between the screws also takes place at higher screw speed.

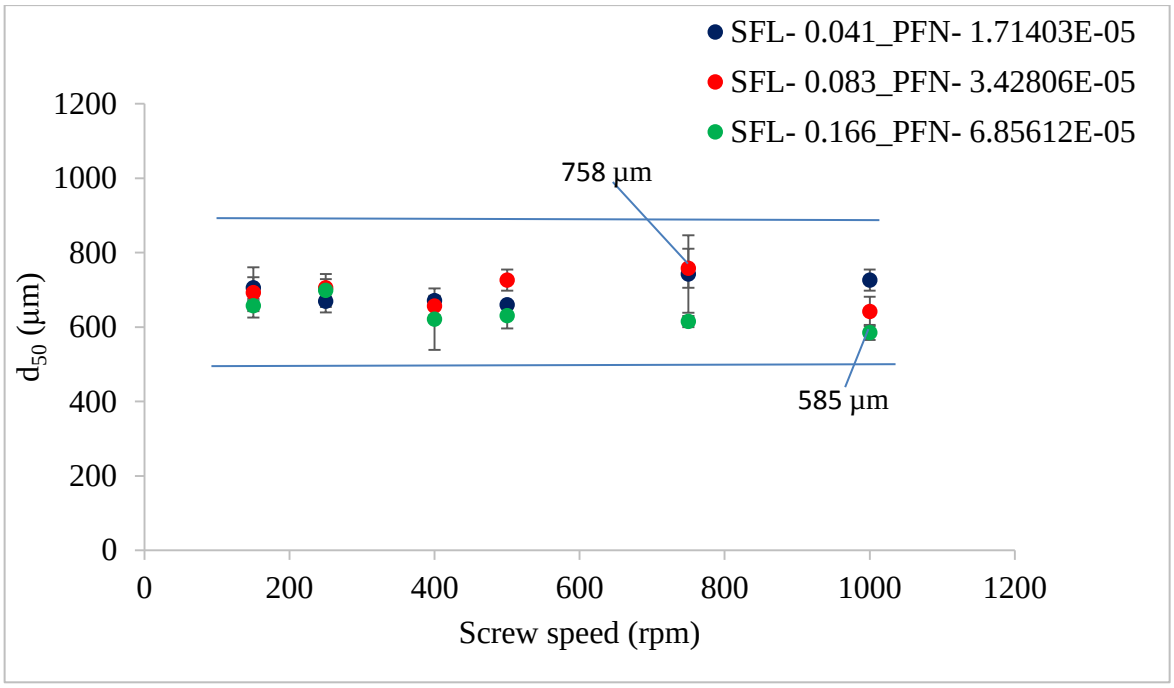

Figure 6-5 Median granule size at different SFL-PFN at varying screw speed (L/S- 0.048)

Figure 6-6 shows effect of varying screw speed on median granule size while granulating lactose powder at relatively higher L/S of 0.1 at different fill levels [SFL (0.041-0.166) and PFN (1.71403E-05- 6.85612E-05)]. Similar to low L/S (0.048), granule size was maintained

at varying fill level (SFN-PFN) at different screw speeds. However, over all granule size increased and ranged from 829 µm to 1021 µm. This is expected since the amount of liquid available for the particles to attach was higher at L/S of 0.1. Comparison of results at varying fill levels at different L/S, it is clear that amount of liquid added is critical input variable to be considered while increasing the throughput of the twin screw granulator by increasing the SFL-PFN.

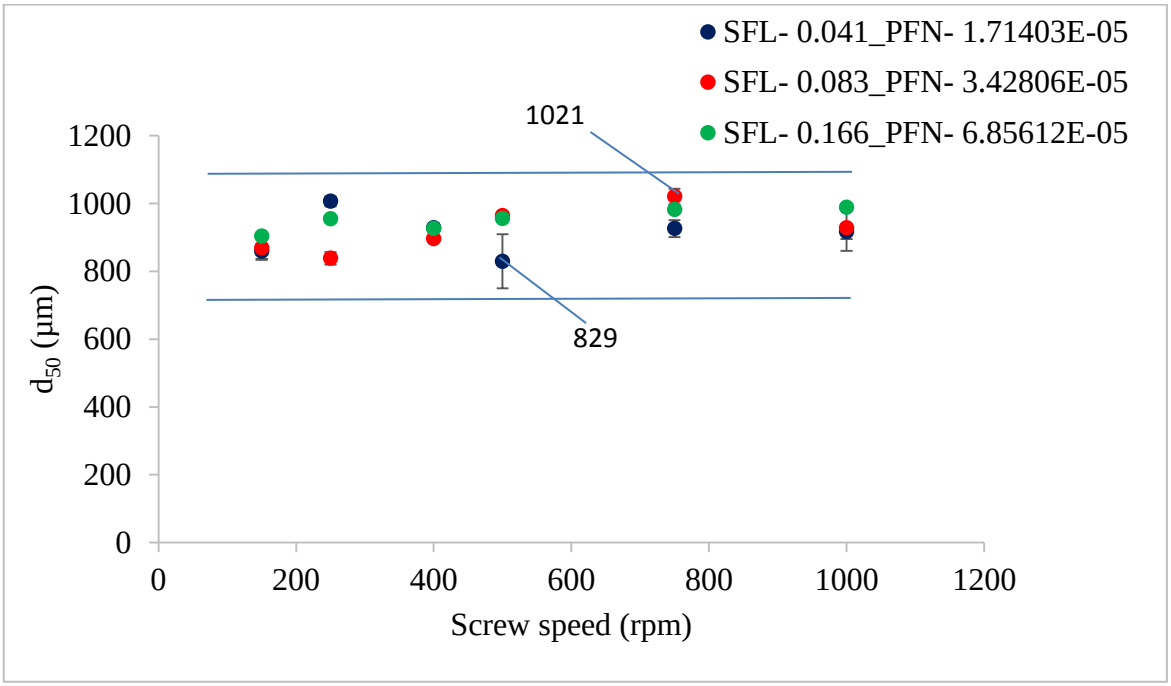

Figure 6-6 Median granule size at different SFL-PFN at varying screw speed (L/S- 0.1)

Figure 6-7 and Figure 6-8 show the size distribution of granules produced at varying SFL-PFN at L/S of 0.048 and 0.1 respectively. The size distribution results support the median granule size data obtained at respective L/S. The low L/S (0.048) produced granules with some degree of bimodality (i.e. mixed amounts of small and bigger granules). On the contrary, higher L/S (0.1) resulted in granules with monomodal size distribution i.e. less proportion of smaller granules compared to that at low L/S.

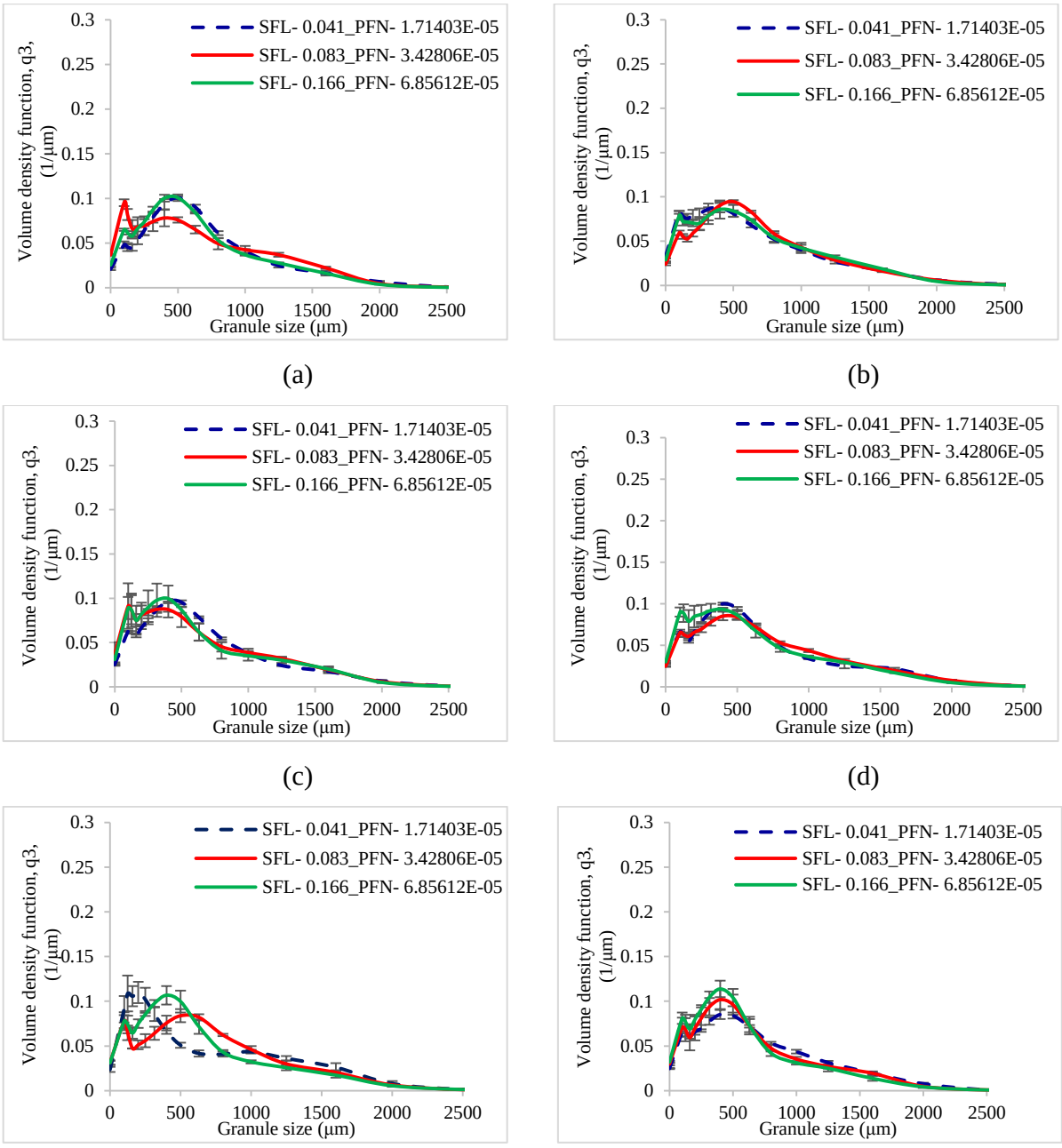

Figure 6-7 Granule size distribution at different SFL-PFN at varying screw speed (at L/S-0.048) (a) 150 rpm (b) 250 rpm (c) 400 rpm (d) 500 rpm (e) 750 rpm (f) 1000 rpm

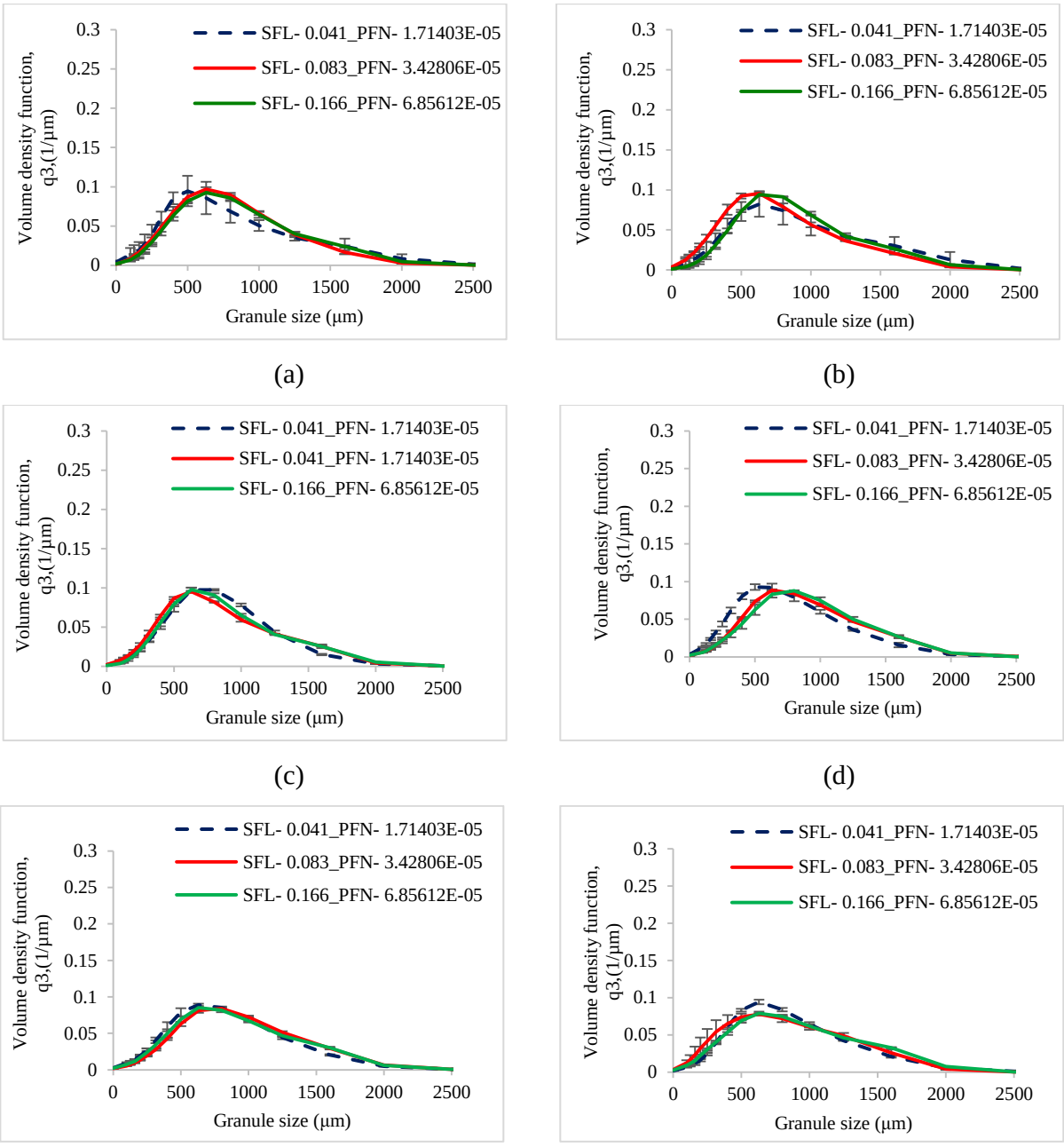

Figure 6-8 Granule size distribution at different SFL-PFN at varying screw speed (at L/S-0.1) (a) 150 rpm (b) 250 rpm (c) 400 rpm (d) 500 rpm (e) 750 rpm (f) 1000 rpm

6.4.3 Effect of varying SFL-PFN at different screw speed and L/S on granule shape

Figure 6-9(a)-(f) show the shape of granules produced at varying screw speed (i.e. peak shear rates) at low L/S (0.048) and low SFL (0.041) and PFN (1.71403E-05). It can be observed from figure that the granule shape (elongation) do not vary noticeably as the screw speed is increased at constant fill level (SFL-PFN). In all cases a mixed proportion of large (elongated) and small granules were produced. These microscopic results support the size distribution of granules at varying fill level where no significant difference in size was observed.

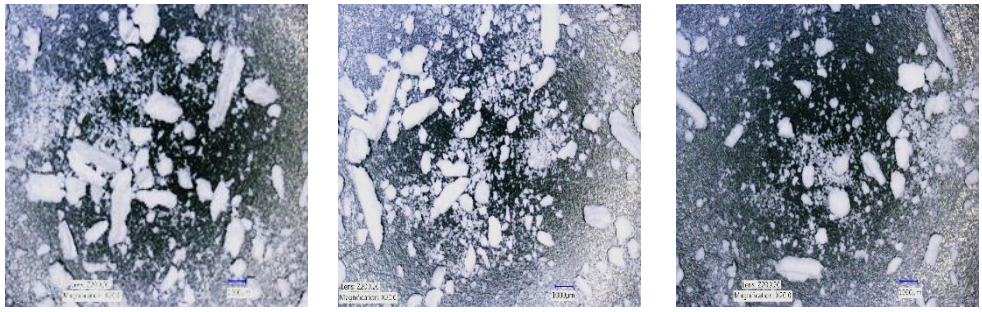

150rpm (a) | 250rpm (b) | 400rpm (c)

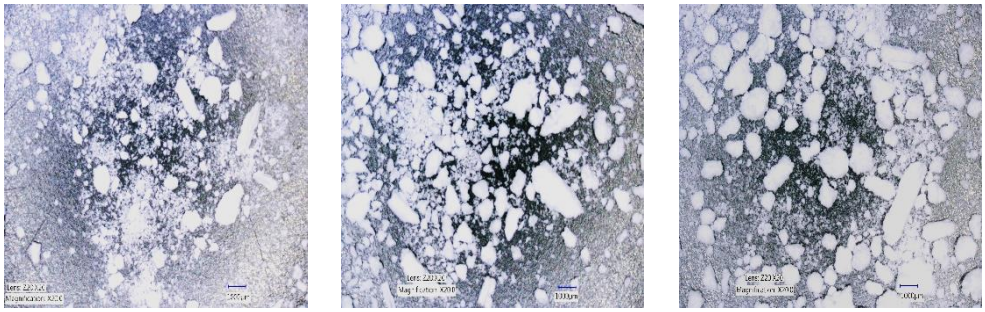

500rpm (d) | 750rpm (e) | 1000rpm (f)

Figure 6-9 Microscopic images of granules produced at varying screw speed at SFL-0.041 and PFN- 1.71403E-05 (L/S- 0.048)

Similar observations were noted for higher fill level of SFL-0.083, PFN- 3.42806E-05 and SFL-0.166, PFN- 6.85612E-05 (see appendix 12.3.1). The results again support the granule size distribution results presented in Figure 6-7-Figure 6-9. Microscopic images for L/S of

0.1 at varying screw speed and SFL-PFN also exhibited similar shape characteristic (see appendix 12.3.1).

6.4.4 Effect of varying SFL-PFN at different screw speed and L/S on tablet tensile strength

Figure 6-10-Figure 6-15 shows the tensile strength of tablets of granules (with varying size ranges) produced at varying screw speed, L/S and SFL-PFN. It can be observed from figures that tablet strength does not vary with significantly at all conditions. The results support the data for granule size which also did not vary at various conditions. Interestingly, granule size ranges also did not affect the tablet tensile strength. It is likely that the compression force used during tablet making was high enough to overcome the strength of all granules in various ranges used in the study.

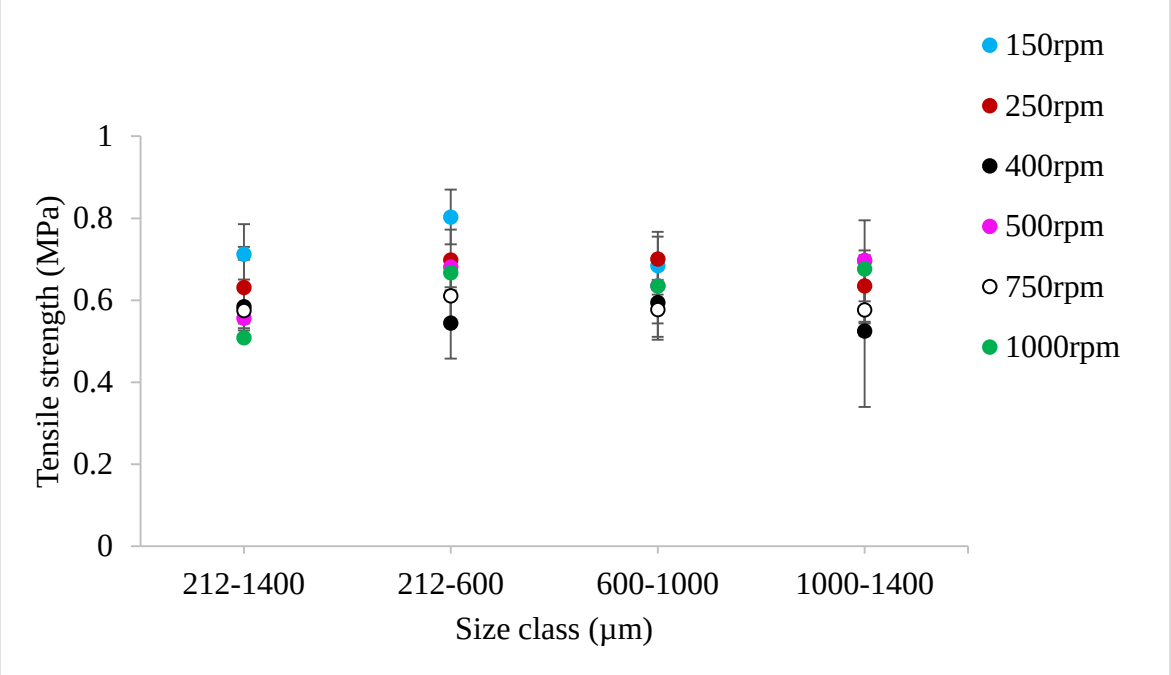

Figure 6-10 Tensile strength of tablets of granules produced at varying screw speed at SFL- 0.041 and PFN- 1.71403E-05 (L/S- 0.048)

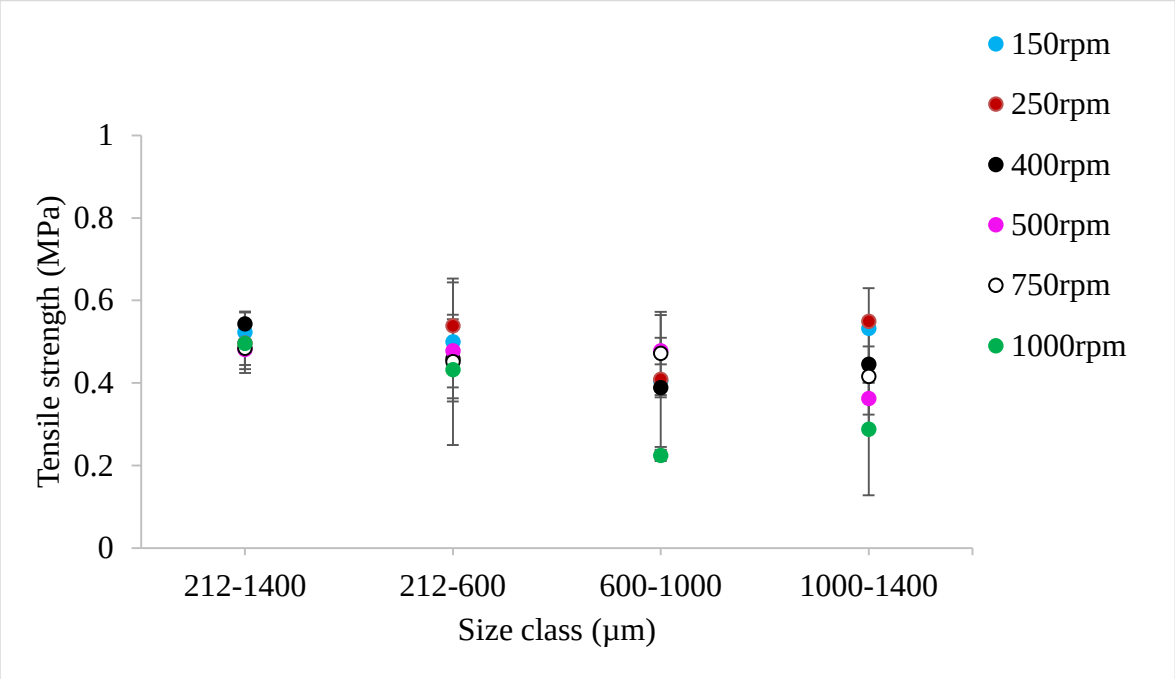

Figure 6-11 Tensile strength of tablets of granules produced at varying screw speed at SFL- 0.041 and PFN- 1.71403E-05 (L/S- 0.1)

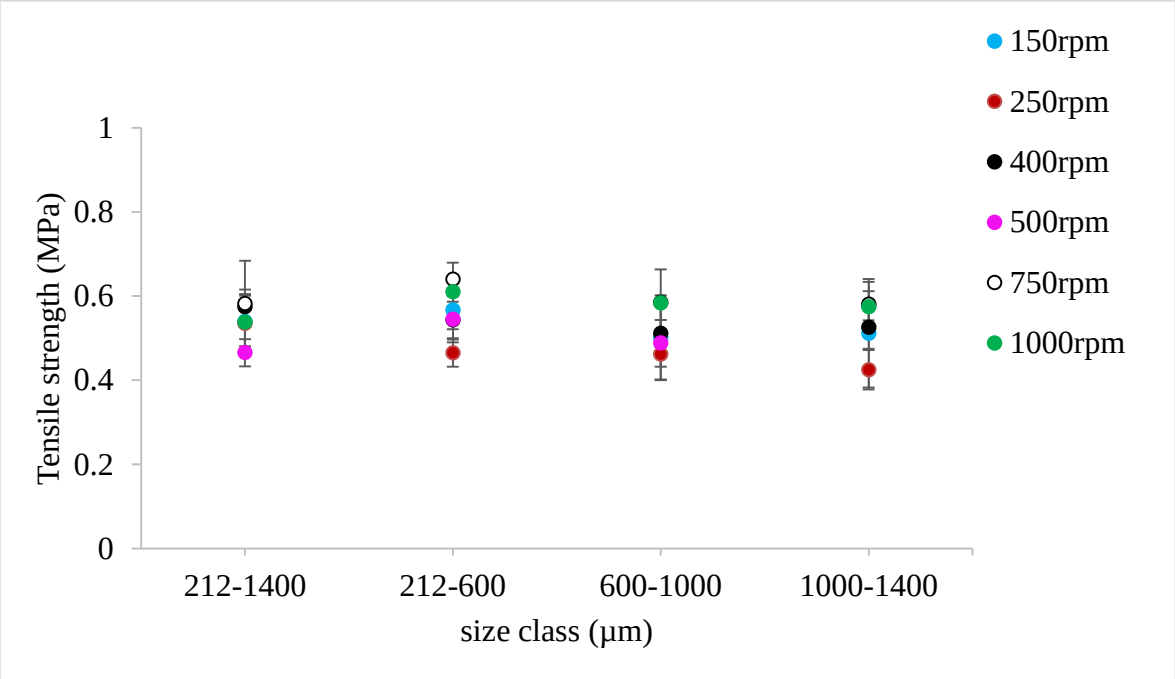

Figure 6-12 Tensile strength of tablets of granules produced at varying screw speed at SFL- 0.083 and PFN- 3.42806E-05 (L/S- 0.048)

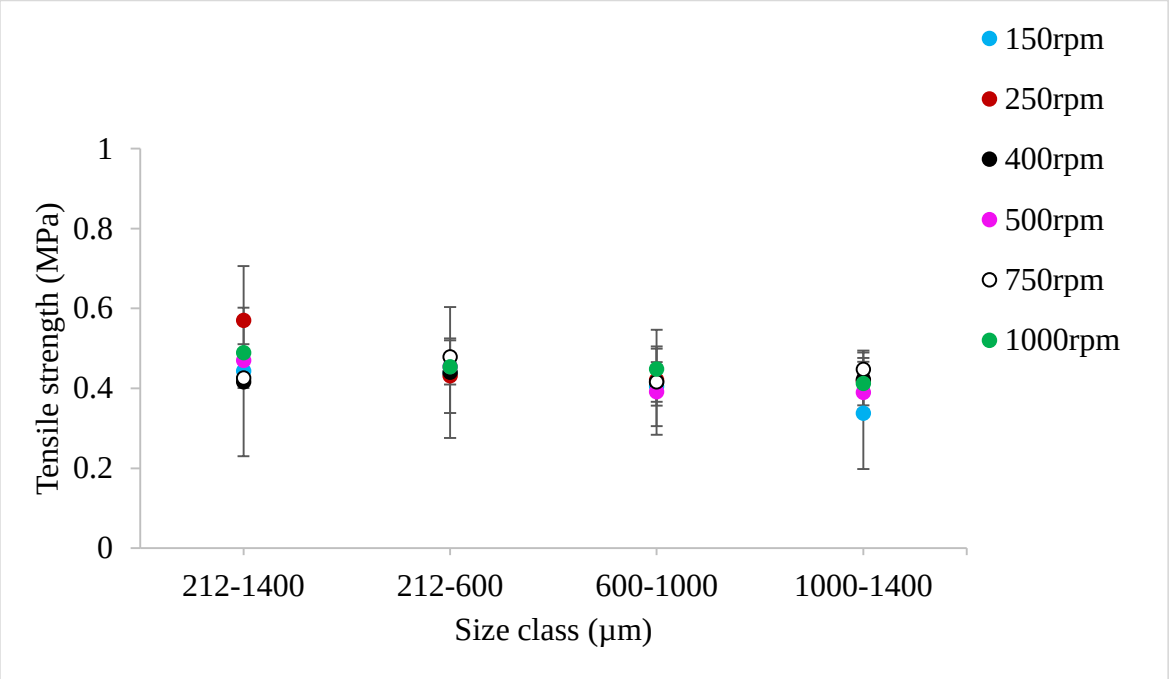

Figure 6-13 Tensile strength of tablets of granules produced at varying screw speed at SFL- 0.083 and PFN- 3.42806E-05 (L/S- 0.1)

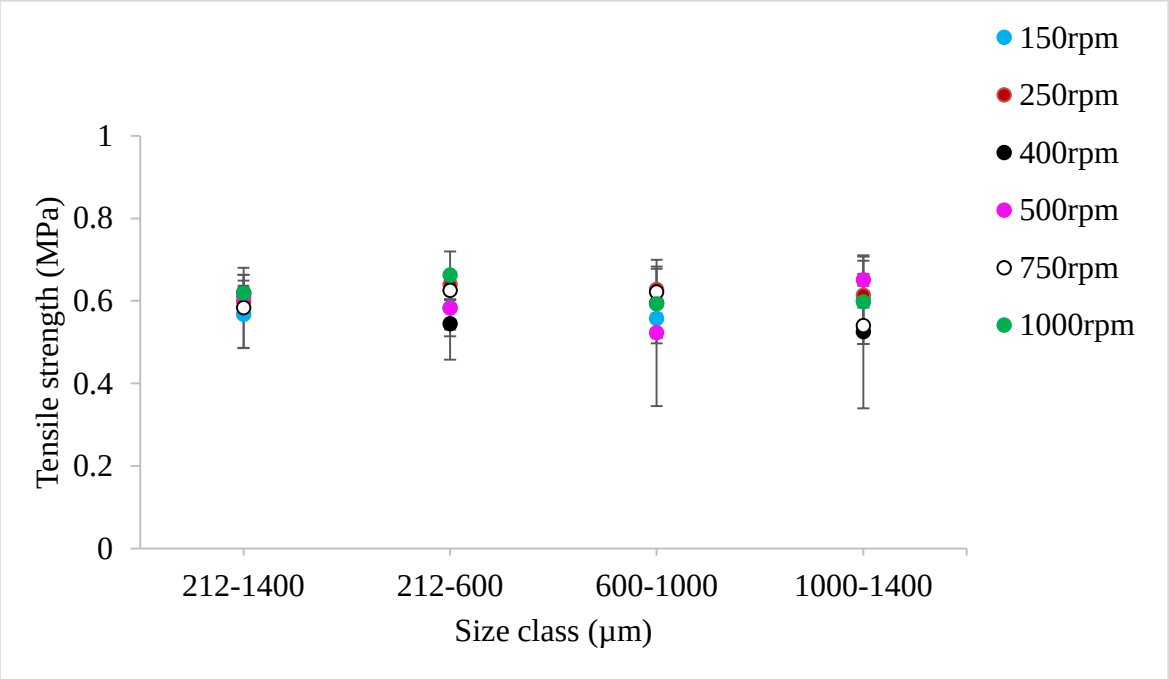

Figure 6-14 Tensile strength of tablets of granules produced at varying screw speed at SFL- 0.166 and PFN- 6.85612E-05 (L/S- 0.048)

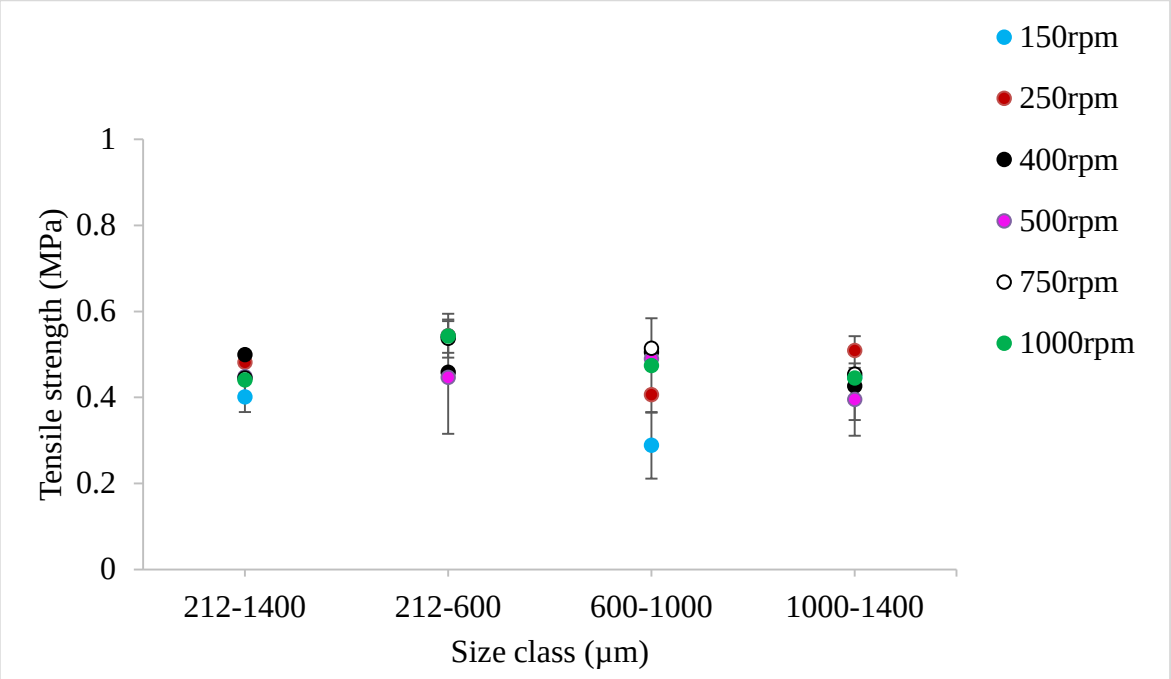

Figure 6-15 Tensile strength of tablets of granules produced at varying screw speed at SFL- 0.166 and PFN- 6.85612E-05 (L/S- 0.1)

6.5 CONCLUSION

From this study it was shown that the powder properties (solubility) and L/S are important variables while investigating effect of barrel fill level on granule properties especially granule size. In case of lactose, effect of changing SFL and PFN (barrel fill level) seemed to be insignificant for water soluble powders such as lactose. The solubility of powder played more important role than fill level. Furthermore, increasing SFL and PFN would increase the fill level in the kneading zone. However, the conveying elements following the kneading zone cut and chopped oversized granules to maintain the granule size at discharge at such L/S. It was also found that the material property plays an important role while studying fill level. Water soluble lactose powder maintained granule size at all fill levels because it dissolved in water and formed liquid bridges which helped to bind material together to form relatively stronger granules. So, it is concluded that along with fill level, material property and residence time are also important factors while considering increasing the throughput (scaling out) of twin screw granulator.

The approach of using SFL-PFN for increasing the machine throughput while maintaining the granule and tablet quality attributes was validated using microcrystalline cellulose (MCC) powder which has different physical and mechanical properties than lactose powder. The results for MCC are presented in Appendix 12.3.2.

7 EFFECTS OF VARYING PRIMARY PARTICLE SIZE

7.1 ABSTRACT

This chapter focuses on developing of understanding the granulation mechanism of three grades of lactose (Pharmatose 450M, Pharmatose 350M and Pharmatose 200M) with varying particle sizes. These powders were granulated at varying L/S and screw speed and their effect on granule properties (size and structure) and tablet tensile strength. It was found that the extent of impact of varying primary particle size and compressibility of powder on the granule attributes depends on the L/S. Powder with smaller particle size granulate to a similar extent to the powder with larger primary particle size at lower L/S.

7.2 INTRODUCTION

In twin screw wet granulation, the effect of primary powder particle size has received limited attention compared to the high shear wet granulation. El Hagrasy et al. (2013b) granulated three different grades of lactose powder (as a major ingredient mixed with 3 minor ingredients namely MCC, HPMC and crosscarmellose sodium) at different liquid to solid ratio (L/S) in TSG. The three grades of lactose used viz., Pharmatose 200M, Supertab 30GR and Impalpable. They noticed that the changes in the lactose grades displayed similar growth behavior at different L/S ratios. They reported that the median granule size showed limited difference among the three lactose grades at low L/S ratios while the results were inconclusive at higher L/S due to potential variability in size measurement using sieve analysis due to the elongated shape of granules. Furthermore, the effect of particle size on the granule porosity was not conclusive since, the middle sized lactose (Supertab 30GR) resulted in lowest porosity followed by small sized (Pharmatose 200M) and large sized lactose (Impalpable).

Fonteyne et al. (2014) studied the influence of particle size of materials (7 different grades of anhydrous theophylline mixed separately with other powders in the formulation) on granule attributes using seven different grades of theophylline powder. They found that the powder with large particle size produce relatively high amount of oversized granules and

low amounts of fines. The powders with small particle size (micronized powders) produced higher amounts of fines.

In the present study, the influence of different types of lactose powders having varying particles sizes were granulated separately at different liquid to solid ratios and screw speeds and their impact on the growth and properties of the granules and attributes of tablet was investigated.

Three types of lactose powder (Pharmatose 200M, Pharmatose 350M and Pharmatose 450M) used in this study differ in their particle size. All three lactose powders are manufactured by slow crystallization of a supersaturated lactose solution below 93.5 °C accompanied by roller drying resulting in single crystals of α-lactose monohydrate (DFE Pharma, Germany). These crystals have tomahawk-like shape and are very hard and brittle. The crystals are then mechanically milled to varying particle size or grades.

7.3 MATERIALS AND METHODS

7.3.1 Materials

7.3.1.1 Powder and granulation liquid

The types of lactose powders (Pharmatose) from DMV-Fonterra Excipient GmbH and co., Goch, Germany used in this study are Pharmatose 450M, Pharmatose 350M and Pharmatose 200M. Distilled water was used as a granulation liquid (liquid binder).

7.3.2 Methods

7.3.2.1 Morphology of powders

The three lactose powders were analysed for particle size and surface, flowability, and compressibility using method described in section 3.2 and Table 7-1.

Table 7-1 Particle size and sphericity of powders used in the study

Powder Grade	Particle size (µm)		
	d_{10}	d_{50}	d_{90}
Pharmatose 450M	7.0	22.5	43.8
Pharmatose 350M	9.8	35.2	74.2
Pharmatose 200M	9.3	42.1	110

The primary particles size of three lactose powders is shown in Table 7-1. It can be seen that Pharmatose 200M have the largest particle size (d_{50}) amongst three powders.

The scanning electron microscopy (SEM) images for three powders is shown in Figure 7-1. The SEM observations complement the particle size data in Table 7-1.

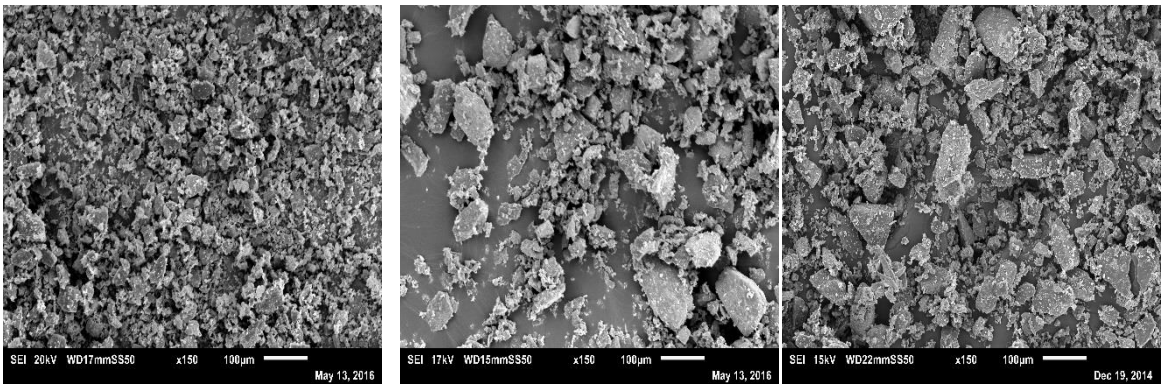

(a) Pharmatose 450M (b) Pharmatose 350M (c) Pharmatose 200M

Figure 7-1 SEM images of powders

7.3.2.2 Preparation of granules

Lactose powders were granulated separately using distilled water in the TSG. The granulation was carried out using full length of the granulator using screw configuration similar to that used in chapter 5 (Figure 5-2). The experimental design is shown in Table 7-1. In total, 48 experiments (3 repetitions of each experiment) were carried out. Each powder was granulated at 4 different L/S (0.048, 0.07, 0.1 and 0.113) and 4 different screw speeds (200 rpm, 450 rpm, 700 rpm and 950 rpm) in order to compare the effects of varying process variables on the granule properties (size and structure) and tensile strength of tablet.

Table 7-2 Experimental conditions and variables used in this study

Powder type	Powder feed rate (kg/h)	Screw speed (rpm)	L/S	Liquid binder
Pharmatose 450M	2	200, 450, 700, 950	0.048,0.07 0.1, 0.113	Distilled water
Pharmatose 350M				
Pharmatose 200M				

The granules were air dried at room temperature for 48 h and analysed for size (d_{50}) and structure using methods described in section 3.2.

The granules were sieved into different size classes (212 µm-1400 µm, 212 µm-600 µm, 600 µm-1000 µm and 1000 µm-1400 µm) and compressed into tablets that were analysed for the tensile strength using methods described in section 3.2.

7.4 RESULTS AND DISCUSSION

7.4.1 Flowability and compressibility factor of different types of powder

Figure 7-2 shows flowability indicators [effective angle of internal friction and flow factor coefficient (ff_c)]. It can be seen from the figure that the effective angle of internal friction increases while ff_c decreases slightly with decreasing primary particle size of lactose. This indicates that the fine, milled lactose has high inter-particle interaction i.e. cohesion, thus, it does not tend to flow well. The results are in agreement with Zhou et al. (2011) who also noticed that the ff_c values increase with an increase in particle size of lactose powder.

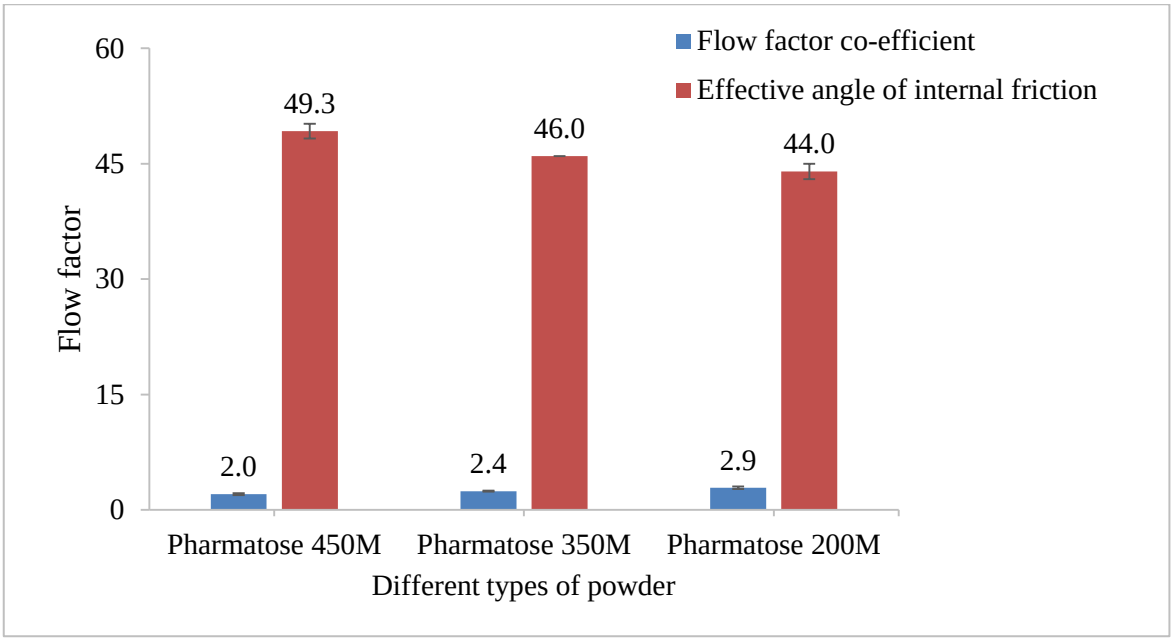

Figure 7-2 Flowability indicators for different powders (Orange columns- Effective angle of internal friction, Blue columns- Flow factor coefficient)

Figure 7-3 shows compressibility factor (K) for different powders. Pharmatose 450M showed the smallest K value meaning high compressibility. The fine, milled lactose have high surface area and tend to form denser compact as the smaller particle fill the inter-particle spaces.

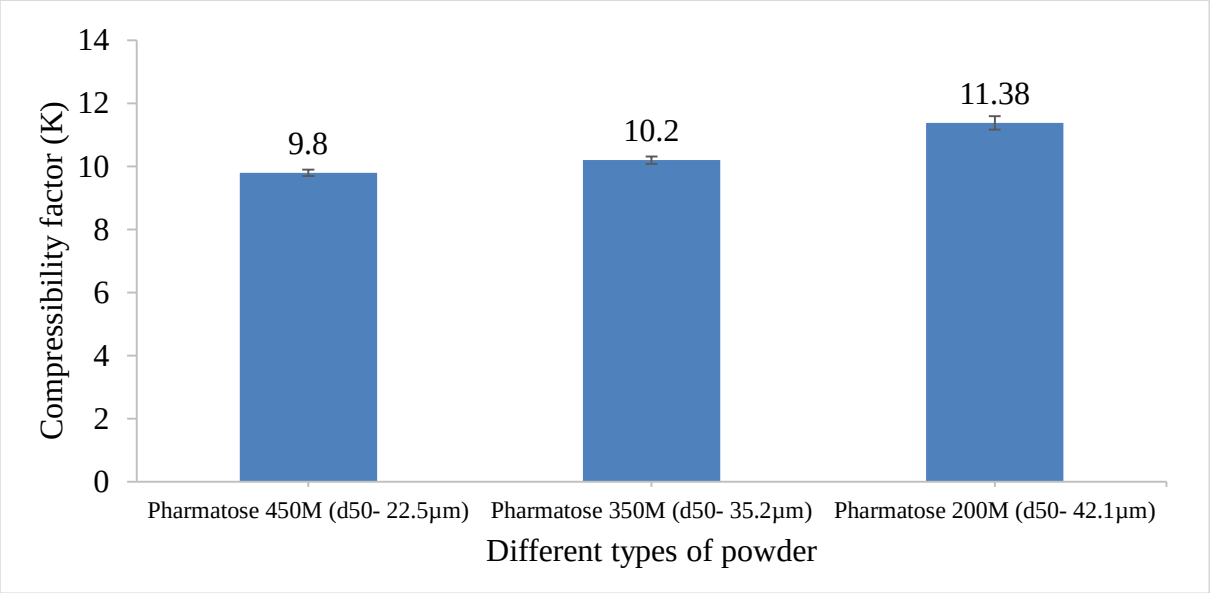

Figure 7-3 Compressibility factor for different powders

7.4.2 Size of granules

Figure 7-4(a)-(b) show the effect of varying L/S, on the size of granules produced from three powders at screw speeds of 200 rpm and 450 rpm respectively. At both screw speeds, increasing L/S from 0.048 to 0.07, did not result in the increase in the granule size for any of the three powders. With further increase in the L/S to 0.1 and 0.113, the granule size increased for all powders.

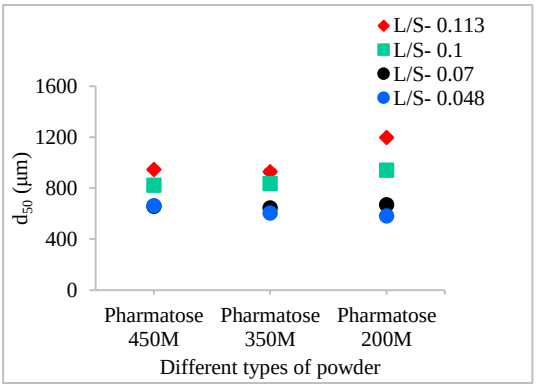

a) 200 rpm

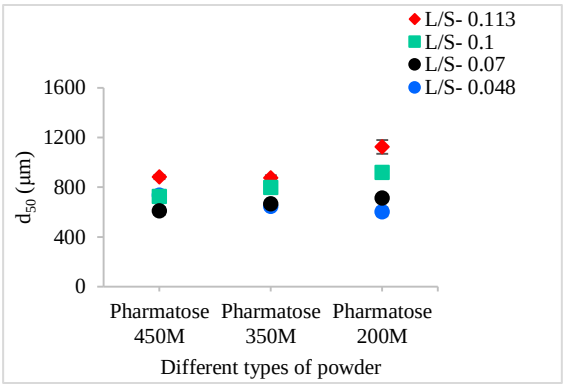

b) 450 rpm

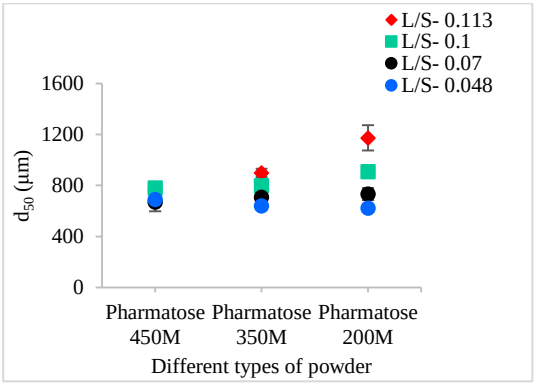

c) 700 rpm

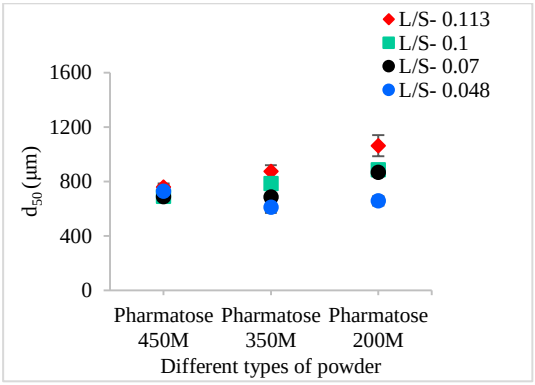

d) 950 rpm

Figure 7-4 Median size of granules for different types of lactose powder at varying L/S and screw speed

The granulation at L/S of 0.113 resulted in the production of the largest granules amongst four L/S. It can also be observed from Figure 7-4(a)-(b) that at low L/S of 0.048 and 0.07 all three powders produced similar size granules. At high L/S of 0.1 and 0.113, Pharmatose 450M and 350M powders produced almost same sized granules while Pharmatose 200M produced relatively larger granules. These type of observations can be described using two

concepts based on amount of liquid added during the granulation. The first concept is that when there is less amount of liquid available (L/S- 0.048 and 0.07), the granulation occurs by consolidation of compressible and cohesive powder (Figure 7-2 and Figure 7-3). The second concept is that in presence of sufficiently high liquid availability (L/S- 0.1 and 0.113) for granulation, the granule growth occurs by coalescence of wetted and saturated granules. The first concept is explained as follows. Amongst the powders used, Pharmatose 350M and 450M powders have smaller particle size (meaning larger specific surface area), higher cohesivity (indicated by higher ff_c values) (Figure 7-2) and higher compressibility (indicated by lower K values) (Figure 7-3) compared to Pharmatose 200M. This could be realised from SEM images presented in Figure 7-5- Figure 7-7 where the granule surface is smoother and more flattened in case of Pharmatose 350M and 450M.

Furthermore, there is also a relationship between the particle size, amount of liquid and inter-particle liquid forces (capillary and viscous forces) that occur during wet granulation. According to Iveson et al. (2001) and Mackaplow et al. (2000), the inter-particle interaction forces [friction, cohesion] are dominant when the particle size is small, even at lower liquid pore saturation (~ in this case lower L/S). Also, at such liquid amount, the inter-particle liquid bridge volume is directly proportional to the primary particle size while the number of inter-particle contact points per unit area for liquid bridge formation is inversely proportional to the particle size (Mackaplow et al. 2000). This means that the added liquid will be used in the formation of liquid bridges between the particles and the number of inter-particle liquid bridges per unit area will be more in case of smaller primary particles. In summary, at lower L/S of 0.048 and 0.07, the wet granules of powder with smaller primary particles (Pharmatose 350M and 450M) grow in size due to relatively better consolidation of moist powder owing to higher compressibility. The relatively larger primary particles (Pharmatose 200M) means smaller specific surface area, lower inter-particle interaction forces and less number of inter-particle contact points per unit area, hence there are fewer liquid bridges between the particles at low L/S which limit the granule growth.

The second concept (results at L/S of 0.1 and 0.113) can be explained as follows. It is well known that higher L/S results in higher pore saturation which according to Holm et al. (1985), shifts the deformation behaviour of wet granules from brittleness (‘crumb’ in wet granulation regime map developed by Iveson et al. (2001) (when L/S or pore saturation low)

to plasticity. As the pore saturation increases, the number and the dimension of inter-particle liquid bridges increase too. Further increase in the saturation can also result in the funicular and capillary state of the particle assembly or granules. This in turn reduces inter-particle interaction forces and wet granules in the granulator become both weaker and more deformable (Mackaplow et al. 2000, Iveson et al. 2001). As the particle size increases, the specific surface area decreases which requires relatively less volume of liquid for surface coverage. Hence, as the particle size increases, the liquid bridge volume in funicular state or volume of liquid surrounding the particles in case of capillary state also increases which reduces the strength of the wet granules or the particle assembly making them more deformable. It is well known that higher the deformability of wet granules, higher is the granule growth by coalescence (Mackaplow et al. 2000). Thus, with increasing particle size at higher L/S, the granule size increased. The results are in agreement with the findings by El Hagrasy et al. (2013b) and Fonteyne et al. (2014) where the granules size increased with the primary particle size of powder at high L/S.

Figure 7-4(c)-(d) show the effect of varying L/S, on the size of granules produced from three powders at screw speed of 700 rpm and 950 rpm respectively. At such higher screw speeds granulation at low or high L/S had limited impact on the granule size for Pharmatose 450M which has the smallest primary particles. Increase in shearing at higher screw speeds minimised the effect of L/S in case of Pharmatose 450M. In case of other Pharmatose 350M and 200M, increasing L/S at screw speeds of 700 rpm and 950 rpm followed similar trends at screw speeds of 200 rpm and 450 rpm.

7.4.3 Surface of granules

Figure 7-5(a)-(d) shows scanning electron microscopic images for Pharmatose 450M at varying L/S (screw speed- 450 rpm). It can be observed that at all L/S some granules exhibit flat surfaces indicating the densification due to high compressibility of Pharmatose 350M powder (Figure 7-6(a)-(d)). In case of Pharmatose 200M (Figure 7-7(a)-(d)), the surface flattening/densification reduced owing to its relatively lower compressibility.

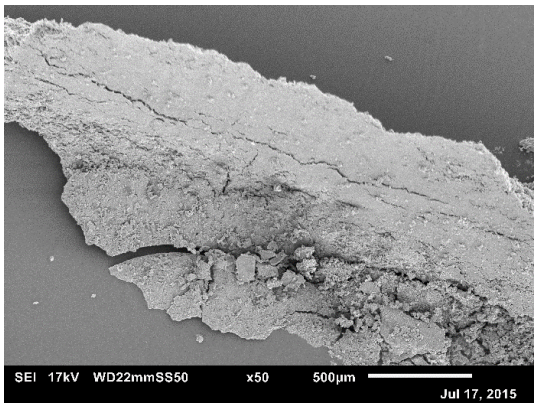

(a) L/S-0.048 Screw speed-450 rpm
(Porosity- 25.5471%)

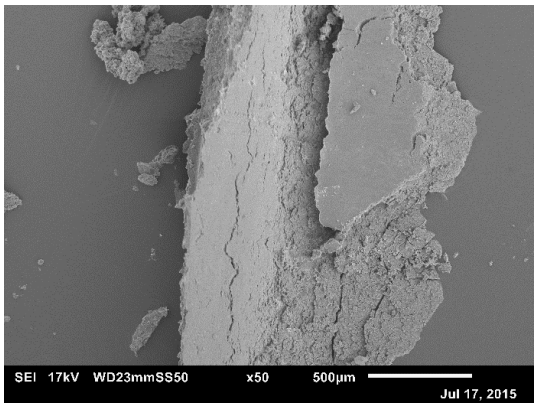

(b) L/S-0.07 Screw speed-450 rpm
(Porosity- 23.5879%)

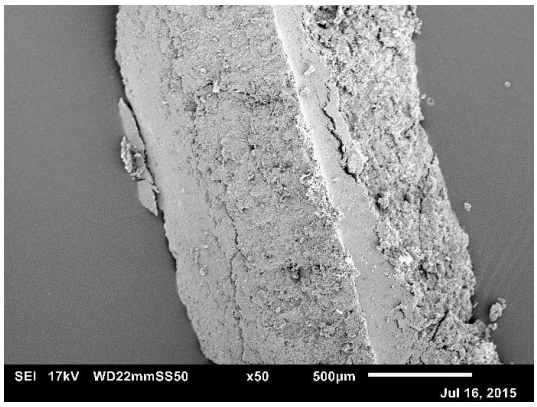

(d) L/S-0.1 Screw speed-450rpm
(Porosity- 20.4568%)

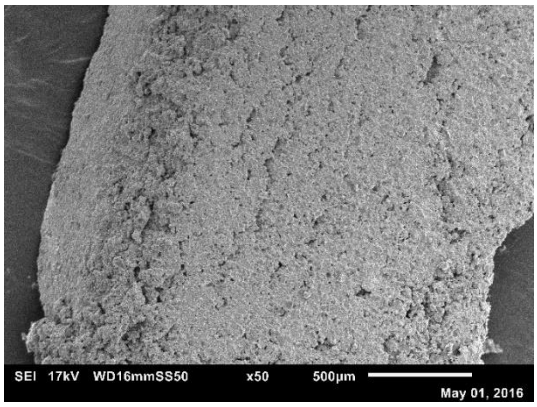

(e) L/S-0.113 Screw speed-450 rpm
(Porosity- 16.855%)

Figure 7-5 Scanning Electron Microscope images of granules produced using Pharmatose 450M at varying L/S

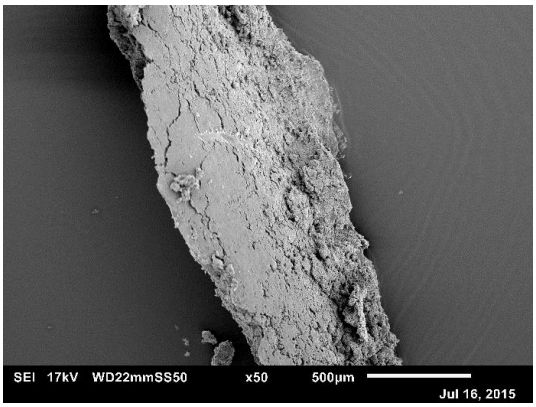

(a) L/S-0.048 Screw speed-450 rpm (Porosity- 28.5469%)

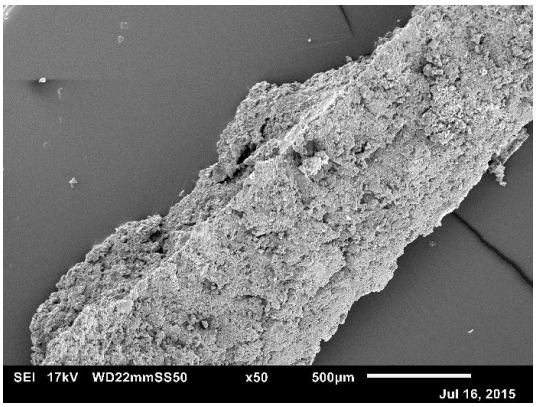

(b) L/S-0.07 Screw speed-450 rpm (Porosity- 25.6123%)

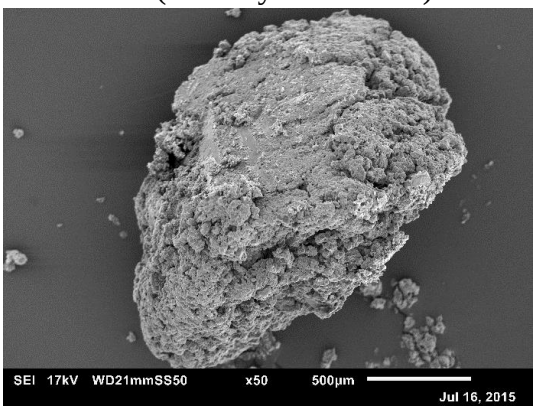

(c) L/S-0.1 Screw speed-450 rpm (Porosity- 21.5489%)

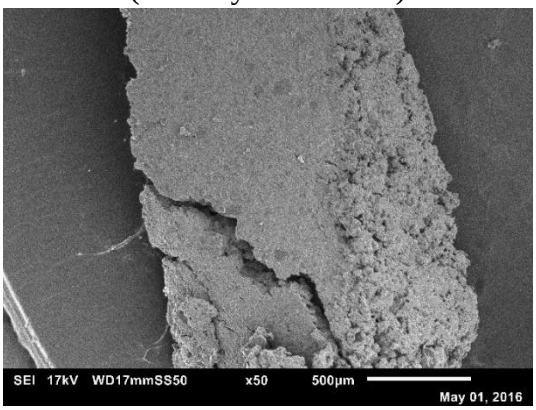

(d) L/S-0.113 Screw speed-450 rpm (Porosity- 20.0548%)

Figure 7-6 Scanning Electron Microscope images of granules produced using Pharmatose 350M at varying L/S

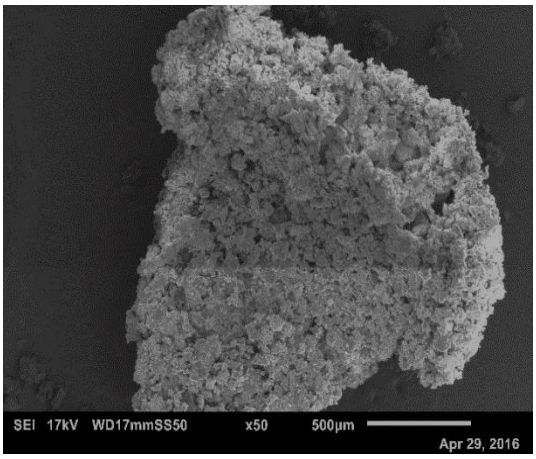

(a) L/S-0.048 Screw speed- 450 rpm (Porosity- 30.3045%)

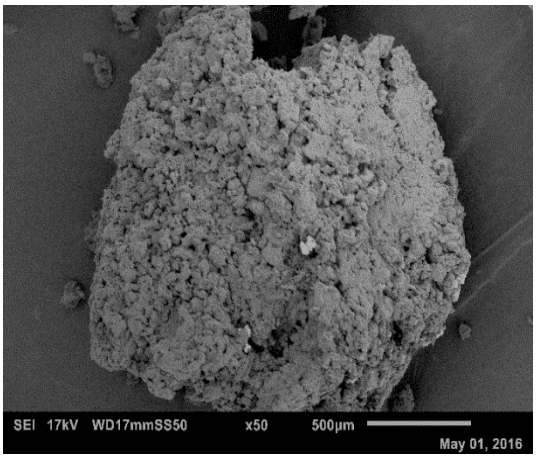

(b) L/S-0.07 Screw speed- 450 rpm (Porosity- 28.4587%)

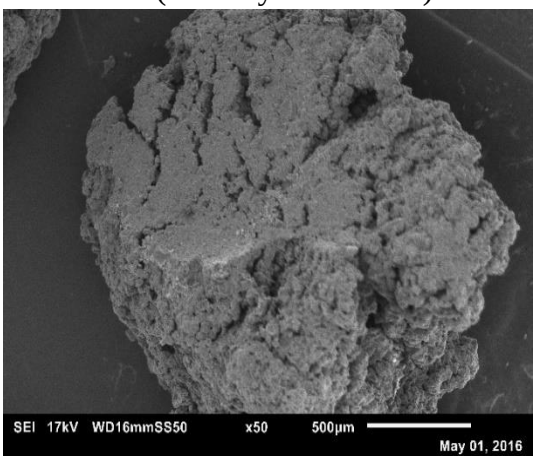

(c) L/S-0.1 Screw speed- 450 rpm (Porosity- 22.2451%)

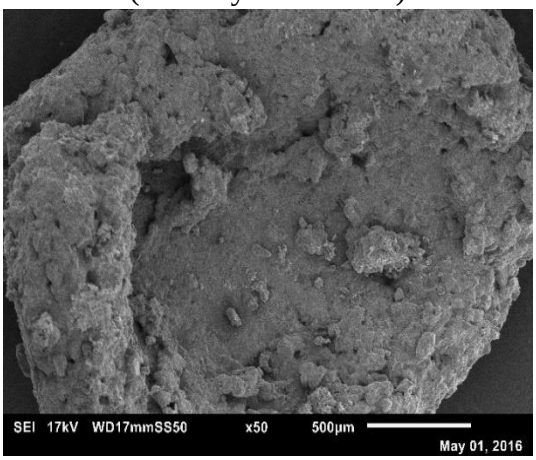

(d) L/S-0.113 Screw speed- 450 rpm (Porosity- 20.0548%)

Figure 7-7 Scanning Electron Microscope images of granules produced using Pharmatose 200M at varying L/S

7.4.4 Granule structure

Figure 7-8(a)-(d) shows X-ray tomographic images for Pharmatose 450M at varying L/S (screw speed- 450 rpm). The respective inter-particle porosity within the granules calculated using ImageJ software is presented in Figure 7-11. The black colour in image represents air or void and the grey represents granulated powder mass. It can be observed that the granule structure became denser (and inter-particle porosity within the granule decreased) with increasing L/S. This may be because, at high liquid levels, the powder mass was more wetted, deformable and hence better consolidated. Similar effect was observed in case of

Pharmatose 350M (Figure 7-9(a)-(d)) and 200M (Figure 7-10(a)-(d)) powders. Increasing particle size increases inter-particle porosity within the granule as shown in Figure 7-11.

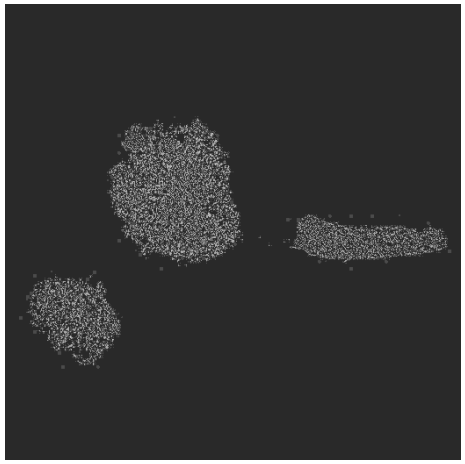

(a) L/S-0.048 Screw speed- 450 rpm (Porosity- 25.5471%)

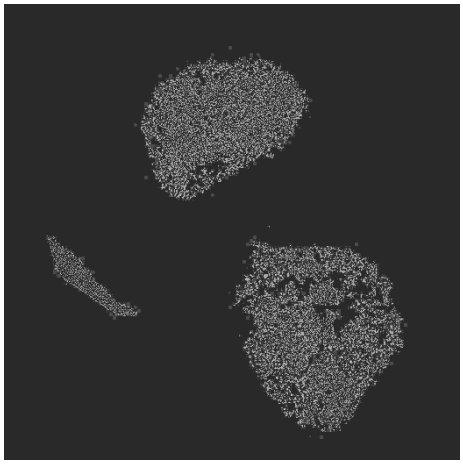

(b) L/S-0.07 Screw speed- 450 rpm (Porosity- 23.5879%)

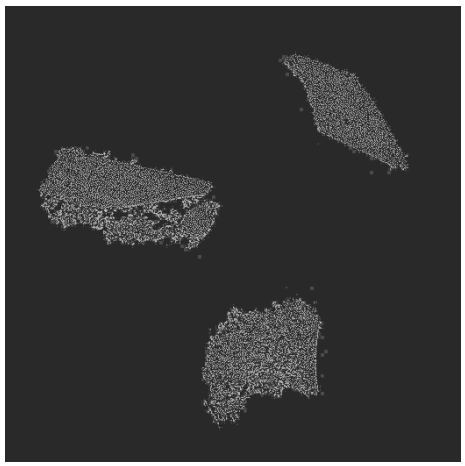

(c) L/S-0.1 Screw speed- 450 rpm (Porosity- 20.4568%)

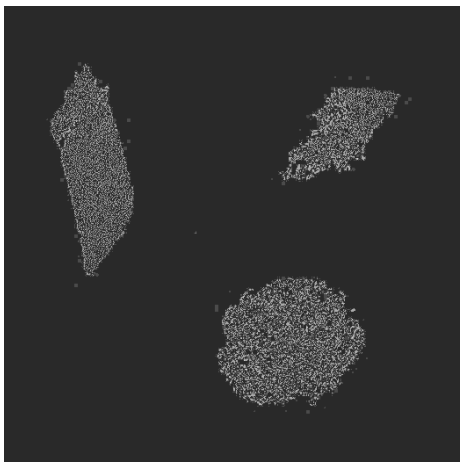

(d) L/S-0.113 Screw speed- 450 rpm (Porosity- 16.855%)

Figure 7-8 X-ray tomographic images of granules produced using Pharmatose 450M (d50- 22.5 µm) at varying L/S

(a) L/S-0.048 Screw speed- 450 rpm (Porosity- 28.5469%)

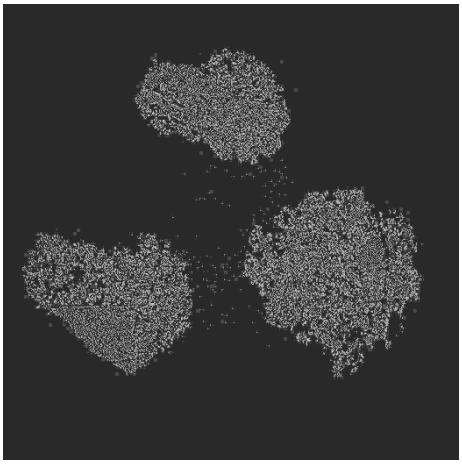

(b) L/S-0.07 Screw speed- 450 rpm (Porosity- 25.6123%)

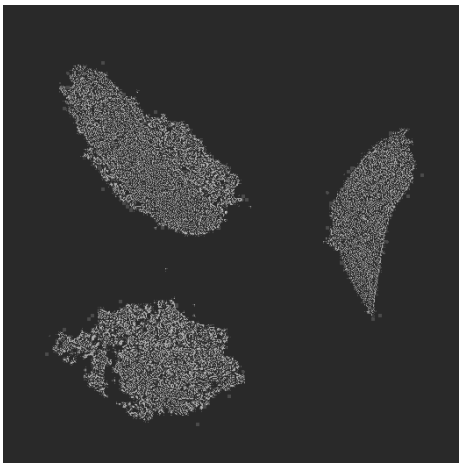

(c) L/S-0.1 Screw speed- 450 rpm (Porosity- 21.5489%)

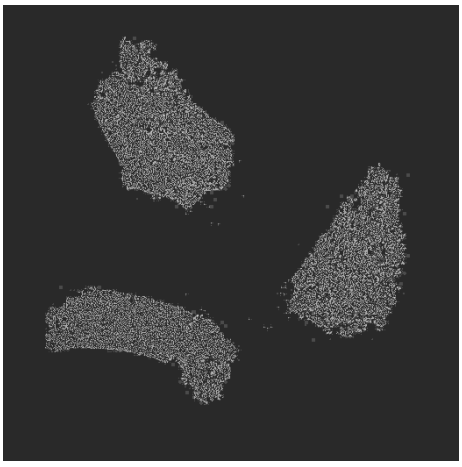

(d) L/S-0.113 Screw speed- 450 rpm (Porosity- 20.0548%)

Figure 7-9 X-ray tomographic images of granules produced using Pharmatose 350M (d50- 35.2 µm) at varying L/S

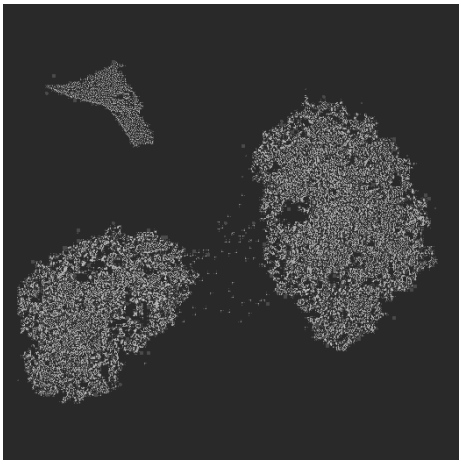

(a) L/S-0.048 Screw speed- 450 rpm (Porosity- 30.3045%)

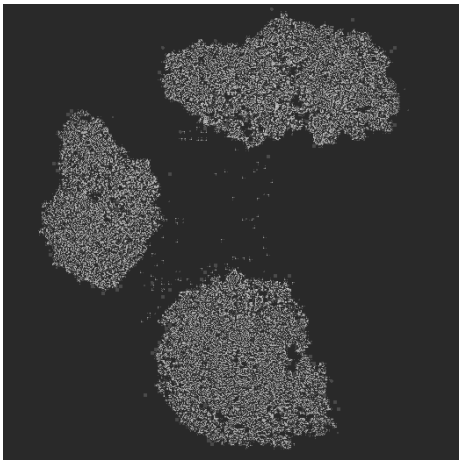

(b) L/S-0.07 Screw speed- 450 rpm (Porosity- 28.4587%)

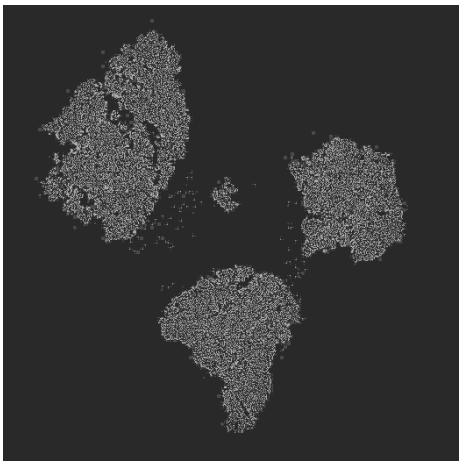

(c) L/S-0.1 Screw speed- 450 rpm (Porosity- 22.2451%)

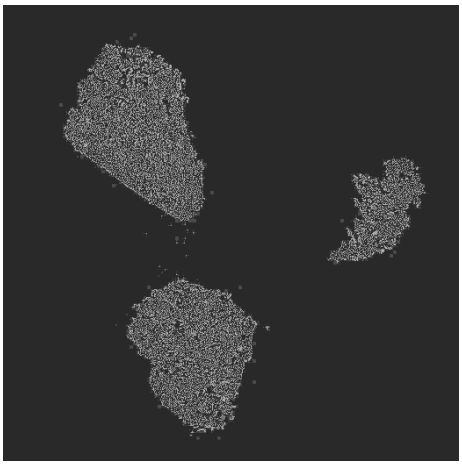

(d) L/S-0.113 Screw speed- 450 rpm (Porosity- 20.0548%)

Figure 7-10 X-ray tomographic images of granules produced using Pharmatose 200M (d50- 42.1 µm) at varying L/S

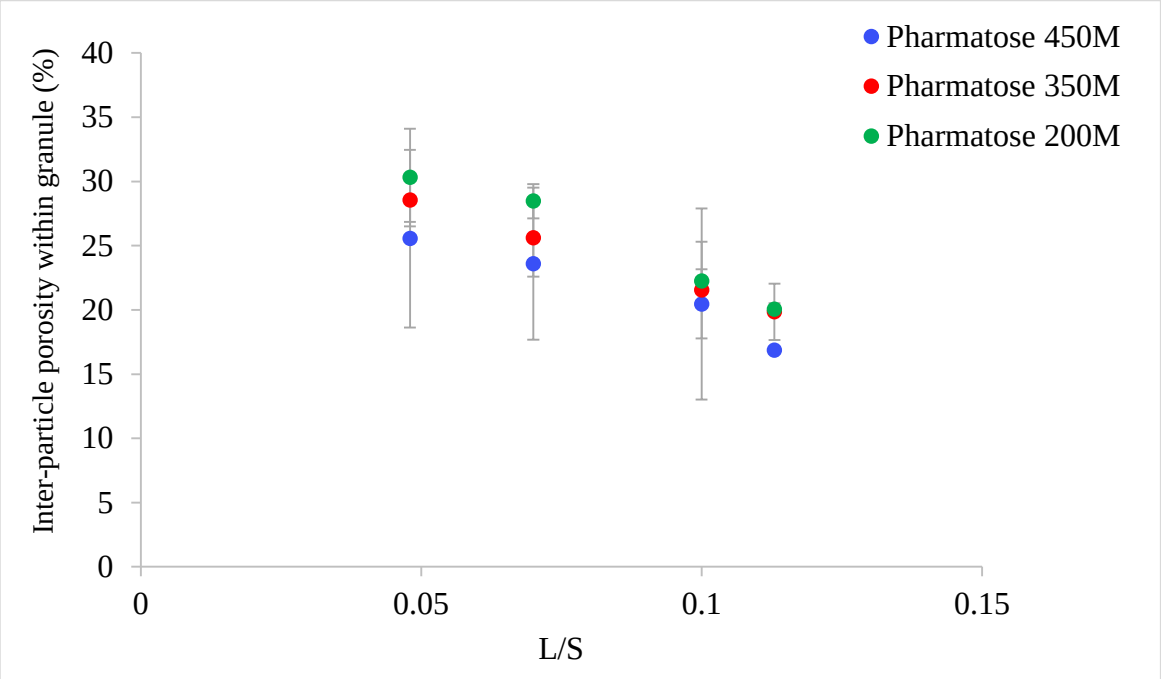

Figure 7-11 Porosity of granules for different sizes of lactose powder at varying L/S (screw speed- 450 rpm)

7.4.5 Tensile strength of tablets

Figure 7-12 show the tensile strength of tablets of Pharmatose 450M granules produced at L/S of 0.048 and 0.113 at different screw speeds (200 rpm, 450 rpm, 700 rpm and 950 rpm) for different granule size ranges (complete range- 212-1400 µm and subdivisions- 212-600 µm, 600-1000 µm, 1000-1400 µm). It can be observed that at lower L/S 0.048, the strength of granules was slightly higher compared to L/S 0.113. This is because granules produced at lower L/S, due to unavailability of sufficient liquid, were weaker compared to those at higher L/S. It can be observed that granule size and screw speed had no significant effect on the tablet tensile strength (despite difference in the granule structure at varying L/S) (Figure 7-4). Similar results were observed for Pharmatose 350M (Figure 7-13) and 200M (Figure 7-14) powders.

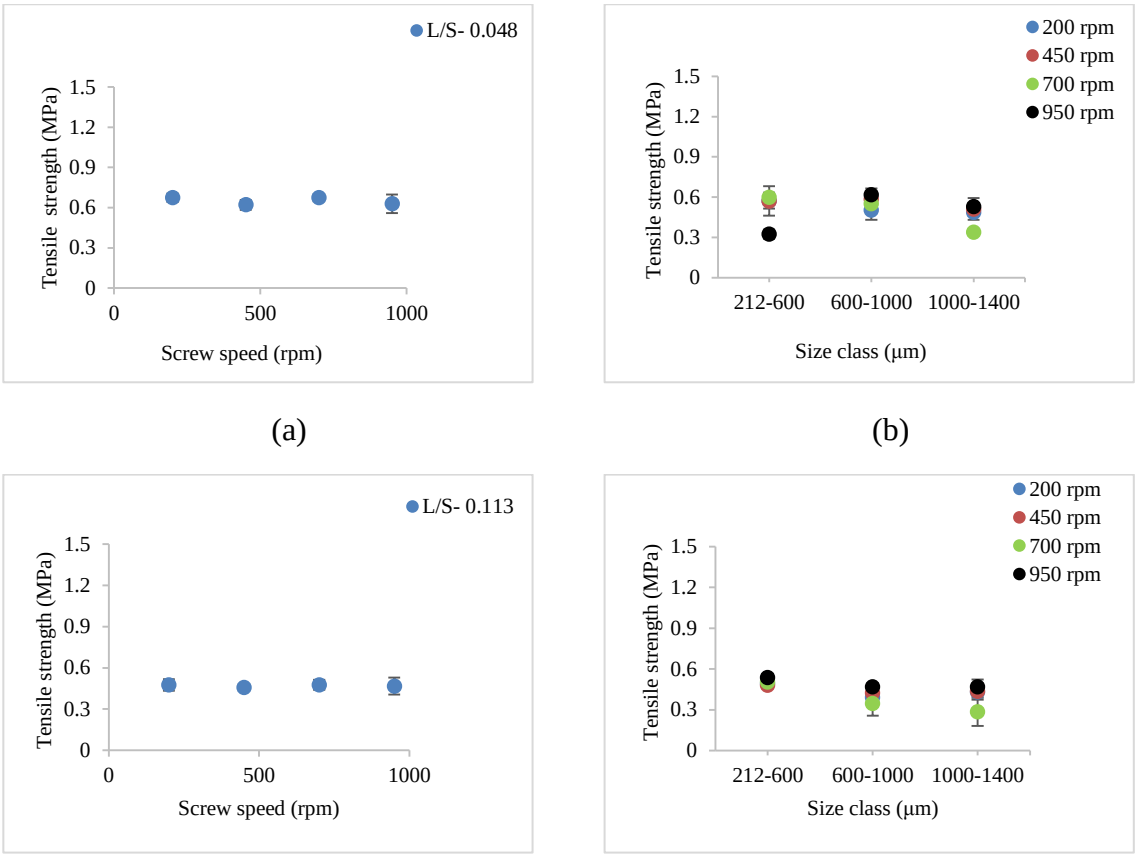

Figure 7-12 Tensile strength of tablet of granules at different size classes of Pharmatose 450M

(a) 212-1400 µm at L/S of 0.048 (b) 212-600 µm, 600-1000 µm, 1000-1400 µm at L/S of 0.048

(c) 212-1400 µm at L/S of 0.113 (d) 212-600 µm, 600-1000 µm, 1000-1400 µm at L/S of 0.113

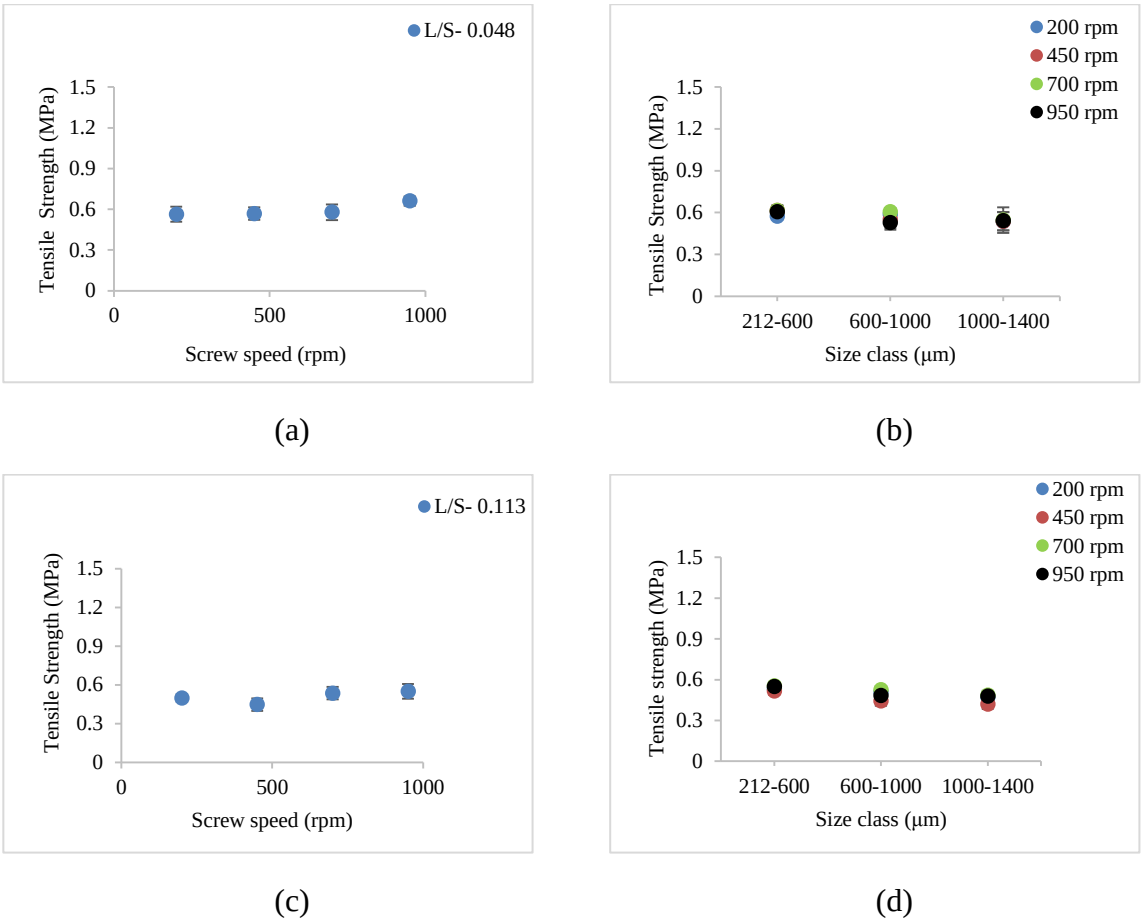

Figure 7-13 Tensile strength of tablet of granules at different size classes of Pharmatose 350M

(a) 212-1400 µm at L/S of 0.048 (b) 212-600 µm, 600-1000 µm, 1000-1400 µm at L/S of 0.048

(c) 212-1400 µm at L/S of 0.113 (d) 212-600 µm, 600-1000 µm, 1000-1400 µm at L/S of 0.113

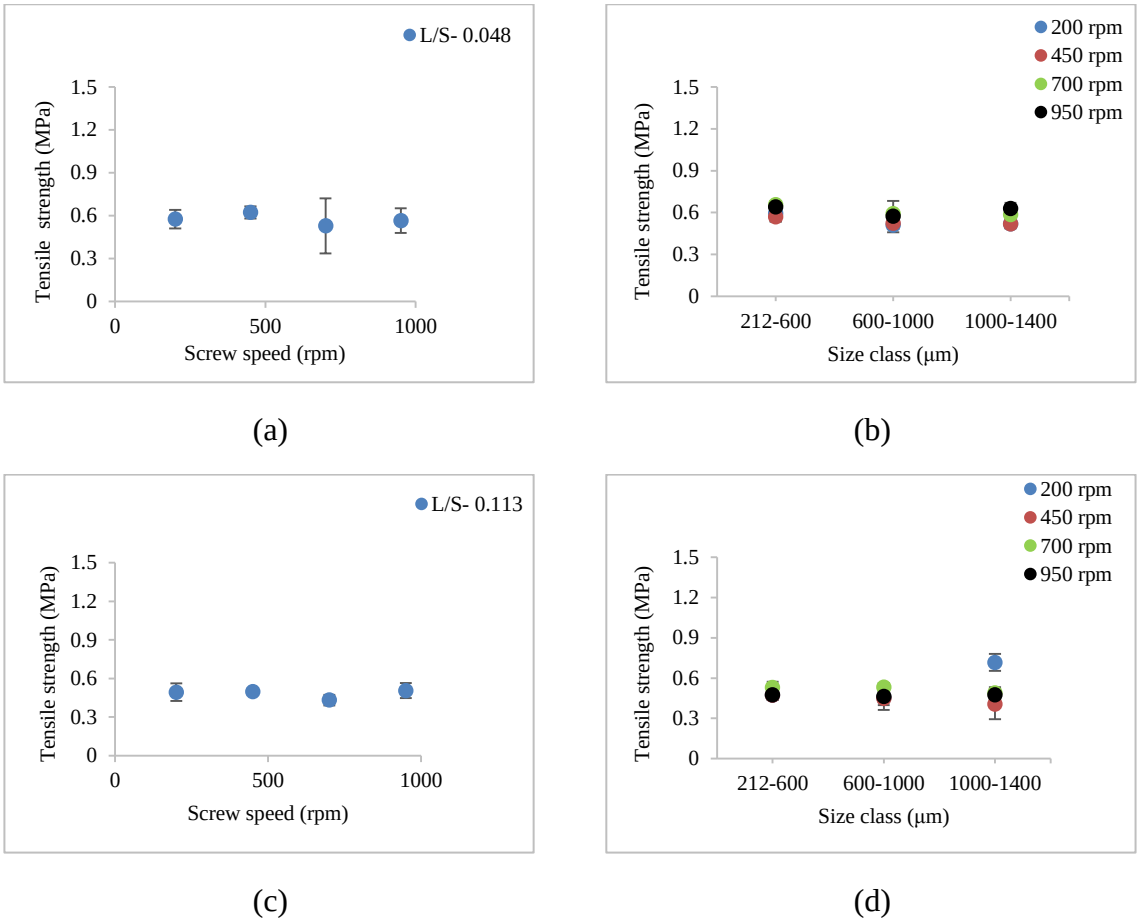

Figure 7-14 Tensile strength of tablet of granules at different size classes of Pharmatose 200M (a) 212-1400 µm at L/S of 0.048 (b) 212-600 µm, 600-1000 µm, 1000-1400 µm at L/S of 0.048 (c) 212-1400 µm at L/S of 0.113 (d) 212-600 µm, 600-1000 µm, 1000-1400 µm at L/S of 0.113

7.5 CONCLUSION

In this study the effects of the properties of powder on granule and tablet properties were studied. It was observed that the change in the granule size with decrease or increase primary particle size (and thus compressibility and flowability) is dependent on the amount of liquid available or L/S. The powders with smaller primary particle size and high compressibility granulated even at low L/S producing granules similar to powder with larger particle size and relatively lower compressibility. Increasing L/S, showed more pronounced effect on granule size in case of powder with larger primary particles. Granules become smoother and

denser with decreasing primary particle size and increasing L/S. The effect of screw speed on granule properties, to some extent, was dependant on the amount of liquid added. Effect of particle size and screw speed on tablet tensile strength was very limited.

8 EFFECTS OF TYPES OF PRIMARY POWDER

8.1 ABSTRACT

This chapter is focused on understanding the granulation mechanism of two types of pharmaceutical powders with varying properties (primary particle size, structure and compressibility). Three grades each of lactose and mannitol were granulated at varying liquid to solid ratio (L/S) and screw speed. It was noticed that primary powder morphology plays an important role in determining the granule size and structure and the tablet tensile strength.

8.2 INTRODUCTION

Amongst various excipient powders available for the wet/ dry granulation and tabletting in the pharmaceutical industry, lactose and mannitol are some of the most common ones. Both lactose and mannitol are commercially available in different grades (sieved, milled, spray-dried, granulated etc.) presenting different attributes, such as surface morphology and degrees of fines etc. (Jivraj et al. 2000, Huang et al. 2013).

In twin screw wet granulation, the effect of primary powder morphology on granulation behaviour and properties of granules and tablets has received very limited attention. Moreover, comparison of the performance of different grades of lactose vs. mannitol powders in twin screw wet granulation has not been studied previously.

The objective of this study is to compare the performance of different grades of lactose and mannitol powders during twin screw wet granulation. Different types of lactose and mannitol powders having different powder morphology were granulated separately at different L/S and screw speeds and their impact on the growth and properties of the granules (size, shape and structure) and tablet (tensile strength) was investigated.

8.3 MATERIAL AND METHOD

8.3.1 Materials

8.3.1.1 Powder and granulation liquid

Different grades of lactose and mannitol powders were used in this study for comparing the effects of their physical properties on the granulation behaviour and granule properties.

Three types of lactose powders were used in the study: α-lactose monohydrate (Pharmatose 200M), spray dried lactose (SuperTab11SD) and anhydrous lactose (SuperTab21AN). All powders were supplied by DMV-Fonterra Excipient GmbH and co., Goch, Germany. α-lactose monohydrate powder is manufactured by slow crystallization of a supersaturated lactose solution below 93.5°C accompanied by roller drying resulting in single crystals of α-lactose monohydrate are further milled to produce Pharmatose 200M grade powder. Anhydrous lactose is also made from crystallisation of supersaturated solution of lactose but it is rapidly dried at high temperature (above 93.5°C) by roller drying. The particles are then milled and sieved to produce SuperTab21AN grade powder. Spray dried lactose consists of particles of α-lactose monohydrate. Finely milled α-lactose monohydrate is suspended in water and spray dried to make spherical agglomerates to produce SuperTab11SD.

The three types of mannitol powders, used in respective comparison with three lactose powders, were milled crystalline mannitol (Pearlitol 50C), spray dried mannitol (Pearlitol 200SD) and granulated mannitol (Pearlitol 300DC). All mannitol powders were supplied by Roquette (France). Milled crystalline mannitol powder is manufactured by slow crystallization of a supersaturated solution to produce crystals of mannitol which are then crushed to produce Pearlitol 50C. Spray dried mannitol (Pearlitol 200SD) as name suggests is manufactured by spray drying suspension of mannitol powder in water to produce spherical agglomerates. The granulated mannitol (Pearlitol 300DC) is produced by pouring hot slurry of mannitol powder on the cold rotating drum and then crushed into desired size.

Powders were analysed for the size, shape, surface and compressibility using methods described in section 3.2.

8.3.1.2 Preparation of granule

Lactose and mannitol powders were granulated separately using distilled water in the TSG. The granulation was carried out using full length of the granulator using screw configuration similar to that used in chapter 5 (Figure 5-2). About 60 g of granules from each experiment were collected for analysis. The experimental design is shown in Table 8-1. In total, 288 experiments (i.e. 16 combinations × 3 repeats of each combination × 6 powders) were carried out. Each powder was granulated at 4 different L/S and 4 different screw speeds in order to compare its performance under varying process variables and its effects on the properties of granules (size, shape and structure) and tablets (tensile strength). The granulator was cleaned in between different conditions (change of powders).

Non randomised approach was used to run various trial conditions. While investigating effects of various powders, granulator was cleaned in between the powders. For each powder granulator was allowed to run empty after trial condition was finished to discharge material held in the granulator before starting next condition.

Table 8-1 Experimental conditions and variables used in the study

Powder type	Powder feed rate (kg/h)	Screw speed (rpm)	L/S	Liquid binder
Pharmatose 200M	2	200, 450, 700, 950	0.048, 0.07, 0.1, 0.113	Distilled water
SuperTab11SD				
SuperTab21AN				
Pearlitol 50C				
Pearlitol 200SD				
Pearlitol 300DC				

The granules were air dried at room temperature for 48h and analysed for size and structure using methods described in section 3.23.2. The granules produced at two extremes of L/S i.e. 0.048 and 0.113 at 4 screw speeds were sieved into different size classes (212 µm-600 µm, 600 µm-1000 µm, 1000 µm-1400 µm and 212 µm-1400 µm) and compressed into tablets that were analysed for the tensile strength using methods described in section 3.2.

8.4 RESULTS AND DISCUSSION

8.4.1 Morphology of powder

The morphology of powder (size and shape) is discussed in this section. The primary particle size of six different powders is shown in Table 8-2. It can be seen that SuperTab21AN and Pearlitol 300DC have the largest particle size (d_{50}) amongst lactose and mannitol powders respectively.

Table 8-2 Primary particle size of powders used in the study

Powder Grade	Particle size (µm)		
	d_{10}	d_{50}	d_{90}
Pharmatose 200M	9.3	42.1	110.0
SuperTab11SD	45.0	113.4	191.3
SuperTab21AN	27.5	172.3	330.0
Pearlitol 50C	10.1	33.9	114.9
Pearlitol 200SD	26.0	145.3	200.9
Pearlitol 300DC	58.3	249.9	385.9

The scanning electron microscopy (SEM) images for lactose and mannitol powders are shown in Figure 8-1 and Figure 8-2 respectively. The SEM images for lactose and mannitol powders clearly show the difference in shape. Pharmatose 200M is a crystalline milled lactose with tomahawk like shape (Figure 8-1 (a)-(b)). SuperTab11SD is spray dried lactose with relatively spherical particles and its structure is made from α-lactose monohydrate (Figure 8-1 (c)-(d)). SuperTab21AN is crystalline anhydrous lactose which is aggregation of lactose crystals (Figure 8-1(e)-(f)). Pearlitol 50C powder has elongated particles (Figure 8-2 (a)-(b)) with smaller particle sticking on the larger ones. Pearlitol 200SD has more spherical shaped primary particles (Figure 8-2 (c)-(d)) having porous shells with elongated thread-like smaller particles embedded in them. Pearlitol 300DC is a granulated mannitol powder with compact and rounded particles (Figure 8-2 (e)-(f)).

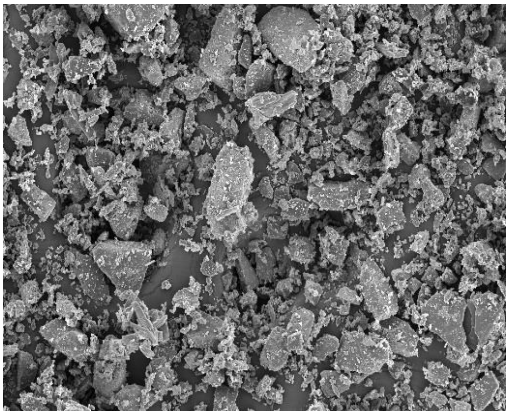

(a) Pharmatose 200M (×150)

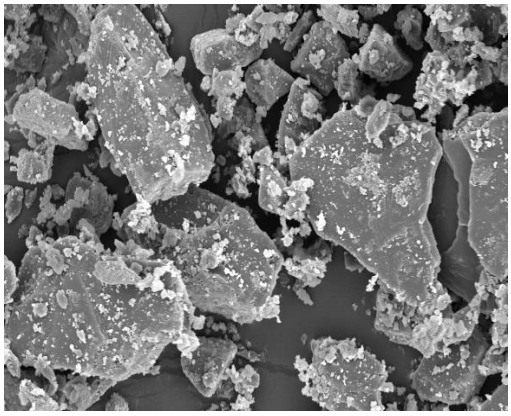

(b) Pharmatose 200M (× 500)

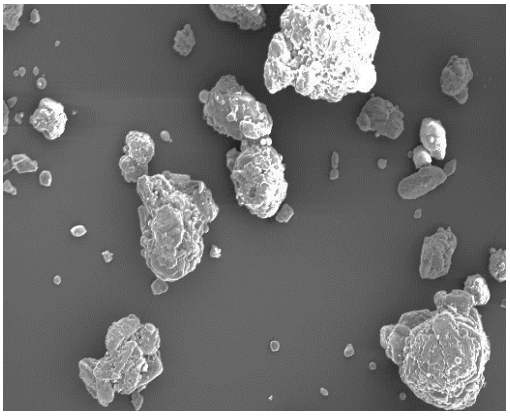

(c) SuperTab11SD (×150)

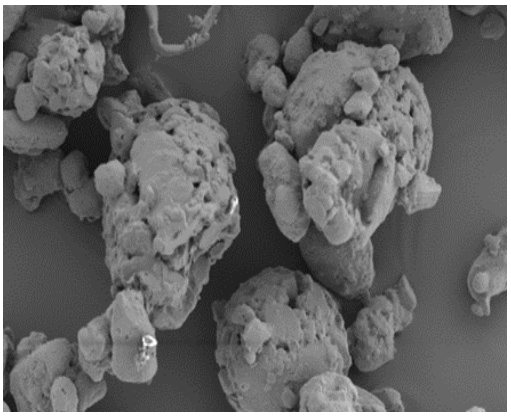

(d) SuperTab11SD (× 500)

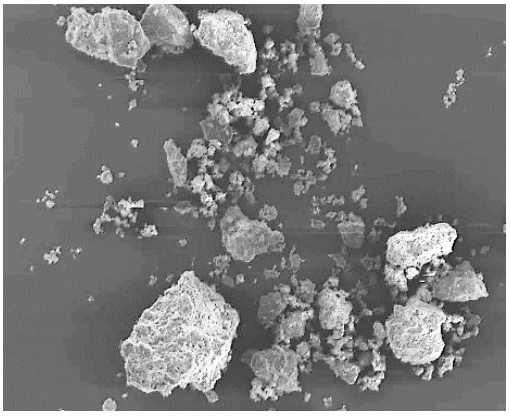

(e) SuperTab21AN (×150)

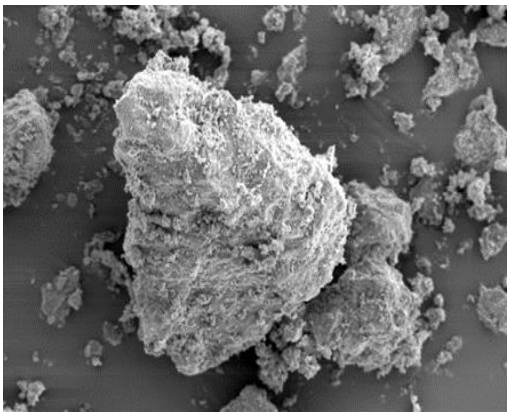

(f) SuperTab21AN (× 500)

Figure 8-1 Scanning Electron Microscope images of lactose powder

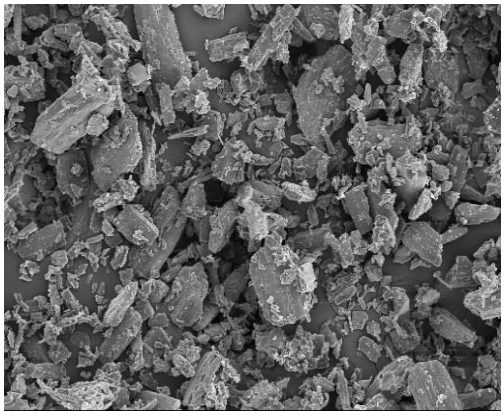

(a) Pearlitol 50C (×150)

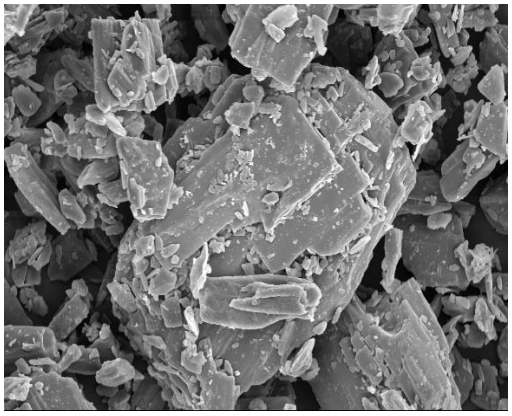

(b) Pearlitol 50C (×500)

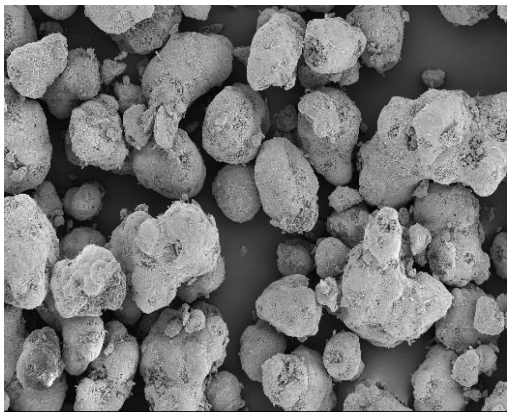

(c) Pearlitol 200SD (×150)

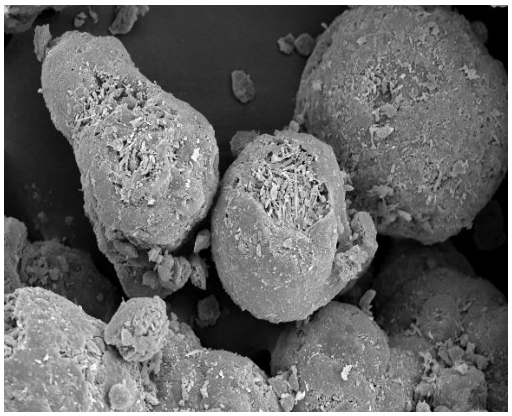

(d) Pearlitol 200SD (×500)

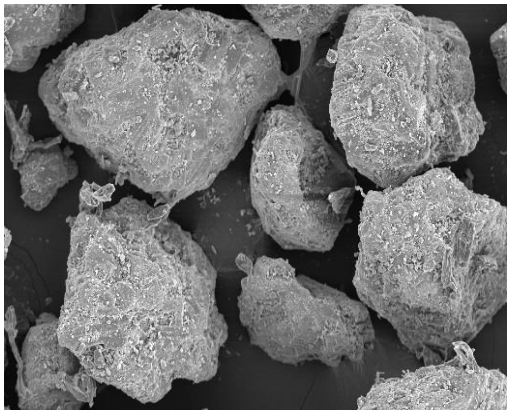

(e) Pearlitol 300DC (×150)

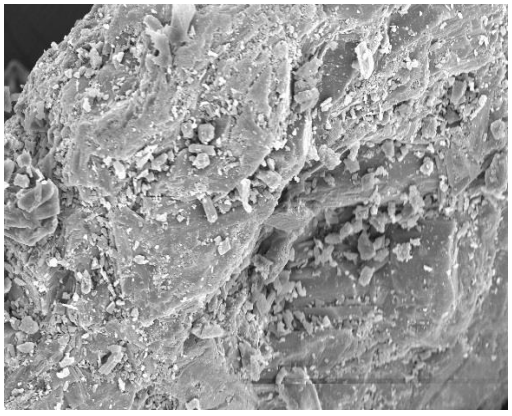

(f) Pearlitol 300DC (×500)

Figure 8-2 Scanning Electron Microscope images of mannitol powders

8.4.2 Compressibility factor for powders

Figure 8-3 shows the compressibility factor (K) for different powders. The compressibility factor results for lactose and mannitol powders were anomalous. The K value was SuperTab11SD < SuperTab21AN < Pharmatose 200M for lactose and Pearlitol 200SD < Pearlitol 300DC < Pearlitol 50C for mannitol while based on the particle size, the expected trend for K value was Pharmatose 200M < SuperTab11SD < SuperTab21AN for lactose and Pearlitol 50C < Pearlitol 200SD < Pearlitol 300DC for mannitol, however, it was not the case. The K value was higher for crystalline Pharmatose 200M and Pearlitol 50C having smaller particle size while it was lower for spray dried large sized (meaning higher compressibility) SuperTab11SD and Pearlitol 200SD respectively. It was also expected that the pre-processed SuperTab21AN and Pearlitol 300DC (which are suitable for direct compression in tableting), to have lower K than SuperTab11SD and Pearlitol 200SD respectively but it was not the case. This can be attributed to the structure of the spray dried lactose and mannitol particles. SEM images of SuperTab11SD particles (Figure 8-1(c)-(d)) show that they are aggregates of several particles. According to Omar et al. (2015), when compressed, such aggregated SuperTab11SD particles fracture into smaller particles and potentially improve the compressibility (even better than SuperTab21AN). Similar is the case for spray dried mannitol or Pearlitol 200SD where the SEM images (Figure 8-2 (c)-(d)) clearly show the presence of elongated, smaller particles embedded in the spherical shell. According to Mitra et al. (2016), during compression such Pearlitol 200SD particles may possibly break into smaller fragments and thereby improve compressibility. It can also be noticed from Figure 8-3 that Pearlitol 200SD has lower K value (i.e. higher compressibility) compared to Pearlitol 300DC which is a granular compact.

Some example curves showing linearity of compressibility is shown in Appendix 12.4.1.4

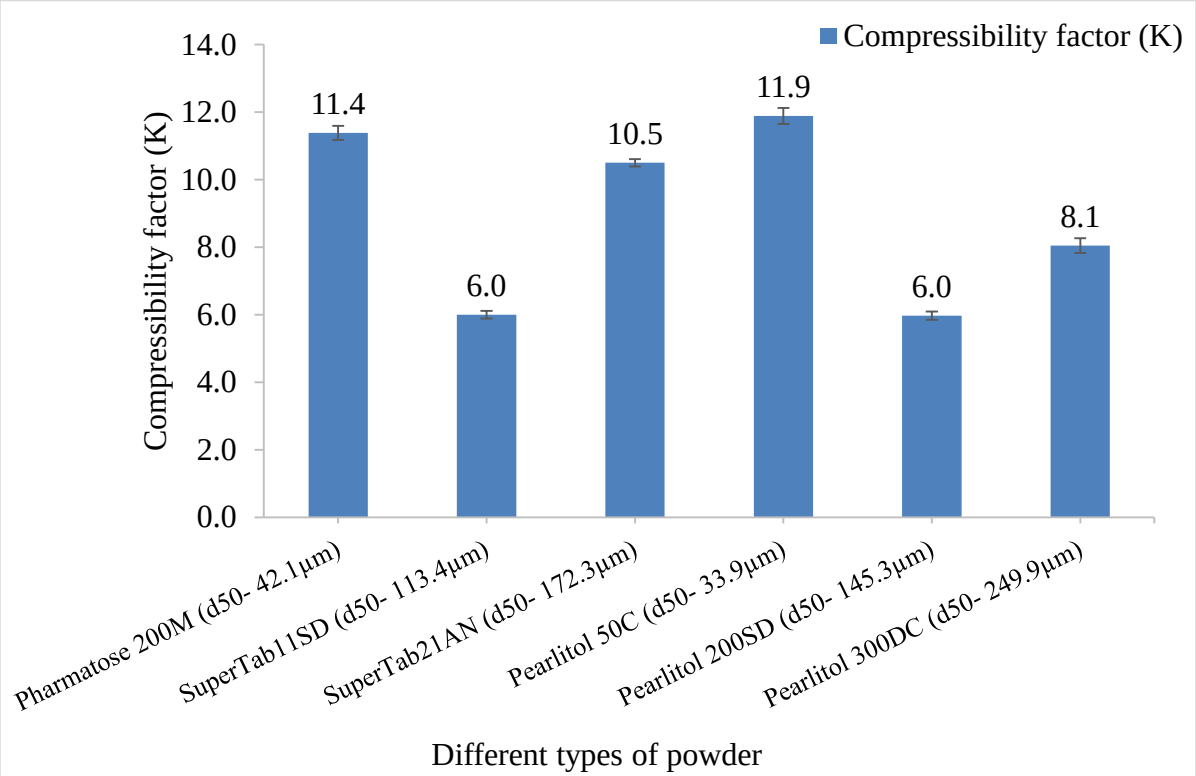

Figure 8-3 Compressibility factor for different powders

8.4.3 Size of granules

8.4.3.1 Lactose

Figure 8-4(a)-(d) show median size of granules produced using different grades of lactose powder at varying L/S and screw speed. For the ease of understanding the results are discussed in two parts viz. effect of different powder properties on the granule size at varying L/S and the same at varying screw speed.

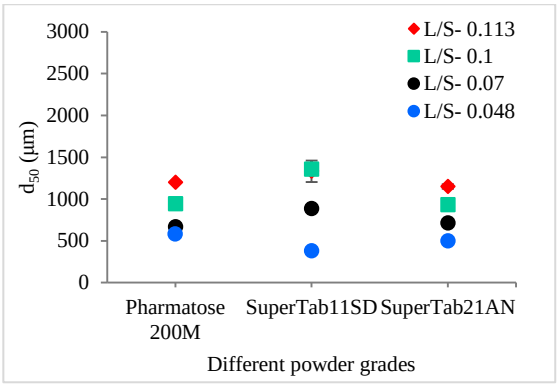

(a) 200 rpm

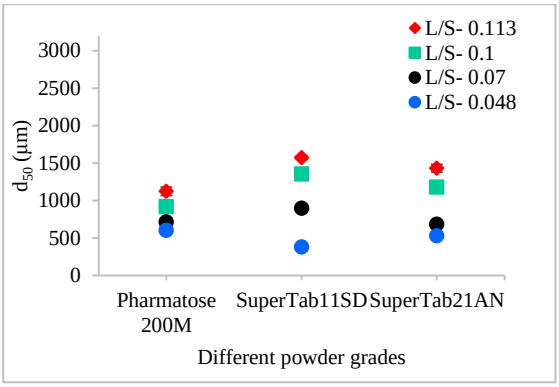

(b) 450 rpm

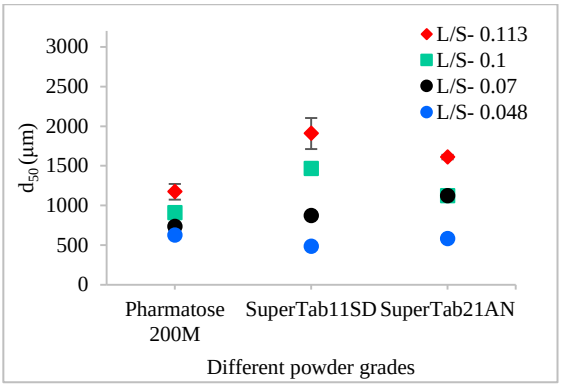

(c) 700 rpm

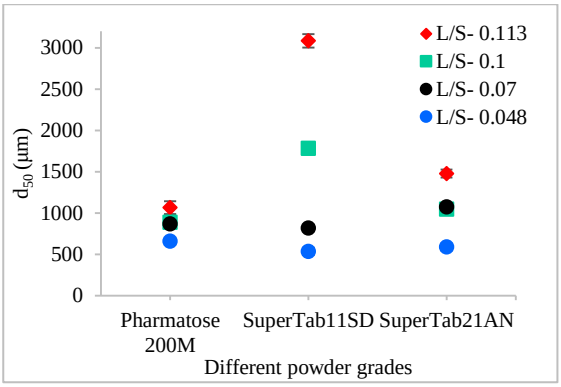

(d) 950 rpm

Figure 8-4 Median size of granules for different grades of lactose powder at varying L/S and screw speed

8.4.3.1.1 Effect of varying L/S

From Figure 8-4(a)-(d), it can be noticed that the granule size increased as the L/S increased for all three lactose powders. At the lowest L/S of 0.048, although, Pharmatose 200M has the smallest primary particle size (d_{50}) amongst three lactose powders, it produced granules comparable to SuperTab21AN which has larger primary particle size. This indicates that the smaller particles of Pharmatose 200M exhibited larger surface area which promoted the dissolution of particle surface potentially contributing to the formation of stronger liquid bridges between the particles and thus to the granule growth. As shown in Table 8-2, SuperTab21AN powder has larger primary particle size (d_{50}- 172.3 µm) meaning relatively smaller surface area and hence limited dissolution of particle surface and limited granule growth. At same L/S (i.e. 0.048) and screw speed of 200 rpm and 450 rpm, SuperTab11SD

which has larger and more compressible primary particles also produced similar sized granules. This may be because, at such low L/S, larger primary particles remained poorly wetted and were broken into smaller fragments owing to high compressibility limiting the overall granule growth. No significant change in the granule size was observed at higher screw speeds of 700 rpm and 950 rpm (at same L/S of 0.048). Although, some differences were observed amongst three powders at various screw speeds, the overall maximum granule size was limited to ~650 µm due to low availability of liquid at L/S of 0.048. This can be explained as follows. In twin screw wet granulation process the wetted/partially wetted powder passes through the zone of kneading elements where shearing and consolidation occurs (Lute et al. 2016). This results in the squeezing of interstitial liquid from the wetted powder helping primary particles to attach with each other (Iveson et al. 2001, Lute et al. 2016). However, due to insufficient availability of liquid, the granules did not grow significantly for any of the three lactose powders.

At L/S of 0.07 and screw speed of 200 rpm and 450 rpm, SuperTab11SD produced relatively bigger granules amongst three powders. At screw speed of 700 rpm and 950 rpm, SuperTab21AN had the largest median granule size amongst three powders. This indicated that at L/S of 0.07 the effect of screw speed was not consistent and it depended on the properties of the primary powder.

With further increase in the L/S to 0.1 and 0.113, the solubility of lactose powders expectedly increased resulting in the formation of stronger and more number of liquid bridges between the primary particles meaning formation of bigger and stronger granules. However, apart from the solubility, there are other factors such as compressibility which can also play key role during wet granulation. Pharmatose 200M is a crystalline lactose which is smaller in size (thus high surface area and expectedly more soluble amongst 3 lactose powders) and less compressible. SuperTab11SD is more compressible and spherical powder compared to other two lactose powders. SuperTab21AN is also crystalline lactose which is more compressible compared to Pharmatose 200M and less compressible compared to SuperTab11SD. At L/S of 0.1 and 0.113 (at all screw speeds except 200 rpm), SuperTab11SD produced the largest granules amongst all three powders. At such higher L/S, shearing action from the kneading elements promoted an even distribution of liquid into the SuperTab11SD powder. This liquid distribution helped to produce plastic mass of powder

which promoted granules to coalesce and grow further rapidly at all screw speeds. Despite smaller primary particles and higher solubility, Pharmatose 200M produced relatively smaller granules at higher L/S compared to other powders.

8.4.3.1.2 Effect of varying screw speed

Figure 8-4 (a)-(d) also shows that the increase in the screw speed had varying effects on granule size depending on the amount of liquid (L/S). In case of Pharmatose 200M, the effect of increasing screw speed on the granule size was not prominent. This is in agreement with the observation by Dhenge et al. (2010). In case of SuperTab11SD, at lower L/S of 0.048 and 0.07 (at all screw speeds), no significant difference was observed due to the porous structure of SuperTab11SD where liquid was absorbed into the powder particles reducing the availability of liquid on the surface (Dhenge et al. 2010). The absorbed interstitial liquid did not squeeze out sufficiently on the surface of granules due to low granule-granule and granule-barrel wall impact at lower screw speed. At lower screw speed, fill level also goes up increasing the attrition forces controlling the granule growth (Jonathan Bouffard 2005). Increasing screw speed at higher L/S of 0.1 and 0.113, granule size increased significantly. The granule growth at low L/S and high screw speed and high L/S and low screw speed can be explained using regime map described by Hapgood et al. (2003) where high liquid amount condition was described as ‘drop controlled regime’ while high shearing condition was indicated by ‘mechanical agitation controlled regime’.

In case of SuperTab21AN, increasing screw speed at lower L/S of 0.048 did not show significant effect on the granule growth because liquid was not sufficient to form adequate number of liquid bridges between the particles. Increasing screw speed from 200 rpm to 450 rpm at L/S of 0.07, there was no significant change in granule size but as the screw speed was increased further to 700 rpm and 950 rpm, the granule size increased noticeably. This is because at lower screw speed 200 rpm and 450 rpm, the barrel fill level was high. This resulted in more attrition and breakage of formed granules which controlled the granule size. At higher screw speeds of 700 rpm to 950 rpm, the granule size increased because of high impact forces that helped granules to squeeze-out interstitial liquid on the surface promoting growth. Increasing screw speed at further higher L/S of 0.1 and 0.113 resulted in granule growth due to higher availability and better distribution of granulation liquid.

8.4.3.2 Mannitol

In case of mannitol (Figure 8-5(a)-(d)), increasing the primary particle size of powder at varying L/S and screw speed had varying influences on the median granule size. Similar to lactose, for the ease of understanding the results are discussed in two parts viz. effect of increasing powder particle size on granule size at varying L/S and the same at varying screw speed.

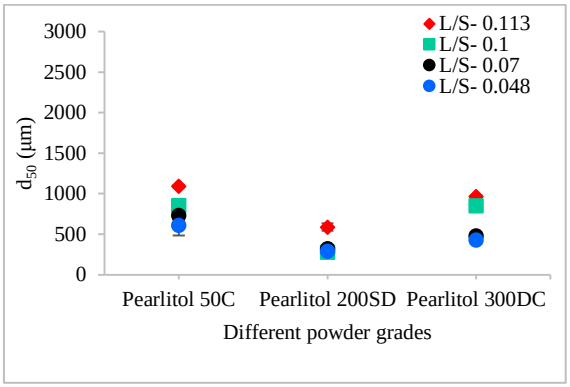

(a) 200 rpm

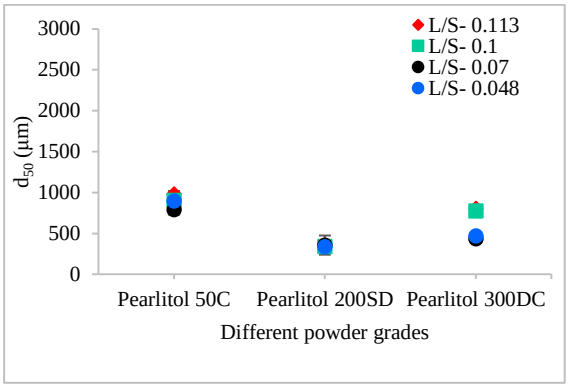

(b) 450 rpm

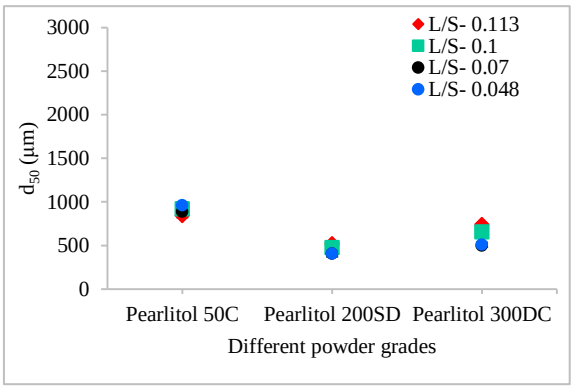

(c) 700 rpm

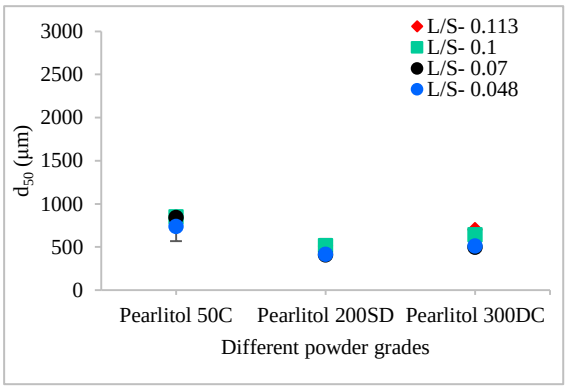

(d) 950 rpm

Figure 8-5 Median size of granules for different grades of mannitol powder at varying L/S and screw speed

8.4.3.2.1 Effect of varying L/S

From Figure 8-5(a)-(d) it can be observed that increasing L/S had powder dependent effect on the granule size. In case of Pearlitol 50C and Pearlitol 200SD, varying L/S at constant screw speed of 200 rpm (Figure 8-5(a) showed an obvious increase in granule size at L/S of

0.113 only. The granule size did not vary significantly at lower L/S. Varying L/S at screw speed of 450 rpm, 700 rpm and 950 rpm, resulted in no change in granule size for Pearlitol 50C and Pearlitol 200SD. In case of Pearlitol 300DC, the granule size did not vary noticeably at L/S of 0.048 and 0.07 but increased at L/S of 0.1 and 0.113 (at all screw speeds).

Comparing three powders, Pearlitol 50C, which has the smallest primary particle size (d_{50}) amongst all mannitol powders, generally produced relatively larger granules in almost all cases while Pearlitol 200SD produced small size granules. This was not the case with similar size lactose powder i.e. Pharmatose 200M (similar to Pearlitol 50C) where granule size was either similar or smaller than other two lactose powders at various conditions. Pearlitol 300DC which has the largest primary particles amongst three mannitol powders produced granules comparable to Pearlitol 50C. This indicates that there are more dominant variable(s)/properties that controlled the granule size than the primary particle size of the powder. As discussed in the Section 8.4.1 and section 8.4.4 the powders are significantly different in their size, shape, structure and compressibility. One or more properties of the primary powder can dominate the granulation process outcome. For instance, Pearlitol 50C has the smallest size, elongated shape and low compressibility. The small particle size of Pearlitol 50C meant a larger surface area which potentially promoted the dissolution of particle surface contributing to the formation of stronger liquid bridges between the particles and thus to the granule growth (similar to Pharmatose 200M). Pearlitol 200SD on the other hand has larger particles (small surface area) with porous structure and high compressibility. This means that part of the liquid added may have been absorbed into the particle structure leaving insufficient amount to promote the formation of sufficient number of liquid bridges between the particles, hence, very limited granule growth in case of Pearlitol 200SD, even at moderately high L/S (0.07- 0.113). This suggests that either the binding capacity of Pearlitol 200SD is poor or it requires further increase in L/S (> 0.113) to exhibit increase in the granule size at increasing shear i.e. at higher screw speeds. Additionally, the low compressibility factor (Figure 8-4) also supports the fact that Pearlitol 200SD particles are fragile (Souihi et al. 2013). Thus, the overall change in growth may be concealed by the volume reduction due to excellent compressibility and or the breakage of poorly saturated particles. However, spray dried lactose powder (SuperTab11SD) which has similar compressibility factor to Pearlitol 200SD produced larger granules at high L/S (0.1 and

0.113) at all four screw speeds. An attempt was made to understand this contrasting granule growth behaviour of these two spray dried powders (SuperTab11SD and Pearlitol 200SD) by determining difference between their drop penetration time, single particle strength and dissolution rate (refer Figure 12-25, Figure 12-26 and Figure 12-27). However, none of these additional measurements justified the difference in the granule growth behaviour of SuperTab11SD and Pearlitol 200SD. This remains a topic for the further investigation in the future where the known fact about the spray dried lactose that it consists of spherical agglomerates of crystalline lactose monohydrate in a matrix of amorphous lactose (Omar et al. 2015) can be explored for differentiating its behaviour from spray dried mannitol.

Compared to Pearlitol 200SD, Pearlitol 300DC has the larger particle size, however, it is relatively low in compressibility (than porous Pearlitol 200SD). It behaves similar to Pearlitol 50C at higher L/S. The Pearlitol 300DC has large particle size but they are not porous as in case of Pearlitol 200SD. This means that the liquid was not absorbed in the structure and was available for the inter-particle liquid bridge formation. Additionally, there was less reduction in the volume due to relatively lower compressibility. Hence, it can be concluded that when there is significant difference in the structure and the compressibility, the granule growth is not just controlled by the primary particle size of powder in twin screw wet granulation. The effect on granule size can be a combination of one or more properties of a powder.

8.4.3.2.2 Effect of varying screw speed

Figure 8-5(a)-(d) also shows the effect of screw speed on the median size of granules produced using three mannitol powders. Increasing screw speed at all L/S had limited impact on the granule size.

8.4.4 Structure of granules

Figure 8-6-Figure 8-8 show the XRT images of granules produced using different lactose powders at varying L/S (constant screw speed- 450 rpm). The respective inter-particle porosity within the granules calculated using ImageJ software is presented in Figure 8-9.

The XRT images and the respective calculated inter-particle porosity indicate that the granules generally densify with increase in the L/S at a set screw speed in all three lactose powders. Comparing the XRT images of granules from 3 powders, SuperTab11SD and SuperTab21AN granules appeared to be relatively more porous (due to higher inter-granular porosity) (Dhenge et al. 2011) due to larger primary particle size. However, they show localized densification (lower inter-particle porosity) within the granule structure owing to their porous primary particles and high compressibility.

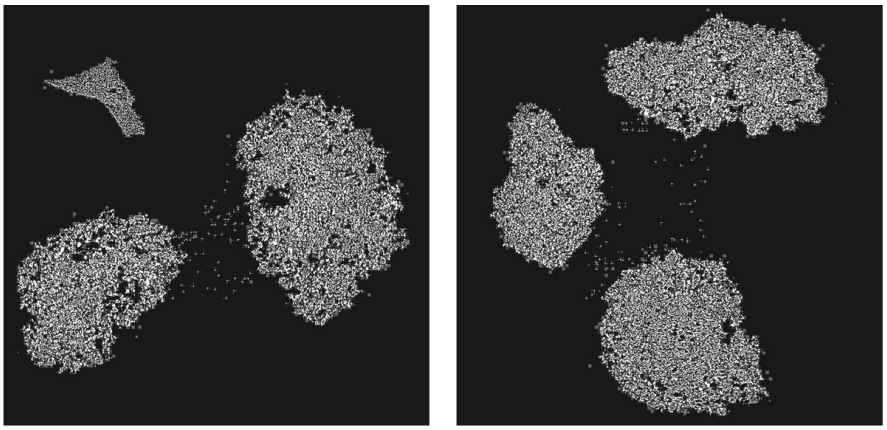

(a) L/S-0.048 Screw speed-450rpm (b) L/S-0.07 Screw speed-450rpm

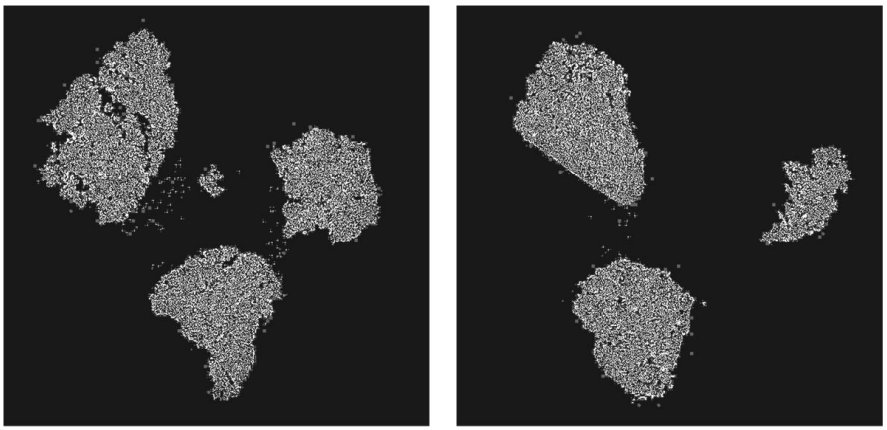

(c) L/S-0.1 Screw speed-450rpm (d) L/S-0.113 Screw speed-450rpm

Figure 8-6 X-ray tomographic images of granules produced using Pharmatose 200M (d50- 42.1 µm) at varying L/S (screw speed- 450 rpm)

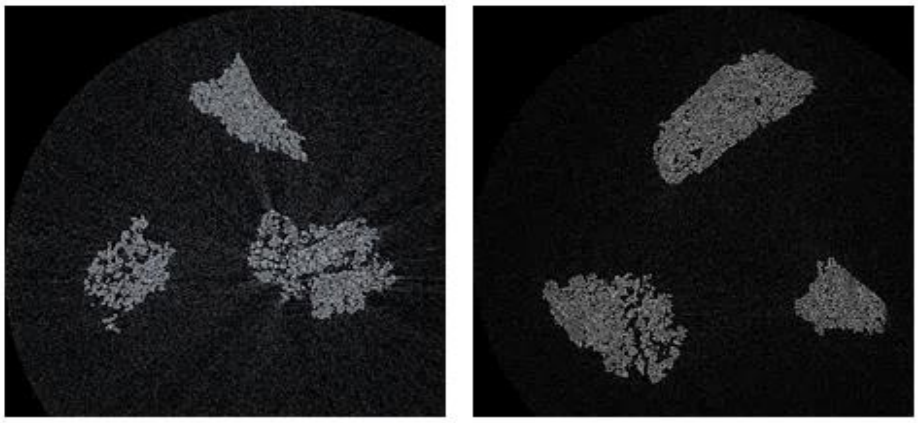

(a) L/S-0.048 Screw speed-450rpm (b) L/S-0.07 Screw speed-450rpm

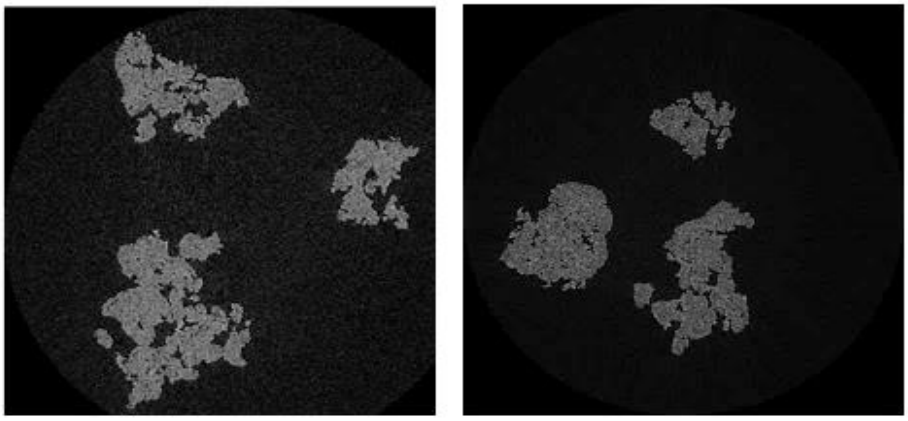

(c) L/S-0.1 Screw speed-450rpm (d) L/S-0.113 Screw speed-450rpm

Figure 8-7 X-ray tomographic images of granules produced using SuperTab11SD at varying (d50- 113.48 µm) L/S (screw speed- 450 rpm)

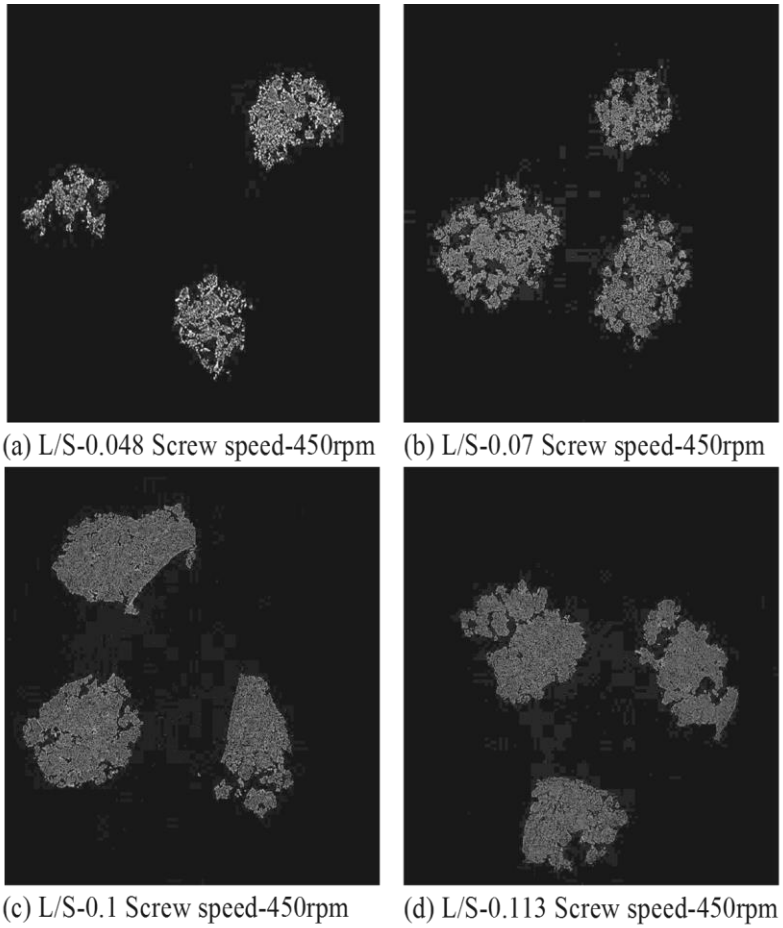

Figure 8-8 X-ray tomographic images of granules produced using SuperTab21AN at varying (d50- 172.3 µm) L/S (screw speed- 450 rpm)

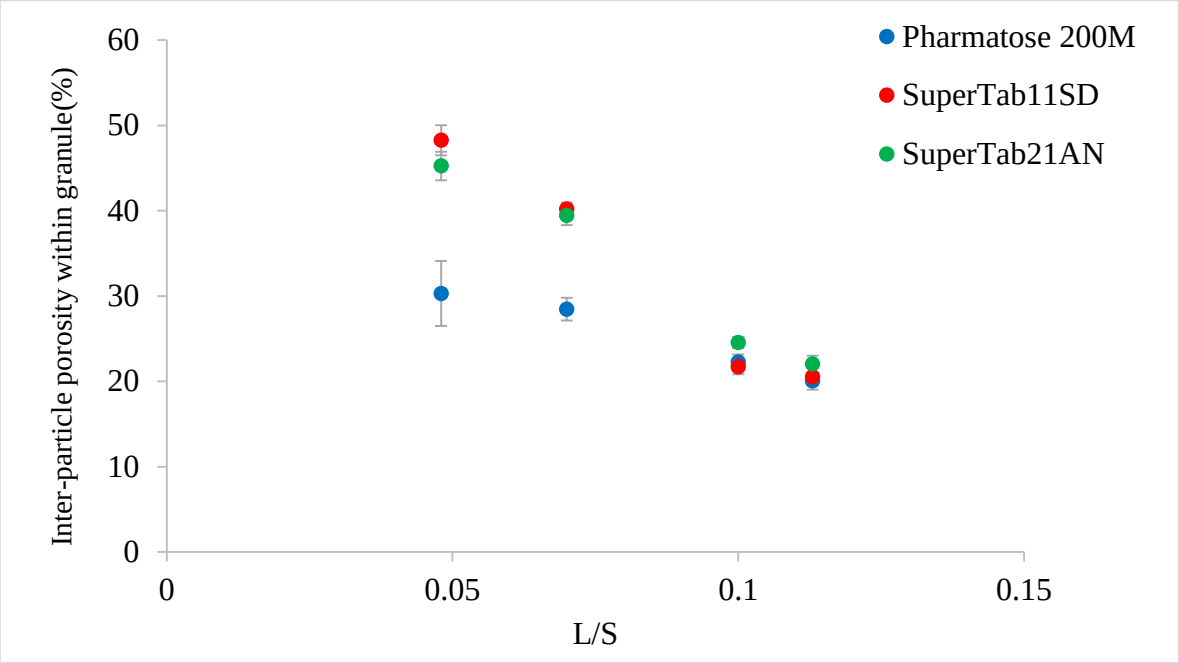

Figure 8-9 Porosity of granules for different grades of lactose powder at varying L/S (screw speed- 450 rpm)

XRT images of granules produced using different grades of mannitol are presented in Figure 8-10-Figure 8-12. The respective inter-particle porosity within the granules calculated using ImageJ software is presented in Figure 8-13. Pearlitol 50C (Figure 8-10(a)-(d) and Pearlitol 200SD (Figure 8-11(a)-(d)) showed less significant change in structure of larger granules with increasing L/S. However, few densified, elongated granules could be seen at L/S of 0.07-0.113 in case of Pearlitol 200SD (Figure 8-11(b)-(d)). The effect of L/S on granule structure was more obvious in case of Pearlitol 300DC (Figure 8-12(a)-(d) where granules became denser with increasing L/S. At L/S of 0.048 (Figure 8-12(a)), individual large size particles of Pearlitol 300DC could still be identified in the granule structure. The inter-particle porosity within the granules (Figure 8-13) supported the observation from XRT images for Pearlitol 300DC. The inter-particle porosity within the granules (Figure 8-13) also supported the observation from XRT images for Pearlitol 50C where porosity did not vary significantly with increasing L/S. However, in case of Pearlitol 200SD, the inter-particle porosity decreased with increasing L/S. This is due to the localised densification within the granules.

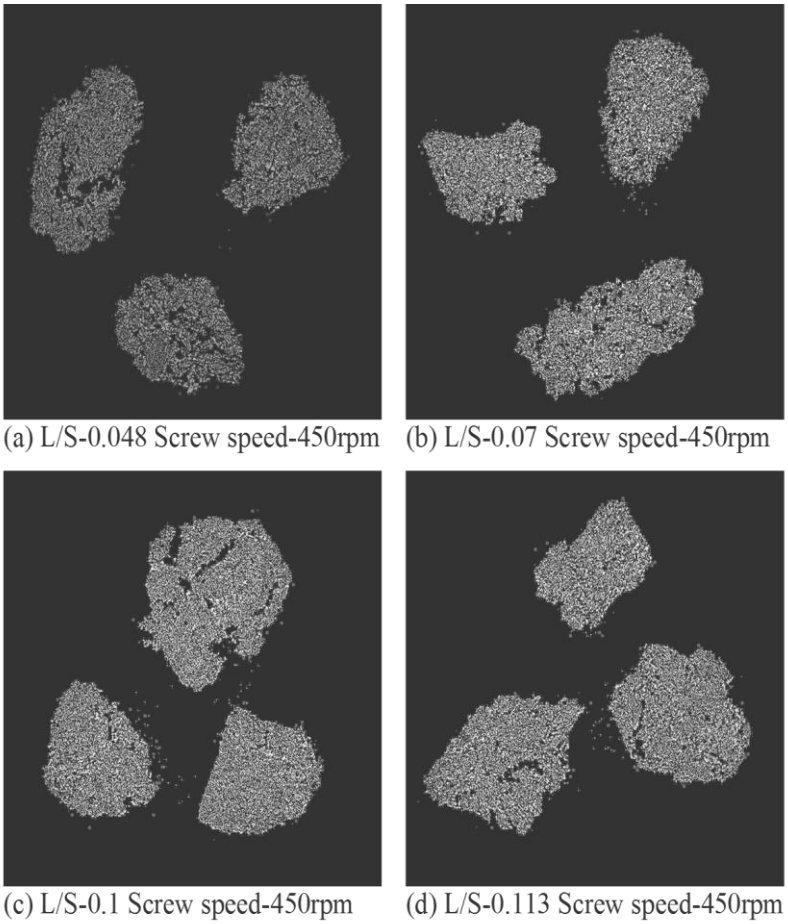

Figure 8-10 X-ray tomographic images of granules produced using Pearlitol 50C at varying (d50- 33.9µm) L/S (screw speed- 450 rpm)

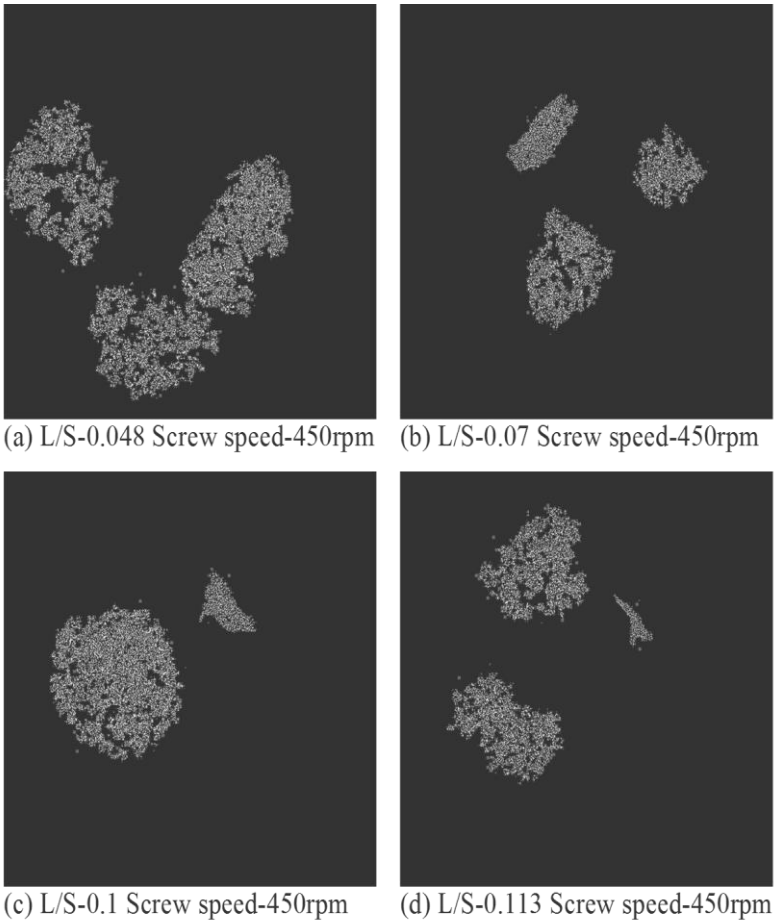

Figure 8-11 X-ray tomographic images of granules produced using Pearlitol 200SD at (d50-145.3µm) varying L/S (screw speed- 450 rpm)

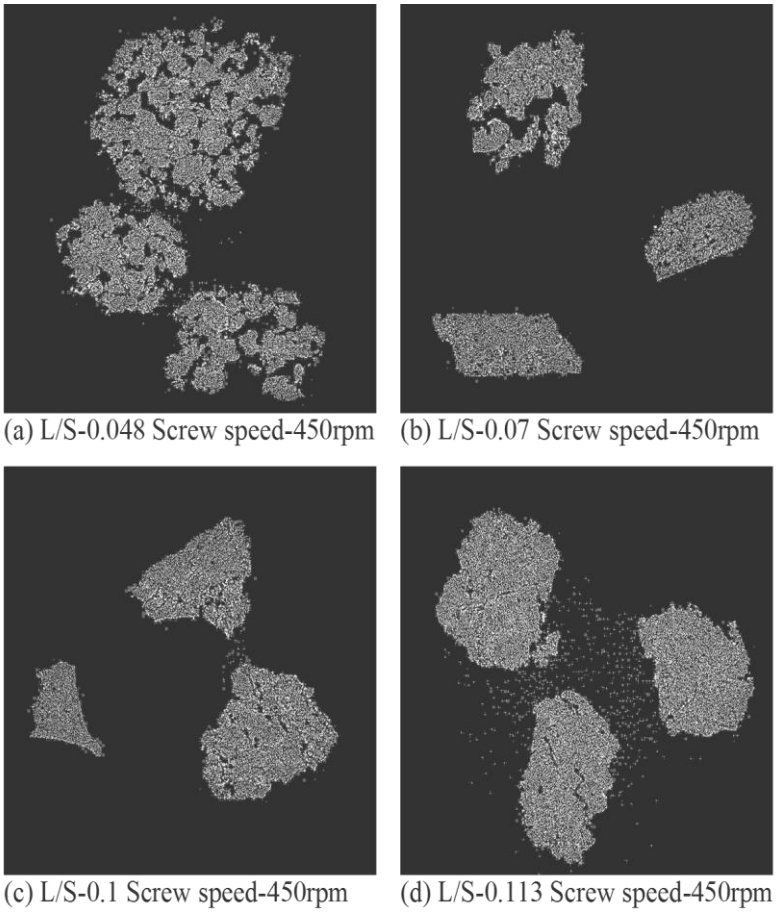

Figure 8-12 X-ray tomographic images of granules produced using Pearlitol 300DC at (d50- 249.9 µm) varying L/S (screw speed- 450 rpm)

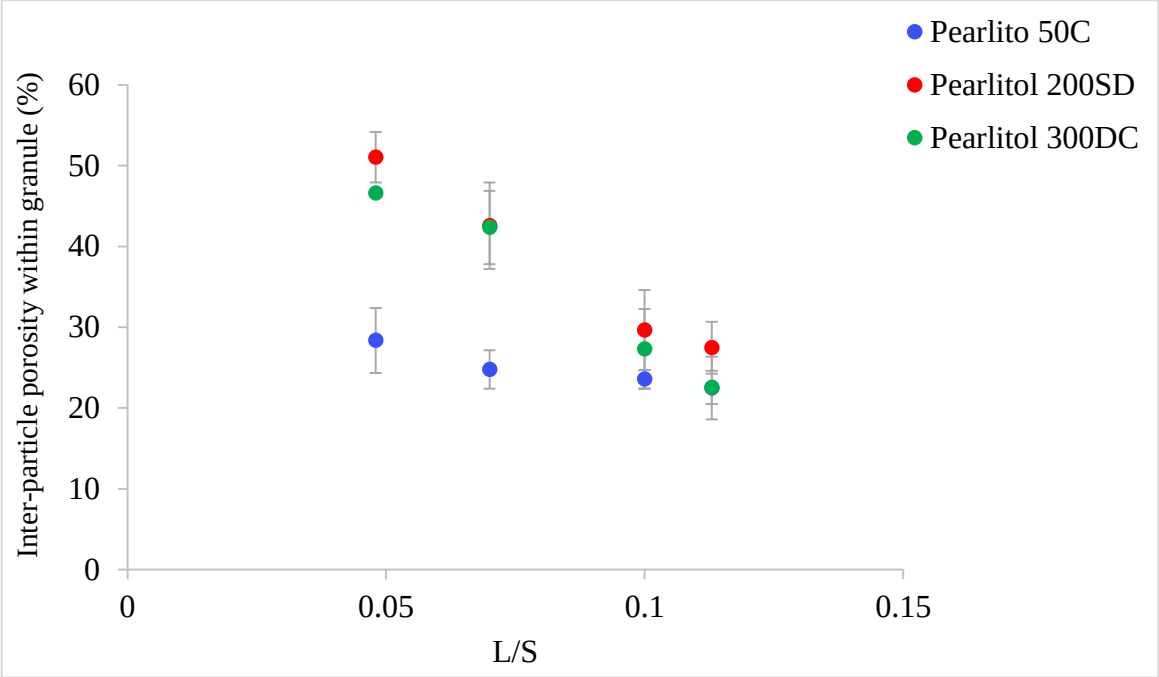

Figure 8-13 Porosity of granules for different grades of mannitol powder at varying L/S (screw speed- 450 rpm)

8.4.5 Tensile strength of tablets

Granules produced at L/S of 0.048 and 0.113 were sieved in size range of 212-1400 µm and into further subdivisions of 212-600 µm, 600-1000 µm, 1000-1400 µm. This was done to study the effect of different granule size range on the tableting and tablet tensile strength.

8.4.5.1 Pharmatose 200M

Figure 8-14(a)-(d) show the tensile strength of tablets of Pharmatose 200M granules produced at L/S of 0.048 and 0.113 at different screw speeds (200 rpm, 450 rpm, 700 rpm and 950 rpm) for different granule size ranges (complete range- 212-1400 µm and subdivisions- 212-600 µm, 600-1000 µm, 1000-1400 µm). It was found that the tensile strength of tablet was similar at both L/S (and at all screw speeds). The granule size also had very limited impact on the tablet strength. It appears that compression force applied during tableting overcame the granule strength (at low or high L/S or screw speeds), thus a minimum effect on the tablet strength.

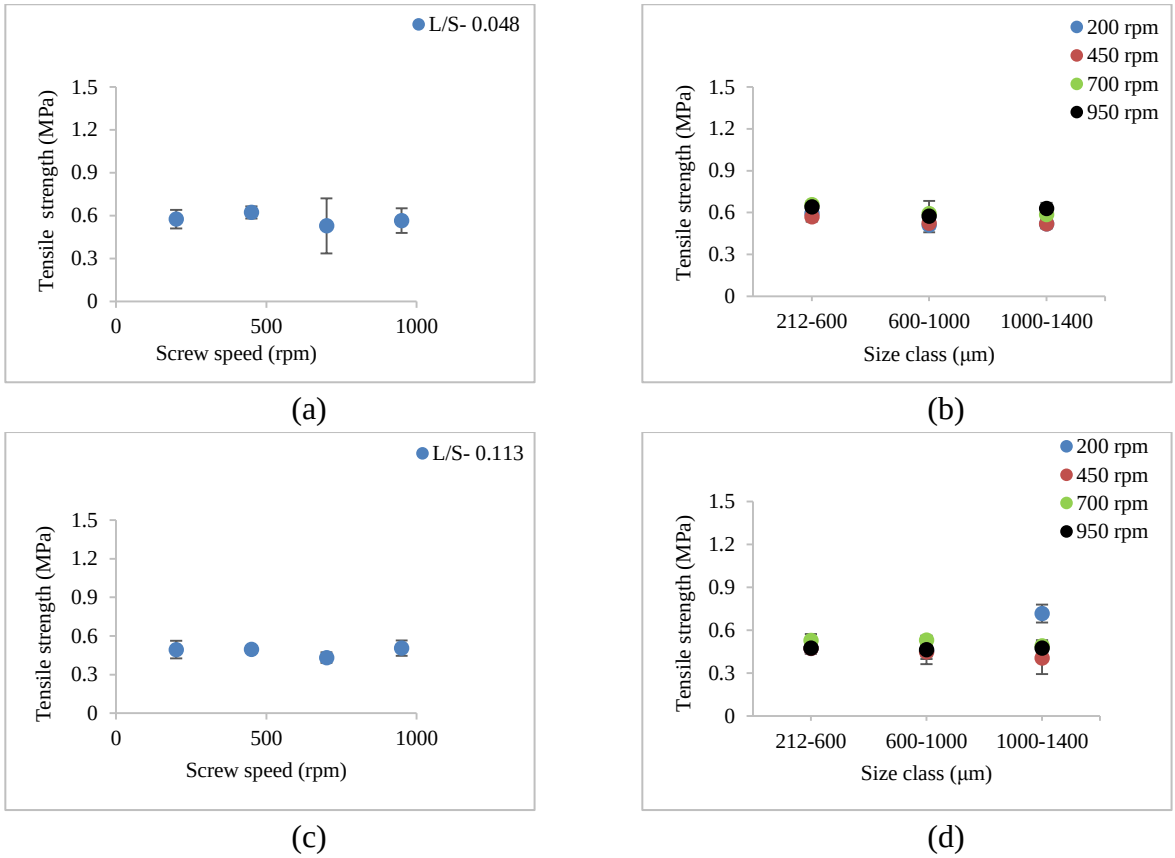

Figure 8-14 Tensile strength of tablet of granules at different size classes of Pharmatose 200M (a) 212-1400 µm at L/S of 0.048 (b) 212-600 µm, 600-1000 µm, 1000-1400 µm at L/S of 0.048 (c) 212-1400 µm at L/S of 0.113 (d) 212-600 µm, 600-1000 µm, 1000-1400 µm at L/S of 0.113

8.4.5.2 SuperTab11SD

Figure 8-15(a)-(d) show the tensile strength of tablets of SuperTab11SD granules produced at L/S of 0.048 and 0.113 (at varying screw speed) for different size classes. Similar to Pharmatose 200M, tablet strength was similar at all conditions.

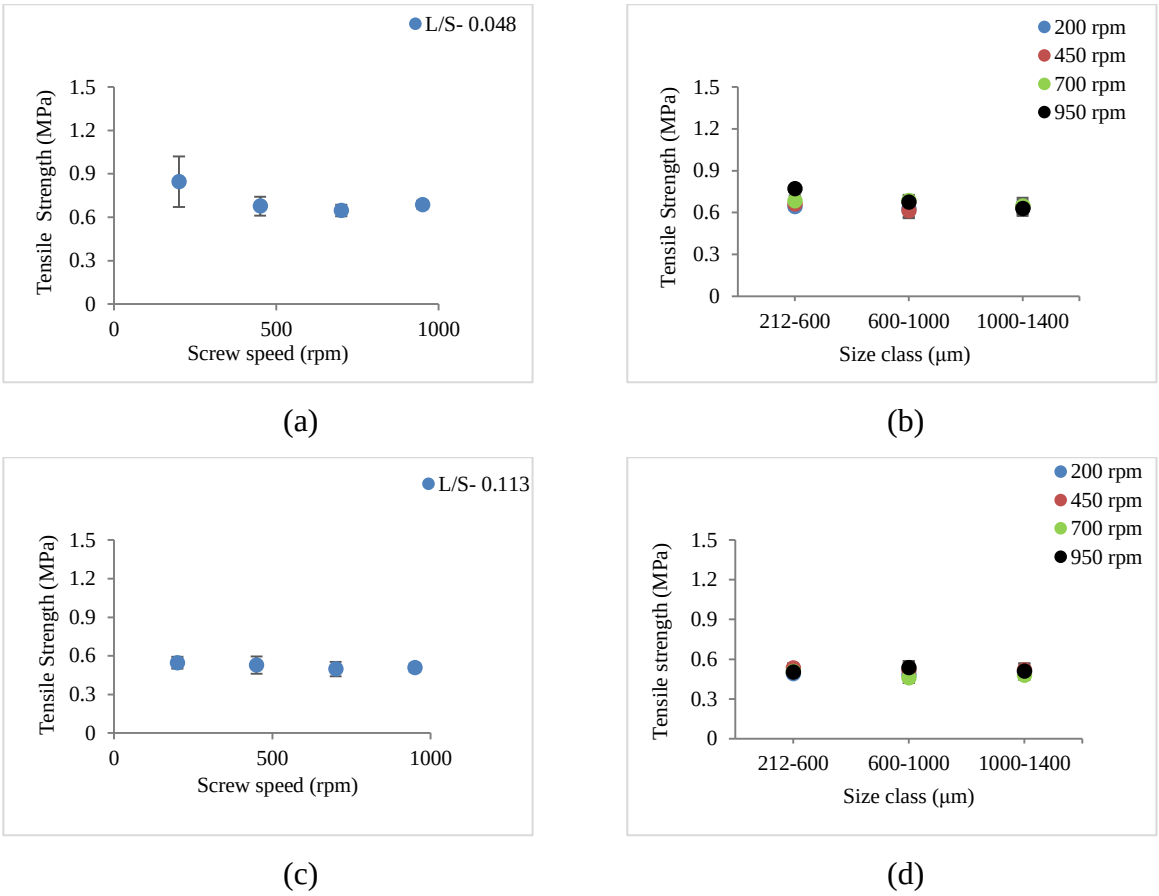

Figure 8-15 Tensile strength of tablet of granules at different size classes of SuperTab11SD a) 212-1400 µm at L/S of 0.048 (b) 212-600 µm, 600-1000 µm, 1000-1400 µm at L/S of 0.048 (c) 212-1400 µm at L/S of 0.113 (d) 212-600 µm, 600-1000 µm, 1000-1400 µm at L/S of 0.113

8.4.5.3 SuperTab21AN

Figure 8-16(a)-(d) show the tensile strength of tablets of SuperTab21AN granules produced at L/S of 0.048 and 0.113 (at varying screw speed) for different size classes. Similar to Pharmatose 200M and SuperTab11SD, tablet strength did not change (for broader granule size class of 212-1400 µm) with increase in the L/S and screw speed (Figure 8-16(a)-(c)). Subdividing the granules into narrower size classes, showed a screw speed dependent effect on the tablet strength to some extent (Figure 8-16(b)). The tablet strength increased at lower screw speed of 200 rpm and 450 rpm while it decreased at higher screw speed of 700 rpm and 950 rpm with increasing granule size class from 212-600 µm to 600-1000 µm and then to 1000-1400 µm. It may be interpreted that the granules in the size of 600-1000 µm and 1000-1400 µm, which are bigger and stronger, dictated the trend of decrease in the tablet strength with increasing screw speed in the broader granule size range (212-1400 µm). At

higher L/S of 0.113, the effect of screw speed was concealed by the liquid amount available for the granulation.

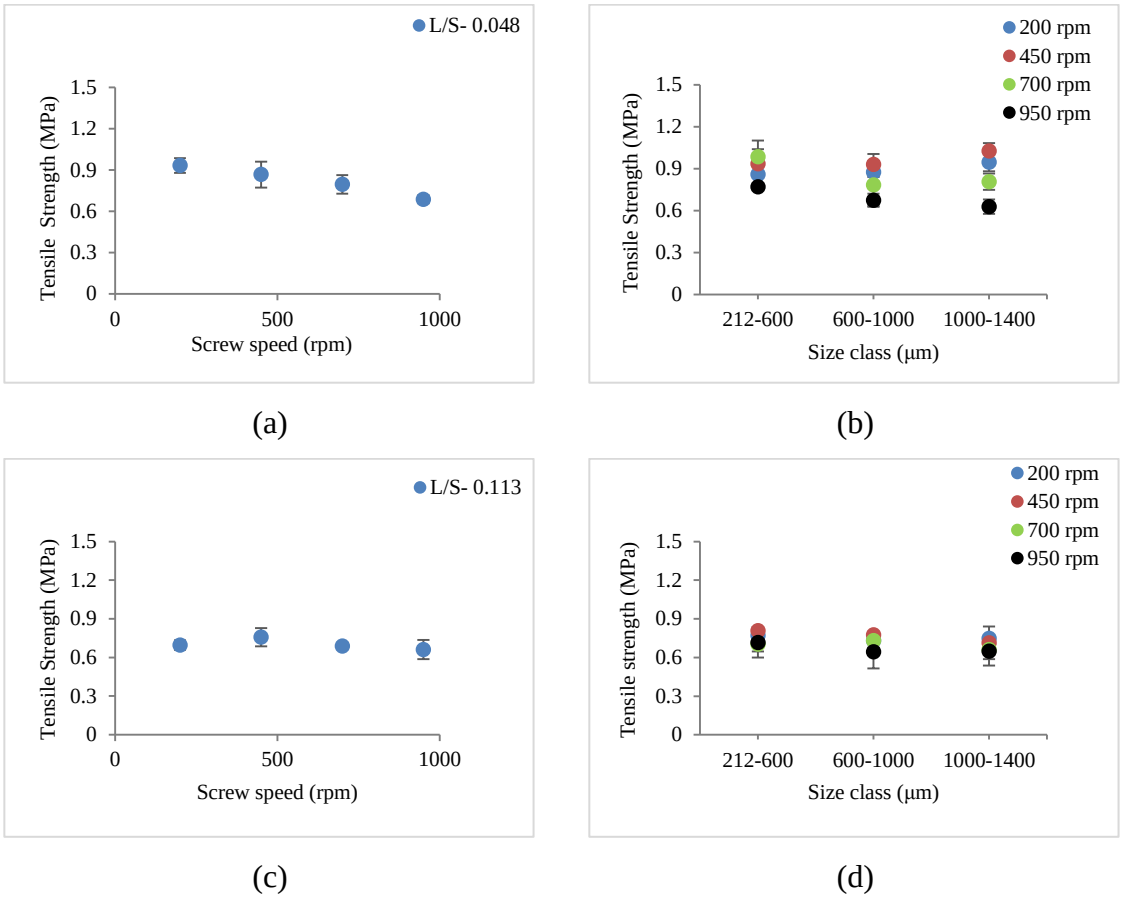

Figure 8-16 Tensile strength of tablet of granules at different size classes of SuperTab21AN (a) 212-1400 µm at L/S of 0.048 (b) 212-600 µm, 600-1000 µm, 1000-1400 µm at L/S of 0.048 (c) 212-1400 µm at L/S of 0.113 (d) 212-600 µm, 600-1000 µm, 1000-1400 µm at L/S of 0.113

8.4.5.4 Pearlitol 50C

Figure 8-17(a)-(d) show the tensile strength of tablet of Pearlitol 50C granules produced at varying L/S and screw speed for different size ranges. It can be seen that the tablets produced using broader granule size range (212-1400 µm) does not vary significantly upon increasing screw speed at both L/S (Figure 8-17(a) and Figure 8-17(c)). But subdividing the granules from 212-1400 µm into 212-600 µm, 600-1000 µm and 1000-1400 µm showed effect of granule size on the tablet tensile strength at different screw speed (Figure 8-17(b)). Increasing the granule size range from 212-600 µm to 600-1000 µm and to 1000-1400 µm, decreased the tensile strength of tablet. The smaller granule size range (212-600 µm) produced stronger tablet. This is because the small particles had higher surface area which

helped them to make more number of inter-particle bonds and pack better making stronger tablet. As granule size range increased to 600-1000 µm and to 1000-1400 µm, the surface area decreased and so did the number of bonds between the particles resulting in weaker tablet. As the L/S was increased to 0.113, availability of sufficient liquid promoted the formation of stronger granules that masked the effect of screw speed.

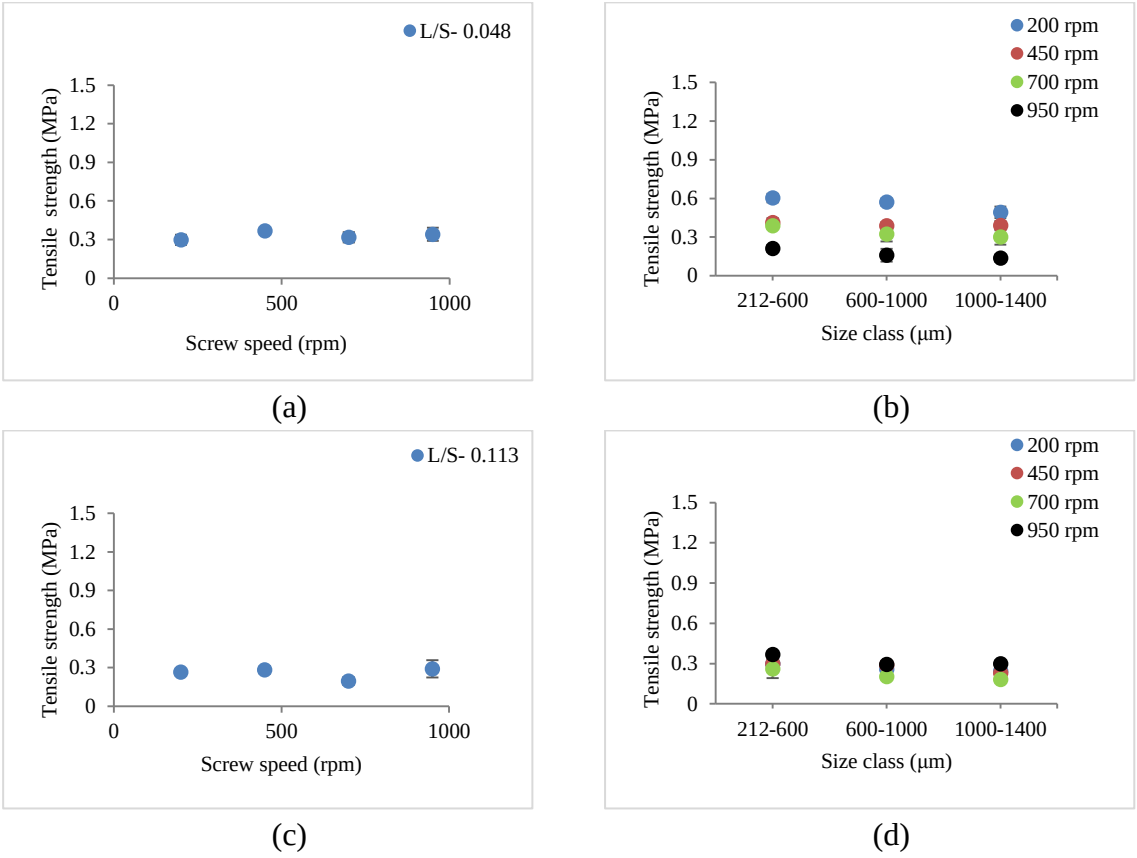

Figure 8-17 Tensile strength of tablet of granules at different size classes of Pearlitol 50C (a) 212-1400 µm at L/S of 0.048 (b) 212-600 µm, 600-1000 µm, 1000-1400 µm at L/S of 0.048 (c) 212-1400 µm at L/S of 0.113 (d) 212-600 µm, 600-1000 µm, 1000-1400 µm at L/S of 0.113

8.4.5.5 Pearlitol 200SD

Figure 8-18(a)-(d) show the tensile strength of tablet of Pearlitol 200SD produced at varying L/S and screw speed for different size ranges. Similar to Pearlitol 50C, varying screw speed or L/S for broader granule size range (212-1400 µm) showed no prominent effect on the tensile strength of tablets (Figure 8-18(a) and Figure 8-18(c)). Subdividing the broader range into 212-600 µm, 600-1000 µm and 1000-1400 µm also showed no significant effect on the tablet strength at various screw speed and L/S (Figure 8-18(b) and Figure 8-18(d)).

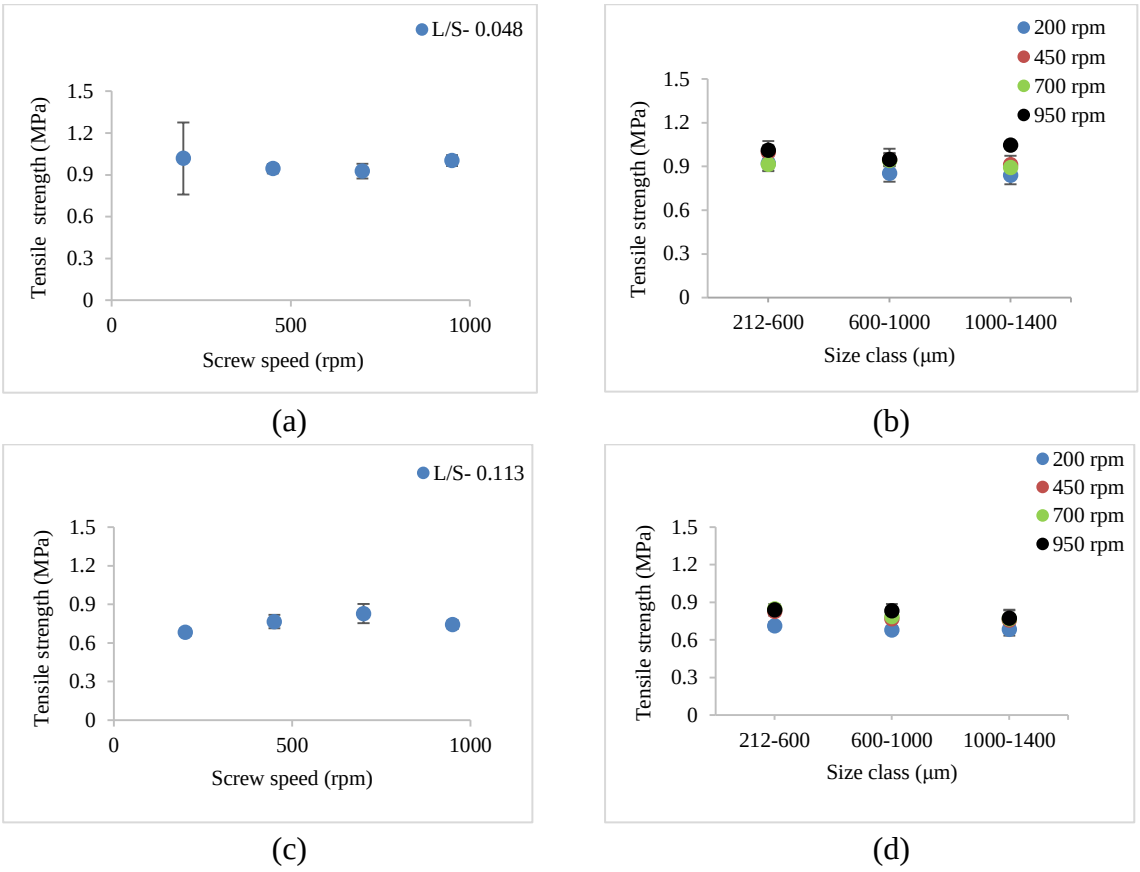

Figure 8-18 Tensile strength of tablet of granules at different size classes of Pearlitol 200SD (a) 212-1400 µm at L/S of 0.048 (b) 212-600 µm, 600-1000 µm, 1000-1400 µm at L/S of 0.048 (c) 212-1400 µm at L/S of 0.113 (d) 212-600 µm, 600-1000 µm, 1000-1400 µm at L/S of 0.113

8.4.5.6 Pearlitol 300DC

Figure 8-19(a)-(d) show tensile strength of tablets of Pearlitol 300DC produced at varying L/S and screw speed for different size ranges. It is clear that tensile strength of tablet was similar but very low at both lower and higher L/S at all screw speeds.

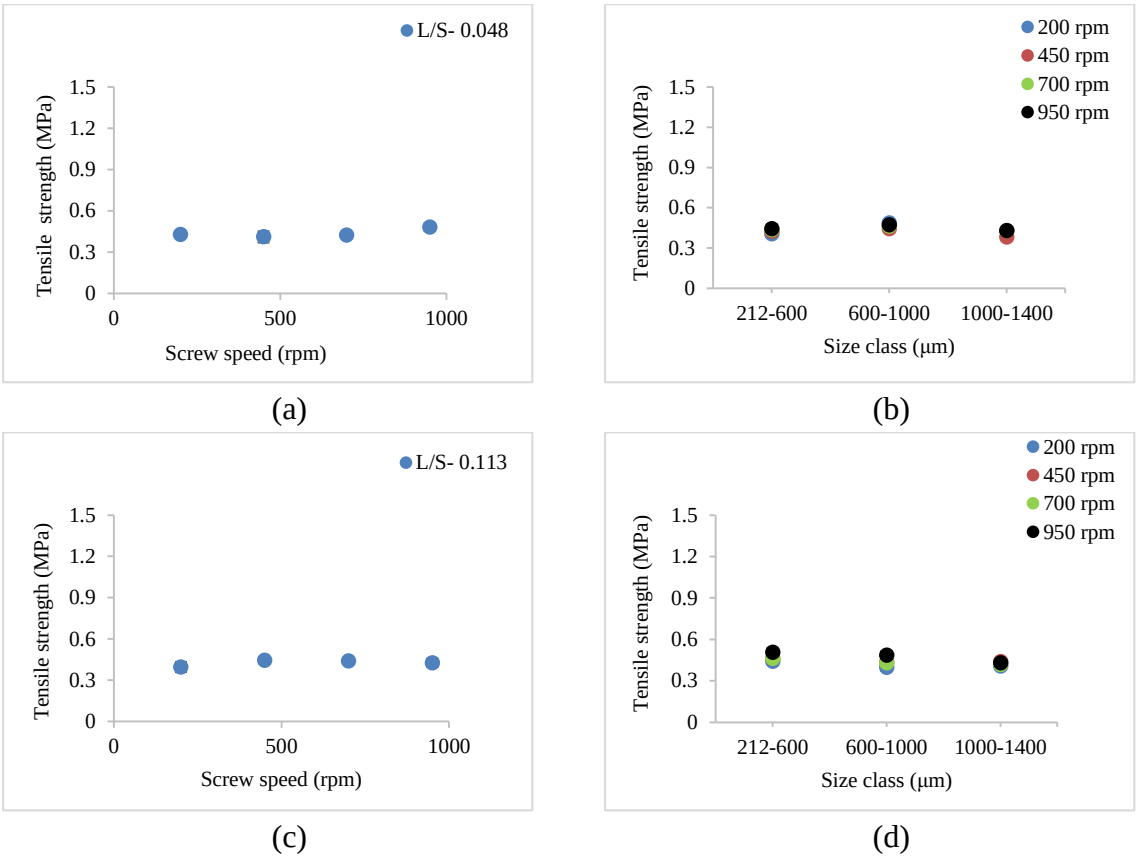

Figure 8-19 Tensile strength of tablet of granules at different size classes of Pearlitol 300DC (a) 212-1400 µm at L/S of 0.048 (b) 212-600 µm, 600-1000 µm, 1000-1400 µm at L/S of 0.048 (c) 212-1400 µm at L/S of 0.113 (d) 212-600 µm, 600-1000 µm, 1000-1400 µm at L/S of 0.113

It is clear that tensile strength of tablet was low for all three mannitol powders at both lower and higher L/S at all screw speeds. It is likely that the differences in the granule strength or compressibility may have been concealed by the compression force used in the study.

8.5 CONCLUSION

Powders differ in their size and structure due to the way of manufacture for the intended application (suitability for dry or wet granulation or direct compaction). In this study the effects of the properties of powder on twin screw wet granulation behaviour and properties of so produced granules and tablets were studied. It was found that granulation behaviour of powder is controlled by size, structure and compressibility of primary powder. The porous structure of particle may enhance the compressibility in dry granulation or direct compaction but in wet granulation it can limit the binding between the particles due to absorption of water in the structure of the particles. In general, increasing L/S resulted in increase in the

granule size and weaker tablets in all powders. The effect of screw speed on granule properties was dependant on the amount of liquid added.

9 POPULATION BALANCE MODELING OF TWIN SCREW GRANULATION TO DEVELOP MECHANISTIC UNDERSTANDING

9.1 ABSTRACT

This chapter aims to develop the mechanistic understanding of twin screw granulation process by using PBM based models incorporated in an advanced process modelling platform i.e. gSolids followed by the experimental validation (experiments similar to chapter 4). Using gSolids, the breakage and layering rate processes were studied for twin screw wet granulation. This was done by optimising rate constants for breakage and layering within gSolids in order to develop a database for future granule size prediction using gSolids platform. The experimental conditions were simulated using gSolids and the granule size distribution from both (experimental and gSolids simulation) was compared. During experiments, granule size evolution along the barrel length was understood at varying L/S. This was done by granulating the lactose powder (using distilled water) using systematically changed screw configuration (i.e. by stepwise increment in number of kneading and conveying elements in order to get a final screw configuration). The modelling was also carried out for each incremental screw configuration. The comparison of modelling and experimental results showed good agreement in most of the conditions. It was concluded that the combined model for the entire screw length can be used to track the evolution of granule size from any combination of kneading and conveying element at two different L/S. The model can also be improved with the addition of aggregation term.

9.2 INTRODUCTION

As mentioned earlier (section 2.3), screw configuration which includes different screw elements (e.g. kneading and conveying elements) is one of the most important process parameters to influence different granule attributes such as granule size and porosity and its effect has been studied before in detail in the literature. In this chapter, an attempt has been made to understand and describe the specific roles of kneading and conveying screw elements in determining the granulation behaviour, granule growth evolution along the length of the screw mechanistically using mathematical modelling based on PBM.

Population balance modelling technique has been extensively used in wet granulation processes. In order to understand and describe the rate processes involved in twin screw wet granulation using PBM based models in gSolids, it important to understand the basics of PBM. This technique is focussed on change in number of population of particles as they undergo different rate processes such as aggregation and breakage (Verkoeijen et al. 2002, Cameron et al. 2005). The PBM is a class of integro-differential equations which describes the change in the number of particles within each size class where each particles are subjected to different rate processes such as liquid addition, consolidation, aggregation and breakage. The screw speed of TSG in gSolids is determined by residence time. The powder and liquid feed rate can also vary depending on the values entered before simulation. Successful collision between two particles happens when particles with liquid layer of > =5 micron collides with each other. Successful collision results in aggregation.

A general form of the population balance equation is given in Eq. 9 (Ramkrishna 2000).

$$\frac{\partial F(x,t)}{\partial t} + \frac{\partial}{\partial x}\left[F(x,t)\frac{dx}{dt}(x,t)\right] = R_{formation}(x,t) - R_{depletion}(x,t) \qquad \text{Eq. 9}$$

Where, F is the number of particles or particle density as a function particle coordinates and time. The set of particle properties can also include different properties such as size, wetness, porosity and composition etc. (Ramkrishna 2000, J.D. Ennis 2004). Vector x represents these particle coordinates. The source terms $R_{\text{formation}}$ and $R_{\text{depletion}}$ represent the change in number of particles within each size class from aggregation, breakage, or Nucleation. In Eq. 9, the first term on left hand side (LHS) represents the changes in number of particles or number density over time. The second term on LHS represents changes in the particle co-ordinates. The possibilities also include the change in the solid volume in the particle due to layering. While the first term on the right hand side (RHS) is the rate of formation of particle of state x at time t due to rate mechanisms such as Nucleation, breakage and aggregation; the second term on RHS represents depletion of particles due to those rate processes.

Depending on different rate processes, some of the important properties of theoretical, experimental and mechanistic kernels which are widely found in literature and used in

granulation studies involving aggregation and breakage mechanisms are discussed here to provide an overview.

9.2.1 Aggregation kernel

The formation and depletion of granules due to aggregation is represented by Eq. 10 which can be determined using the semi-empirical aggregation kernel *β*, as shown in Eq. 11

$$R_{agg}(x,t) = R_{agg}^{form}(x,t) - R_{agg}^{dep}(x,t) \quad \text{Eq. 10}$$

The aggregation is a measure of successful collision of two particles. The aggregation kernel $\beta_{i,j}(t)$ among the classes *i* and *j* is defined as the product of the collision frequency $\beta_{i,j}$ of the particles and aggregation efficiency, $\beta_0(t)$.

$$\beta_{i,j}(t) = \beta_0(t).\beta_{i,j} \quad \text{Eq. 11}$$

As shown in the chapter 4 (Figure 4-14-Figure 4-16) the kneading elements helps for aggregation of particles. But, the aggregation kernel is absent in gSolids while breakage and layering has taken into consideration when experimental data and gSolids simulation were compared.

9.2.2 Breakage kernel

Breakage happens when particles disintegrate into two or more fragments due to impact and attrition. The breakage rate describes the change in breakage of larger R_{break}^{dep} granules and formation of smaller particles R_{break}^{form} as shown in Eq. 12 and Eq. 13.

$$R_{break}(x,t) = R_{break}^{form}(x,t) - R_{break}^{dep}(x,t) \quad \text{Eq. 12}$$

$$Breakage = \int_{v}^{\infty} K_{break}\, B_{break} n_x dx \quad \text{Eq. 13}$$

Where, K_{break} - breakage rate kernel

B_{break} - number of fragments due to breakage of bigger particle

n_x - number of particles of size x

9.2.3 Layering kernels

Layering is related to the surface area of granules, amount of fines present in the system and amount of liquid available on the surface of granules. Ridade Sayin (2016) found that, no layering will occur if the granule has an external liquid layer with less than five-micron thickness and this external layer is called critical moisture content. The following correlation is used to calculate the growth rate G is shown in Eq. 14 (Cameron et al. 2005).

$$G = G_m = \frac{M_{powder}}{k \sum M_i + M_{powder}} . \exp[-\alpha(x_w - x_{wc})^2] \quad \text{Eq. 14}$$

where, G_m is the maximum growth rate, M_{powder} is the mass of fine powder below the lower bound of the particle classes, M_i is the mass of particles in the ith size class, x_w is moisture content, x_{wc} is the critical moisture content, k and α are fitting parameters.

9.2.4 Population balance modelling in twin screw wet granulation

Compared to its batch counterparts, population balance modelling of twin screw granulation process has received relatively limited attention in literature. A 1-D five compartmental PBM for twin screw granulation was developed by Kumar, Vercruysse, et al. (2016), dividing the screws into liquid addition port, 2 blocks of 6 kneading elements each and conveying elements before and after 2nd kneading block where aggregation rate increases in the first block of kneading elements. It was noticed that aggregation rate reduces and breakage rate increases in the further sections during granulation. Similarly, four compartmental PBM for conveying element only was studied (Ridade Sayin 2016). Additionally, a 2-D three compartmental PBM developed by Barrasso et al. (2015) helps to track particle size and liquid distributions of conveying elements along an axial co-ordinate,

while taking into account the rate processes of aggregation, breakage, liquid addition, and consolidation, as well as powder flow. The liquid content and porosity of each particle size class was tracked by lump parameter approach.

The aim of the study is to develop the mechanistic understanding through experimental validation of 1-D PBM model developed and incorporated in gSolids (within gPROMS Formulated Products software by Process Systems Enterprise). Population balance modelling for twin screw granulation using gSolids is a multi-phase approach where fine powder is granulated by addition of liquid to form granules. The model takes into account the granule size as a distributed parameter.

It is known that the screw configuration in TSG is responsible for transport of material along the screw/barrel and the degree to which breakage, layering and consolidation occur. The granule breakage during granulation results in decrease in granule size. This breakage process induces layering by increasing the available granule surface area. Based on this mechanistic approach, the entire screw length is modelled as a series of parts or compartments where, each compartment is modelled separately on an element by element basis under the same processing conditions. The combined model for the whole screw length can then be used to track the evolution of granule properties from any combination of elements.

9.3 MATERIALS AND METHODS

9.3.1 Materials

Granules were produced using the method shown in chapter 4 using lactose (Pharmatose 200M) powder and distilled water as a granulation liquid.

9.3.2 Methods

The granules were air dried at room temperature for 48 h and then size of the granules was analysed using sieve shaker (Retsch, Germany) with series sieve of 212 µm. This was done to separate the granules from poorly granulated powder. The sieving was done at an

amplitude of 0.75 mm for 1 min at an interval of 10 s. gSolids was used to done simulation to compare with experimental data. The different parameters and values used in the simulation is shown in Table 9-1

Table 9-1 Parameter type and values used in the gSolids simulations

Parameter	Type	Value
Powder feed rate	Process parameter	2 kg/h
Liquid feed rate	Process parameter	0.2 kg/h for L/S-0.1 and 0.096 kg/h for L/S - 0.048
Conveying element residence time	Process parameter	1.1578 s/cm
Kneading element residence time	Process parameter	3.35 s/cm
Liquid drop diameter	Material property	2.6 mm
Screw diameter	Equipment geometry	16 mm
Breakage rate constant	Material property	0.03 s^{-1} for L/S- 0.048 0.02 s^{-1} for L/S- 0.1
Layering rate constant	Material property	35 µm/s for L/S- 0.048 50 µm/s for L/S- 0.1
v **and** w	Material property	Different particles of respective volumes(m3)
$\boldsymbol{\beta, \gamma, \emptyset}$	Material property	Fragment distribution function

9.3.2.1 Compartmental approach and screw configurations studied

Figure 9-1 is the screw configuration plan used in the experiment (also used in chapter 4). The whole screw length was divided into 10 parts and each part was treated as different compartment or part in modelling the twin screw granulator.

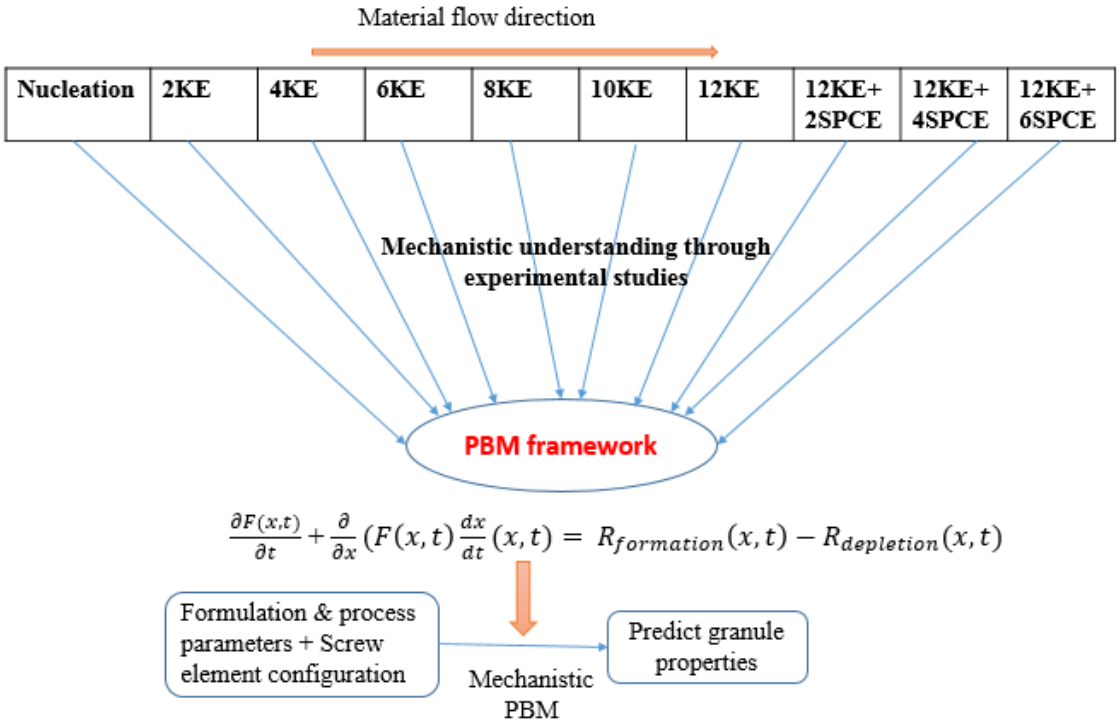

Figure 9-1 Mechanistic approach for PBM based modelling of twin screw wet granulation in gSolids

9.3.2.2 Population balance modelling in gSolids and experimental plan

The PBM based modelling in gSolids has very simple approach to understand each rate process. It considers experimentally measured mean residence time for each type of screw element. The model considers Austin 1976 breakage distribution function which is given by Eq. 15.

$$\textit{Breakage distribution function} = \frac{\emptyset\gamma}{3w}\frac{v}{w}_3^{\gamma-1} + \frac{(1-\emptyset)\beta}{3w}\frac{v}{w}_3^{\beta-1} \quad \text{Eq. 15}$$

Where, v, w = different particles of respective volumes (m^3)

$\beta, \gamma, \emptyset$ = Fragment distribution fuction

In the present work, the population balance model in gSolids was studied for each compartment in TSG and the dominant granulation rate processes in every compartment were understood by granulating lactose powder using distilled water (methodology similar to chapter 4) (using lactose powder). The pictorial representation of rate processes taking place in each compartment or part is given in Figure 9-2 (at L/S of 0.048 and 0.1 and screw

speed of 500 rpm). It can be noted from Figure 9-2 that twin screw wet granulation is a regime separated granulation process where various rate processes are more or less physically separated. It can also be noticed from Figure 9-2 that at low L/S of 0.048, granule size decrease along the length of the screw with increasing number of screw elements. At lower L/S of 0.048, the liquid is generally insufficient (in case of lactose) to aggregate powder particles together, thus, as the number of kneading elements increase, consolidation, coalescence and breakage of granules occur. As the L/S increases to 0.1, median granule size increase with increasing number of KE, because granule growth occurs due to predominant consolidation and coalescence. Presence of conveying elements after KE results in breakage due to shearing and cutting action of SPCE.

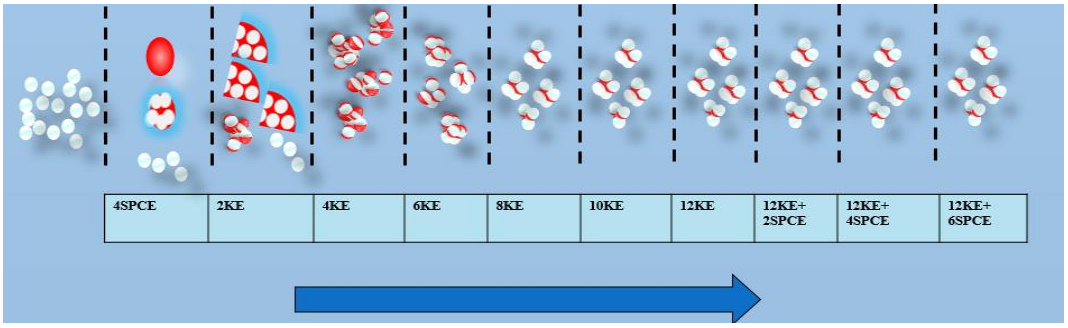

(a)

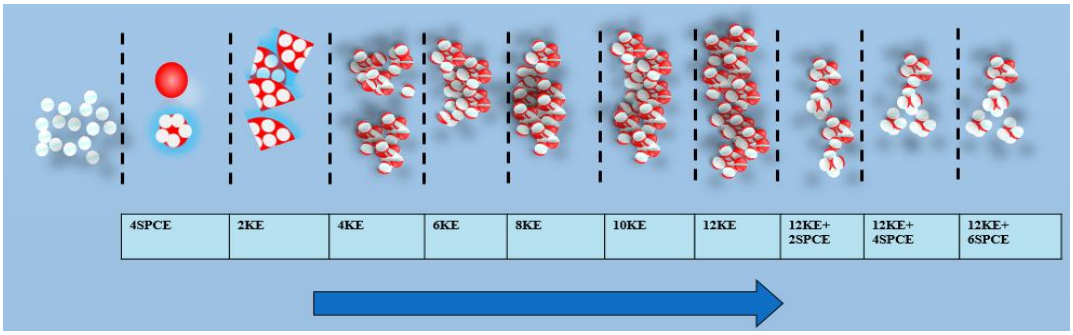

(b)

Figure 9-2 Physical separation (dominance) of granulation mechanisms/regimes (a) Low liquid to solid ratio (0.048) (b) High liquid to solid ratio (0.1)

9.4 RESULTS AND DISCUSSION

Figure 9-3 and Figure 9-4 present the granule size distribution results for the different number of kneading and conveying elements along the length of the barrel at L/S 0.048 and 0.1 respectively.

In Figure 9-3(a) and Figure 9-4(a) (Nucleation) the amount of fines is underestimated by simulated data compared to experimental data.

In Figure 9-3(L/S- 0.048) the model is able to predict the granule size distribution more effectively at lower L/S of 0.048 ratio with some discrepancy in the fraction of fines. It can also be seen from figure at lower L/S 0.048 that the size distribution of granules is maintained along the length of barrel due to less availability of liquid that results in more breakage of granules rather than aggregation.

At higher L/S 0.1, it is possible to predict granule size distribution effectively at configurations where breakage happens (12KE+2CE, 12KE+4CE, 12KE+6CE) (Figure 9-4 (h)-(j)).

Figure 9-4(a)-(f) shows the granule size distribution of kneading elements at higher sizes were underestimated by the model (Figure 9-4). A possible explanation is that aggregation is not taken into consideration in the model. Further studies on the aggregation rate will strengthen the predictive power of the model.

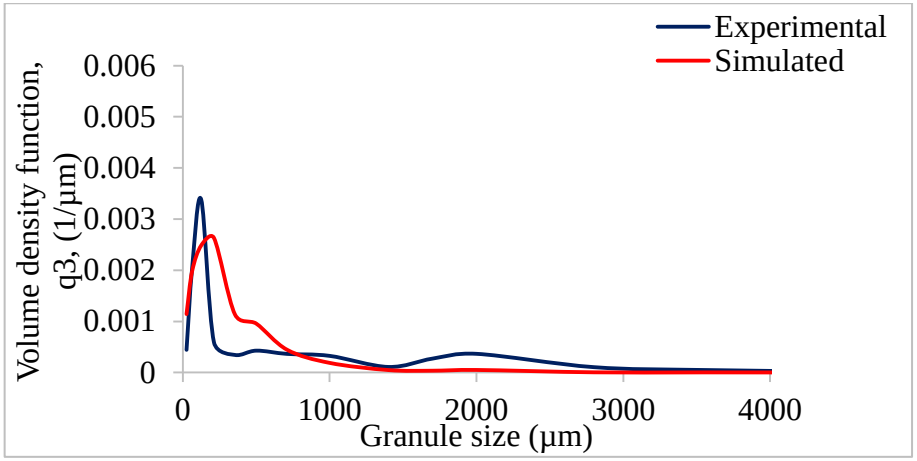

(a) Nucleation

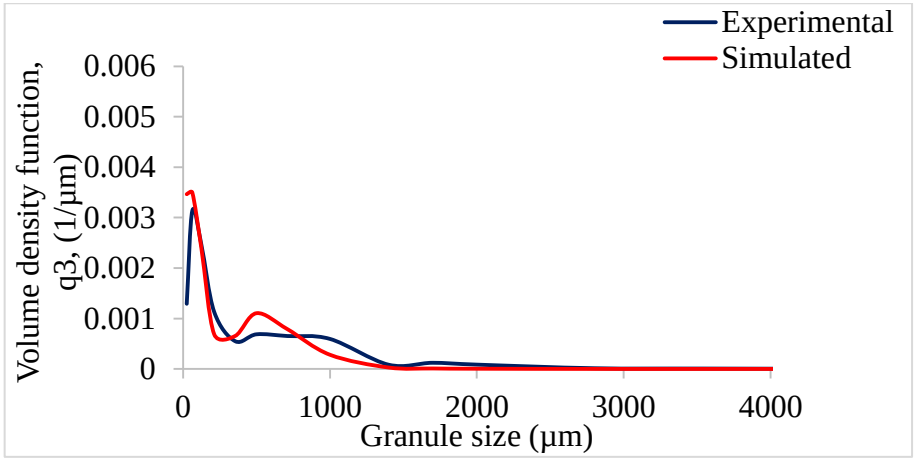

(b) 2KE

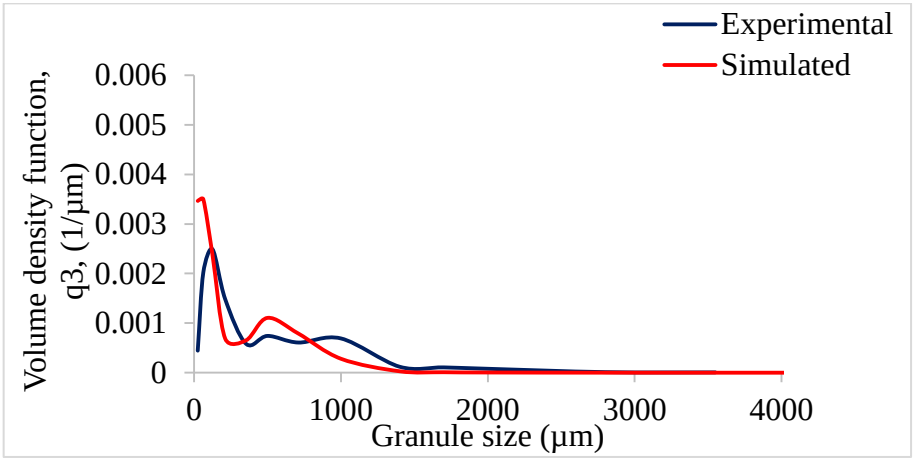

(c) 4KE

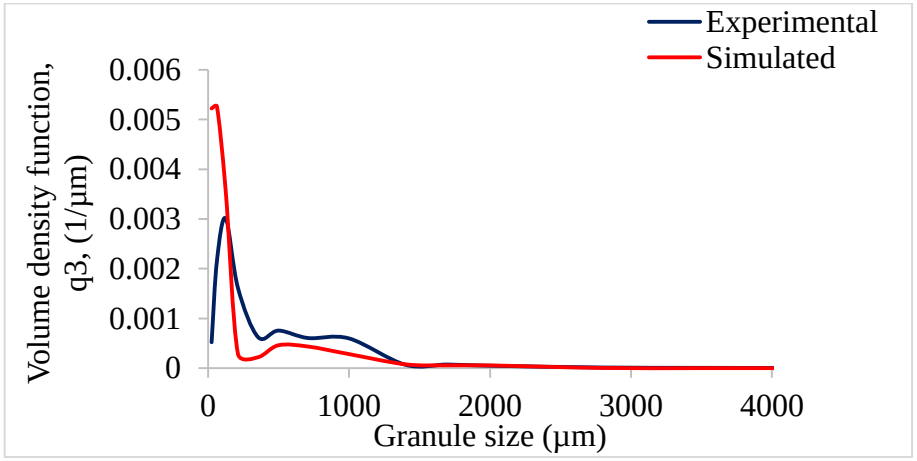

(d) 6KE

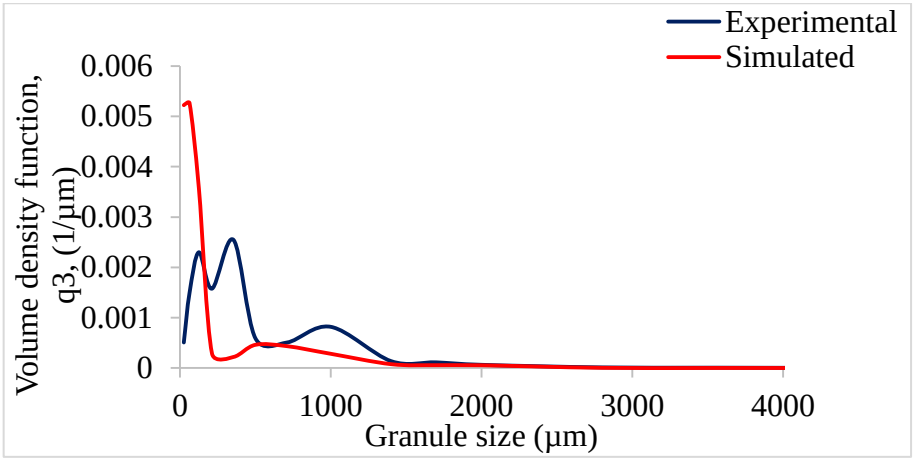

(e) 8KE

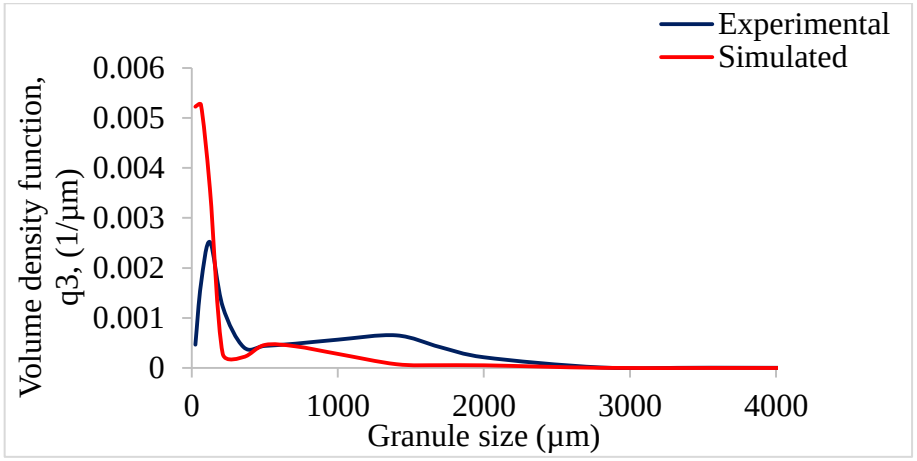

(f) 10KE

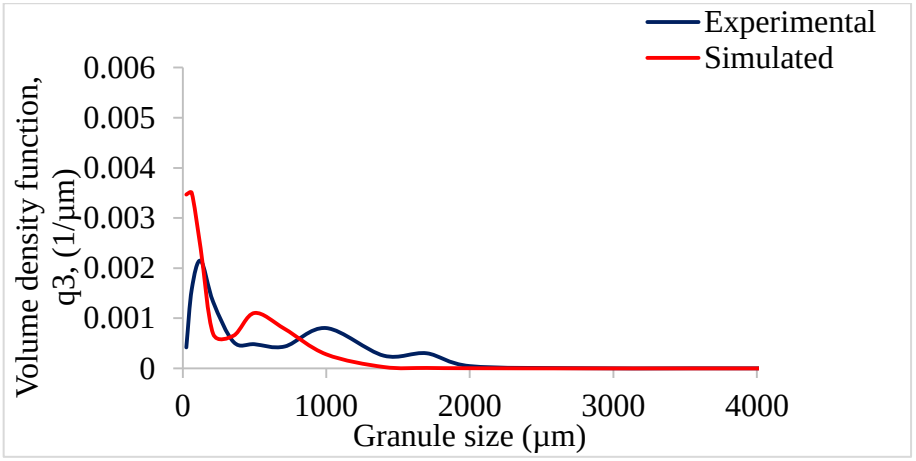

(g) 12KE

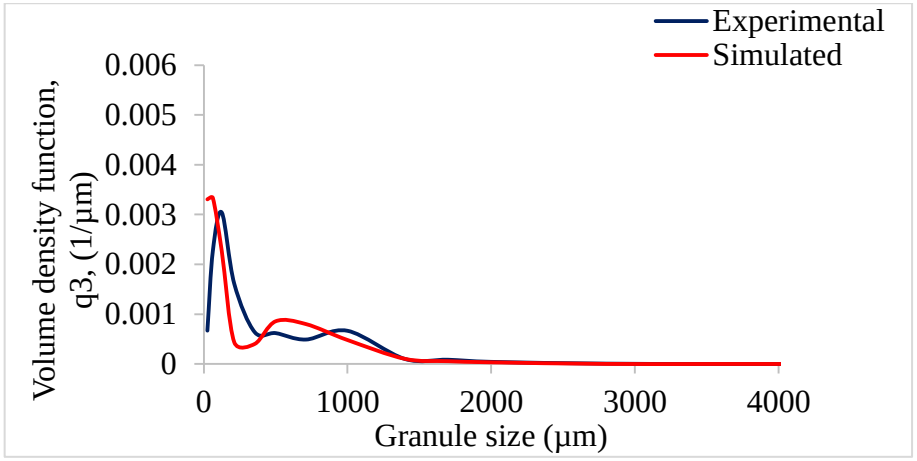

(h) 12KE+2SPCE

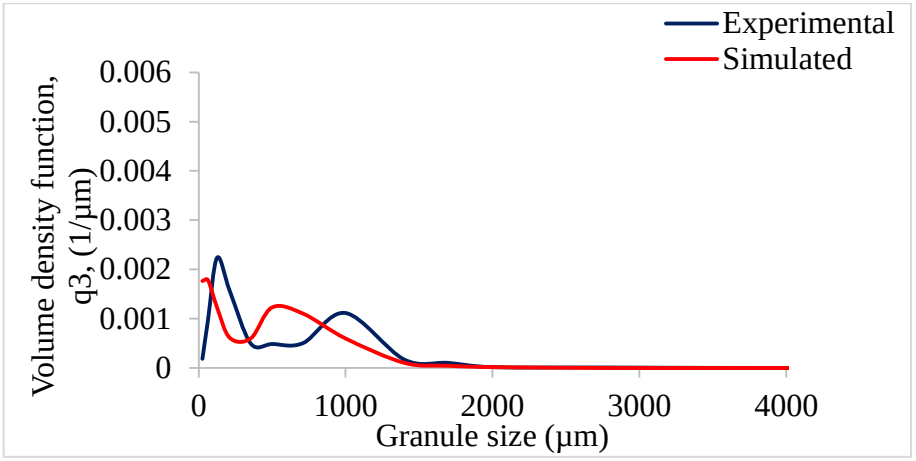

(i) 12KE+4SPCE

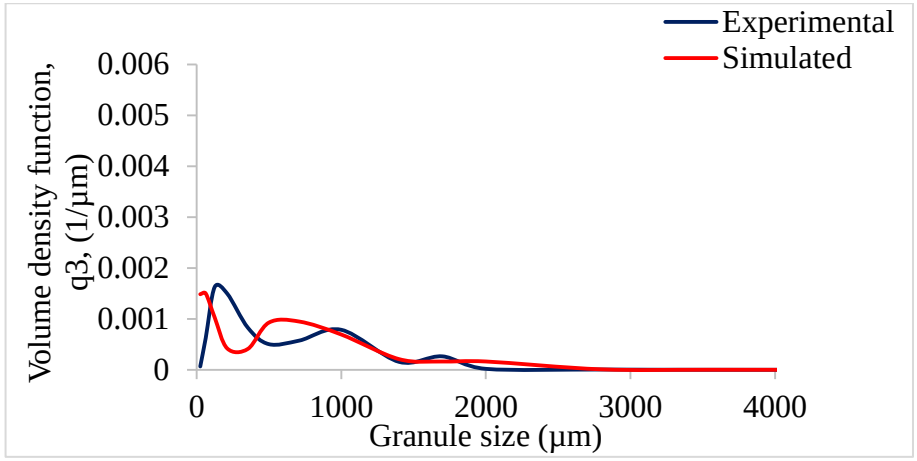

(j) 12KE+6SPCE

Figure 9-3 Experimental and simulated product size distributions of runs used in validation at (a) Nucleation (b) 2KE (c) 4KE (d) 6KE (e) 8KE (f) 10KE (g) 12KE (h) 12KE+2SPCE (i) 12KE+4SPCE (j) 12KE+6SPCE L/S 0.048 with breakage kernel - Austin 1976, breakage rate constant - 0.03 $\mathbf{s^{-1}}$ and maximum growth rate by layering - 35 µm/s

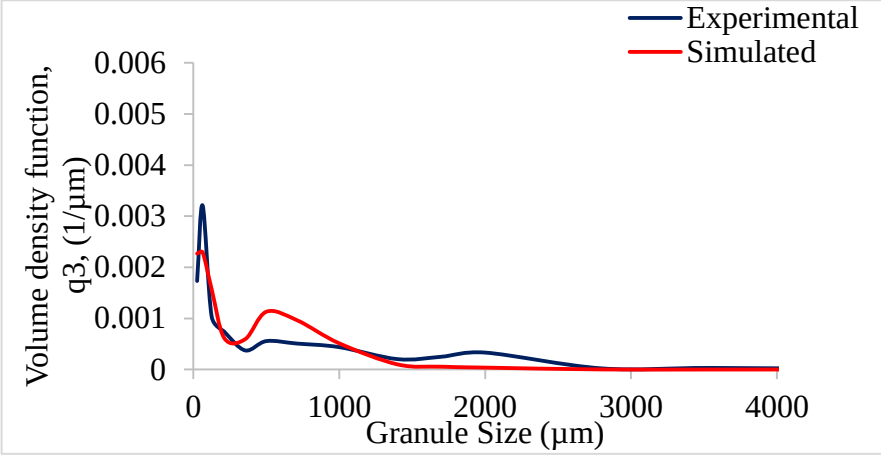

(a) Nucleation

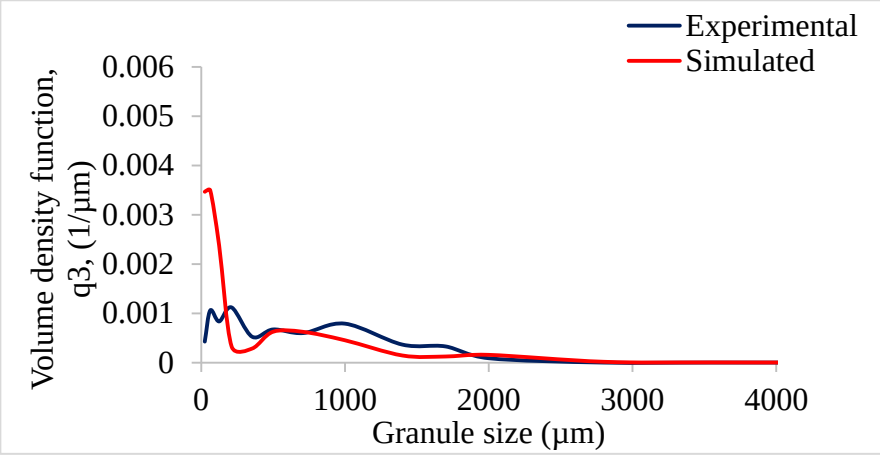

(b) 2KE

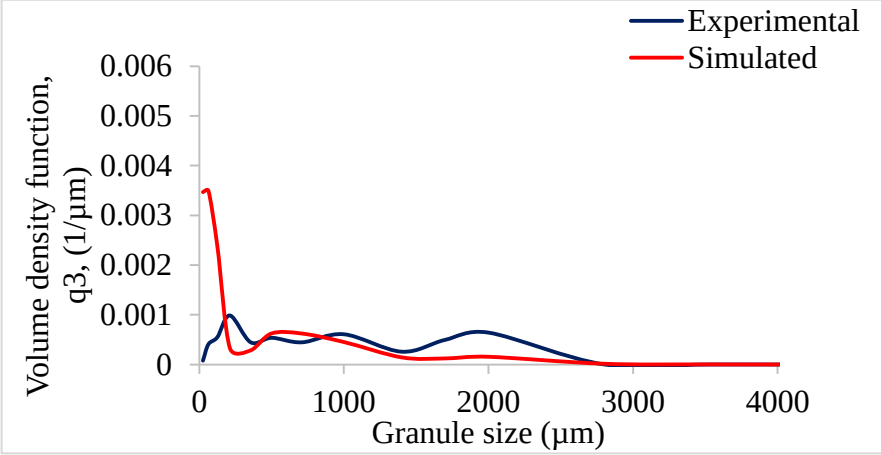

(c) 4KE

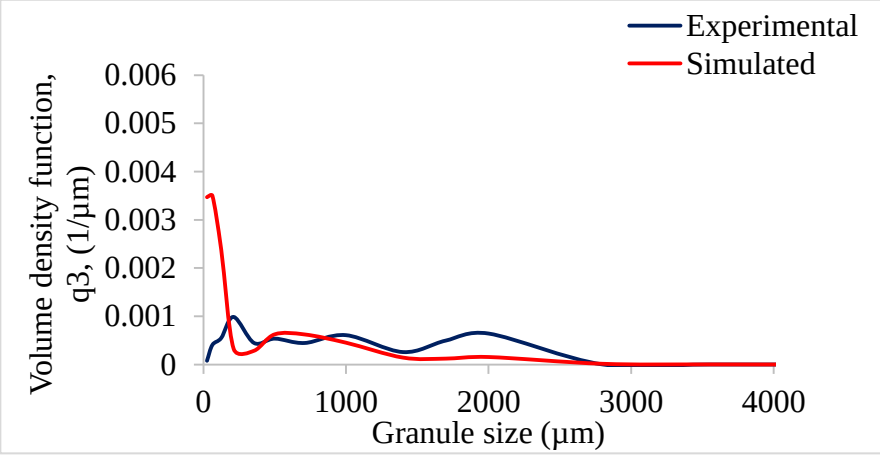

(d) 6KE

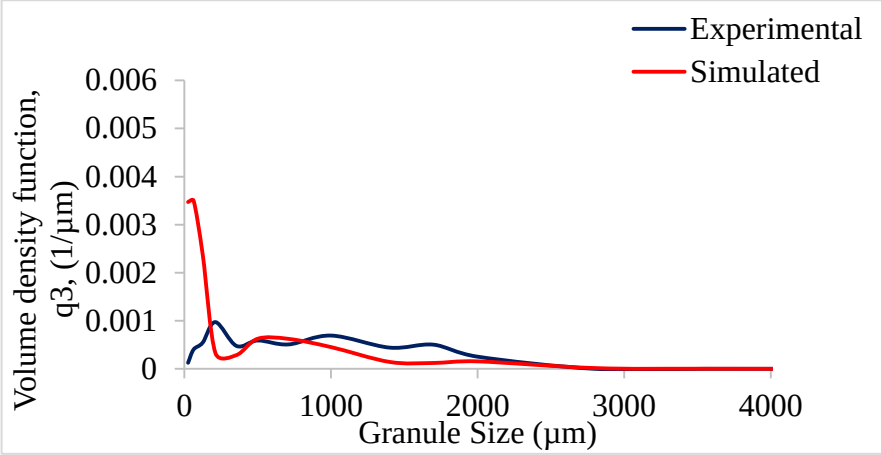

(e) 8KE

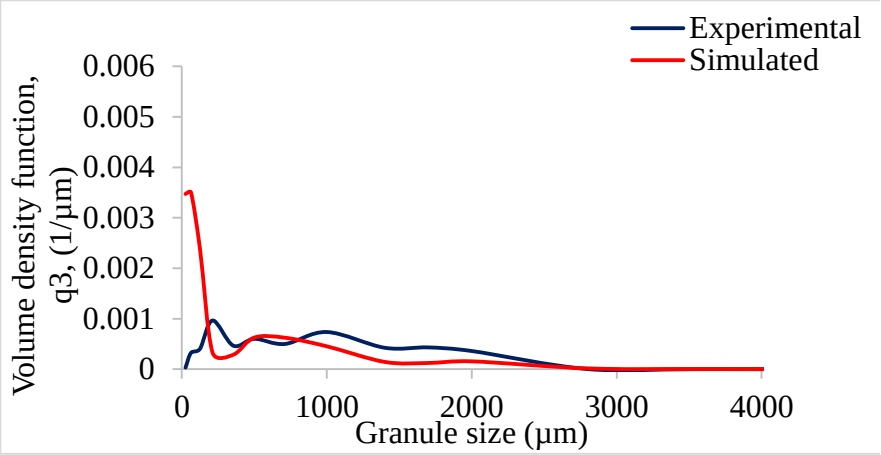

(f) 10KE

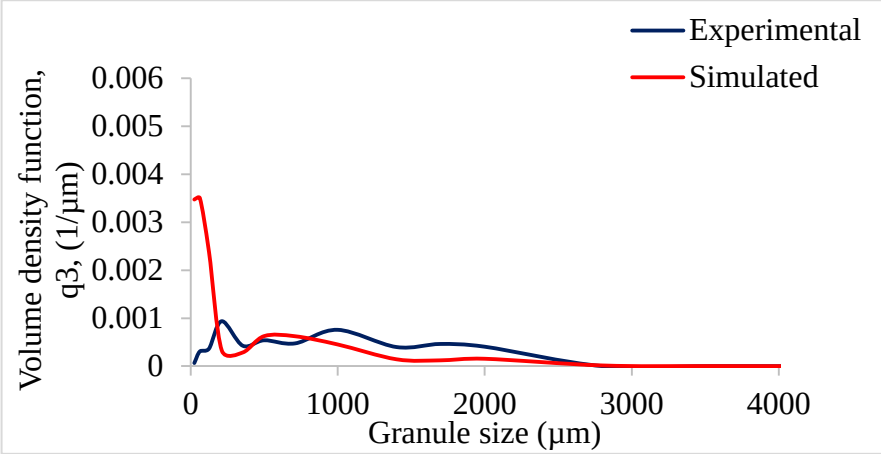

(g) 12KE

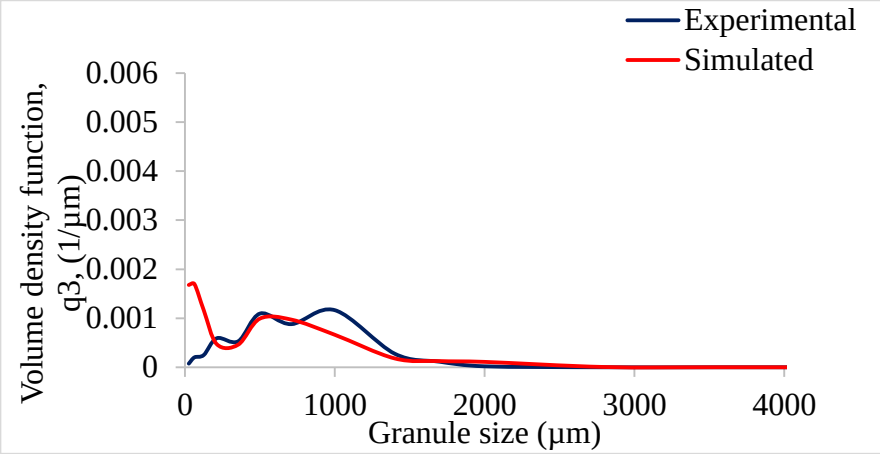

(h) 12KE+2SPCE

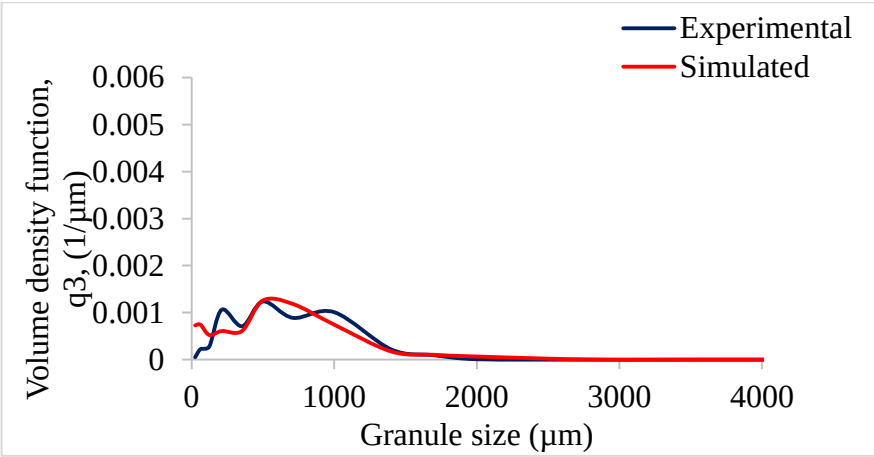

(i) 12KE+4SPCE

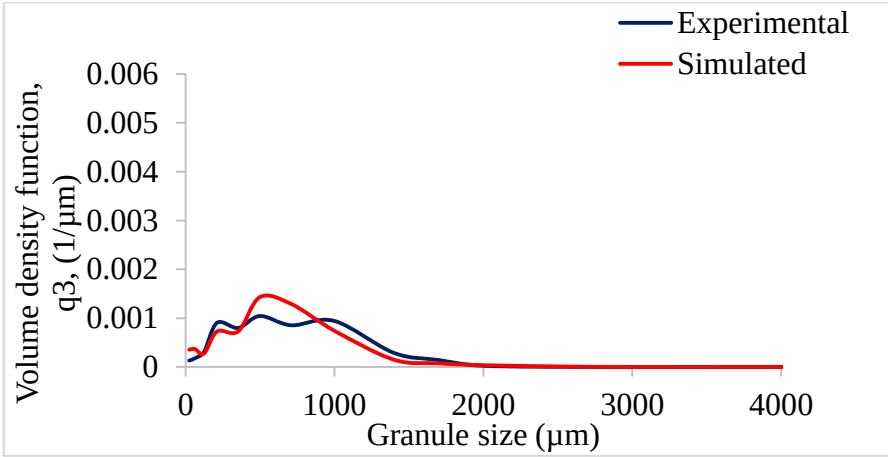

(j) 12KE+6SPCE

Figure 9-4 Experimental and simulated product size distributions of runs used in validation, at (a) Nucleation (b) 2 KE (c) 4KE (d) 6KE (e) 8KE (f) 10KE (g) 12KE (h) 12KE+2SPCE (i) 12KE+4SPCE (j) 12KE+6SPCE L/S 0.1 with breakage kernel - Austin 1976, breakage rate constant - 0.021 $\mathbf{s^{-1}}$ and maximum growth rate by layering - 50µm/s

9.5 CONCLUSION

In the present work, the effect of the L/S on granule size distribution along the length of the barrel at different number of kneading and conveying elements was studied using experimental and PBM based modelling approach (i.e. gSolids). The results show good agreement with experimental data in some cases, but have some discrepancies in the size distributions at high L/S. The model was able to predict fairly close trend for the granule size distributions along the length of the barrel at lower L/S 0.048. At higher L/S 0.1, it is possible to predict granule size distribution at the end part (12KE+2CE, 12KE+4CE, 12KE+6CE) where breakage occurs. However, it is not possible to predict the size distribution trends at the configurations comprising kneading elements where aggregation occurs. Further understanding of aggregation rate function is needed to predict the size distributions from this configuration accurately. Nevertheless, it can be realised that mathematical modelling approach using gSolids is promising and may prove really useful for process understanding and can potentially be applied to different size granulation equipment, different formulations and process parameters. Such approach may reduce the number of experiments that need to be performed during product development in pharmaceutical industry.

10 SUMMARY, CONCLUSIONS AND FUTURE WORK

10.1 SUMMARY

The current work furthered the existing understanding about the twin screw wet granulation by developing mechanistic understanding of the roles of the screw elements (kneading and conveying) in the screw configuration, effects of fill level (powder feed rate/screw speed), processing temperatures and different powders on granulation behaviours and granules properties and thereby development of the capacity to control granule and tablet properties. This study also demonstrated that advanced modelling platforms such as gSolids, which are based on population balance methods, can be used with some changes to predict the granulation outcomes. The outcomes from this study should contribute towards establishing twin screw granulator as a continuous wet granulation equipment.

10.2 CONCLUSIONS

Based on the results of different experiments carried out in this study the following conclusions were put forward.

10.2.1 Understanding granulation mechanism for lactose powder along the barrel length

In this chapter, it was demonstrated that granule attributes can be controlled if the mechanism of granulation along the length of the granulator is understood to a level of discrete screw element. It was understood that the granule formation and growth in the TSG is a function of the type and number of elements in the screw configuration and the L/S. For instance, increasing the number of kneading elements at higher L/S, the granules become bigger in size, elongated, smoother and denser due to high shear and compaction forces acting on them. However, addition of conveying elements after kneading elements in the screw configuration results in decrease in size and elongation of granules due to shearing and cutting action of the conveying elements. Increasing the channel width of conveying elements results in an increase in granule size and structural voids indicating the coalescence or re-agglomeration.

10.2.2 Effects of varying barrel temperature

This chapter proved that granulation mechanism in TSG can also be influenced by the change in the processing temperature (barrel temperature) and L/S. The study showed that lower L/S and higher barrel temperature are important process conditions in the twin screw wet granulation as they directly influence the granule attributes.

10.2.3 Effects of fill level

This chapter demonstrated that the specific feed load (powder feed rate divided by screw speed) or powder feed number can act as a surrogate for the barrel fill level that can be used to control and maintain the granule size, shape and tablet tensile strength. It was also shown that the material property plays important role while studying fill level. For instance, lactose maintains granule size at all fill levels because it dissolves in water and forms liquid bridges which helps binding material together to form relatively stronger granules.

10.2.4 Effects of varying primary particle size

This chapter was focused on developing of understanding the granulation mechanism of three grades of lactose (Pharmatose 450M, Pharmatose 350M and Pharmatose 200M) with varying particle sizes. These powders were granulated at varying L/S and screw speed and their effect on granule properties (size, shape and structure) and tablet tensile strength. It was found that the extent of impact of varying primary particle size and compressibility of powder on the granule attributes depends on the L/S. Powder with smaller particle size granulate to a similar extent to the powder with larger primary particle size at lower L/S.

10.2.5 Effects of types of primary powder

This chapter showed that the primary powder morphology plays an important role in determining the granule size and structure and the tablet tensile strength. This study also showed that the porous structure of particle may enhance the compressibility in dry granulation or direct compaction but in wet granulation it can limit the binding between the particles due to absorption of water in the structure of the particles.

10.2.6 Population balance modelling of twin screw granulation to develop mechanistic understanding

This study demonstrated that PBM based mechanistic model used within advanced modelling platforms such as gSolids can be used to predict the granulation outcomes in twin screw granulation. It was also shown that by using PBM model in such platform, the effect of the L/S on granule size distribution along the length of the barrel at different number of kneading and conveying elements can be quantified, and the calibrated model can be used as a predictive tool within the experimental space. The results show good agreement with experimental data, but have some discrepancies in the size distributions at high L/S.

10.3 FUTURE WORK

10.3.1 Further investigation into experimental findings

The findings from the present work provide an interesting insight into the granulation mechanism and its relation with the granule attributes. To expand the knowledge pool of the twin screw granulation process, the more experiments can be performed using kneading discs with varying thickness in order to increase or decrease the shear stress on the wet granules which will potentially control the liquid distribution and thereby uniform granules with desired size, structure (porosity) and shape of granules. In another experiment conveying elements with longer pitch and larger channel volume can be used as 'Nucleation zone' to increase the rolling effect and thereby sphericity. Also, in another experiment, the short pitch conveying elements in binder addition location or Nucleation zone can be replaced with cut-conveyers or distributive feed screws in order to remove Nucleation regime and induce early consolidation prior kneading zone.

The pharmaceutical formulation generally comprised of active pharmaceutical ingredient and one or more bulking ingredients or excipients. The lactose and MCC powder are the most commonly used excipients in the pharmaceutical formulation. They are added in certain proportion to improve the physical and mechanical properties of the formulation when it is granulated or compressed into the tablets. It is not very clear from the literature how these 2 ingredients behave when added in varying proportions. The previous studies were based on fixed proportions of these two powders in a placebo formulation. Therefore, future study can include investigating the effect of varying proportions of lactose and MCC powder on granulation mechanism and the granule size, shape and structure. The research can also be expanded to cover range excipient with different physical and mechanical properties and water affinity (viz., di-calcium phosphate and mannitol).

In addition, there is also scope to understand relationship between mechanical properties of powders such as hardness of single particle and the granulation behaviour in twin screw granulation. This can be achieved by measuring hardness of particles using nano-indentation method.

10.3.2 Understanding and reducing product fluctuations

The twin screw granulator is known to produce irregular granules with bimodal size distribution. The work carried out so far in the present study clearly addresses and troubleshoots this issue. However, there is an opportunity to improve and further this knowledge by understanding and reducing the product fluctuations (size and shape with time) during twin screw granulation. The product fluctuation can be indicated by the machine torque (measured in real time). In the future experiments, the granules can be collected and the size and shape can be characterised in real time and related with the real time torque. This will provide direct correlation of the granules properties and the torque. The correlation can be studied in both steady and unsteady state granulation. Additionally, attempt can be made to measure the normal stress acting on the granules using stress sensor (inserted into the barrel, flushed to the barrel wall) as a function of the product fluctuations.

10.3.3 Population Balance Modelling in TSG

The work presented in this thesis can be further using multi component population balance equation considering liquid distribution and porosity along with size. Other screw elements such as distributive feed screws and mixing elements can also be studied using single and multi-component population balance modelling of twin screw granulation process. Further studies on the aggregation rates will also strengthen the predictive power of the model in kneading elements.

11 REFERENCES

Ainsworth, P., S. Ibanoglu and G. D. Hayes (1997). "Influence of process variables on residence time distribution and flow patterns of tarhana in a twin-screw extruder." Journal of Food Engineering **32**(1): 101-108.

Barrasso, D., A. El Hagrasy, J. D. Litster and R. Ramachandran (2015). "Multi-dimensional population balance model development and validation for a twin screw granulation process." Powder Technology **270**(Part B): 612-621.

Bilgi Boyaci, B., J.-Y. Han, M. T. Masatcioglu, E. Yalcin, S. Celik, G.-H. Ryu and H. Koksel (2012). "Effects of cold extrusion process on thiamine and riboflavin contents of fortified corn extrudates." Food Chemistry **132**(4): 2165-2170.

Cameron, I. T., F. Y. Wang, C. D. Immanuel and F. Stepanek (2005). "Process systems modelling and applications in granulation: A review." Chemical Engineering Science **60**(14): 3723-3750.

Chan Seem, T., N. A. Rowson, I. Gabbott, M. de Matas, G. K. Reynolds and A. Ingram (2016). "Asymmetric distribution in twin screw granulation." European Journal of Pharmaceutics and Biopharmaceutics **106**(Supplement C): 50-58.

Chokshi, R. (2004). "Hot-Melt Extrusion Technique: A Review." Ira. J. Pharm. Res. **3**: 3-16.

Debord, B., C. Lefebvre, A. M. Guyot-Hermann, J. Hubert, R. Bouché and J. C. Cuyot (1987). "Study of Different Crystalline forms of Mannitol: Comparative Behaviour under Compression." Drug Development and Industrial Pharmacy **13**(9-11): 1533-1546.

Dhenge, R. M., J. J. Cartwright, D. G. Doughty, M. J. Hounslow and A. D. Salman (2011). "Twin screw wet granulation: Effect of powder feed rate." Advanced Powder Technology **22**(2): 162-166.

Dhenge, R. M., J. J. Cartwright, M. J. Hounslow and A. D. Salman (2012a). "Twin screw granulation: Steps in granule growth." International Journal of Pharmaceutics **438**(1): 20-32.

Dhenge, R. M., J. J. Cartwright, M. J. Hounslow and A. D. Salman (2012b). "Twin screw wet granulation: Effects of properties of granulation liquid." Powder Technology **229**(Supplement C): 126-136.

Dhenge, R. M., R. S. Fyles, J. J. Cartwright, D. G. Doughty, M. J. Hounslow and A. D. Salman (2010). "Twin screw wet granulation: Granule properties." Chemical Engineering Journal **164**(2): 322-329.

Dhenge, R. M., K. Washino, J. J. Cartwright, M. J. Hounslow and A. D. Salman (2013). "Twin screw granulation using conveying screws: Effects of viscosity of granulation liquids and flow of powders." Powder Technology **238**(Supplement C): 77-90.

Djuric, D. and P. Kleinebudde (2008). "Impact of screw elements on continuous granulation with a twin-screw extruder." Journal of Pharmaceutical Sciences **97**(11): 4934-4942.

Djuric, D. and P. Kleinebudde (2010). "Continuous granulation with a twin-screw extruder: impact of material throughput." Pharm Dev Technol **15**(5): 518-525.

Djuric, D., B. Van Melkebeke, P. Kleinebudde, J. P. Remon and C. Vervaet (2009). "Comparison of two twin-screw extruders for continuous granulation." European Journal of Pharmaceutics and Biopharmaceutics **71**(1): 155-160.

El Hagrasy, A. S., J. R. Hennenkamp, M. D. Burke, J. J. Cartwright and J. D. Litster (2013a). "Twin screw wet granulation: Influence of formulation parameters on granule properties and growth behavior." Powder Technology **238**: 108-115.
El Hagrasy, A. S., J. R. Hennenkamp, M. D. Burke, J. J. Cartwright and J. D. Litster (2013b). "Twin screw wet granulation: Influence of formulation parameters on granule properties and growth behavior." Powder Technology **238**(Supplement C): 108-115.

Fell, J. T. and J. M. Newton (1970). "Determination of Tablet Strength by the Diametral-Compression Test." Journal of Pharmaceutical Sciences **59**(5): 688-691.

Fonteyne, M., H. Wickström, E. Peeters, J. Vercruysse, H. Ehlers, B.-H. Peters, J. P. Remon, C. Vervaet, J. Ketolainen, N. Sandler, J. Rantanen, K. Naelapää and T. D. Beer (2014). "Influence of raw material properties upon critical quality attributes of continuously produced granules and tablets." European Journal of Pharmaceutics and Biopharmaceutics **87**(2): 252-263.

Gorringe, L. J., G. S. Kee, M. F. Saleh, N. H. Fa and R. G. Elkes (2017). "Use of the channel fill level in defining a design space for twin screw wet granulation." International Journal of Pharmaceutics **519**(1): 165-177.

Han, C. D. (1969). " On the operation of a continuous granulation plant-manufacturing of fertiliser granules." J. KIChE **7**(4): 214-220.

Hansuld, E. M., L. Briens, A. Sayani and J. A. B. McCann (2012). "Monitoring quality attributes for high-shear wet granulation with audible acoustic emissions." Powder Technology **215-216**(Supplement C): 117-123.

Hapgood, K. P., J. D. Litster and R. Smith (2003). "Nucleation regime map for liquid bound granules." AIChE Journal **49**(2): 350-361.

Hirth, M., A. Leiter, S. M. Beck and H. P. Schuchmann (2014). "Effect of extrusion cooking process parameters on the retention of bilberry anthocyanins in starch based food." Journal of Food Engineering **125**(Supplement C): 139-146.

Holm, P., T. Schaefer and H. G. Kristensen (1985). "Granulation in high-speed mixers Part V. Power consumption and temperature changes during granulation." Powder Technology **43**(3): 213-223.

Huang, W., Y. Shi, C. Wang, K. Yu, F. Sun and Y. Li (2013). "Using spray-dried lactose monohydrate in wet granulation method for a low-dose oral formulation of a paliperidone derivative." Powder Technology **246**: 379-394.

Isaac, G.-S., L. Mayur and M. Matthew (2003). Twin-Screw Wet Granulation. Pharmaceutical Extrusion Technology, Informa Healthcare.

Iveson, S. M., J. D. Litster, K. Hapgood and B. J. Ennis (2001). "Nucleation, growth and breakage phenomena in agitated wet granulation processes: a review." Powder Technology **117**(1): 3-39.

J.D. Ennis, B. J., and Litster (2004). "The Science and Engineering of Granulation Processes ".

Jenike, A. W. (1964). Storage and flow of solids. Salt Lake City, University of Utah.

Jivraj, M., L. G. Martini and C. M. Thomson (2000). "An overview of the different excipients useful for the direct compression of tablets." Pharmaceutical Science & Technology Today **3**(2): 58-63.

Johanson, J. R. (1965). "A Rolling Theory for Granular Solids." Journal of Applied Mechanics **32**(4): 842-848.

Jonathan Bouffard, M. K., Hubert Dumont (2005). "Influence of Process Variable and Physicochemical Properties on the Granulation Mechanism of Mannitol in a Fluid Bed Top Spray Granulator." Drug Development and industrial Pharmac **3**.
Keleb, E. I., A. Vermeire, C. Vervaet and J. P. Remon (2002). "Continuous twin screw extrusion for the wet granulation of lactose." International Journal of Pharmaceutics **239**(1): 69-80.

Keleb, E. I., A. Vermeire, C. Vervaet and J. P. Remon (2004). "Twin screw granulation as a simple and efficient tool for continuous wet granulation." International Journal of Pharmaceutics **273**(1): 183-194.

Kibbe, A. H. (2000). Handbook of pharmaceutical excipients. Washington, D.C., American Pharmaceutical Association.

Kleinebudde, P., M. Jumaa and F. El Saleh (2000). "Influence of the degree of polymerization on the behavior of cellulose during homogenization and extrusion/spheronization." AAPS pharmSci [electronic resource] **2**(3).

Kohlgrüber, K. (2008). Co-Rotating Twin-Screw Extruders. Co-rotating Twin-screw Extruder, Hanser**:** I-XIII.

Kolter, K., M. Karl and A. Gryczke (2012). "Hot-Melt Extrusion with BASF Pharma Polymers." Extrusion Compendium 2nd Revised and Enlarged Edition BASF SE, Ludwigshafen.

Kumar, A., M. Alakarjula, V. Vanhoorne, M. Toiviainen, F. De Leersnyder, J. Vercruysse, M. Juuti, J. Ketolainen, C. Vervaet, J. P. Remon, K. V. Gernaey, T. De Beer and I. Nopens (2016). "Linking granulation performance with residence time and granulation liquid distributions in twin-screw granulation: An experimental investigation." European Journal of Pharmaceutical Sciences **90**(Supplement C): 25-37.

Kumar, A., J. Dhondt, J. Vercruysse, F. De Leersnyder, V. Vanhoorne, C. Vervaet, J. P. Remon, K. V. Gernaey, T. De Beer and I. Nopens (2016). "Development of a process map: A step towards a regime map for steady-state high shear wet twin screw granulation." Powder Technology **300**(Supplement C): 73-82.

Kumar, A., J. Vercruysse, G. Bellandi, K. V. Gernaey, C. Vervaet, J. P. Remon, T. De Beer and I. Nopens (2014). "Experimental investigation of granule size and shape dynamics in twin-screw granulation." International Journal of Pharmaceutics **475**(1): 485-495.

Kumar, A., J. Vercruysse, S. T. F. C. Mortier, C. Vervaet, J. P. Remon, K. V. Gernaey, T. De Beer and I. Nopens (2016). "Model-based analysis of a twin-screw wet granulation system for continuous solid dosage manufacturing." Computers & Chemical Engineering **89**(Supplement C): 62-70.

Kumar, A., J. Vercruysse, M. Toiviainen, P.-E. Panouillot, M. Juuti, V. Vanhoorne, C. Vervaet, J. P. Remon, K. V. Gernaey, T. De Beer and I. Nopens (2014). "Mixing and transport during pharmaceutical twin-screw wet granulation: Experimental analysis via chemical imaging." European Journal of Pharmaceutics and Biopharmaceutics **87**(2): 279-289.

Lee, K. T., A. Ingram and N. A. Rowson (2012). "Twin screw wet granulation: The study of a continuous twin screw granulator using Positron Emission Particle Tracking (PEPT) technique." European Journal of Pharmaceutics and Biopharmaceutics **81**(3): 666-673.

Li, H., M. R. Thompson and K. P. O'Donnell (2014). "Understanding wet granulation in the kneading block of twin screw extruders." Chemical Engineering Science **113**(Supplement C): 11-21.

Liu, H., S. C. Galbraith, B. Ricart, C. Stanton, B. Smith-Goettler, L. Verdi, T. O'Connor, S. Lee and S. Yoon (2017). "Optimization of critical quality attributes in continuous twin-screw wet granulation via design space validated with pilot scale experimental data." International Journal of Pharmaceutics **525**(1): 249-263.

Liu, L. X., R. Smith and J. D. Litster (2009). "Wet granule breakage in a breakage only high-hear mixer: Effect of formulation properties on breakage behaviour." Powder Technology **189**(2): 158-164.

Liu, Y., M. R. Thompson and K. P. O'Donnell (2015). "Function of upstream and downstream conveying elements in wet granulation processes within a twin screw extruder." Powder Technology **284**(Supplement C): 551-559.

Lute, S. V., R. M. Dhenge, M. J. Hounslow and A. D. Salman (2015). "Twin screw wet granulation: Effect of fill level." 7th International Granulation Workshop, Sheffield, UK.

Lute, S. V., R. M. Dhenge, M. J. Hounslow and A. D. Salman (2016). "Twin screw granulation: Understanding the mechanism of granule formation along the barrel length." Chemical Engineering Research and Design **110**(Supplement C): 43-53.

Mackaplow, M. B., L. A. Rosen and J. N. Michaels (2000). "Effect of primary particle size on granule growth and endpoint determination in high-shear wet granulation." Powder Technology **108**(1): 32-45.

Meier, R., K.-P. Moll, M. Krumme and P. Kleinebudde (2017). "Impact of fill-level in twin-screw granulation on critical quality attributes of granules and tablets." European Journal of Pharmaceutics and Biopharmaceutics **115**(Supplement C): 102-112.

Meier, R., M. Thommes, N. Rasenack, K. P. Moll, M. Krumme and P. Kleinebudde (2016). "Granule size distributions after twin-screw granulation – Do not forget the feeding systems." European Journal of Pharmaceutics and Biopharmaceutics **106**(Supplement C): 59-69.

Mitra, B., J. Hilden and J. D. Litster (2016). "Effects of the granule composition on the compaction behavior of deformable dry granules." Powder Technology **291**(Supplement C): 487-498.

Morkhade, D. M. (2017). "Comparative impact of different binder addition methods, binders and diluents on resulting granule and tablet attributes via high shear wet granulation." Powder Technology **320**(Supplement C): 114-124.

Mu, B. and M. R. Thompson (2012). "Examining the mechanics of granulation with a hot melt binder in a twin-screw extruder." Chemical Engineering Science **81**(Supplement C): 46-56.

Omar, C. S., R. M. Dhenge, J. D. Osborne, T. O. Althaus, S. Palzer, M. J. Hounslow and A. D. Salman (2015). "Roller compaction: Effect of morphology and amorphous content of lactose powder on product quality." International Journal of Pharmaceutics **496**(1): 63-74.

Osorio, J. G., R. Sayin, A. V. Kalbag, J. D. Litster, L. Martinez-Marcos, D. A. Lamprou and G. W. Halbert (2017). "Scaling of continuous twin screw wet granulation." AIChE Journal **63**(3): 921-932.

Pradhan, S. U., M. Sen, J. Li, J. D. Litster and C. R. Wassgren (2017). "Granule breakage in twin screw granulation: Effect of material properties and screw element geometry." Powder Technology **315**(Supplement C): 290-299.

Ramkrishna, D. (2000). Population Balances: Theory and Applications to Particulate Systems in Engineering.
Ridade Sayin, D. B. (2016). "Population balance modeling of twin screw wet granulation through mechanistic understanding."

Saleh, M. F., R. M. Dhenge, J. J. Cartwright, M. J. Hounslow and A. D. Salman (2015a). "Twin screw wet granulation: Binder delivery." International Journal of Pharmaceutics **487**(1): 124-134.

Saleh, M. F., R. M. Dhenge, J. J. Cartwright, M. J. Hounslow and A. D. Salman (2015b). "Twin screw wet granulation: Effect of process and formulation variables on powder caking during production." International Journal of Pharmaceutics **496**(2): 571-582.

Sayin, R., A. S. El Hagrasy and J. D. Litster (2015). "Distributive mixing elements: Towards improved granule attributes from a twin screw granulation process." Chemical Engineering Science **125**(Supplement C): 165-175.
Sayin, R., L. Martinez-Marcos, J. G. Osorio, P. Cruise, I. Jones, G. W. Halbert, D. A. Lamprou and J. D. Litster (2015). "Investigation of an 11mm diameter twin screw granulator: Screw element performance and in-line monitoring via image analysis." International Journal of Pharmaceutics **496**(1): 24-32.

Schæfer, T., D. Johnsen and A. Johansen (2004). "Effects of powder particle size and binder viscosity on intergranular and intragranular particle size heterogeneity during high shear granulation." European Journal of Pharmaceutical Sciences **21**(4): 525-531.

Schæfer, T. and C. Mathiesen (1996). "Melt pelletization in a high shear mixer. VIII. Effects of binder viscosity." International Journal of Pharmaceutics **139**(1): 125-138.

Souihi, N., M. Dumarey, H. Wikström, P. Tajarobi, M. Fransson, O. Svensson, M. Josefson and J. Trygg (2013). "A quality by design approach to investigate the effect of mannitol and dicalcium phosphate qualities on roll compaction." International Journal of Pharmaceutics **447**(1–2): 47-61.

Thiele, W., Ed. (2003). Twin-screw extrusion and screw design, in: Ghebre-Sellasie, I., Martin, C. (Eds.), Chapter 4, Pharmaceutical Extrusion Technology. New York, Marcel Dekker.

Thompson, M. R. and J. Sun (2010). "Wet Granulation in a Twin-Screw Extruder: Implications of Screw Design." Journal of Pharmaceutical Sciences **99**(4): 2090-2103.

Tu, W.-D., A. Ingram and J. Seville (2013). "Regime map development for continuous twin screw granulation." Chemical Engineering Science **87**(0): 315-326.

Van Melkebeke, B., C. Vervaet and J. P. Remon (2008). "Validation of a continuous granulation process using a twin-screw extruder." International Journal of Pharmaceutics **356**(1): 224-230.

Vanhoorne, V., B. Bekaert, E. Peeters, T. De Beer, J. P. Remon and C. Vervaet (2016). "Improved tabletability after a polymorphic transition of delta-mannitol during twin screw granulation." International Journal of Pharmaceutics **506**(1): 13-24.

Vanhoorne, V., L. Janssens, J. Vercruysse, T. De Beer, J. P. Remon and C. Vervaet (2016). "Continuous twin screw granulation of controlled release formulations with various HPMC grades." International Journal of Pharmaceutics **511**(2): 1048-1057.

Vercruysse, J., A. Burggraeve, M. Fonteyne, P. Cappuyns, U. Delaet, I. Van Assche, T. De Beer, J. P. Remon and C. Vervaet (2015). "Impact of screw configuration on the particle size distribution of granules produced by twin screw granulation." International Journal of Pharmaceutics **479**(1): 171-180.

Vercruysse, J., D. Córdoba Díaz, E. Peeters, M. Fonteyne, U. Delaet, I. Van Assche, T. De Beer, J. P. Remon and C. Vervaet (2012). "Continuous twin screw granulation: Influence of process variables on granule and tablet quality." European Journal of Pharmaceutics and Biopharmaceutics **82**(1): 205-211.

Vercruysse, J., U. Delaet, I. Van Assche, P. Cappuyns, F. Arata, G. Caporicci, T. De Beer, J. P. Remon and C. Vervaet (2013). "Stability and repeatability of a continuous twin screw granulation and drying system." European Journal of Pharmaceutics and Biopharmaceutics **85**(3, Part B): 1031-1038.

Vercruysse, J., M. Toiviainen, M. Fonteyne, N. Helkimo, J. Ketolainen, M. Juuti, U. Delaet, I. Van Assche, J. P. Remon, C. Vervaet and T. De Beer (2014). "Visualization and understanding of the granulation liquid mixing and distribution during continuous twin screw granulation using NIR chemical imaging." European Journal of Pharmaceutics and Biopharmaceutics **86**(3): 383-392.

Verkoeijen, D., G. A. Pouw, G. M. H. Meesters and B. Scarlett (2002). "Population balances for particulate processes—a volume approach." Chemical Engineering Science **57**(12): 2287-2303.

Verstraeten, M., D. Van Hauwermeiren, K. Lee, N. Turnbull, D. Wilsdon, M. am Ende, P. Doshi, C. Vervaet, D. Brouckaert, S. T. F. C. Mortier, I. Nopens and T. D. Beer (2017). "In-depth experimental analysis of pharmaceutical twin-screw wet granulation in view of detailed process understanding." International Journal of Pharmaceutics **529**(1): 678-693.

Vervaet, C. and J. P. Remon (2005). "Continuous granulation in the pharmaceutical industry." Chemical Engineering Science **60**(14): 3949-3957.

Wade, A. and P. J. Weller (1994). Handbook of pharmaceutical excipients. Washington; London, American Pharmaceutical association ; pharmaceutical press.

Westermarck, S., A. M. Juppo, L. Kervinen and J. Yliruusi (1998). "Pore structure and surface area of mannitol powder, granules and tablets determined with mercury porosimetry and nitrogen adsorption." European Journal of Pharmaceutics and Biopharmaceutics **46**(1): 61-68.

Willecke, N., A. Szepes, M. Wunderlich, J. P. Remon, C. Vervaet and T. De Beer (2017). "Identifying overarching excipient properties towards an in-depth understanding of process and product performance for continuous twin-screw wet granulation." International Journal of Pharmaceutics **522**(1): 234-247.

Yao, K., F. Gao and F. Allgöwer (2008). "Barrel temperature control during operation transition in injection molding." Control Engineering Practice **16**(11): 1259-1264.

Yu, S., G. K. Reynolds, Z. Huang, M. de Matas and A. D. Salman (2014). "Granulation of increasingly hydrophobic formulations using a twin screw granulator." International Journal of Pharmaceutics **475**(1): 82-96.

Zhou, Q., L. Qu, I. Larson, P. J. Stewart and D. A. V. Morton (2011). "Effect of mechanical dry particle coating on the improvement of powder flowability for lactose monohydrate: A model cohesive pharmaceutical powder." Powder Technology **207**(1): 414-421.

12 APPENDIX

12.1 PUMP CALIBRATION

In twin screw wet granulation, the granules are produced by injecting the granulation liquid using peristaltic pump on the powder. In the above research the granulation was done by using positive displacement peristaltic pump 101U (Watson Marlow, UK). The pump has a roller enclosed in a box. The roller compress the tube on the upper and lower walls of the box and traps the liquid to be conveyed. The feed rate of the pump depends on rotation of the pump per minute. For different liquid to solid ratio different liquid flow rates were required accordingly. So, it was necessary to find out the liquid flow rate per hour at different rpm. Figure 12-1 shows the pump speed (rpm) and their corresponding liquid flow rate (kg/h).

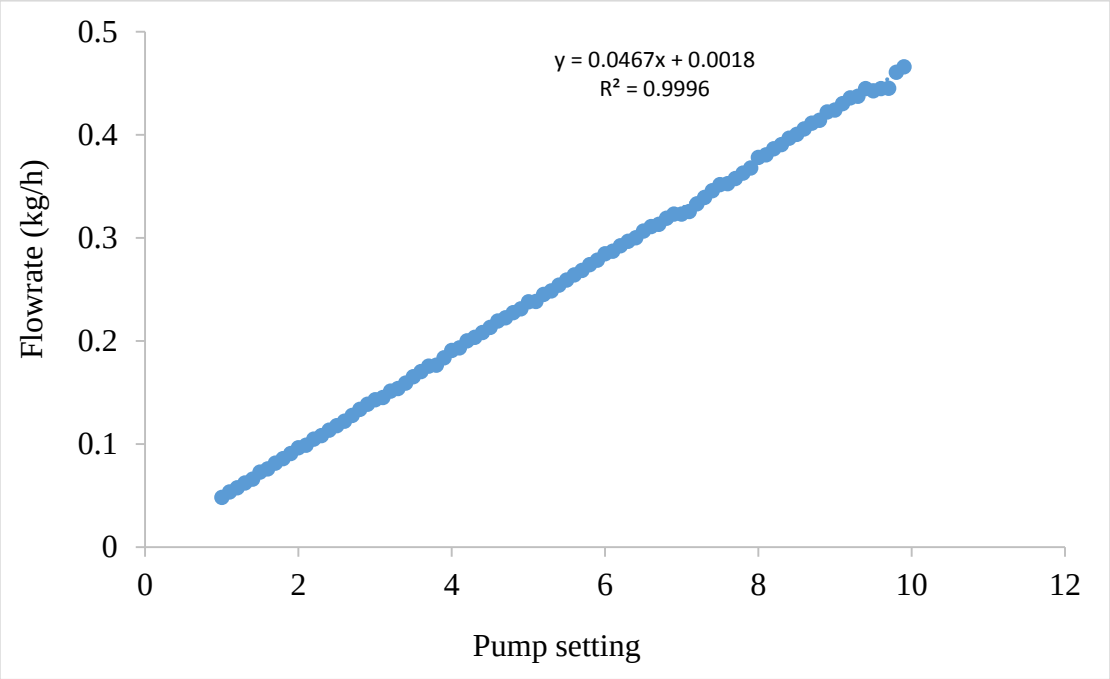

Figure 12-1 Peristaltic pump calibration for granulation liquid

12.2 GRANULE SIZE DISTRIBUTION ALONG THE LENGTH OF THE BARREL

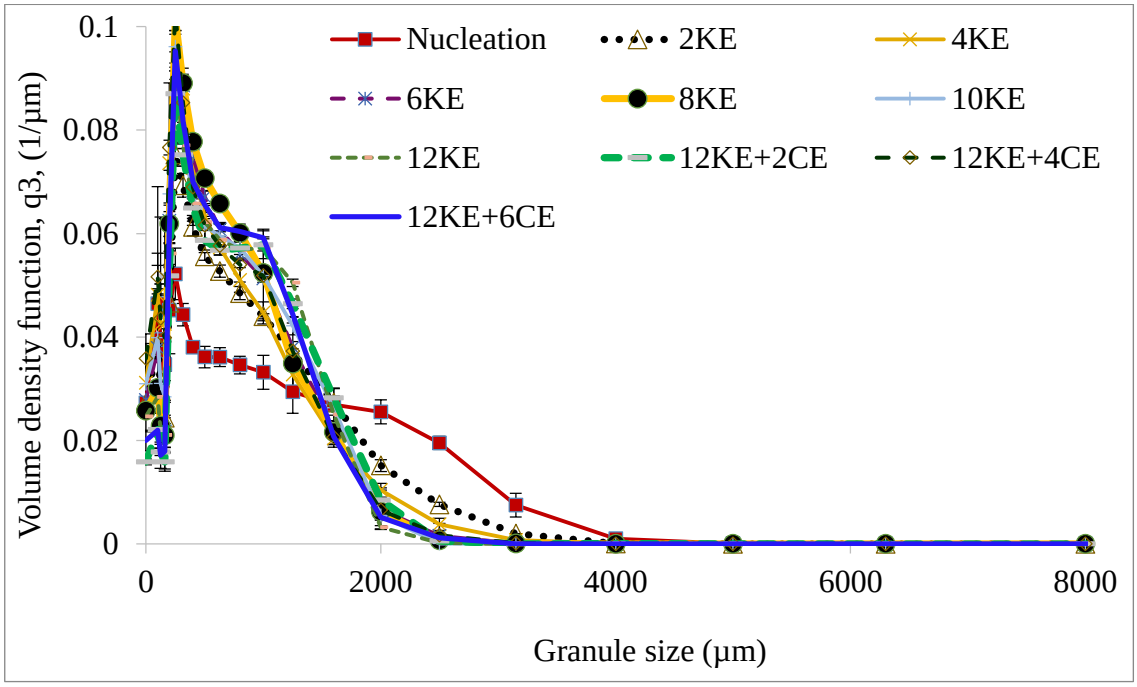

Figure 12-2 Size distribution (after sieving) in different Parts at L/S- 0.048 (at 250 rpm)

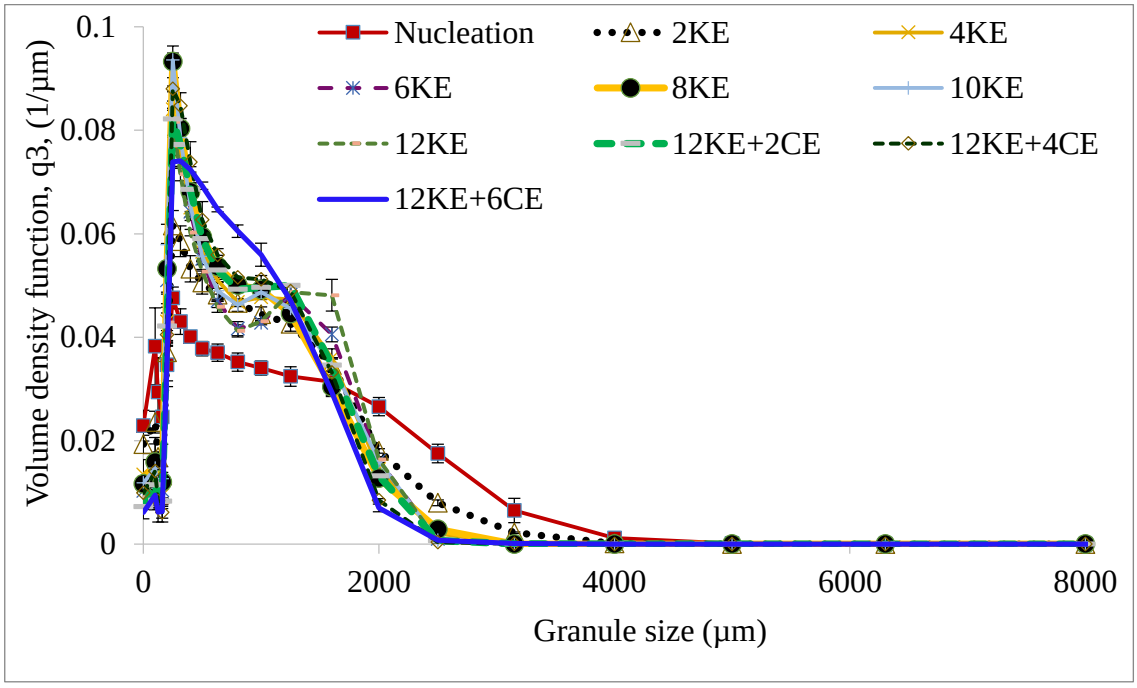

Figure 12-3 Size distribution (after sieving) in different Parts at L/S- 0.07 (at 250 rpm)

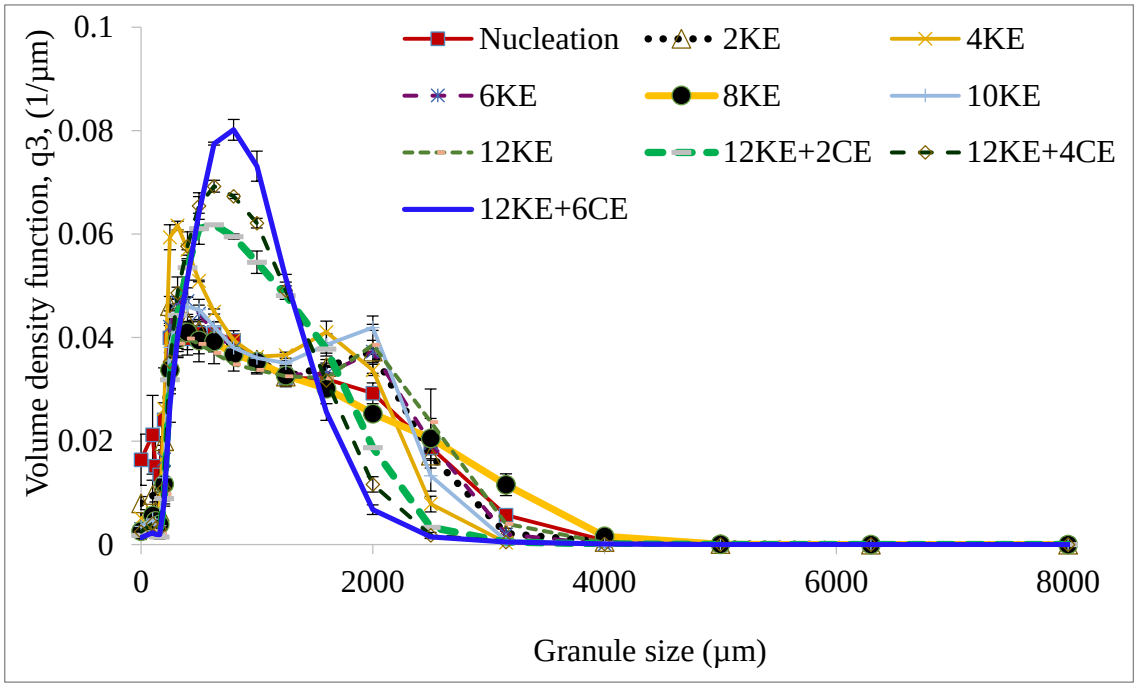

Figure 12-4 Size distribution (after sieving) in different Parts at L/S- 0.1 (at 250 rpm)

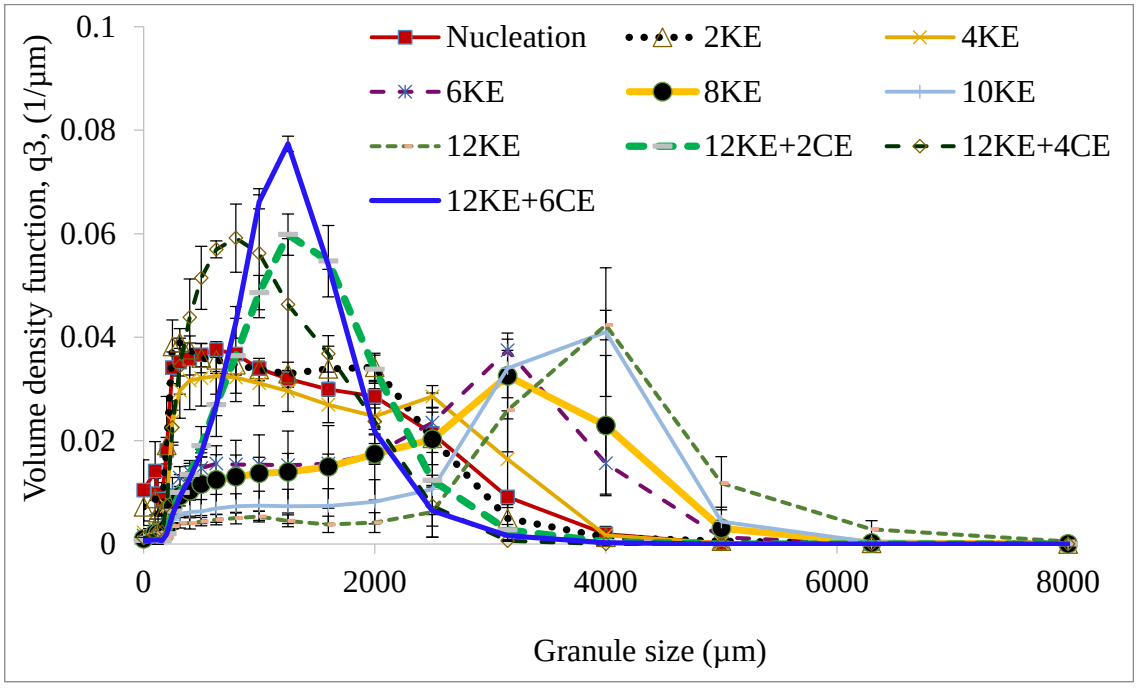

Figure 12-5 Size distribution (after sieving) in different Parts at L/S- 0.113 (at 250 rpm)

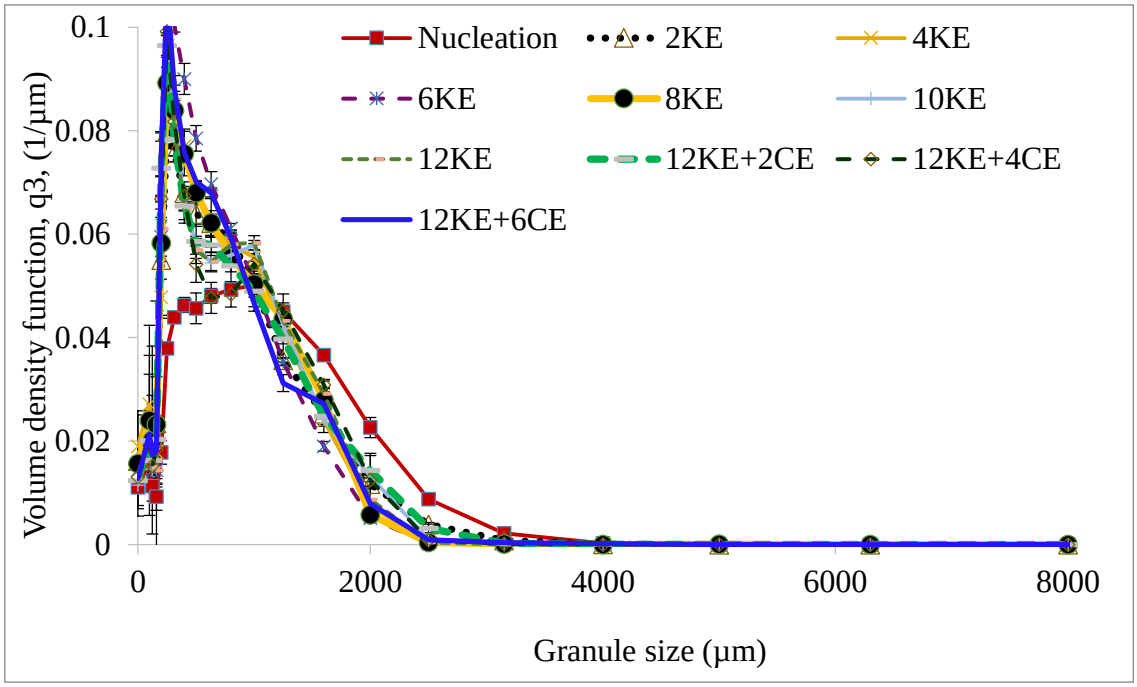

Figure 12-6 Size distribution (after sieving) in different Parts at L/S- 0.048 (at 500 rpm)

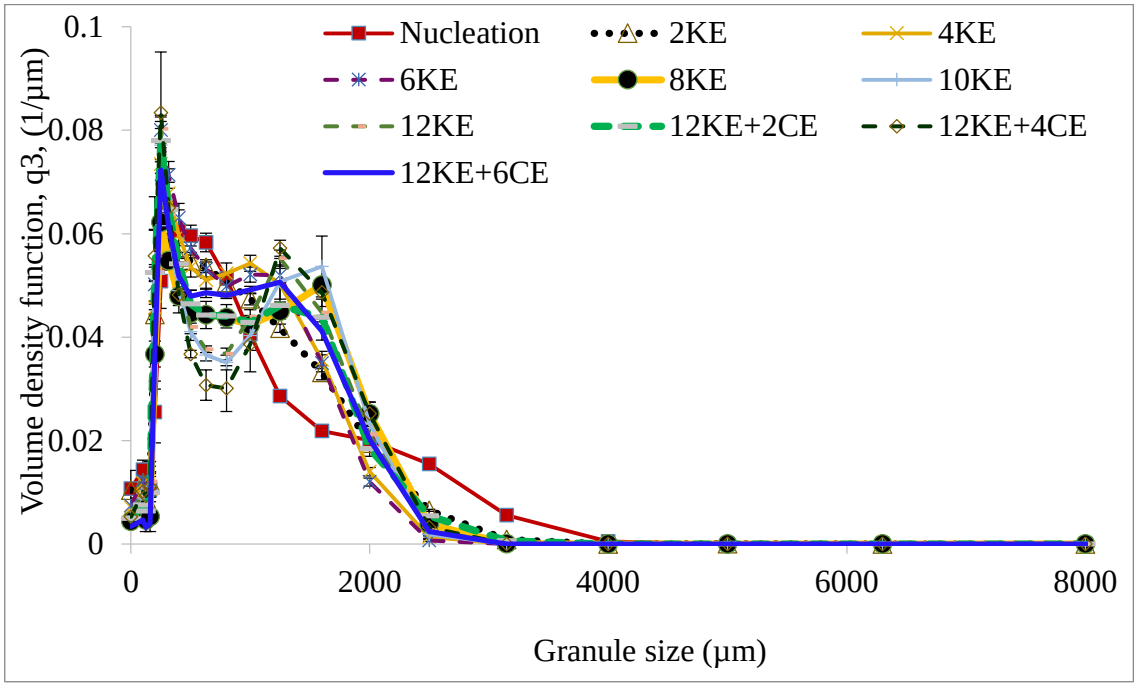

Figure 12-7 Size distribution (after sieving) in different Parts at L/S- 0.07 (at 500 rpm)

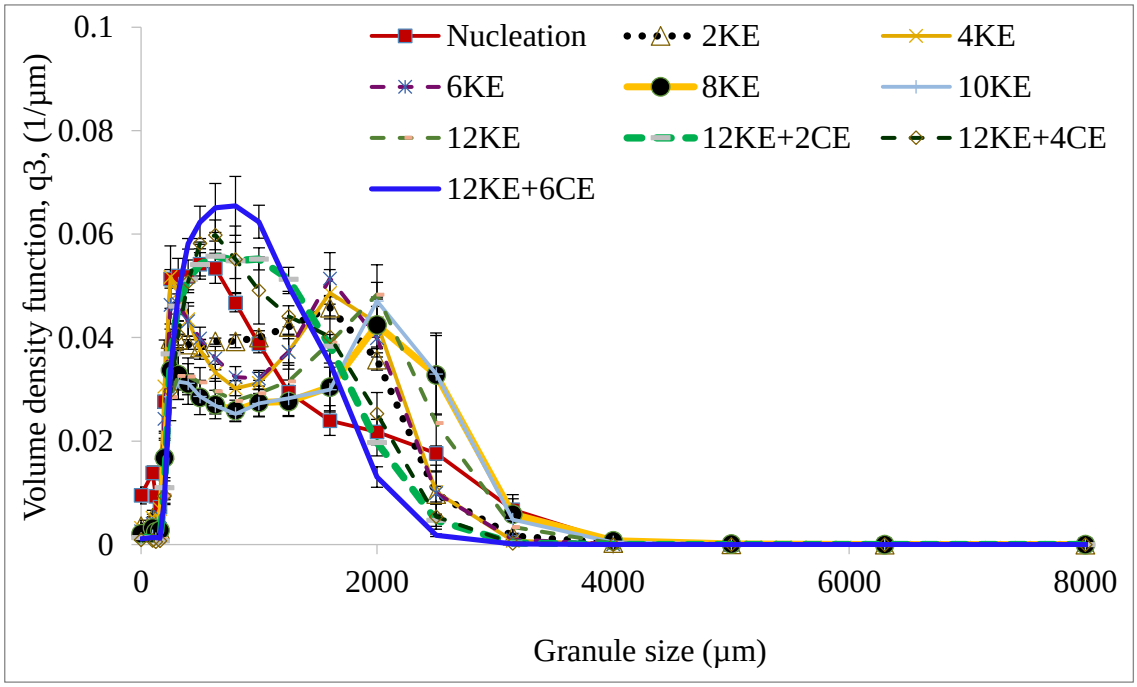

Figure 12-8 Size distribution (after sieving) in different Parts at L/S- 0.1 (at 500 rpm)

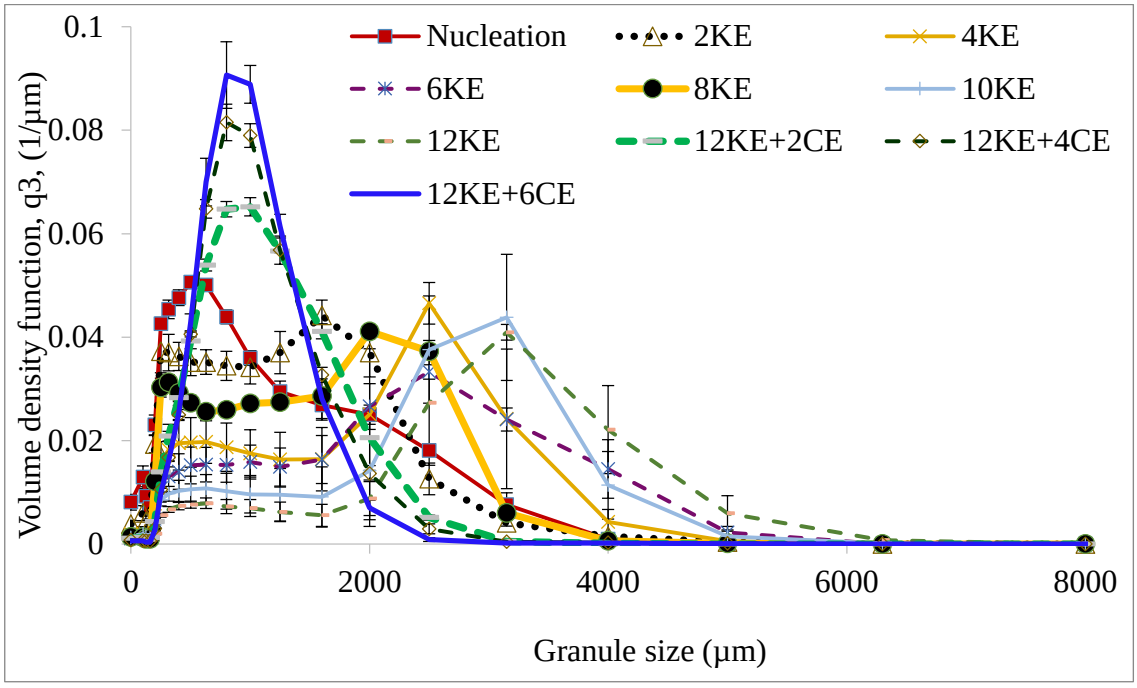

Figure 12-9 Size distribution (after sieving) in different Parts at L/S- 0.113 (at 500rpm)

12.3 EFFECTS OF FILL LEVEL

12.3.1 Lactose Powder

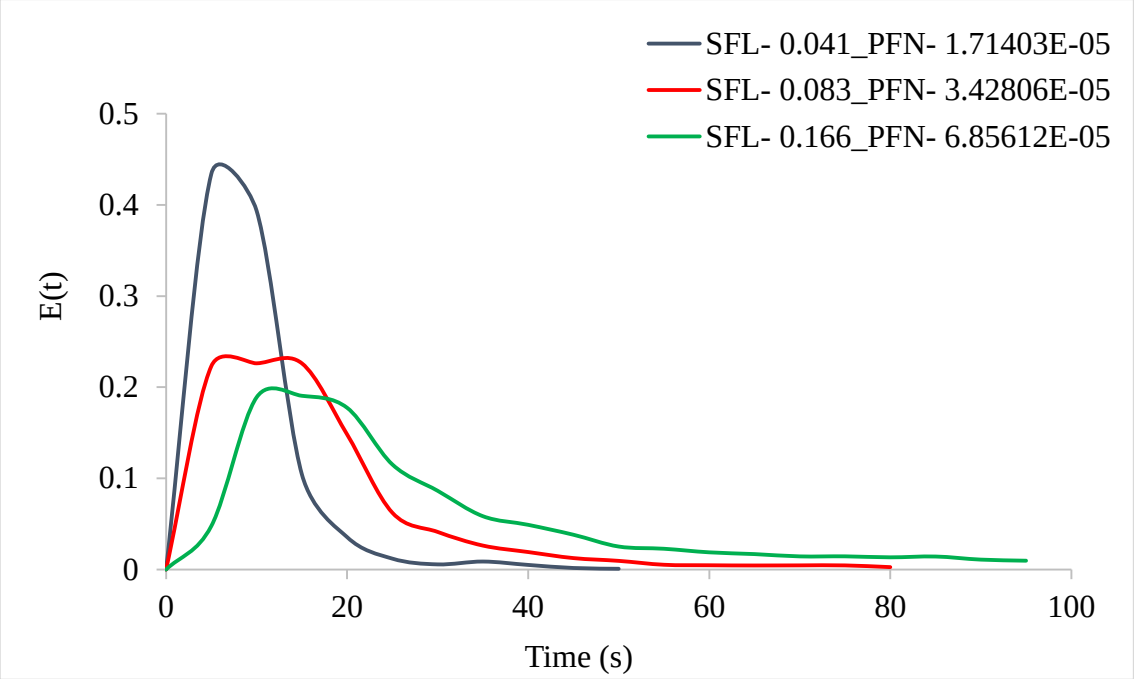

Figure 12-10 Residence time distribution curves at different powder fill level

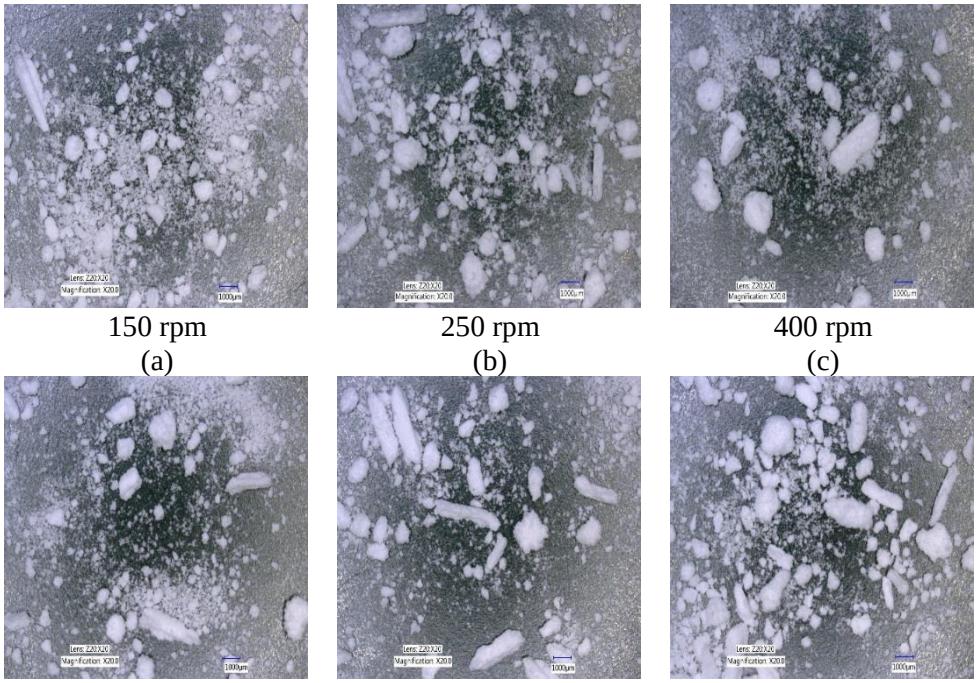

150 rpm (a) | 250 rpm (b) | 400 rpm (c)

500 rpm (d) | 750 rpm (e) | 1000 rpm (f)

Figure 12-11 Microscopic images of lactose granules produced at varying screw speed at SFL-0.083 and PFN- 3.42806E-05 (L/S-0.048)

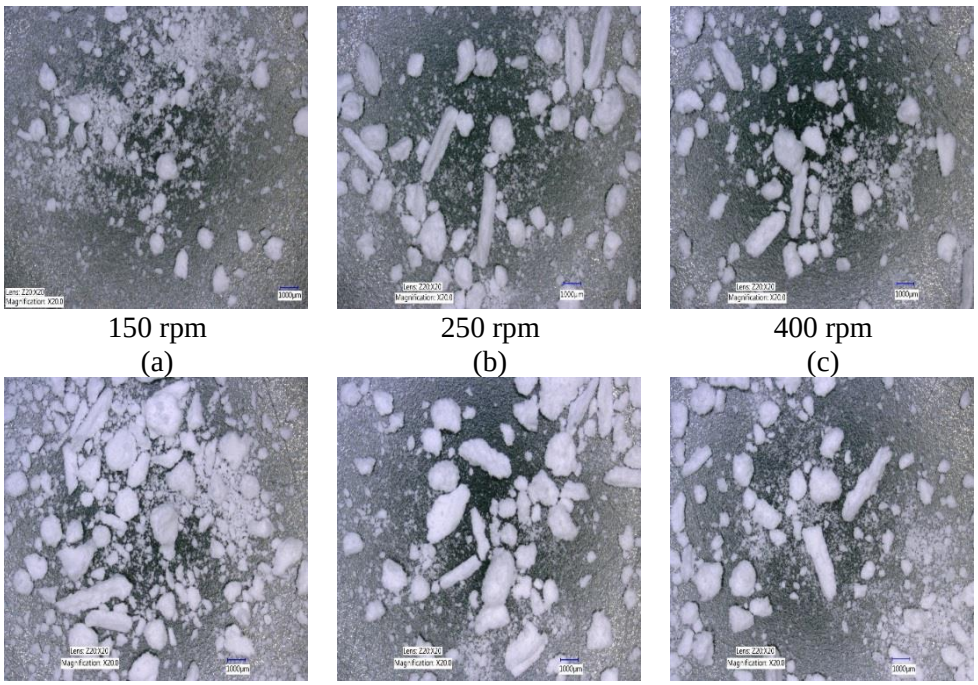

150 rpm (a) | 250 rpm (b) | 400 rpm (c)

500 rpm (d) | 750 rpm (e) | 1000 rpm (f)

Figure 12-12 Microscopic images of lactose granules produced at varying screw speed at SFL-0.166 and PFN- 6.85612E-05 (L/S-0.048)

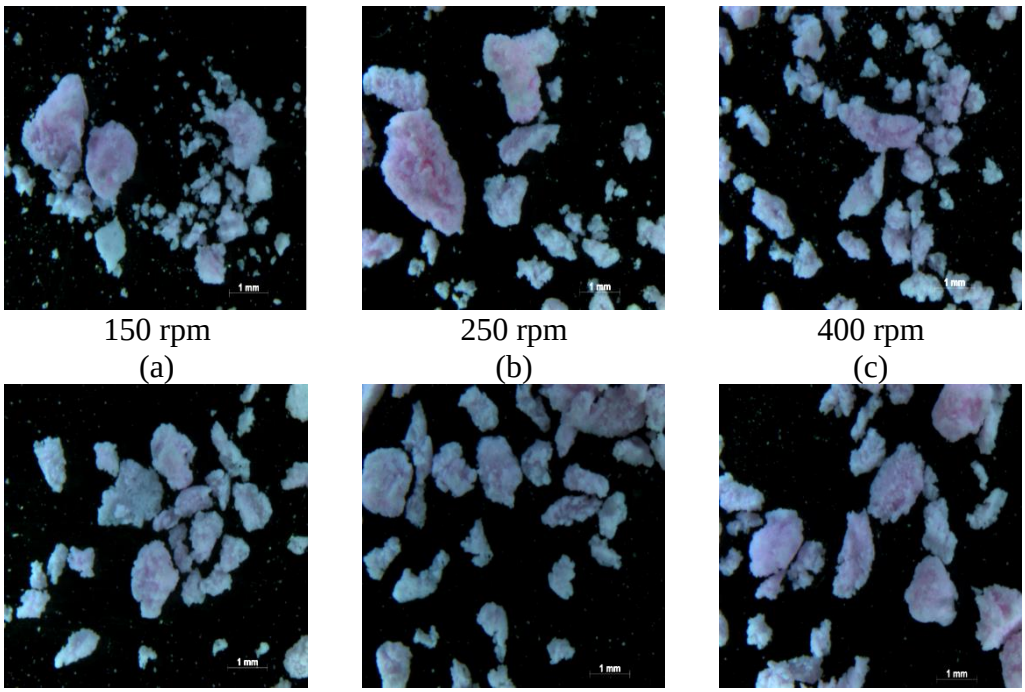

150 rpm (a) 250 rpm (b) 400 rpm (c)

500 rpm (d) 750 rpm (e) 1000 rpm (f)

Figure 12-13 Microscopic images of lactose granules produced at varying screw speed at SFL-0.041 and PFN- 1.71403E-05 (L/S- 0.1)

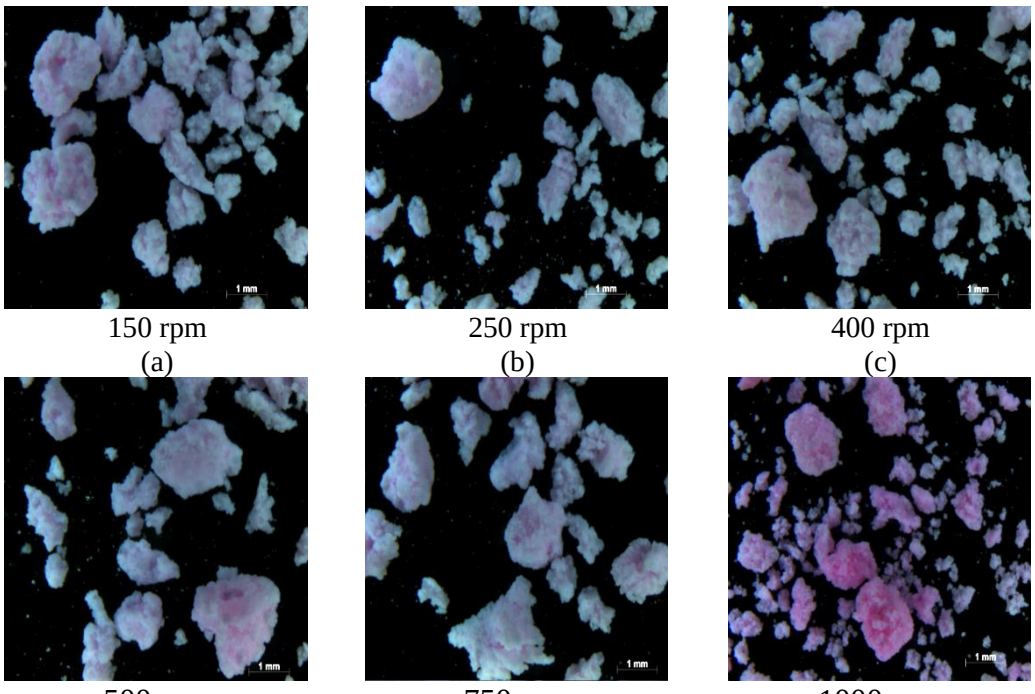

150 rpm (a) 250 rpm (b) 400 rpm (c)

500 rpm (d) 750 rpm (e) 1000 rpm (f)

Figure 12-14 Microscopic images of lactose granules produced at varying screw speed at SFL-0.083 and PFN- 3.42806E-05 (L/S-0.1)

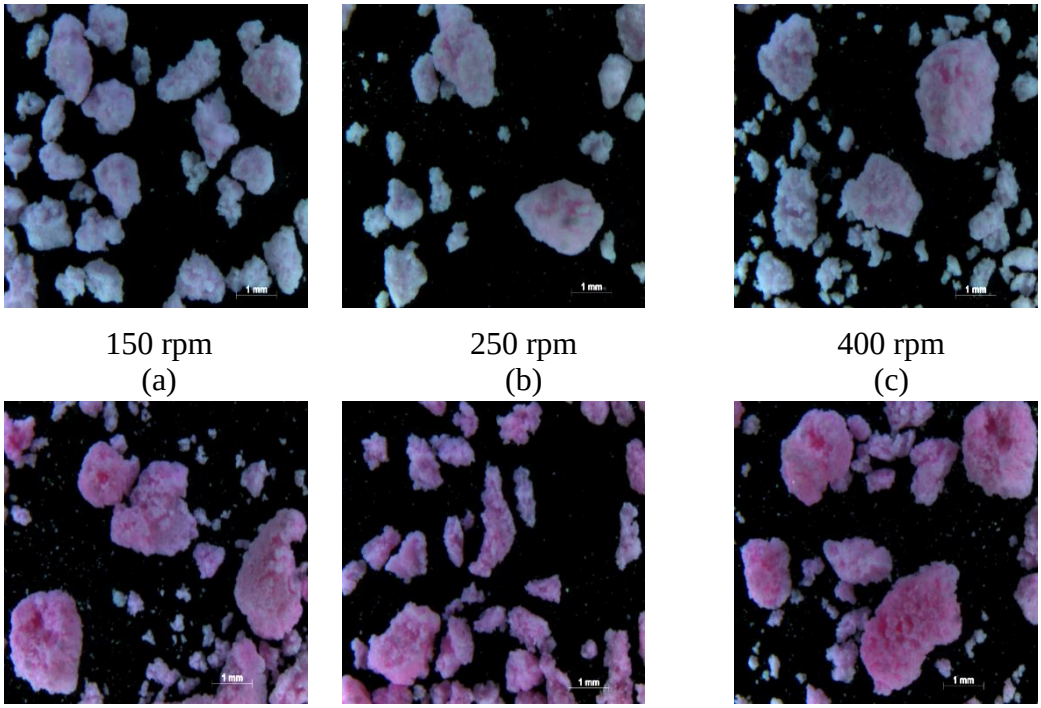

150 rpm (a) | 250 rpm (b) | 400 rpm (c)

500 rpm (d) | 750 rpm (e) | 1000 rpm (f)

Figure 12-15 Microscopic images of lactose granules produced at varying screw speed at SFL-0.166 and PFN- 6.85612E-05 (L/S-0.1)

12.3.2 Microcrystalline cellulose powder

In order to validate the approach of using SFL-PFN for increasing the machine throughput while maintaining the granule and tablet quality attributes, microcrystalline cellulose (MCC) powder which has different physical and mechanical properties than lactose powder was tested for the effect of fill. The experimental plan and the results for MCC are presented below.

The MCC powder (bulk density- 0.3 g/ml) was granulated using distilled water as a granulating liquid in twin screw granulator. The liquid was also adjusted to maintain the L/S of 1. The screw configuration used for the experiments was kept constant and is shown in chapter 5.3.1.2 (Figure 5-2). The free volume (68.67 cm^3) for the screw configuration under consideration was determined using Screw Configuration software from ThermoFisher.

The experimental design for the granulation of MCC powder at varying specific feed load (in g) (SFL) (Eq. 4) and powder feed number (PFN) (-) (Eq. 5) is shown in Table 12-1. Three different SFLs: 0.041, 0.083, 0.166 and were selected to cover lower and upper extremes of the granulation conditions while studying the effect on the residence time and granule attributes. Each time the powder feed rate and screw speed were adjusted accordingly to maintain the SFL. Liquid feed rate was also changed according to powder feed rate in order to maintain respective L/S. PFN was further obtained from SFL using powder bulk density and free space in the twin screw granulator. The liquid was also adjusted to maintain the L/S of 1.0. The barrel temperature was maintained at 25°C (in all barrel compartments). In total, 24 experiments (3 repeats of each experiment) were carried out.

Table 12-1 Experimental plan

Expt no.	Powder feed rate (g/min)	Screw speed (rpm)	SFL (g)	PFN (-) for MCC
1	6.25	150	0.041	3.37093E-05
2	10.4167	250		
3	16.6667	400		
4	20.8333	500		
5	31.25	750		
6	41.6667	1000		
7	12.5	150	0.083	6.74185E-05
8	20.8333	250		
9	33.3333	400		
10	41.6667	500		
11	62.5	750		
12	83.3333	1000		
13	25	150	0.166	1.34837E-04
14	41.6667	250		
15	66.6667	400		
16	83.3333	500		
17	125	750		
18	166.667	1000		

12.3.2.1 Effect of varying SFL-PFN at different screw speed on mean residence time

Figure 12-16 shows effect of varying screw speed (i.e. peak shear rate) on the MRT measured while granulating MCC powder at constant L/S of 1 at different fill levels [SFL (0.041-0.166) and PFN (3.37093E-05- 1.34837E-04)]. It can be noticed from the Figure 12-16 that mean residence time decreased with increasing screw speed at all three fill levels (SFN-PFN). Comparing three SFL-PFN values, the MRT values drop significantly at high SFL (0.166)-PFN (1.34837E-04). These results for MCC powder are similar in terms of trend to that for lactose powder (at L/S of and 0.1) (Figure 6-2) where MRT decreased with increasing screw speed. However, the magnitude of MRT for MCC is clearly smaller than lactose. This can be described based on the difference in the PFN values and powder-liquid interaction for MCC and lactose. The PFN values for MCC are almost double the lactose

PFN values (Table 6-1). The PFN values take into consideration the bulk density of the powder which in case of MCC is higher than lactose.

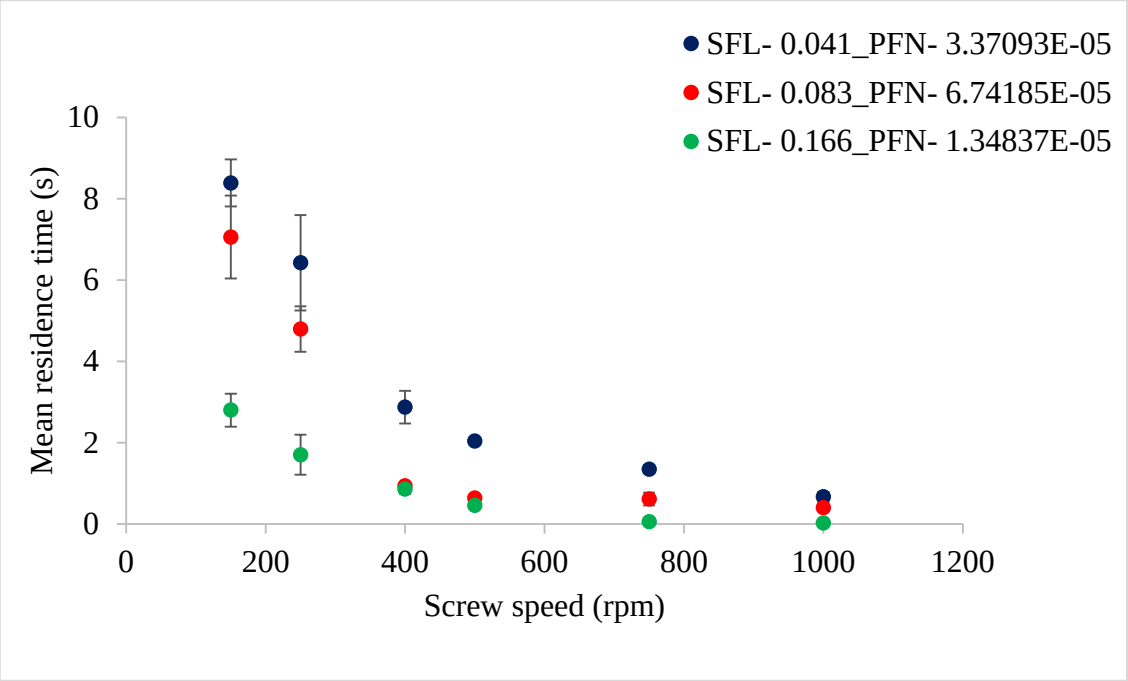

Figure 12-16 Mean residence time of MCC at different SFL-PFN at varying screw speed (L/S- 1)

Thus the overall barrel fill level for MCC is higher compared to lactose. Furthermore, unlike lactose, MCC granules do not become sticky (due to its insolubility in water) and flow better within granulator. Therefore, due to higher fill level and better flowability, MCC granules spent relatively shorter time within granulator, hence lower MRT.

12.3.2.2 Effect of varying SFL-PFN at different screw speed on granule size

Figure 12-17 shows median size of granules of MCC produced at three different fill levels (SFL-PFN) at varying screw speed and constant L/S of 1. The median granule size was similar at two fill levels [SFL (0.041 and 0.083) and PFN (3.37093E-05 and 6.74185E-05)] at varying screw speeds. As the fill level increased further (SFL-0.166, PFN-1.34837E-04), the granule size remained similar at varying screw speed but it was smaller compared to other two fill levels. There are two potential reasons for this effect: either very short residence time (due to high throughput force at high fill level) for the MCC powder to form sufficiently strong granules or high shearing and friction between the granules- barrel wall

and granules-granules due to relatively high barrel fill level that reduce the overall granule size. The MRT exhibited almost no impact on granule size in case of lactose powder due to its solubility in water, however in case of MCC (due to its insolubility in water), MRT showed its effect owing to short duration for powder-liquid interaction to occur at high fill level and greater flowability of MCC powder within the granulator.

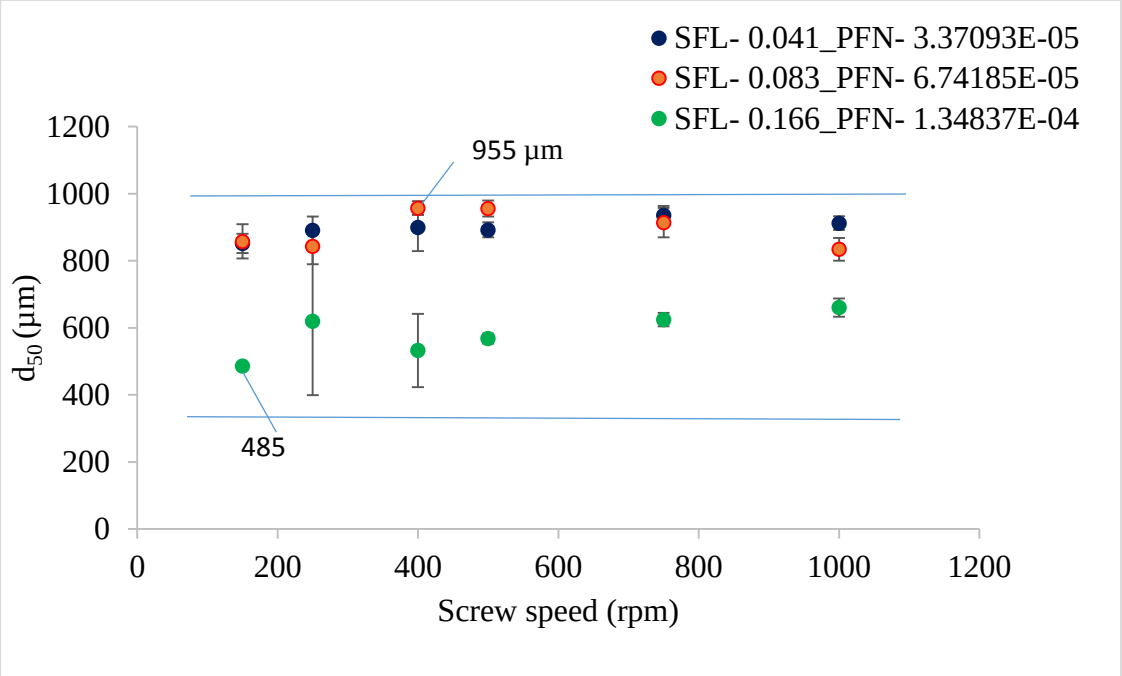

Figure 12-17 Median size of granules (d50) of MCC at different SFL-PFN at varying screw speed (L/S- 1)

Shows the size distribution of granules produced at varying SFL-PFN at L/S of 1. The size distribution results support the median granule size data obtained at various SFL-PFN. At all three fill levels or SFLs-PFNs, the granule size distributions were bimodal at all screw speeds. High fill level (SFL-0.166, PFN-1.34837E-04) resulted in more fines or small granules compared to other two fill levels. As mentioned in case of median granule size, the production of small size granules or fines was potentially because of reduced powder-liquid interaction due to shorter residence time or high shearing.

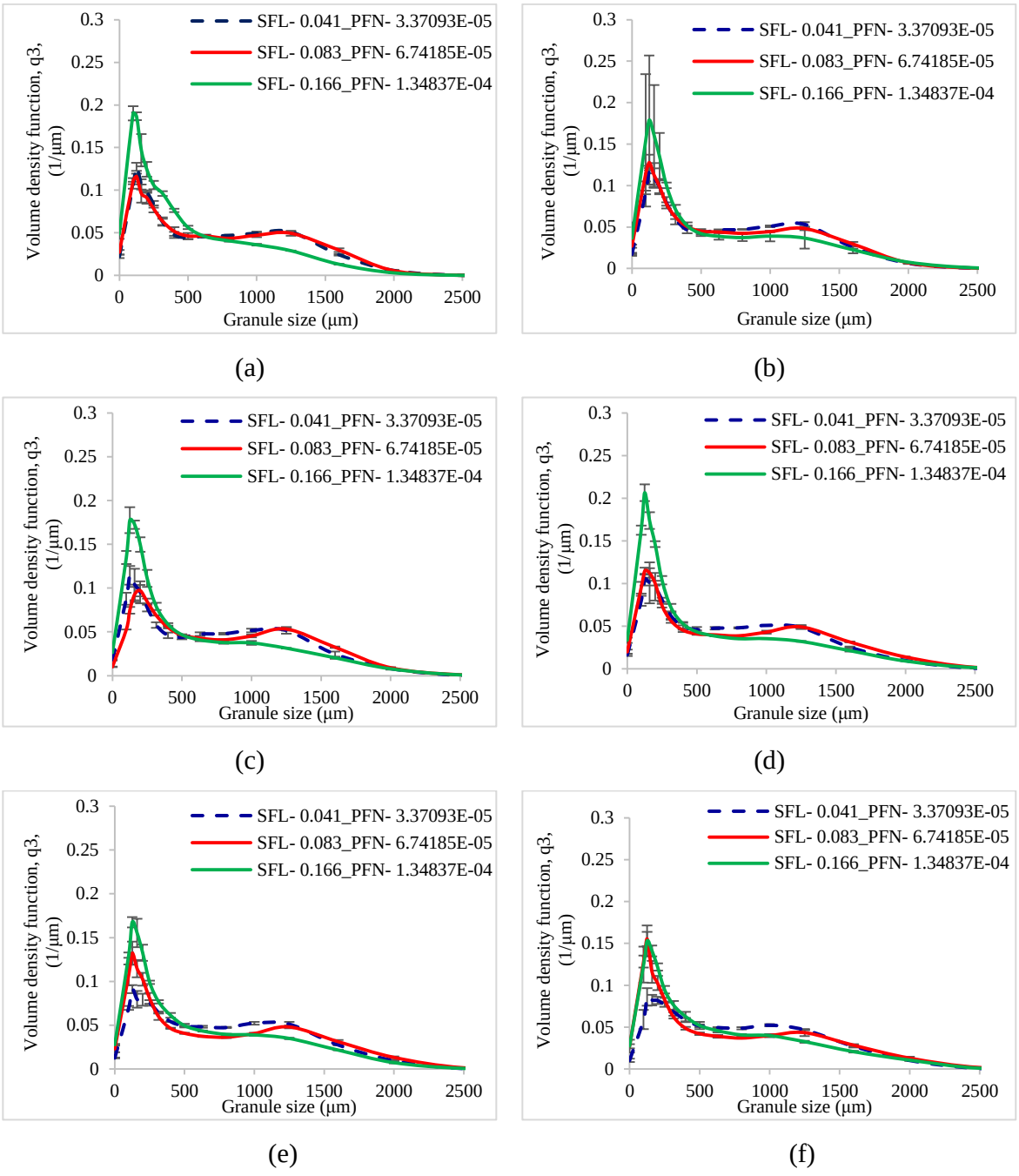

Figure 12-18 Granule size distribution of MCC (L/S- 1) at different SFL- PFN at varying screw speed (a)150 rpm (b)250 rpm (c)400 rpm (d)500 rpm (e)750 rpm (f)1000 rpm

12.3.2.3 Effect of varying SFL-PFN at different screw speed on granule shape

The effect of varying SFL-PFN at different screw speed on granule shape is presented in Figure 12-19(a)-(f), Figure 12-20(a)-(f) and Figure 12-21(a)-(f). In all cases, the granules so produced were elongated in shape and comprised of small and large granules. This supports the size distribution of granules at three different fill levels where higher fill level (SFL-0.166, PFN-1.34837E-04) showed the presence of more fines compared to lower fill levels.

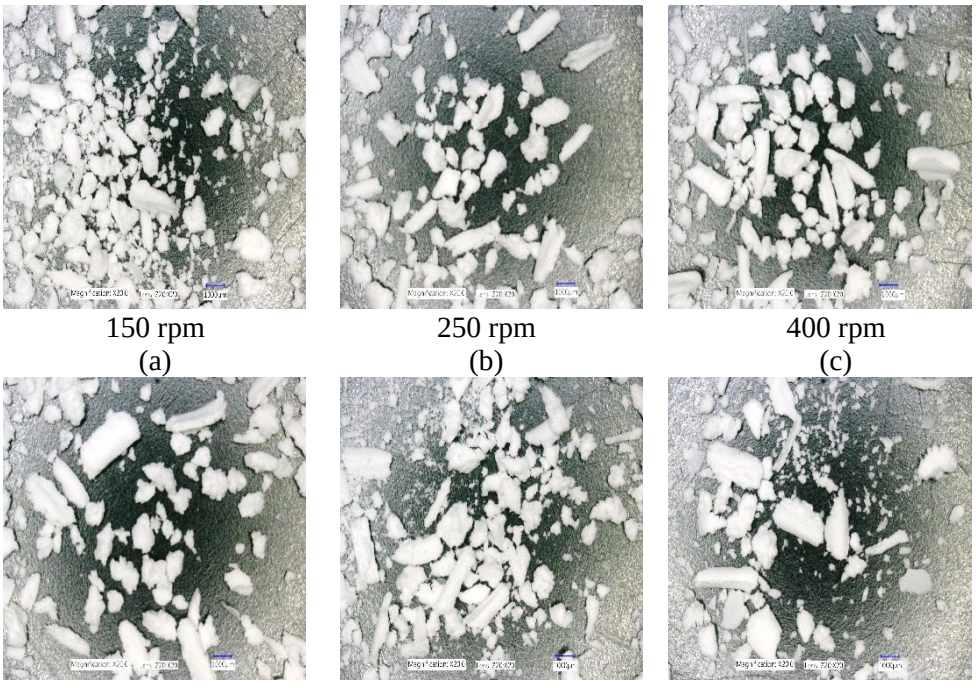

150 rpm (a) 250 rpm (b) 400 rpm (c)

500 rpm (d) 750 rpm (e) 1000 rpm (f)

Figure 12-19 Microscopic images of MCC granules produced at varying screw speed at SFL-0.041 and PFN- 3.37093E-05

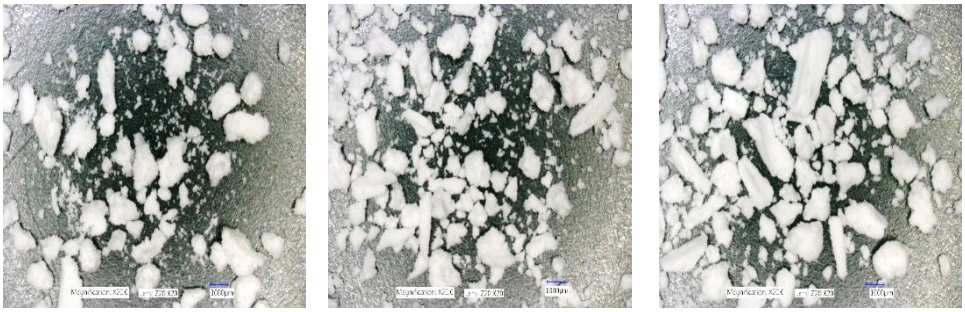

150 rpm (a) 250 rpm (b) 400 rpm (c)

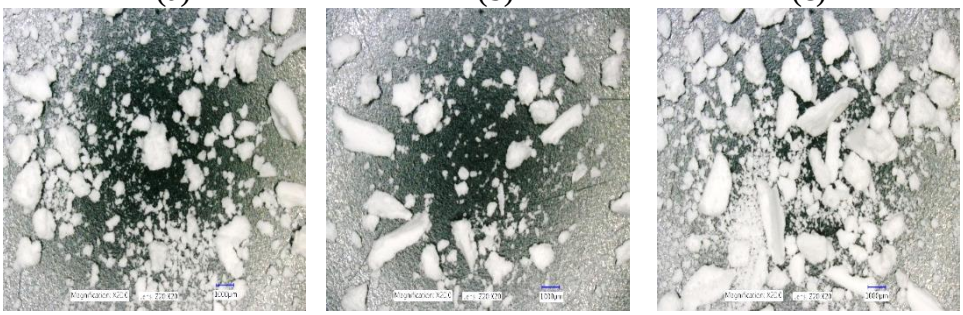

500 rpm (d) 750 rpm (e) 1000 rpm (f)

Figure 12-20 Microscopic images of MCC granules produced at varying screw speed at SFL- 0.083 and PFN- 6.74185E-05

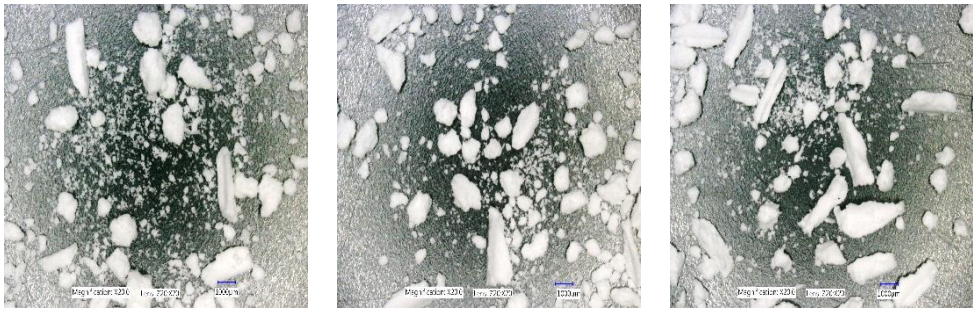

150 rpm (a) 250 rpm (b) 400 rpm (c)

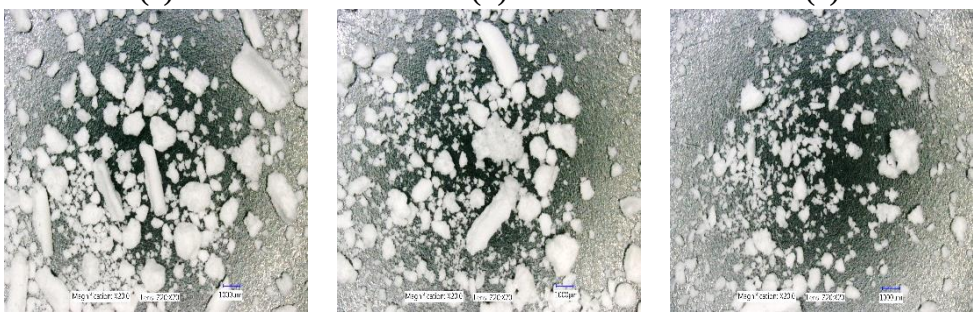

500 rpm (d) 750 rpm (e) 1000 rpm (f)

Figure 12-21 Microscopic images of MCC granules produced at varying screw speed at SFL- 0.166 and PFN- 1.34837E-04

12.3.2.4 Effect of varying SFL-PFN at different screw speed on tablet tensile strength

Figure 12-22-Figure 12-24 show the tensile strength of tablets of MCC granules (with varying size ranges) produced at varying screw speed and SFL-PFN at L/S of 1.0. The tensile strength of tablets does not change significantly at varying size or SFL-PFN. In all cases, the tensile strength of tablets of MCC granules ranged between ~2 MPa to 3 MPa which is clearly higher than the tablets of lactose granules. It is known that MCC is water insoluble, plastically deforming powder with high compressibility while lactose is water soluble and brittle in nature and has lower compressibility (Kleinebudde et al. 2000). Hence, the so produced granules of lactose may be relatively stronger than MCC granules. The weaker MCC granules compressed better than stronger lactose granules and produced stronger tablets. Furthermore, the tablet tensile strength results for MCC are not fully aligned to the granule size results. The granule size at SFL of 0.041 and 0.083 was similar while higher SFL of 0.166 had resulted in relatively smaller granules (Figure 12-18). The tablet tensile for all three SFL was similar. As mentioned earlier, this may be due to high compression force during tableting that overcome the strength of granules in various size ranges.

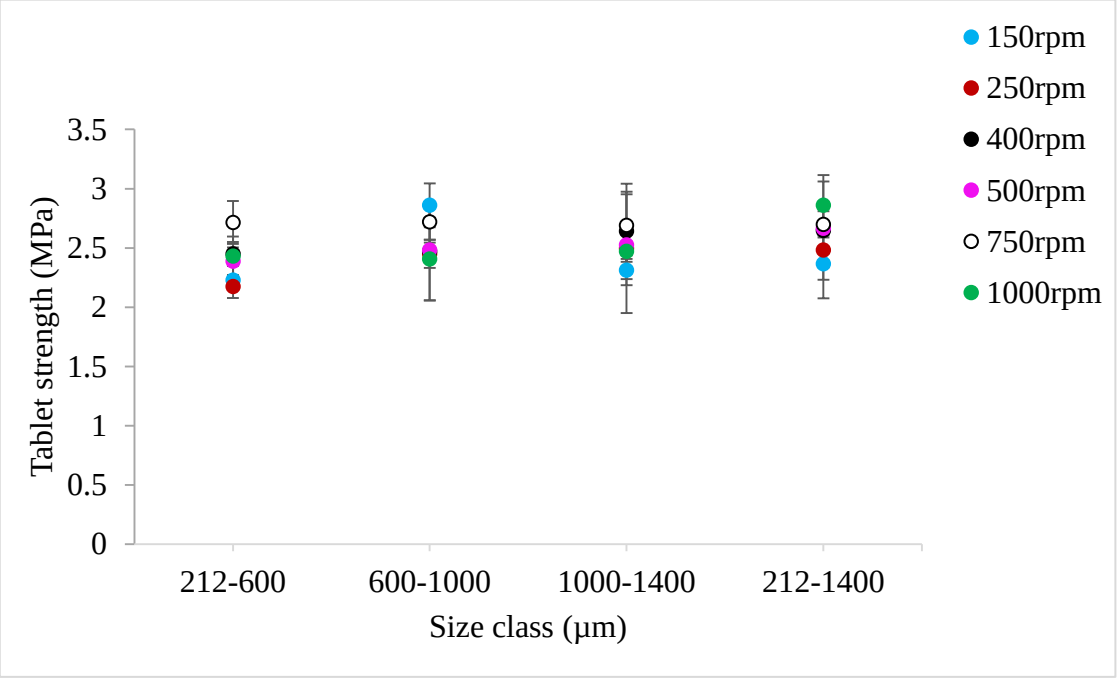

Figure 12-22 Tensile strength of tablets of MCC granules produced at varying screw speed at SFL- 0.041 and PFN- 3.37093E-05 (L/S- 1)

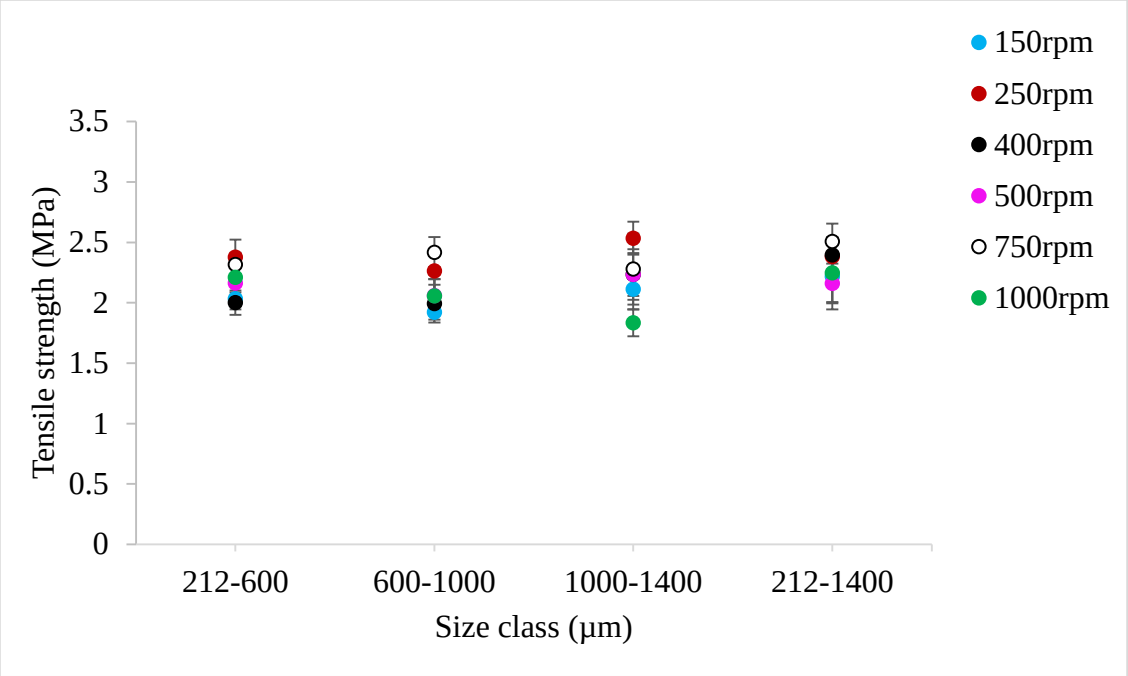

Figure 12-23 Tensile strength of tablets of MCC granules produced at varying screw speed at SFL- 0.083 and PFN- 6.74185E-05 (L/S- 1)

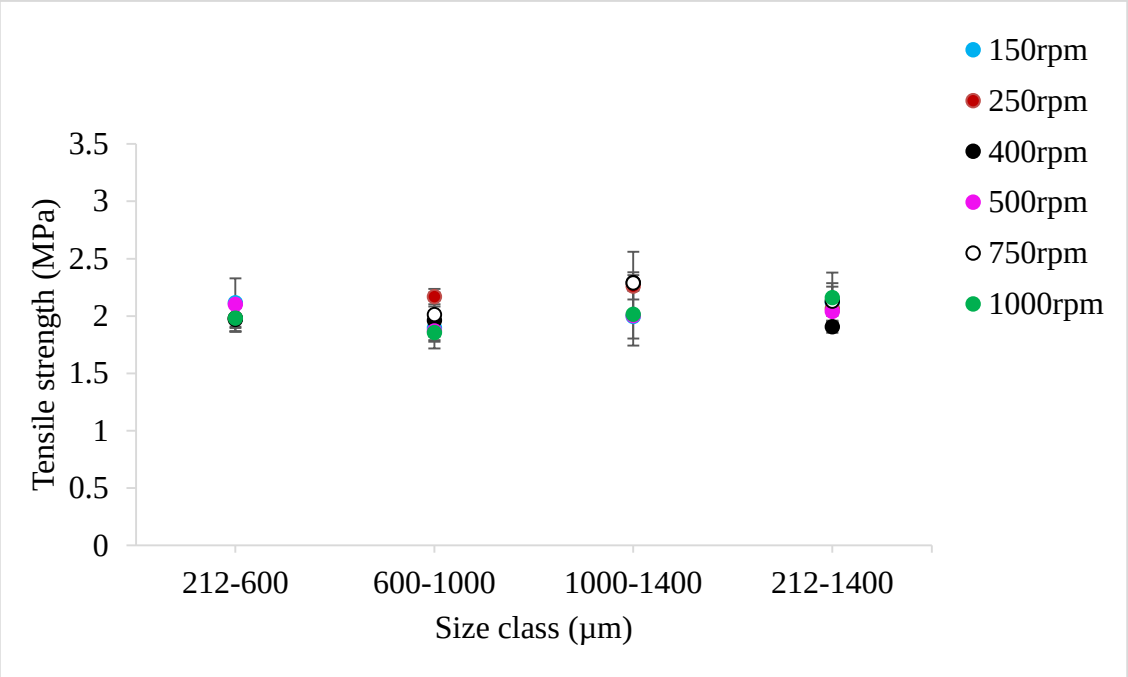

Figure 12-24 Tensile strength of tablets of MCC granules produced at varying screw speed at SFL- 0.166 and PFN- 1.34837E-04 (L/S- 1)

12.3.2.5 Conclusion

From this study it was shown that the specific feed load or powder feed number can act as a surrogate for the barrel fill level that can be used to control and maintain the granule size, shape and tablet tensile strength. It was also found that the material property plays important role while studying fill level. MCC which is insoluble in water produced more proportion of smaller granules at higher fill level owing to limited interaction between powder and liquid due to high throughput force and short residence time. So, it is concluded that along with fill level, material property and residence time are also important factors while considering increasing the throughput (scaling out) of twin screw granulator.

12.4 EFFECTS OF TYPES OF PRIMARY POWDER

12.4.1 Determination of different properties of lactose and mannitol powders

12.4.1.1 Drop penetration time

A drop penetration test was carried out for each of the powders to study the liquid-powder interactions (Figure 12-25). Loose powder beds were prepared. Powder were loosely packed into a petri dish (depth 25mm, diameter 100mm) without using compression machine. The powder was then levelled off to provide a relatively smooth surface for landing of droplet. The petri dishes were handled very gently to avoid tapping or applying direct pressure on the powder surface. The drop penetration was then studied by filming single drops of granulation liquid (distilled water) while it penetrates into the beds of different powders. An electronic pipette was used to produce drop of ~15μL which was released from 20 mm on the surface of the powder bed placed on a substrate. The drop penetration kinetics on powder bed was captured using high speed camera (Photron, Fastcam, 100 K, USA) at frame rate of 2000 frames/s. This was repeated about 10 times for each powder. The frames were then analysed using ImageJ software to measure the drop penetration time. The penetration time was taken as the time taken for the drop to touch the surface of the powder to the time the drop completely disappeared into the powder. It was calculated by counting the number of frames from drop touching the surface of the powder until its complete draining into the powder and dividing it by the frame rate.

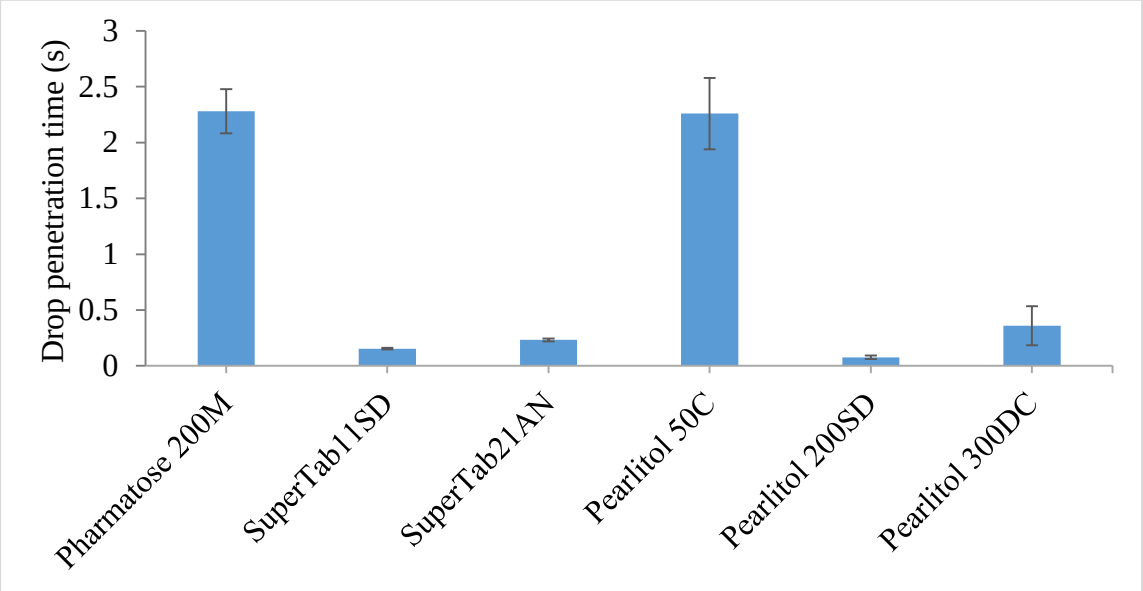

Figure 12-25 Drop penetration time for lactose and mannitol powders

12.4.1.2 Dissolution rate

The rate of dissolution of powders were measured using refractometer PR-43-AP-73-E25. K-Patents refractometer determines the concentration of dissolved solids by making an optical measurement of a solution's refractive index. About 15 g each of lactose and mannitol powders were separately dissolved in 750 ml of water at constant temperature of 25°C and the concentration change with time was recorded (Figure 12-26).

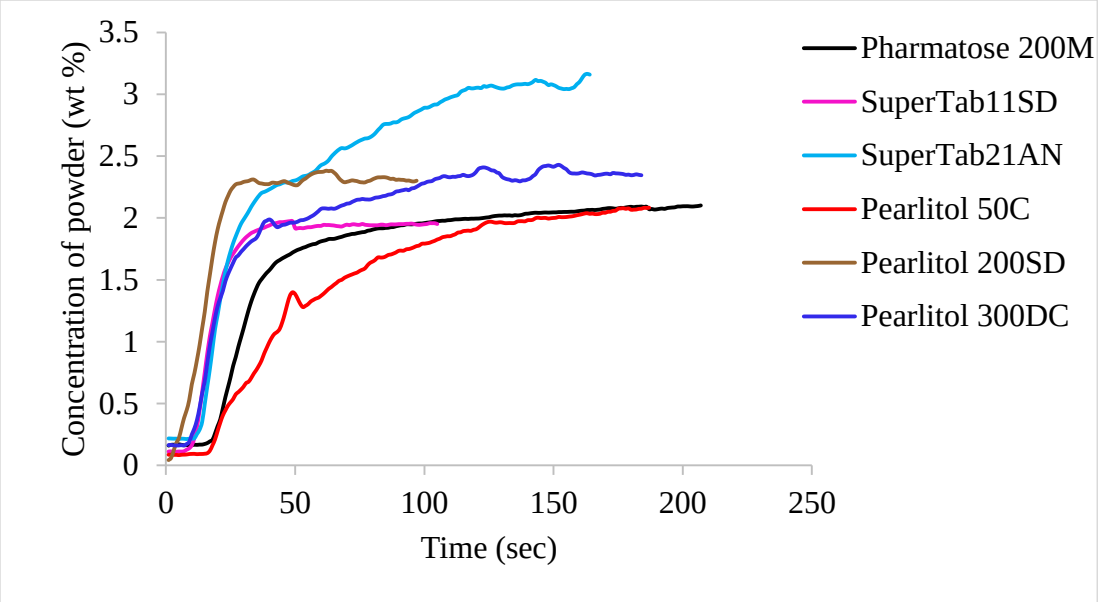

Figure 12-26 Dissolution rate for lactose and mannitol powders

12.4.1.3 Single particle strength

The strength of single powder particle (size- 212 to 250 µm) was determined by using Zwick/ Roell (Figure 12-27). The single particle was compressed using punch with load cell of 1N and the force required to fracture was measured.

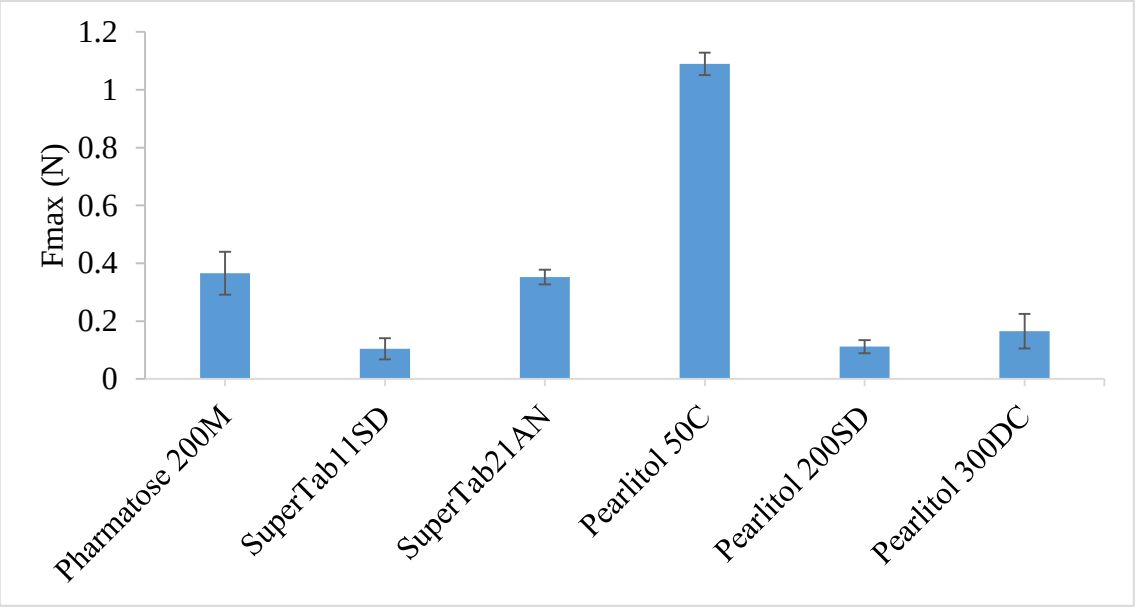

Figure 12-27 Single particle strength of lactose and mannitol powders

12.4.1.4 Compressibility factor (K)

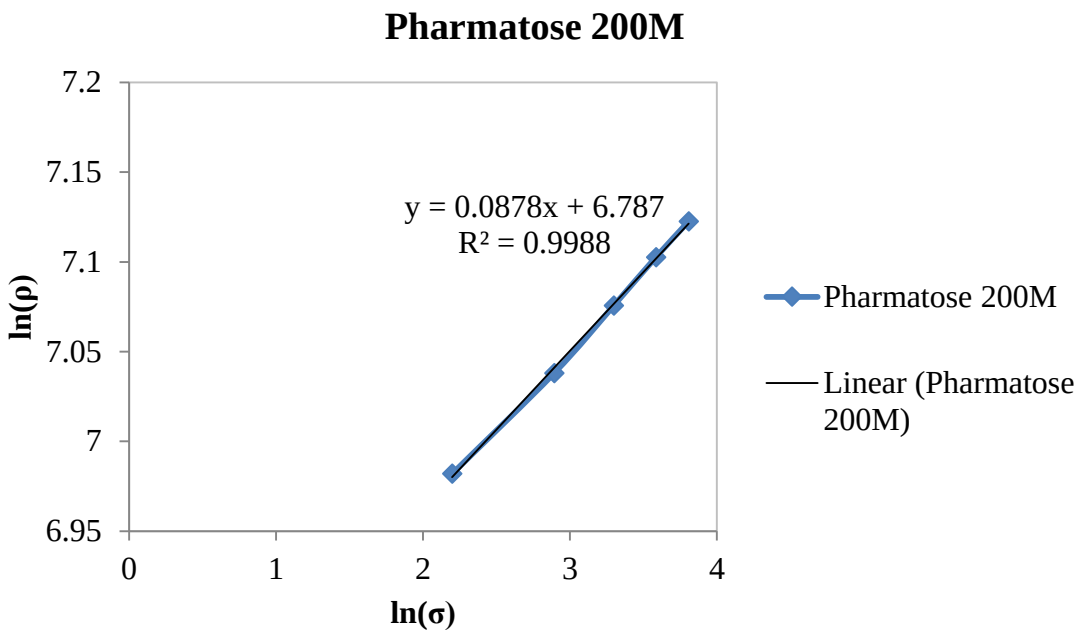

Figure 12-28 Linearity curve for compressibility factor (K) for Pharmatose 200M

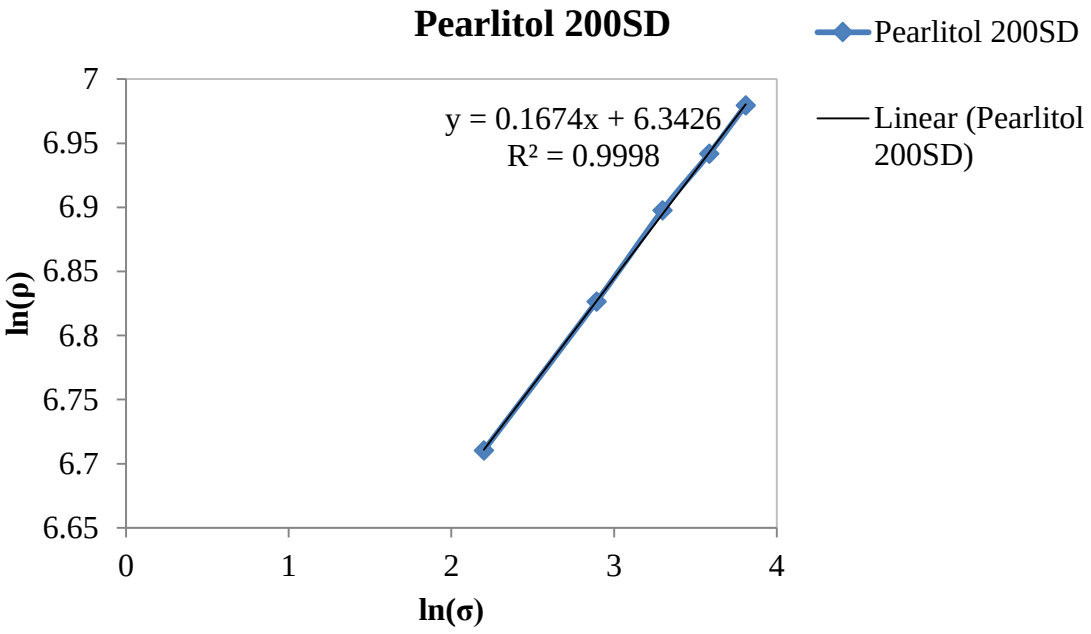

Figure 12-29 Linearity curve for compressibility factor (K) for Pearlitol 200SD